44769

National Library of Canada | Bibliothèque nationale du Canada

Canadian Theses Division | Division des thèses canadiennes

Ottawa, Canada
K1A 0N4

PERMISSION TO MICROFILM — AUTORISATION DE MICROFILMER

- Please print or type — Écrire en lettres moulées ou dactylographier

Full Name of Author — Nom complet de l'auteur

AH-DONG, LEU

Date of Birth — Date de naissance

Jan. 13 1937

Country of Birth — Lieu de naissance

REPUBLIC OF CHINA

Permanent Address — Résidence fixe

10923 86 AVE., EDMONTON, AB., T6G 0W8

Title of Thesis — Titre de la thèse

SOLVATED ELECTRON OPTICAL ABSORPTION SPECTRA IN ALCOHOL-WATER SOLUTIONS

University — Université

THE UNIVERSITY OF ALBERTA

Degree for which thesis was presented — Grade pour lequel cette thèse fut présentée

PH. D.

Year this degree conferred — Année d'obtention de ce grade

1980

Name of Supervisor — Nom du directeur de thèse

PRF. G. R. FREEMAN

Permission is hereby granted to the NATIONAL LIBRARY OF CANADA to microfilm this thesis and to lend or sell copies of the film.

The author reserves other publication rights, and neither the thesis nor extensive extracts from it may be printed or otherwise reproduced without the author's written permission.

L'autorisation est, par la présente, accordée à la BIBLIOTHÈQUE NATIONALE DU CANADA de microfilmer cette thèse et de prêter ou de vendre des exemplaires du film.

L'auteur se réserve les autres droits de publication; ni la thèse ni de longs extraits de celle-ci ne doivent être imprimés ou autrement reproduits sans l'autorisation écrite de l'auteur.

Date

Jan. 3rd 1980

Signature

Ah-dong Leu

NL-91 (4/77)

National Library of Canada
Collections Development Branch

Canadian Theses on
Microfiche Service

Bibliothèque nationale du Canada
Direction du développement des collections

Service des thèses canadiennes
sur microfiche

NOTICE

The quality of this microfiche is heavily dependent upon the quality of the original thesis submitted for microfilming. Every effort has been made to ensure the highest quality of reproduction possible.

If pages are missing, contact the university which granted the degree.

Some pages may have indistinct print especially if the original pages were typed with a poor typewriter ribbon or if the university sent us a poor photocopy.

Previously copyrighted materials (journal articles, published tests, etc.) are not filmed.

Reproduction in full or in part of this film is governed by the Canadian Copyright Act, R.S.C. 1970, c. C-30. Please read the authorization forms which accompany this thesis.

THIS DISSERTATION
HAS BEEN MICROFILMED
EXACTLY AS RECEIVED

AVIS

La qualité de cette microfiche dépend grandement de la qualité de la thèse soumise au microfilmage. Nous avons tout fait pour assurer une qualité supérieure de reproduction.

S'il manque des pages, veuillez communiquer avec l'université qui a conféré le grade.

La qualité d'impression de certaines pages peut laisser à désirer, surtout si les pages originales ont été dactylographiées à l'aide d'un ruban usé ou si l'université nous a fait parvenir une photocopie de mauvaise qualité.

Les documents qui font déjà l'objet d'un droit d'auteur (articles de revue, examens publiés, etc.) ne sont pas microfilmés.

La reproduction, même partielle, de ce microfilm est soumise à la Loi canadienne sur le droit d'auteur, SRC 1970, c. C-30. Veuillez prendre connaissance des formules d'autorisation qui accompagnent cette thèse.

LA THÈSE A ÉTÉ
MICROFILMÉE TELLE QUE
NOUS L'AVONS REÇUE

Ottawa, Canada
K1A 0N4

NL-339 (Rev. 8/80)

THE UNIVERSITY OF ALBERTA

SOLVATED ELECTRON OPTICAL ABSORPTION SPECTRA IN ALCOHOL-WATER SOLUTIONS

BY

© AH-DONG LEU, M.Sc.

A THESIS
SUBMITTED TO THE FACULTY OF GRADUATE STUDIES AND RESEARCH
IN PARTIAL FULFILMENT OF THE REQUIREMENTS FOR THE DEGREE
OF
DOCTOR OF PHILOSOPHY

DEPARTMENT OF CHEMISTRY

EDMONTON, ALBERTA
SPRING, 1980

THE UNIVERSITY OF ALBERTA

FACULTY OF GRADUATE STUDIES AND RESEARCH

The undersigned certify that they have read, and recommend to the Faculty of Graduate Studies and Research for acceptance, a thesis entitled

"SOLVATED ELECTRON OPTICAL ABSORPTION SPECTRA IN ALCOHOL-WATER SOLUTIONS"

submitted by AH-DONG LEU in partial fulfilment of the requirements for the degree of Doctor of Philosophy.

G.R. Freeman
Supervisor

Fraser W. Birss

M.J. Robins

J.A. Kernahan

S. Huzinaga

Hugh A. Gillis
External Examiner

Dec 20/79
Date

TO MY PARENTS

ABSTRACT

Optical absorption spectra of excess electrons in binary mixtures of water with a number of alcohols have been studied by the pulse radiolysis method. Composition and temperature were varied in order to determine their effects on spectrum parameters such as E_{Amax} and $W_{\frac{1}{2}}$.

The values of E_{Amax} in the pure compounds have been remeasured and some new values have been suggested. The values decrease as follows: methanol ≈ primary alcohols (except ethanol) > water > secondary alcohols > t-butanol. The values of $W_{\frac{1}{2}}$ decrease as follows: primary alcohols > methanol > secondary alcohols > t-butanol ≈ water.

In the vicinity of pure alcohols, the E_{Amax} for the solutions has two trends, i.e., it decreases as mole % water increases in methanol and primary alcohols, and increases for secondary alcohols and t-butanol. Around 10 mole % water in primary alcohols, the E_{Amax} reaches a minimum that is close to or slightly less than the value for pure water. The value of $W_{\frac{1}{2}}$ decreases with increasing mole % water in all the alcohols except t-butanol, in which it is independent of composition. Both E_{Amax} and $W_{\frac{1}{2}}$ are nearly independent of composition between 50 and 97 mole % water in all the alcohols. The electrons are selectively solvated by water. In

the vicinity of pure water, the E_{Amax} increases significantly upon the addition of 2 - 3 mole % of any alcohol, but the $W_{\frac{1}{2}}$ remains constant. This increase is related to a modification of the liquid structure of water.

The minimum of E_{Amax} in primary alcohols containing around 10 mole % water suggests that a peculiar solution structure exists at that composition.

In the 50 to 98 mole % water region the excess electron rests preferentially in a slightly modified water structure.

The spectrum shape is more sensitive to composition change than to temperature. The temperature coefficient of E_{Amax} is negative in all solutions and in the pure compounds. By contrast, that of $W_{\frac{1}{2}}$ can be positive, negative or nearly zero. The behavior of the ratio $W_{\frac{1}{2}}/E_{Amax}$ indicates that increasing the temperature favors selective solvation by water.

The behavior of $-dE_{Amax}/dT$ and $dW_{\frac{1}{2}}/dT$ as a function of composition are similar to that of E_{Amax} itself. The behavior of $W_{\frac{1}{2}}$ itself with composition is quite different from these.

ACKNOWLEDGEMENT

I am deeply indebted to Professor G. R. Freeman for his guidance and patience during the course of the work.

It is a pleasure to express my gratitude to Drs. K. N. Jha and F. Y. Jou for their invaluable discussions and advice, and to Drs. and Mrs. Tomoki C. S. Ruo and R. C. Lin for their continuous encouragement.

I am very grateful for the help I received from Mrs. Mary Waters, Miss Mary Morrison, and Mr. Steve Nicely in the course of this thesis.

I would like to thank Mr. Larry Coulson for his assistance in computer programming, and to Mr. R. J. Gardner and his staff for their technical assistance.

Thanks are due to the members of the glass and machine shops and of the Xeroxing room for the excellent work they have done, and to the members of the Radiation Chemisty Group for their helpful cooperation.

Appreciation is extended to the National Research Council of Canada for financial assistance.

承蒙

技佐、技士、技正 諸仁兄 ， 利器善事；
MR. LARRY COULSON ， 編寫算程；
MR. STEVE NICELY ， 修飾辞藻；
MRS. MARY WATERS ， 謄繕文稿；
MISS MARY MORRISON ， 校對紕漏．
此恩此惠 ， 銘諸肺腑．

幸獲

DRS. K. N. JHA 和 F. Y. JOU ，
兩位學長 ， 時賜教益；
DRS. TOMOKI C. S. RUO 和 R. C. LIN，
學兄夫婦 ， 慰勉有嘉．
此功此德 ， 銘肌鏤骨．

能得

PROFESSOR GORDON R. FREEMAN ，
誨我教我 ， 督我促我；
以啓思路 ， 以匡不逮．
鑽之彌堅 ， 仰之彌高；
浩瀚師恩 ， 倫比再造．

另特致謝 加國"國科會"之獎助．

呂阿東

1979年12月21日
于 CHEMISTRY DEPARTMENT,
UNIVERSITY OF ALBERTA,
EDMONTON, ALBERTA,
CANADA T6G 2G2

TABLE OF CONTENTS

PAGE

I. INTRODUCTION.................................. 1

A. General.................................. 1

B. Historical.................................. 6

1. Solvated Electrons in Pure Liquids.... 6

2. Solvated Electrons in Binary Mixtures. 10

C. Theory.................................. 12

1. The Polaron Model.................... 18

2. The Cavity Model.................... 21

3. The Continuum Model.................. 25

4. The Semi-Continuum Model............. 28

5. The Molecular Field Model............ 35

6. The Two Absorber Model............... 36

D. The Present Study..................... 37

II. EXPERIMENTAL.................................. 39

A. Materials.................................. 39

B. Apparatus.................................. 40

1. The Sample Cells.................... 40

2. The Bubbling System.................. 41

3. The Irradiation, Detection and Control System.............................. 41

(a) The van de Graaff Accelerator (VDGA)......................... 45

(b) The Secondary Emission Monitor (SEM).......................... 46

PAGE

(c) The Temperature Control System....... 48

(d) Optical Detection Systems............ 52

(i) The Light Source............... 52

(ii) The Monochromator, Grating and Filters........................ 55

(iii) Detectors and Amplifiers....... 57

(iv) Digital Voltmeter (DVM) and Oscilloscope................... 60

(e) The Timing and Control Systems....... 63

C. Techniques.................................. 67

1. Sample Preparation........................ 67

2. Analysis of Polaroid Photographs......... 71

(a) Analysis of Optical Absorption from Photograph 'i'..................... 71

(b) Analysis of Optical Absorption from Photograph 'ii'.................... 74

3. Analysis of Absorption Spectra........... 75

(a) Primary Parameters................... 75

(b) Secondary Parameters................. 75

(c) High Energy Side of the Spectra...... 76

(d) Area Measurements.................... 76

D. Irradiation and Dosimetry.................. 81

III. RESULTS...................................... 83

A. Alcohol/Water Mixture, 298K................ 83

B. Spectrum Shape............................. 87

1. Effect of composition.................. 87

(a) Methanol/Water..................... 87

PAGE

(b) Ethanol/Water........................ 91

(c) 1-Propanol/Water...................... 95

(d) 2-Propanol/Water...................... 99

(e) 1-Butanol/Water....................... 103

(f) Iso-Butanol (2-Methyl-1-propanol/Water............................ 107

(g) 2-Butanol (sec-Butyl Alcohol)/Water.. 111

(h) tert-Butanol (2-Methyl-2-propanol)/Water............................ 115

Summary............................... 119

2. Effect of Temperature.................... 124

C. Effect of Composition upon Temperature Coefficients.................................. 210

IV. DISCUSSION.................................... 214

A. E_{Amax} of Pure Alcohols from C_1 to C_4 at 298K. 214

B. Effect of Composition........................ 223

1. Composition Dependence of E_{Amax} for C_1 to C_4 Alcohol/Water Solutions........... 223

(i) Pure Alcohols....................... 225

(ii) In the Low Mole % Water Region.... 227

(iii) In the High Mole % Water Region... 235

(iv) Around 10 Mole % Water Region..... 238

(v) In the Remaining Composition Range 242

2. Composition Dependence of $W_{\frac{1}{2}}$ for Alcohol/Water Mixtures.......................... 243

3. Composition Dependence of W_b and W_r...... 252

PAGE

4. Composition Dependence of Gε_{max} 257

C. Effect of Temperature.......................... 260

1. Temperature Dependence of Spectra Shape of Alcohol/Water Mixtures...................... 260

2. Temperature Dependence of E_{Amax}.......... 260

3. Temperature Dependence of $W_{\frac{1}{2}}$.............. 263

D. Summary.................................... 276

1. Pure Solvents.............................. 276

2. Alcohol/Water Mixtures.................... 276

(a) Effect of Composition................ 276

(b) Effect of Temperature................ 278

(c) Composition Dependence of Temperature Coefficient.......................... 279

REFERENCES.. 280

V. APPENDIX.. 304

A. Deconvolution of Absorption Spectra.......... 304

B. High Energy Side of the Absorption Spectra... 353

C. Area Measurements............................ 353

D. The Secondary Parameters..................... 353

LIST OF TABLES

TABLE		PAGE
III-1	Parameters of Solvated Electrons in Methanol/Water at 298K	89
III-2	Parameters of Solvated Electrons in Ethanol/Water at 298K	93
III-3	Parameters of Solvated Electrons in 1-Propanol/Water at 298K	97
III-4	Parameters of Solvated Electrons in 2-Propanol/Water at 298K	101
III-5	Parameters of Solvated Electrons in 1-Butanol/Water at 298K	105
III-6	Parameters of Solvated Electrons in iso-Butanol/Water at 298K	109
III-7	Parameters of Solvated Electrons in 2-Butanol/Water at 298K	113
III-8	Parameters of Solvated Electrons in t-Butanol/Water at 298K	117
III-9	Parameters of Solvated Electrons in Water at Different Temperatures	125
III-10	Parameters of Solvated Electrons in Methanol/Water at Different Temperatures	126
III-11	Parameters of Solvated Electrons in Ethanol/Water at Different Temperatures	128
III-12	Parameters of Solvated Electrons in 1-Propanol/Water at Different Temperatures	130

TABLE		PAGE
III-13	Parameters of Solvated Electrons in 2-Propanol/Water at Different Temperatures	132
III-14	Parameters of Solvated Electrons in 1-Butanol/Water at Different Temperatures	134
III-15	Parameters of Solvated Electrons in iso-Butanol/Water at Different Temperatures	136
III-16	Parameters of Solvated Electrons in 2-Butanol/Water at Different Temperatures	138
III-17	Parameters of Solvated Electrons in tert-Butanol/Water at Different Temperatures	140
IV-1	Values of E_{Amax} in Pure Alcohols and in Water	217
IV-2	The Temperature Coefficient of $W_{\frac{1}{2}}/E_{Amax}$ in Alcohol/Water Mixtures	270
V-1	Parameters for Deconvoluting the Absorption Spectra of Methanol into Gaussian Bands at 298K	309
V-2	Secondary Parameters of Solvated Electrons in Water at Different Temperatures	311

TABLE PAGE

V-3 Secondary Parameters of Solvated Electrons in Methanol/Water at Different Temperatures 312

V-4 Secondary Parameters of Solvated Electrons in Ethanol/Water at Different Temperatures 315

V-5 Secondary Parameters of Solvated Electrons in 1-Propanol/Water at Different Temperatures 318

V-6 Secondary Parameters of Solvated Electrons in 2-Propanol/Water at Different Temperatures 321

V-7 Secondary Parameters of Solvated Electrons in 1-Butanol/Water at Different Temperatures 324

V-8 Secondary Parameters of Solvated Electrons in iso-Butanol/Water at Different Temperatures 327

V-9 Secondary Parameters of Solvated Electrons in 2-Butanol/Water at Different Temperatures 330

V-10 Secondary Parameters of Solvated Electrons in t-Butanol/Water at Different Temperatures 333

V-11 The Values of α for Alcohol/Water Mixtures at 298K 354

LIST OF FIGURES

FIGURE		PAGE
I-1	Definition of the Distances Involved in the Semi-Continuum Model	29
II-1	Suprasil Quartz Optical Cells	42
II-2	The Sample Bubbler Manifold for Use with Quartz Cells	43
II-3	The Block Diagram of Optical Detection System	44
II-4	The Secondary Emission Monitor (SEM)	47
II-5	The Path of the Analyzing Light	53
II-6	Circuit for Pulsing the Xe Lamp	54
II-7	Block Diagram of the Detectors and the Amplifiers for IR, Visible, and UV Measurements	58
II-8	Amplifier Circuit for the IR Light Detector	59
II-9	Amplifier Circuit for the Visible Light Detector	61
II-10	Amplifier Circuit for the UV Light Detector	62
II-11	The Time Sequence of an Absorption Experiment	64
II-12	Direct Current Absorption Amplifier	68
II-13	The Sealing Technique for Type (b) Cells	70
II-14	Typical Oscilloscope Trace Photograph	72

FIGURE		PAGE
II-15	Graph Used to Obtain Primary Parameters	77
II-16	Graph for Obtaining Secondary Parameters	78
II-17	Plot of $\ln(A/A_{max})$ vs $\ln(E)$	79
II-18	Graph Used to Measure the Area	80
III-1	Plot of E_{Amax} vs Composition	84
III-2	Plot of $G\varepsilon_{max}$ vs Composition	85
III-3	The Optical Absorption Spectrum of Solvated Electrons in Methanol/Water at 298K and Various Compositions	88
III-4	Composition Dependence of Spectrum Parameters in Methanol/Water	90
III-5	The Optical Absorption Spectrum of Solvated Electrons in Ethanol/Water at 298K and Various Compositions	92
III-6	Composition Dependence of Spectrum Parameters in Ethanol/Water	94
III-7	The Optical Absorption Spectrum of Solvated Electrons in 1-Propanol/Water at 298K and Various Compositions	96
III-8	Composition Dependence of Spectrum Parameters in 1-Propanol/Water	98
III-9	The Optical Absorption Spectrum of Solvated Electrons in 2-Propanol/Water at 298K and Various Compositions	100

FIGURE		PAGE
III-10	Composition Dependence of Spectrum Parameters in 2-Propanol/Water	102
III-11	The Optical Absorption Spectrum of Solvated Electrons in 1-Butanol/Water at 298K and Various Compositions	104
III-12	Composition Dependence of Spectrum Parameters in 1-Butanol/Water	106
III-13	The Optical Absorption Spectrum of Solvated Electrons in iso-Butanol/Water at 298K and Various Compositions	108
III-14	Composition Dependence of Spectrum Parameters in iso-Butanol/Water	110
III-15	The Optical Absorption Spectrum of Solvated Electrons in 2-Butanol/Water at 298K and Various Compositions	112
III-16	Composition Dependence of Spectrum Parameters in 2-Butanol/Water	114
III-17	The Optical Absorption Spectrum of Solvated Electrons in tert-Butanol/Water at 298K and Various Compositions	116
III-18	Composition Dependence of Spectrum Parameters in t-Butanol/Water	118
III-19	Composition Dependence of E_{Amax} for Alcohol/Water Mixtures at 298K	120
III-20	Composition Dependence of $W_{\frac{1}{2}}$ for Alcohol/Water Mixtures at 298K	122

FIGURE PAGE

III-21 Composition Dependence of W_b and W_r for Alcohol/Water Mixtures at 298K 123

III-22 The Optical Absorption Spectrum of Solvated Electrons in Water at Different Temperatures 142

III-23 Temperature Dependence of Spectrum Parameters in Water 143

III-24 The Optical Absorption Spectrum of Solvated Electrons in Methanol at Different Temperatures 144

III-25 Temperature Dependence of Spectrum Parameters in Methanol 145

III-26 The Optical Absorption Spectrum of Solvated Electrons in a Solution of 10 Mole % Water in Methanol at Different Temperatures 146

III-27 Temperature Dependence of Spectrum Parameters in a Solution of 10 Mole % Water in Methanol 147

III-28 The Optical Absorption Spectrum of Solvated Electrons in a Solution of 50 Mole % Water in Methanol at Different Temperatures 148

III-29 Temperature Dependence of Spectrum Parameters in a Solution of 50 Mole % Water in Methanol 149

FIGURE PAGE

III-30 The Optical Absorption Spectrum of Solvated Electrons in a Solution of 98 Mole % Water in Methanol at Different Temperatures 150

III-31 Temperature Dependence of Spectrum Parameters in a Solution of 98 Mole % Water in Methanol 151

III-32 The Optical Absorption Spectrum of Solvated Electrons in Ethanol at Different Temperatures 152

III-33 Temperature Dependence of Spectrum Parameters in Ethanol 153

III-34 The Optical Absorption Spectrum of Solvated Electrons in a Solution of 10 Mole % Water in Ethanol at Different Temperatures 154

III-35 Temperature Dependence of Spectrum Parameters in a Solution of 10 Mole % Water in Ethanol 155

III-36 The Optical Absorption Spectrum of Solvated Electrons in a Solution of 50 Mole % Water in Ethanol at Different Temperatures 156

III-37 Temperature Dependence of Spectrum Parameters in a Solution of 50 Mole % Water in Ethanol 157

III-38 The Optical Absorption Spectrum of Solvated Electrons in a Solution of 98 Mole % Water in Ethanol at Different Temperatures 158

FIGURE		PAGE
III-39	Temperature Dependence of Spectrum Parameters in a Solution of 98 Mole % Water in Ethanol	159
III-40	The Optical Absorption Spectrum of Solvated Electrons in 1-Propanol at Different Temperatures	160
III-41	Temperature Dependence of Spectrum Parameters in 1-Propanol	161
III-42	The Optical Absorption Spectrum of Solvated Electrons in a Solution of 10 Mole % Water in 1-Propanol at Different Temperatures	162
III-43	Temperature Dependence of Spectrum Parameters in a Solution of 10 Mole % Water in 1-Propanol	163
III-44	The Optical Absorption Spectrum of Solvated Electrons in a Solution of 50 Mole % Water in 1-Propanol at Different Temperatures	164
III-45	Temperature Dependence of Spectrum Parameters in a Solution of 50 Mole % Water in 1-Propanol	165
III-46	The Optical Absorption Spectrum of Solvated Electrons in a Solution of 98 Mole % Water in 1-Propanol at Different Temperatures	166
III-47	Temperature Dependence of Spectrum Parameters in a Solution of 98 Mole % Water in 1-Propanol	167

FIGURE		PAGE
III-48	The Optical Absorption Spectrum of Solvated Electrons in 2-Propanol at Different Temperatures	168
III-49	Temperature Dependence of Spectrum Parameters in 2-Propanol	169
III-50	The Optical Absorption Spectrum of Solvated Electrons in a Solution of 10 Mole % Water in 2-Propanol at Different Temperatures	170
III-51	Temperature Dependence of Spectrum Parameters in a Solution of 10 Mole % Water in 2-Propanol	171
III-52	The Optical Absorption Spectrum of Solvated Electrons in a Solution of 50 Mole % Water in 2-Propanol at Different Temperatures	172
III-53	Temperature Dependence of Spectrum Parameters in a Solution of 50 Mole % Water in 2-Propanol	173
III-54	The Optical Absorption Spectrum of Solvated Electrons in a Solution of 98 Mole % Water in 2-Propanol at Different Temperatures	174
III-55	Temperature Dependence of Spectrum Parameters in a Solution of 98 Mole % Water in 2-Propanol	175
III-56	The Optical Absorption Spectrum of Solvated Electrons in 1-Butanol at Different Temperatures	176

FIGURE PAGE

III-57 Temperature Dependence of Spectrum Parameters in 1-Butanol 177

III-58 The Optical Absorption Spectrum of Solvated Electrons in a Solution of 10 Mole % Water in 1-Butanol at Different Temperatures 178

III-59 Temperature Dependence of Spectrum Parameters in a Solution of 10 Mole % Water in 1-Butanol 179

III-60 The Optical Absorption Spectrum of Solvated Electrons in a Solution of 50 Mole % Water in 1-Butanol at Different Temperatures 180

III-61 Temperature Dependence of Spectrum Parameters in a Solution of 50 Mole % Water in 1-Butanol 181

III-62 The Optical Absorption Spectrum of Solvated Electrons in a Solution of 98 Mole % Water in 1-Butanol at Different Temperatures 182

III-63 Temperature Dependence of Spectrum Parameters in a Solution of 98 Mole % Water in 1-Butanol 183

III-64 The Optical Absorption Spectrum of Solvated Electrons in iso-Butanol at Different Temperatures 184

III-65 Temperature Dependence of Spectrum Parameters in iso-Butanol 185

FIGURE PAGE

III-66 The Optical Absorption Spectrum of Solvated Electrons in a Solution of 10 Mole % Water in iso-Butanol at Different Temperatures 186

III-67 Temperature Dependence of Spectrum Parameters in a Solution of 10 Mole % Water in iso-Butanol 187

III-68 The Optical Absorption Spectrum of Solvated Electrons in a Solution of 50 Mole % Water in iso-Butanol at Different Temperatures 188

III-69 Temperature Dependence of Spectrum Parameters in a Solution of 50 Mole % Water in iso-Butanol 189

III-70 The Optical Absorption Spectrum of Solvated Electrons in a Solution of 98 Mole % Water in iso-Butanol at Different Temperatures 190

III-71 Temperature Dependence of Spectrum Parameters in a Solution of 98 Mole % Water in iso-Butanol 191

III-72 The Optical Absorption Spectrum of Solvated Electrons in 2-Butanol at Different Temperatures 192

III-73 Temperature Dependence of Spectrum Parameters in 2-Butanol 193

FIGURE		PAGE
III-74	The Optical Absorption Spectrum of Solvated Electrons in a Solution of 10 Mole % Water in 2-Butanol at Different Temperatures	194
III-75	Temperature Dependence of Spectrum Parameters in a Solution of 10 Mole % Water in 2-Butanol	195
III-76	The Optical Absorption Spectrum of Solvated Electrons in a Solution of 50 Mole % Water in 2-Butanol at Different Temperatures	196
III-77	Temperature Dependence of Spectrum Parameters in a Solution of 50 Mole % Water in 2-Butanol	197
III-78	The Optical Absorption Spectrum of Solvated Electrons in a Solution of 98 Mole % Water in 2-Butanol at Different Temperatures	198
III-79	Temperature Dependence of Spectrum Parameters in a Solution of 98 Mole % Water in 2-Butanol	199
III-80	The Optical Absorption Spectrum of Solvated Electrons in t-Butanol at Different Temperatures	200
III-81	Temperature Dependence of Spectrum Parameters in t-Butanol	201
III-82	The Optical Absorption Spectrum of Solvated Electrons in a Solution of 10 Mole % Water in t-Butanol at Different Temperatures	202

FIGURE		PAGE
III-83	Temperature Dependence of Spectrum Parameters in a Solution of 10 Mole % Water in t-Butanol	203
III-84	The Optical Absorption Spectrum of Solvated Electrons in a Solution of 50 Mole % Water in t-Butanol at Different Temperatures	204
III-85	Temperature Dependence of Spectrum Parameters in a Solution of 50 Mole % Water in t-Butanol	205
III-86	The Optical Absorption Spectrum of Solvated Electrons in a Solution of 98 Mole % Water in t-Butanol at Different Temperatures	206
III-87	Temperature Dependence of Spectrum Parameters in a Solution of 98 Mole % Water in t-Butanol	207
III-88	$-dE_{Amax}/dT$ of Alcohol/Water Solutions as a Function of Composition	211
III-89	$dW_{\frac{1}{2}}/dT$ of Alcohol/Water Solutions as a Function of Composition	213
IV-1	The Relative Viscosity, η/η_{H_2O} of Pure Alcohols and Alcohol/Water Mixtures at 298K	215
IV-2	Excess Enthalpies of Mixing of Alcohol and Water at 298K	216

FIGURE PAGE

IV-3 Plot of E_{Amax} vs the Number of Carbon Atoms in n-Alcohols at 298K 221

IV-4 Composition Dependence of $E_{Amax}/E_{Amax}^{H_2O}$ for Alcohol/Water Mixtures at 298K (a) 224

IV-5 Proposed Two Kinds of Contribution to Account for the Observed E_{Amax} in Alcohol/Water Mixtures at 298K (a) 229

IV-6 Proposed Two Kinds of Contribution to Account for the Observed E_{Amax} in Alcohol/Water Mixtures at 298K (b) 233

IV-7 Composition Dependence of E_{Amax}/E_{Amax}^{ROH} for n-Alcohol/Water Mixtures at 298K 234

IV-8 Viscosity, η, and $d\eta/dC$ of Ethanol/Water Mixtures at 298K 236

IV-9 Composition Dependence of $E_{Amax}/E_{Amax}^{H_2O}$ for Alcohol/Water Mixtures at 298K (b) 237

IV-10 Proposed Solution Structure for Alcohol/Water Mixtures Around 10 Mole % Water at 298K 240

IV-11 Proposed Two Kinds of Contribution to Account for the Observed $W_{\frac{1}{2}}$ in Alcohol/Water Mixtures at 298K 245

IV-12 Plot of $W_{\frac{1}{2}}$ vs the Number of Carbon Atoms in n-Alcohols at 298K 247

IV-13 Plot of $W_{\frac{1}{2}}$ vs the Number of α-H in Alcohols at 298K 249

FIGURE PAGE

IV-14 Composition Dependence of $W_{1/2}/W_{1/2}^{ROH}$ for Alcohol/Water Mixtures at 298K 250

IV-15 Composition Dependence of W_b/W_r for Alcohol/Water Mixtures at 298K 254

IV-16 Plot of W_b/W_r vs the Number of Carbon Atoms in n-Alcohols at 298K 256

IV-17 Partial Molar Volumes in Ethanol/Water Mixtures at 293K 258

IV-18 Plot of $-dE_{Amax}/dT$ vs the Number of α-H in Alcohols 262

IV-19 Composition Dependence of $(dW_{1/2}/dT)/(dE_{Amax}/dT)$ for Alcohol/Water Mixtures 267

IV-20 Composition Dependence of $(dW_{1/2}/dT)/E_{Amax}^{298}$ for Alcohol/Water Mixtures 268

IV-21 Temperature Dependence of $W_{1/2}/E_{Amax}$ for Methanol/Water Mixtures 272

IV-22 Temperature Dependence of $W_{1/2}/E_{Amax}$ for 1-Propanol/Water Mixtures 273

IV-23 Temperature Dependence of $W_{1/2}/E_{Amax}$ for 2-Propanol/Water Mixtures 274

IV-24 Temperature Dependence of $W_{1/2}/E_{Amax}$ for t-Butanol/Water Mixtures 275

FIGURE		PAGE
V-1	The Band Deconvolution of the Optical Absorption Spectrum of Solvated Electrons in Methanol at 298K (a)	305
V-2	Band Deconvolution in Methanol at 298K (b)	306
V-3	Band Deconvolution in Methanol at 298K (c)	307
V-4	Band Deconvolution in Water at 298K	336
V-5	Band Deconvolution in Methanol at 298K (d)	337
V-6	Band Deconvolution in Methanol Containing 10 Mole % Water at 298K	338
V-7	Band Deconvolution in Methanol Containing 50 Mole % Water at 298K	339
V-8	Band Deconvolution in Methanol Containing 98 Mole % Water at 298K	340
V-9	Band Deconvolution in 1-Propanol at 298K	341
V-10	Band Deconvolution in 1-Propanol Containing 10 Mole % Water at 298K	342
V-11	Band Deconvolution in 1-Propanol Containing 50 Mole % Water at 298K	343
V-12	Band Deconvolution in 1-Propanol Containing 98 Mole % Water at 298K	344
V-13	Band Deconvolution in 2-Propanol at 298K	345
V-14	Band Deconvolution in 2-Propanol Containing 10 Mole % Water at 298K	346
V-15	Band Deconvolution in 2-Propanol Containing 50 Mole % Water at 298K	347
V-16	Band Deconvolution in 2-Propanol Containing 98 Mole % Water at 298K	348
V-17	Band Deconvolution in t-Butanol at 298K	349
V-18	Band Deconvolution in t-Butanol Containing 10 Mole % Water at 298K	350

FIGURE PAGE

V-19 Band Deconvolution in t-Butanol Containing 50 Mole % Water at 298K 351

V-20 Band Deconvolution in t-Butanol Containing 98 Mole % Water at 298K 352

V-21 Composition Dependence of $E_1/E_1^{H_2O}$ for Alcohol/Water Mixtures at 298K 356

V-22 Composition Dependence of $E_2/E_2^{H_2O}$ for Alcohol/Water Mixtures at 298K 357

V-23 Composition Dependence of $g_1/g_1^{H_2O}$ for Alcohol/Water Mixtures at 298K 358

V-24 Composition Dependence of $g_2/g_2^{H_2O}$ for Alcohol/Water Mixtures at 298K 359

V-25 Composition Dependence of $f_1/f_1^{H_2O}$ for Alcohol/Water Mixtures at 298K 360

V-26 Composition Dependence of $f_2/f_2^{H_2O}$ for Alcohol/Water Mixtures at 298K 361

V-27 Composition Dependence of $f_3/f_3^{H_2O}$ for Alcohol/Water Mixtures at 298K 362

I. INTRODUCTION

A. GENERAL

A convenient method of putting electrons into liquids for study is to generate them inside the liquid with a pulse of high energy radiation.

$$M \rightsquigarrow M^{+} + e^{-} \qquad [1]$$

An electron is knocked off a molecule and travels a certain distance away from its "parent ion" before losing all its excess energy. Thus the electron is thrust into the body of the liquid. It loses its excess energy by ionizing and exciting the medium. If the liquid is electrophilic in nature, the slowed-down electron becomes attached to a molecule to form a negative molecular ion. If the electron does not become attached to a molecule, it ultimately reaches a state of thermal equilibrium with the medium. It is then called a "thermalized electron" and may be either quasifree or localized.

Electron localization in a polar liquid is due to a coulombic potential well created by several suitably oriented dipoles (1,2). Localization in a nonpolar liquid such as *n*-hexane (3) is presumably related to the anisotropic polarizability of the molecules.

Two states of localized electrons, in addition to that of direct binding to individual molecules, can be distinguished: the trapped state and the solvated state.

In reaction [i], a bound electron is liberated and set in motion away from the simultaneously produced positive ion (parent ion). As it travels further from the parent ion, it may generate tertiary electrons and so on. The energetic electron loses energy by ionizing as well as by exciting the medium and by suffering electrostatic repulsion. Thus the electron passes over a series of potential energy barriers and loses kinetic energy by interactions with the molecules, until finally it cannot get over the next potential barrier. At this point, it is in a region of relatively low potential energy, that is, in an interstitial position, and it is trapped there by short range repulsive forces.

Using the particle model of an electron, the amount of space occupied by the trapped electron must be sufficiently large that the electron zero-point energy (4) is less than the potential energy of the barrier. On the basis of the charge-cloud model of an electron, the trapped electron can be considered to have most of its charge located in a central cavity with some of the cloud penetrating into adjacent interstitial holes that are connected to the central cavity.

Just before an electron is trapped, its kinetic energy, in regions of low potential energy, has probably been reduced to 1 eV or less. Since electronic polarization of molecules occurs in less than 10^{-15} sec, the trapped electron immediately finds itself in an electronically polarized cavity. The potential well of this cavity deepens as the various types of polarization of the medium occur. There is a balance between the tendency of the internal pressure of the liquid to localize the electron in a small volume and the zero-point energy requirement which tends to enlarge the volume occupied by the electron. The trapped electron is transformed into a solvated electron over a period of about 10^{-12} sec in liquid that has a dielectric relaxation time of 10^{-12} sec. The main difference between the depths of the potential wells of solvated electrons in polar and non-polar liquids is caused by the difference in orientation polarization.

Blue solutions of alkali metals in liquid ammonia were first prepared in 1863 (5), but it was not until 1922 that it was demonstrated that they contained solvated electrons (6,7). Later, solvated electrons were also formed by dissolving alkali metals in certain amines (8), ethers (9), alcohols (10,11), and ice (10). The solvated electrons can be identified by means of their optical absorption spectra.

The absorption spectrum of solvated electrons in liquid ammonia has a very broad and unstructured absorption peak (11). The absorption spectra of solvated electrons in other solvents are very similar to this, but the wavelength of the absorption maximum shifts from one solvent to another (12). The optical absorption spectra have been used to identify the formation of solvated electrons in the radiolysis of water (13), alcohols (14), and even in ethers (15) and hydrocarbons (16,17). The "effective radius" of a solvated electron can be estimated according to its optical absorption energy (1,18).

The thermodynamic data for solvated electrons are not known very accurately. They can therefore be used only with certain reservations for further calculations (19). Nevertheless, the standard potential (20), the solvation energy (18) and entropy (18) of solvated electrons in water have been estimated.

Data on the mobility of solvated electrons can be obtained from conductivity studies of their solutions (21,22). The mobilities of solvated electrons in water (23) and in liquid ammonia (24) are three to five times higher than those of normal ions (e.g., Na^+ (24,25) and Cl^- (25,26). However, the mobility of electrons solvated in water is smaller than that of H^+ (25). In nonpolar liquids, the mobilities depend strongly on the structure of the molecules (27-31).

The solvated electron is paramagnetic in nature. This can be confirmed by ESR (32) and ortho-para hydrogen conversion (19,33) measurements.

Solvated electrons have a strongly negative redox potential (20). They can react with many substances such as :

(1) liquid water (34) or alcohols (35);

(2) simple neutral molecules of oxygen (36), iodine (37), carbon monoxide and carbon dioxide (38), nitrous oxide and nitrogen oxide (39), hydrogen peroxide (40), and tetranitromethane (41);

(3) cations of metal ions, e.g., silver I (36,39), cadmium II (36,42), copper II (36,40), lanthanum III (37);

(4) anions of oxo metals, e.g., permanganate and dichromate (37), as well as the oxo anions of nitrogen, nitrous ion (37), of bromine, bromate (42), of chlorine, chlorate (37);

(5) aliphatic compounds of olefins, aldehydes, and ketones (38, 39, 42, 43), and of halogenated hydrocarbons and fatty acids (except fluorinated compounds) (44);

(6) aromatic compounds of benzene, aniline, napthalene, anthracene, biphenyl, and terphenyl (43-46);

(7) heterocyclic compounds of pyridine, uracil, thymine and adenosine (43).

The two physical properties that have been useful in giving information about the behavior of solvated electrons have been the optical absorption spectrum and the mobility. The values of these two properties are understood qualitatively, but their variations with molecular structure have not yet been completely explained (31,47).

B. HISTORICAL

1. Solvated Electrons in Pure Liquids

It is about sixty years since Kraus (48) suggested that solvated electrons were produced when alkali metals were dissolved in liquid ammonia, and it is nearly twenty years since Stein (49) and Platzman (50) postulated that solvated electrons were formed when water is subjected to ionizing radiation. In 1962 the optical absorption spectrum of solvated electrons in irradiated water was first observed by Hart and Boag (13,51).

The spectrum of the solvated electron in water

(13,51-58), as well as in ammonia (59-83), aliphatic alcohols (10,14,84-110), amines (12,69,72,98,99, 105, 111-119), ethers (12,15,17,69,98,99,113,120-127), aliphatic hydrocarbons (98,122,128-148), and other organic liquids (69,111,149-155), has since then been investigated very extensively.

At room temperature, the absorption spectrum of the solvated electron in these compounds has several features in common:

(i) it has a single, broad, structureless band;

(ii) the plot of absorbance vs wavelength is bell-shaped;

(iii) the plot of absorbance vs photon energy (eV) shows an asymmetric shape which is skewed toward high energy.

The behavior of the absorption maximum, E_{Amax}(eV), and of the band width at half the absorption maximum, $W_{\frac{1}{2}}$(eV), in different solvents is as follows.

In all the solvents, E_{Amax} decreases with increasing temperature. For water, the temperature coefficient is from 3.0 to 2.4 meV/K (53,52), whereas the coefficient for ammonia is between 2.7 and 1.4 meV/K (67,81,82), depending on the temperature range of the study. In alcohols (105), amines (69) and ethers (125) the coefficient differs for particular compounds in each category.

The behavior of $W_{½}$ is much more variable. $W_{½}$ increases slightly with increasing temperature in water (52-54) and liquid propane (144). It decreases slightly in ethers (17,18). In alcohols (95,105) and amines (114), $W_{½}$ behaves differently depending on the particular compound. The temperature coefficient in almost all cases is less than 1.0 meV/K, although for 2-methyl-n-amylamine (2-MAA), it is as high as 3.4 meV/K (114). The asymmetry of the absorption spectrum decreases with increasing temperature.

At constant temperature, for organic solvents, the value of E_{Amax} depends upon:

(i) type of alkyl group, e.g., 1.65 for cyclohexanol and 1.83 for n-hexanol (91,97), 1.94 for n-butanol (85,86), 1.67 for s-butanol (91) and 1.08 for t-butanol (84,85,89,91,97); 1.29 for 2-methyl-1-propylamine (98) and 1.08 for 1-methyl-1-propylamine (98,114); 1.76 for ethanol (14,84,86,91,93,104,106,108), 1.93 for n-propanol (84,85), 1.94 for n-butanol (85,86), 1.97 for methanol (14,84,86,87,91,92,97,104,108); and 0.91 for 3-methyl-3-pentanol (91,97) and 0.82 for 3-ethyl-3-pentanol (91);

(ii) number of alkyl groups attached to the functional group, e.g., 1.76 for ethanol (14,84,86,91,93,97, 104,106,108), 0.59 for diethylether (17,69) and 1.29 for isobutylamine (98), 0.83 for diisopropyl amine (98,114), and 0.74 for tripropylamine (114);

(iii) number of functional groups, e.g., 1.93, 2.17 and 2.31 for 1-propanol, 1,2-propanediol and 1,2,3-propanetriol, respectively (84,85); 0.69 for ethylamine (69,111,117) and 0.94 for ethylenediamine (69,72,95).

Differences in E_{Amax} and in $W_{\frac{1}{2}}$ are observed for electrons in liquids of contrasting polarity. Electrons in polar solvents such as ammonia, water, and alcohols show an absorption maximum in the visible to near infrared region. In non-polar solvents such as aliphatic hydrocarbons, the maximum is in the infrared region. Weakly polar solvents, for instance ethers and amines, yield a maximum in between those for polar and non-polar solvents. In addition, there is an overlap in the region of absorption maxima of polar and weak-polar compounds as well as of non-polar and weak-polar compounds. For organic compounds, the overlap is due either to the type of alkyl group in the carbon chain skelton or to the number of alkyl groups attached to the functional group and to the number of functional groups contained in the compound. Hence it is due either to the steric effects or to the inductive effects and to the over-all effects of these two. $W_{\frac{1}{2}}$ tends to be narrower with increasing polarity of the compounds with the same category.

2. Solvated Electrons in Binary Mixtures

The nature of the absorption spectrum of solvated electrons in binary liquids and the dependence of absorption maximum upon the composition of such systems are now known for a variety of compounds (12,17,72,91, 97,105,112,120,122,152,156-175).

At room temperature, the absorption spectum in a binary system exhibits a single absorption band with a maximum that is intermediate to the maxima in the pure components. The value of E_{Amax} varies continuously with composition between the two limits. The composition dependence of E_{Amax} and of $W_{\frac{1}{2}}$ exhibits a very broad range of behavior which is due primarily to the molecular structure and polarity of the components and to the molecular interaction of the two components.

At temperatures low enough, some of these binary mixtures become glassy in nature. In this glassy state, the absorption spectrum of the solvated electron shows either one or two peaks depending upon the polarity of the components. For components of similar polarity, the spectrum behaves as for mixtures at room temperature. When the components have different polarity, the spectrum possesses two peaks, similar to those in the pure components.

The behavior of E_{Amax} as a function of composition in these studies is as follows.

(i) For mixtures of two strongly polar liquids A and B, and of a strongly polar with a moderately or weakly polar liquid, three patterns have been observed:

(a) E_{Amax} increases in an S-shaped manner from 0 to 100 mol % B, as in ethylenediamine (EDA)/water (72), ammonia/water (12,72,156), triethylamine (TEA)/ethanol, 1,2-propanediamine (1,2-PDA)/TEA; sec-butylamine (s-BuA)/ethanol and diisopropylamine (DIPA)/ethanol (168);

(b) E_{Amax} increases or decreases up to a certain point, then changes very little to pure B, as in methanol/water and 2-propanol/water (105), tetrahydrofuran (THF)/water (12,17,112), hexamethylphosphoric triamide (HMPTA)/EDA (152,175), dioxane/water and HMPTA/water (159);

(c) E_{Amax} changes almost linearly, as in methanol/2-propanol (105) and THF/EDA (12). Besides, the degradation of (b) and (c) has been observed in dimethylsulfoxide (DMSO)/water (160), diethylether (DEE)/EDA and 2-methyltetrahydrofuran (MTHF)/EDA (17).

(ii) For mixtures of two moderately or weakly polar liquids and of a nonpolar liquid with a polar liquid, pattern (i)-(b) has been observed in 3-methylpentane (3-MP)/methanol (17), _s_-BuA/TEA, MTHF/TEA, 3-MP/_s_-BuA, and 3-MP/MTHF (168).

$W_{\frac{1}{2}}$ behaves similarly to E_{Amax} in most cases.

C. THEORY

In this section, an outline will be given of a number of models commonly used in the treatment of E_{Amax} and $W_{\frac{1}{2}}$ as well as the temperature coefficient of these two. The common basis of formulation for each model will be described briefly first.

The general form of the Hamiltonian, H_T, for the system consisting of a dielectric medium and an excess electron can be expressed as (1,176)

$$H_T = T_n + H_m + T_e + \sum_i v_{ei} + \sum_n v_{en} \qquad [1]$$

T_n is the kinetic energy of the nuclei. H_m represents the Hamiltonian of the medium in the absence of the excess electron at fixed nuclear configuration.

$$H_m = \frac{-h^2}{8\pi^2 m}\sum_i \nabla^2_{r_i} - \sum_{n,i} \frac{Z_n e^2}{|r_i - r_n|} + \sum_{n<m} \frac{Z_n Z_m e^2}{|r_n - r_m|}$$

$$+ \sum_{i<j} \frac{e^2}{|r_i - r_j|} \qquad [2]$$

where h is Planck's constant, m is the mass of electron, ∇^2 is the Laplacian operator, r_i and r_j represent the coordinates of the medium electrons, r_n and r_m are the coordinates of the medium of the charges Z_n and Z_m. T_e is the kinetic energy of the excess electron, the coordinates of the electron being represented by r_e.

$$T_e = \frac{-h^2}{8\pi^2 m} \nabla^2_{r_e} \qquad [3]$$

v_{ei} and v_{en} represent the interaction energies between the excess electron and a medium electron i or a medium nucleus n; thus

$$v_{ei} = \frac{e^2}{|r_i - r_e|} \qquad [4]$$

$$v_{en} = \frac{-Z_n e^2}{|r_e - r_n|} \qquad [5]$$

The Hamiltonian of the medium, H'_m, is then given by

$$H'_m = H_m + \sum_i v_{ei} + \sum_n v_{en} \qquad [6]$$

and consists of the unperturbed energy and the energy part due to interaction.

Thus, setting

$$H_T = T_n + H'_m + T_e = T_n + H' \qquad [7]$$

the total energy, E_T, of the system can be obtained from the equation

$$H_T|N,e\rangle = E_T|N,e\rangle \qquad [8]$$

where $|N,e\rangle$ is short hand for the eigenfunction of this system. By applying the Born-Oppenheimer approximation (177), this eigenfunction can be separated in the form

$$|N,e\rangle = |N\rangle|e\rangle \qquad [9]$$

where $|N\rangle$ is the nuclear part of the wave function, and $|e\rangle$ is the electronic part of the wave function and depends on the nuclear coordinates, r_n, as parameters. The electronic part can be obtained from the equation

$$H'|e\rangle = E_e(r_n)|e\rangle \qquad [10]$$

while the total energy of the system can be obtained from the expression

$$(T_n + E_e(r_n) - E_T)|N> = 0 \qquad [11]$$

For simplicity, it is convenient to consider the limiting case of infinitely heavy nuclei, when nuclear vibrations can be neglected. The total energy of the system can then be obtained from the condition

$$\frac{\partial E_e(r_n)}{\partial r_n} = 0 \quad \text{for all } r_n \qquad [12]$$

Since equation [10] can not be accurately solved, approximate treatments of the electronic wave function must be applied by using either the adiabatic or the independent-particle self-consistent-field (SCF) approach.

In the adiabatic scheme, the medium electrons are assumed to be affected by a potential of a fixed point charge, excess electron, that is considered to be temporarily at rest. Thus, the electronic wave function, $|e>$, can be formulated in the form

$$|e> = |e_m>|e_a> \qquad [13]$$

$|e_m>$ is the wave function of the medium electrons and depends parametrically on the position r_e of the excess electron.

$|e_a>$ is the wave function of the excess electron. The $|e_m>$ can then be obtained from

$$H_m|e_m> = \varepsilon_e(r_e,r_n)|e_m> \qquad [14]$$

The total energy of fixed nuclear configuration will be obtained from

$$[T_e + \varepsilon_e(r_e,r_n)]|e_a> = E_e(r_n)|e_a> \qquad [15]$$

along with equation [12].

$$\text{Let } \varepsilon_e(r_e,r_n) = U_o + U(P_e,P_D,E_c), \qquad [16]$$

U_o be the unperturbed energy of the unpolarized medium, E_c be the field produced in vacuum by the point sources at r_e, P_e be the electronic component of the polarization, P_D be the permanent polarization, and U represent the polarization energy of the medium. Then the total energy of the system can be obtained from

$$E_T = E_e(r_n) = <e_a|T_e + U|e_a> + U_o \qquad [17]$$

For the independent-particle approximation, the medium electrons are considered to be affected by only the mean charge distribution of the excess electron. Thus, the electronic wave function, $|e>$, can be formulated as

$$|e> = |e'_m>|e_a> \qquad [18]$$

$|e'_m>$ is the wave function of the medium electrons and does not depend parametrically on the position r_e of the excess electron. The electronic energy will be represented in the form

$$E_e(r_n) = <e'_m|<e_a|H'|e'_m>|e_a> \qquad [19]$$

and the total energy of the system can be obtained from

$$E_T \simeq E_e(r_n) = <e_a|T_e|e_a> + <e'_m|H'_m|e'_m> \qquad [20]$$

$$H'_m = H_m + <e_a|\sum_i v_{ei} + \sum_n v_{en}|e_a> \qquad [21]$$

H'_m is determined by the average charge distribution of the excess electron.

It is assumed that the s spin orbitals of the medium electrons can be represented by the appropriate SCF wave function. Hence, the total energy of the system can be obtained from

$$E_T \simeq E_e(r_n) = <e_a|T_e|e_a> + U(P_e,P_D,E_c) + U_o \qquad [22]$$

where U represents the polarization energy of the dielectric medium by the mean charge distribution $e|<e_a|e_a>|^2$, of the excess electron.

The basic difference between these two approaches arises from the fact that, in the SCF scheme, the electronic polarization does contribute to the binding energy of the electron.

It can be seen that the main task is how to formulate U, U_o and V(r) and to construct $|e_a>$. This differs from one model to another. Once this has been accomplished, the ground state and excited state electronic energy of the solvated electron can then be obtained as

$$E_e(n\ell) = <n\ell|H|n\ell>/<n\ell|n\ell> \qquad [23]$$

where

$$H = \frac{-h^2}{8\pi^2 m} \nabla^2 + V(r) \qquad [24]$$

and n and ℓ refer to the quantum numbers of the electronic state. The E_{Amax} and hence its temperature coefficient can then be obtained from

$$E_{Amax} = E_e(2p) - E_e(1s) \qquad [25]$$

The $W_{\frac{1}{2}}$ and its temperature coefficient are treated qualitatively within the constraints of each model, or treated separately.

1. The Polaron Model

Landau (178) proposed that an excess electron can be trapped by polarization of the dielectric medium caused by the electron itself. This idea was mathematically formulated in the work of Pekar (179), who used the term "polaron" for the state of an electron bound by the polarized medium. Davydov (180) and Deigen (181) applied this to electrons trapped in ionic lattices. The electron is treated as free except for its interaction with the medium. If r is the distance from the trapping site, then the potential energy, V(r), resulting from this interaction is

$$V(r) = -De^2/r \qquad [26]$$

$$D = 1/D_{op} - 1/D_{st} \qquad [27]$$

D_{op} is the optical (high frequency) dielectric constant.
D_{st} is the static (low frequency) dielectric constant.

Considering V(r) invariant under transition, Davydov and Deigen derived an equation for E_{Amax} (eV) of the solvated electrons in ammonia as

$$E_{Amax} = E(2p) - E(1s) = 1.93\ D^2(m^*/m) \qquad [28]$$

E(1s) is the energy of the electron in the ground state.
E(2p) is the energy of the electron in the excited state.
m^*/m is the ratio of the effective mass, m^*, of the electron in the liquid to its mass, m, in the free state, and is an unknown parameter.

Jortner (1), taking the electronic polarization into consideration, revised equation [28] as

$$E_{Amax} = [1.93\ D^2 + 1.37\ D(1 - 1/D_{op})](m^*/m) \qquad [29]$$

The correlation of E_{Amax} with this model has been carried out by Dorfman and coworkers (14,108) using $m^*/m = 3.6$. The agreement is quite good for methanol, ethanol, 1-propanol, and 2-propanol, but is poor for water and ammonia.

Mukhomorov et al. (182-184), taking into account fluctuation in the orientational polarization of the medium and using the effective mass method, formulated m^* as a function of temperature as follows

$$\frac{1}{m^*}\left(\frac{dm^*}{dT}\right)_p = -\frac{2}{3}\beta_o \qquad [30]$$

where β_o is the thermodynamic expansion coefficient of the medium. Thus, equation [28] is then revised as

$$E_{Amax} = D_1(m^*/m)(0.805 + 1.138\ D_2/D_1) \qquad [31]$$

with $D_1 = 1 - 1/D_{st}$ and $D_2 = 1/n^2 - 1/D_{st}$

where n is the refractive index of the medium. They also derived the dispersion of the optical spectral band as

$$W_d^{\,2} = 2.69 \times 10^{-3}\ T\ D_2^{\,2} m^*/m[1 + 1.2(D_2/D_1)^2] \qquad [32]$$

and

$$W_{\frac{1}{2}} = (W_d^{\,2})^{\frac{1}{2}} \qquad [33]$$

Thus, the effect of temperature on the E_{Amax} and $W_{\frac{1}{2}}$

can be quantitatively estimated from equations [31] and [32]. A satisfactory agreement between calculated and observed is obtained for water (55, 185), ammonia (78, 186,187), and methanol (185,186).

Bush and Funabashi (188) have proposed two types of traps based on small-polaron formation (189) to account for studies of solvated electrons in alcohol aggregates at low temperature. They assumed that the alkane region forms relatively shallow traps, and the OH region forms deeper ones. They also assumed that there are inhomogeneities within each region, so that, for instance, the depth of a trap at the end of an OH chain will be different from the depth of a trap at the center of a chain. Sophisticated equations have been formulated to simulate the shape of the absorption spectra of solvated electrons. The calculated and observed curves (92) are in good agreement for both E_{Amax} and $W_{\frac{1}{2}}$, but not the shape.

Borisenko and Vannikov (190) applied this alternative two traps model to solvated electrons in the glassy state of 2-propanol. The generated curve fits the experimental one satisfactorily.

2. The Cavity Model

Ogg (7) proposed that the excess electrons in liquid ammonia are self-trapped in physical cavities created in the solvent medium. The potential energy is considered to be independent of surface tension and to be a symmetrical distribution in a spherical cavity of radius r_o, as

$$V(r) = \begin{cases} -Z^2e^2/2r_o & , \quad r \leq r_o \\ 0 & , \quad r > r_o \end{cases} \qquad [31]$$

where r is the distance away from the cavity center. The total energy, E_t, is found to be

$$E_t = h^2/8mr_o^{\,2} - e^2/2r_o \qquad [35]$$

This simple treatment leads to a serious overestimate of the cavity radius. This has been refined by Lipscomb (191) taking into consideration the surface tension, electrostriction, and the electronic polarization of the molecules on the cavity surface, i.e.,

$$E_t = h^2/8mr_o^{\,2} - 0.69\ e^2/r_o + 4\pi r_o^2\gamma \qquad [36]$$

where γ is the surface tension. In order to have a good agreement with observed values of E_{Amax} and r_o, there is a difficulty to choose the proper γ without losing the stability of the cavity.

This difficulty has been further eliminated by Stairs (192), who made a better estimate of the wave functions using a graphical integration method.

Symons and coworkers (193-196) assumed that the electron moves in a discrete centrosymmetrical orbit with a square-well potential of

$$V(r) = \begin{cases} 0 & , \; r \leq r_o \\ \infty & , \; r > r_o \end{cases} \qquad [37]$$

The optical transition is considered to be of the $2p \leftarrow 1s$ type, under invariance of potential energy. The transition is thus determined solely by the kinetic energy of the electron in the ground state. Therefore,

$$E_{Amax} = h^2/8mr_o^2 \qquad [38]$$

This model can provide a qualitative explanation of the observed shape of the solvated electron absorption spectrum, as well as the temperature dependence of E_{Amax} and $W_{\frac{1}{2}}$. The spectrum is considered to be an envelope resulting from many independent optical transitions of electrons in cavities of different sizes. This variability determines the broadness of the spectrum. The asymmetry of the spectrum is then due to the lower probability of transitions to higher excited states. The behavior of E_{Amax} as a function of temperature can be interpreted as resulting from the contracting of the cavity with decreasing temperature, i.e., $dr_o/dT > 0$. Therefore, $dE_{Amax}/dT < 0$. The temperature dependence of $W_{\frac{1}{2}}$ is considered to be due to the breathing vibration of the cavity with changing temperature.

Ishimura, et al., (197) refined the cavity model by considering that the cavity is formed by four or six solvent molecules, and by using the unrestricted open shell treatment (198) based on the intermediate neglect of differential overlap (INDO) approximation (199), to investigate the solvated electron in water, ammonia, and hydrogen fluoride. The calculated values of E_{Amax} for water and ammonia are reasonably in agreement with observed values (74,200).

Recently, the cavity model has been modified by Banerjee and Simons (147) using the Fourier transform of the time-correlation function (201) of the electronic dipole moment to formulate the absorption band shape function. The time dependence appearing in the dipole correlation function is described in terms of both excess electronic motion and solvent molecule motion. The absorption band shape function is expressed in terms of solvent structure information and the electron-solvent interaction potential. The generated band shape for ethanol is in good agreement with the experimental spectrum (92), with respect to E_{Amax}, $W_{\frac{1}{2}}$ and skewedness. For anthracene glass (148), the agreement is good for E_{Amax} and skewedness, but is poor for $W_{\frac{1}{2}}$.

3. The Continuum Model

In Jortner's (202) original work on electrons in ammonia, he modified Landau's potential to allow for a cavity of radius r_o, by solely considering the permanent polarization of the medium,

$$V(r) = \begin{cases} -De^2/r & , \quad r > r_o \\ -De^2/r_o & , \quad r \leq r_o \end{cases} \qquad [39]$$

The electron energy in this potential field can be obtained by

$$E_e(n\ell) = \langle n\ell | (-h^2/8\pi^2 m)\nabla^2 + V(r) | n\ell \rangle \qquad [40]$$

The E_{Amax} can be calculated from

$$E_{Amax} = E_e(2p) - E_e(1s) \qquad [41]$$

considering r_o as an adjustable parameter. The dE_{Amax}/dT can then be obtained by

$$dE_{Amax}/dT = C_1 dD/dT + C_2 dr_o/dT \qquad [42]$$

where C_1 and C_2 are constants, and differ from one system to another. Agreement between the calculated and observed values of E_{Amax} and of dE_{Amax}/dT can be achieved for ammonia (202), but not for water (203) and alcohols (105).

In the case of water, Jortner (176) proposed an alternative approach by treating the excess electron and the medium electrons on an equal basis and by considering the electronic polarization to be contributing to potential formation. The potential energy then becomes

$$V(r) = \begin{cases} e(1 - 1/D_{st})f(r) & , \quad r > r_o \\ e(1-1/D_{st})f(r_o) & ; \quad r \leq r_o \end{cases} \qquad [43]$$

where $\nabla^2 f_{n\ell}(r) = 4\pi e|<n\ell|n>|^2$, since $f_{n\ell}(r)$ is the electrostatic potential due to the average charge distribution, $e|<n\ell|n\ell>|^2$. Again, r_o is considered to be an adjustable parameter. An agreement between the calculated and observed values of E_{Amax} and dE_{Amax}/dT can be achieved for water, when $r_o = 0$. However, this is not realistic (204-206).

This model has been modified by Iguchi (207,208) and by Fueki (209). Iguchi took into account the temperature variation of the dipole moment and volume expansion of the liquid, as well as the dipole-dipole interaction. The results of E_{Amax} and dE_{Amax}/dT are in good agreement with the observed values for alcohols (105). Fueki considered the dielectric saturation effect in the vicinity of the cavity and treated the microscopic dielectric constant as a simple explicit function of distance. The result of E_{Amax} is 3.10 for water, while the experimental is 1.73 (55).

A more elaborate version of the continuum model has been developed by Tachiya et al. (210), taking the orientational polarization as not constant but distributed around the configuration coordinate under which the total energy for the ground state is minimum. For water, the calculated E_{Amax} and $W_{\frac{1}{2}}$ are in relatively good agreement with experimental values.

The validity of the continuum model has been tested by Carmichael and Webster (211), using numerical wave functions for a solvated electron in water and ammonia. The results indicate that the SCF approach, for the particular case of $r_o = 0$, is quite unsuitable.

The continuum model has been modified recently by Funabashi, et al. (212) using the electron transfer concept (213,214), in which the solvated electron is assumed to be coupled with both the low frequency solvent modes and a high-frequency molecular mode, representing the long- and short-range interaction potentials for the electron. The generalized line shape function is then formulated in order to simulate the absorption spectrum of the solvated electron in water. The simulated spectrum consists of contributions from short-distance transfer (bound-bound) and long-distance (bound-free) transfers, the latter being the minor component of the total spectrum. The generated spectrum shape agrees quite well with experimental curves (86) with respect to E_{Amax} and $W_{\frac{1}{2}}$ but not for skewedness.

4. The Semi-Continuum Model

This model is based on the idea proposed by Land and O'Reilly (215,216), in which a few molecules are treated as a discrete solvation layer around the trapping site and the medium beyond must be treated as a continuum. A model developed by Fueki, et al., (FFK Model) (217) was the first one applying this idea to solvated electrons in water. The related work by Copeland, et al., (CKJ Model) (2) was for solvated electrons in ammonia.

In both models, one assumes that the essential feature of the molecule in the first coordination layer is its dipole moment. Thus, the physical ideas for these two formulations are essentially the same, but the details of the calculations, as well as some of the approximations, are different. Essentially, the CKJ Model treats the continuum by the adiabatic approximation, while the FFK Model uses the better SCF version.

The basic coordinates for these two models are given in Figure I-1.

The radius r_v is the void radius of the cavity. The radius r_d is the distance from the center of the

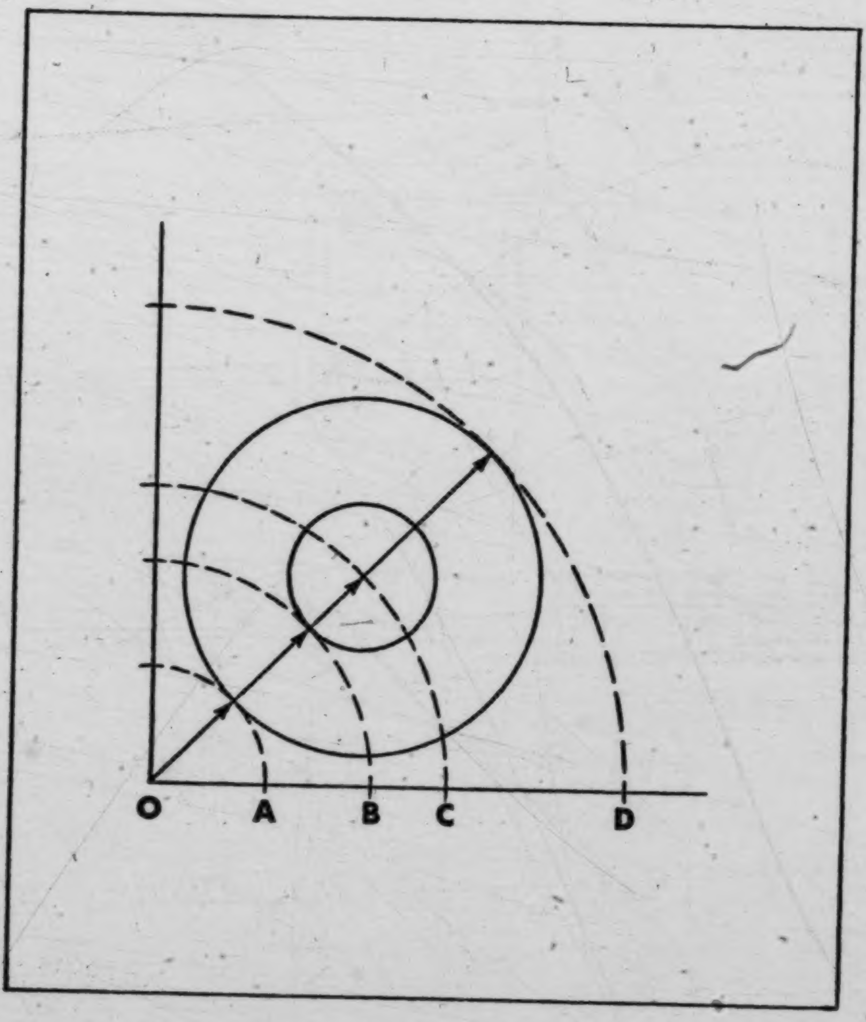

FIGURE I-1. Definition of the Distances Involved in the Semi-Continuum Model.

r_v = OA; R = OB; r_d = OC;

r_c = OD; r_a = BC; r_s = CD

cavity to the center of the molecule (and thus to the dipole), while r_c is the distance from the center of the cavity to the beginning of the continuum beyond the first layer. The r_s is the effective solvent radius, and r_a is the effective hard core of the molecules. R is defined as $r_d - r_a$.

In the FFK Model (107,217,218-226), the solvated electron is considered to interact with a number N of specifically oriented matrix molecule dipoles in the first solvation shell by short-range attractive and repulsive potentials and with the remainder of the matrix molecules beyond the first solvation shell by a long-range polarization potential. Thus, the potential which traps the electron is

$$V(r) = \begin{cases} -Ne\mu/r_d^2 - Ne^2\alpha/2r_d^4 + Af(r_d), & r \leq r_d \\ Af(r) + V_o, & r_d < r \end{cases} \qquad [44]$$

where $A = (e/2)(1 - 1/D_{st})$ and μ and α are the magnitudes of the dipole moment and of the isotropic polarizability, respectively.

$$\mu = \mu_o \langle\cos\theta\rangle \qquad [45]$$

where μ_o is the magnitude of the dipole moment in the gas phase, θ is the angle between the dipole moment vector and the line joining the center of the cavity to the point dipole, and $\langle\cos\theta\rangle$ represents the thermal average of $\cos\theta$ (2). The electrostatic potential f is determined from Poisson's equation (203). V_o is the quasifree electron energy. It is taken to be an adjustable parameter, and is chosen so that the calculated E_{Amax} fits reasonably well with the observed one.

The total energy, $E_T(i)$, of the excess electron in the medium is then given by the sum of the electronic energy, $E_e(i)$, of the electron and the energy necessary to rearrange the medium, $E_M(i)$, because of its interaction with the electron, i.e.,

$$E_T(i) = E_e(i) + E_M(i) \qquad [46]$$

with

$$E_e(i) = E_k(i) + E_e^s(i) + E_q^s(i) + E_e^{\ell}(i) \qquad [47]$$

and

$$E_M(i) = E_m^s(i) + E_m^{\ell}(i) + E_{st} \qquad [48]$$

where i = 1s for ground state; i = 2p for the excited state. E_k is the kinetic energy of the excess electron. E_e^s represents the energy for short-range attractive interactions of the excess electron with point dipoles, while E_q^s represents the energy for short-range repulsion with electrons of the medium. E_e^{ℓ} represents the electronic energy part of long-range polarization interactions, and E_m^{ℓ} represents the medium rearrangement energy portion. E_m^s represents the short range medium rearrangement energy associated with dipole orientation and is a dipole-dipole repulsion term. E_{st} represents the energy required to form a cavity in the medium, and is the surface energy term.

In this FFK Model, the hydrogen-like wave functions using polar coordinates

$$|1s\rangle = A \exp(-ar) \qquad [49]$$

and

$$|2p\rangle = Br \exp(-br) \cos\theta \qquad [50]$$

are employed as eigenfunctions of the ground state and of the excited state respectively, where A and B are normalization factors and a and b are adjustable parameters. The variational procedure is applied to the wave function parameters a and b to obtain the minimum energy for a given r_d. This process is repeated for various r_d to construct configuration coordinate curves and to establish configurational stability. Once this stability has been achieved, the E_{Amax} is then obtained from

$$E_{Amax} = E_T(2p)_\rho - E_T(1s)_\rho \qquad [51]$$

whre $\rho = r_d^o$ is the value of r_d at the configurational minimum of the ground state.

The behavior of E_{Amax} as a function of temperature is considered to be due to the temperature dependence of D_{st}, $\langle\cos\Theta\rangle$, V_o, and μ. The calculated values of E_{Amax} and dE_{Amax}/dT are in reasonable agreement with the observed values, e.g., methanol and ethanol (95), 1-propanol (14,227), and water (55).

In the CKJ Model (2, 228-236), the physical ideas and mathematical formulations are nearly the same as in the FFK Model, except for the following differences (107).

(1) The potential which traps the excess electron:

$$V(r) = \begin{cases} -N\mu e/r_d^{\,2} - \beta e^2/r_c, & 0 < r < R \\ -N\mu e/r_d^{\,2} - \beta e^2/r_c + V_{os}, & R < r < r_d \\ -\beta e^2/r_c + V_{os}, & r_d < r < r_c \\ -\beta e^2/r + V_o, & r_c < r \end{cases} \qquad [52]$$

where V_{os} represents an effective V_o for the first solvation shell and differs from V_o.

(2) The $E_M(i)$:

$$E_M(i) = E_{st} + E_{pv} + E_m^{\,s}(i) + E_m^{\,\ell}(i) + E_{HH} \qquad [53]$$

where E_{pv} represents the pressure volume energy; E_{HH} represents the intermolecular repulsion of the molecules in the first coordination layer and is mainly dominated by the repulsion of hydrogen atoms in most cases.

(3) The potential derived from the SCF approximation (215,216) used for calculating $E_m^{\,\ell}(i)$ is inconsistent with the potential derived from the adiabatic scheme used for calculating the $E_e(i)$.

(4) The temperature coefficient of E_{Amax}:

$$(\partial E_{Amax}/\partial T)_p = (\partial E_{Amax}/\partial T)_\rho + (\partial E_{Amax}/\partial \rho)_T(\partial \rho/\partial_T)_p \quad [54]$$

where ρ represents the density of the medium.

The calculated values of E_{Amax} and dE_{Amax}/dT are in excellent agreement with the observed values for ammonia (74,81,187), although the agreement of $W_{\frac{1}{2}}$ is very poor. In the case of water, the agreement of E_{Amax} (52,53) is very reasonable, but it is quite poor for dE_{Amax}/dT and $W_{\frac{1}{2}}$ (52,53,237).

The validity of a number of assumptions inherent in semi-continuum models, both the CKJ- and FFK-models, has been tested by Webster and Carmichael (238), using numerical solutions of semi-continuum model potentials for a solvated electron in ammonia and in water. The results indicate that the potential representing excess electrons obtained from either the CKJ or FFK models, contains an inadequacy. In particular, the $W_{\frac{1}{2}}$ remains greatly underestimated (55,74). This highlights a basic failure of the proposed models and indicates the need for comparison of any model with a more sensitive property, that is, not with the position of the absorption peak. Static polarizability has been used here by Webster and Carmichael. Neither model even estimates the observed values (239). It appears that this deficiency resides in the coulomb tail associated with the model potentials. They claim that the observed inappropriateness of the coulomb tail has been demonstrated in a number of other studies (239-242).

5. The Molecular Field Model

A number of studies have been made of localized electrons using semi-empirical molecular theories to evaluate the short range electron-solvent interaction. These studies usually consider tetramers such as $(NH_3)_4^-$ or $(H_2O)_4^-$. Some studies have also concentrated on dimer models: $(H_2O)_2^-$ and $(NH_3)_2^-$. These models are formulated in varying degrees of mathematical and conceptual sophistication. The work in these areas includes that of Raff and Phol (244); Natori and Watanabe (245); Natori (246,247); McAloon and Webster (248); Ray (249); Ishimaru and his coworkers (197,250,251); Weissman and Cohan (252,253); Shida et al. (98,99); Naleway and his coworkers (254,255); Howat and Webster (256); Newton (257,258); Tachiya and his coworkers (210,259,260); and Moskowitz et al. (261); Webster (262); Banerjee and Simons (147).

The set of approximate molecular orbital methods employed in these studies includes the ab initio calculation through the approximate theories of INDO, modified intermediate neglect of differential overlap (MINDO), complete neglect of differential overlap version 2 (CNDO/2), complete neglect of differential overlap (CNDO) to extended Hückel and simple Hückel theory.

These studies, although semi-empirical, are able to introduce all the factors which are important in electron-molecule and molecule-molecule interactions in the clusters. They are also capable of considering questions such as optimum orientation of the molecules. These calculations, however, are extremely complicated and it is very difficult to extrapolate the results to other systems.

6. The Two Absorber Model

This model has been proposed by Tuttle (67,263, 264) for studying the behavior of solvated electrons in dilute alkali metal ammonia solutions. Recently, Golden and Tuttle (265) applied this to electrons solvated in binary mixtures of mutually nonreacting polar liquids. The model assumes:

(1) two kinds of solvated electrons in the mixture of solvents S_J *and* S_K*, that correspond to solvated solvent anions* $S_J^-(s)$ *and* $S_K^-(s)$*;*

(2) a chemical equilibrium between solvated electrons and their solvent progenitors, which is described by $S_J^-(s) + S_K \rightleftharpoons$

$S_J + S_K^-(s)$;

(3) a solvated electron absorption band that is an unresolvable composite of intrinsic absorption bands due to $S_J^-(s)$ and $S_K^-(s)$, each of which satisfies Beer's law (ref. 265, p.944).

Under these assumptions, the following formula has been derived

$$\frac{1}{W} \simeq \frac{x_J}{W_J} + \frac{x_K}{W_K} \qquad [55]$$

where W's represent $W_{\frac{1}{2}}$ in the mixtures and in the pure solvents and the x's correspond to the relative mole fractions of $S_J^-(s)$ and $S_K^-(s)$ in the mixtures.

The calculated values of $W_{\frac{1}{2}}$ fit reasonably well for THF/EDA (12) and EDA/HMPTA (175). However, this model fails to account for the behavior of $W_{\frac{1}{2}}$ as a function of composition in water/ammonia (72).

D. The Present Study

Electrons are strongly solvated by hydroxylic solvents and weakly solvated by nonpolar solvents. In a mixed solvent comprised of an alkane and an alcohol, the absorption spectrum is mainly dominated by the latter. The purpose of the present work was to look for more subtle effects in a mixture of two hydroxylic solvents. Both composition and temperature were varied.

Measurements were made of the optical absorption parameters E_{Amax}, $W_{\frac{1}{2}}$, W_r and W_b in C_1 to C_4 aliphatic alcohols mixed with water.

II. EXPERIMENTAL

A. Materials

Water from the laboratory distilled water supply was distilled thrice more from acidic dichromate, alkaline permanganate, then without additive, in a Pyrex triple reflux-distillation unit. The final collection flask was protected from the laboratory atmosphere by a U-tube and bubbler containing distilled water.

The methanol was spectrophotometric reagent grade from Baker Chemical Co.; ethanol was absolute reagent grade from U. S. Industrial Chemical Co.; _n_-propanol, certified grade, Matheson, Coleman and Bell Co.; iso-propanol, spectrophotometric grade, Aldrich Chemical Co.; 1-butanol, spectranalyzed grade, Fisher Scientific Co.; 2-butanol, analytical reagent grade, BDH Chemical Co,; iso-butanol(2-methyl-1-propanol), spectranalyzed grade, Fisher Scientific Co.; _t_-butanol(2-methyl-2-propanol), analytical reagent grade, BDH Chemical Co.

Ethanol was used without further purification because of its exceptionally high purity (266). The other alcohols were further purified as follows. To one liter of alcohol was added one gram of sodium borohydride (Terochem Laboratories Ltd.). The purification was carried out in an apparatus constructed of Pyrex, with grease free ground glass joints. The solution was gently bubbled with Ultra High Purity (UHP) argon

(Matheson Co.), and was refluxed for one day at 5K below its boiling point. The alcohol was then distilled through an 85 cm (length) x 2 cm (inner diameter - i.d.) column packed for 65 cm (length) with 3 mm (i.d.) glass helices. About 90% of the distillate was collected. About 2 grams of freshly cut sodium, washed with the appropriate alcohol, was added to the distillate. The solution was refluxed for another day under UHP argon atmosphere. The alcohol was then fractionally distilled through the column mentioned before. Receivers were rinsed several times with fresh distillate before being used to collect the middle fraction. Treated alcohols were stored under UHP argon atmosphere in Pyrex flasks with stoppers wrapped with Teflon tape. Contact with oxygen or moisture was avoided by fitting the flask with a Pyrex syphon and a gas bubbler, and applying several pounds of UHP argon pressure. Alcohol was obtained by opening a Teflon stopcock on the syphon tubing.

B. Apparatus

1. The Sample Cells

Cells of Suprasil quartz from Pyrocell Manufacturing Company were used at atmospheric pressure for different temperatures. They were of 1.0 x 1.0 x 4.5 cm^3 inside dimensions giving an optical path length of 1.0 cm. The cell was topped by a graded seal so that it could be attached to a Pyrex glass tubing. Different cell designs are illustrated in Figure II-1.

Cells of type (a) were used for dosimetry by using 5 mM KCNS aqueous solution saturated with oxygen. The Pyrex/Teflon stopcocks (No. 1782, Canadian Laboratory Supplies Ltd.) provided a good seal at room temperature, but leaked when the temperature was changed a large amount. Cells of type (b) were used for all temperature studies. The technique for sealing these cells is described in section one of part C (Techniques) in this chapter.

2. The Bubbling Systems

Samples in quartz cells were UHP argon bubbled. The UHP argon bubbling manifold is shown in Figure II-2. A regulator controlled argon pressure at 6 psi. Heavy wall rubber tubing (1/4" i.d. x 1/8" wall thickness) connected the regulator to a column of oxysorb 'G' which removed oxygen from the argon. The main manifold was of Pyrex glass. Pyrex/Teflon stopcocks (No. 7282, Canadian Laboratory Supplies Ltd.) controlled the gas flow through the stainless steel needles (8" long x 0.025" i.d.).

3. The Irradiation, Detection and Control System

Figure II-3 shows this system.

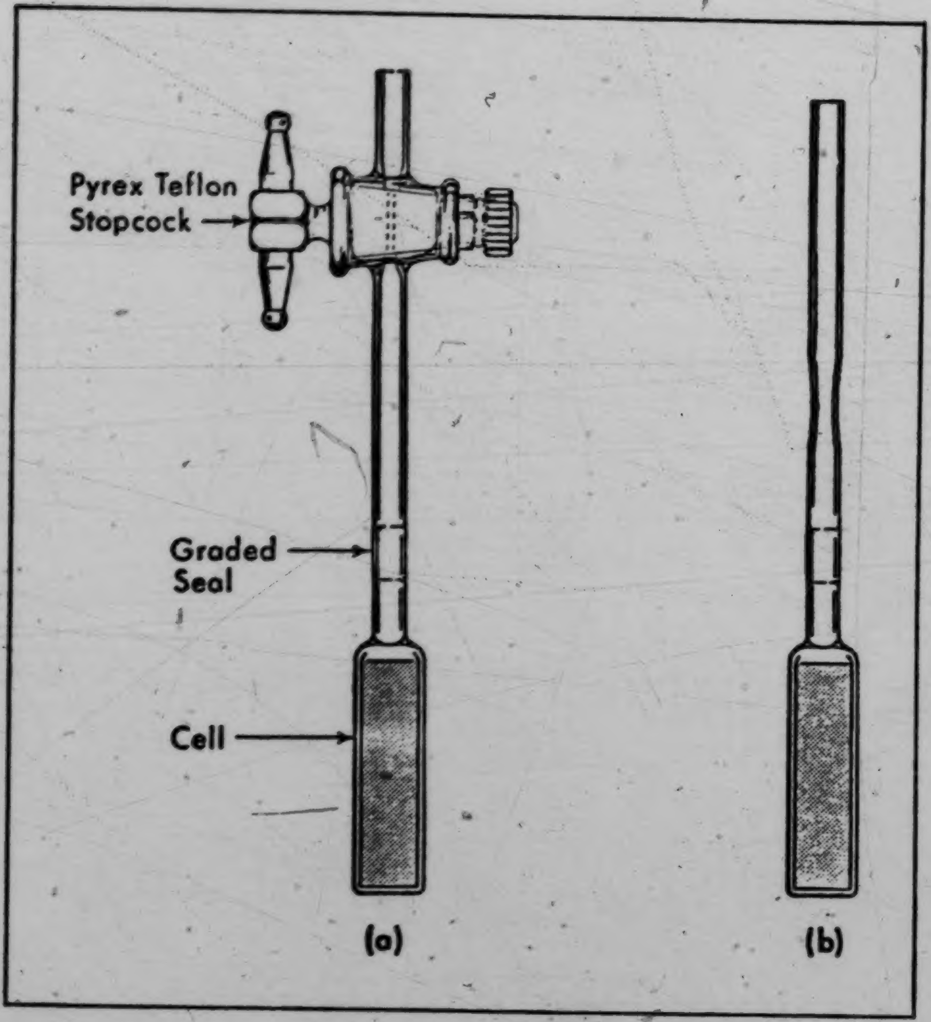
Pyrex Teflon Stopcock
Graded Seal
Cell
(a)
(b)

FIGURE II-1 Suprasil Quartz Optical Cells

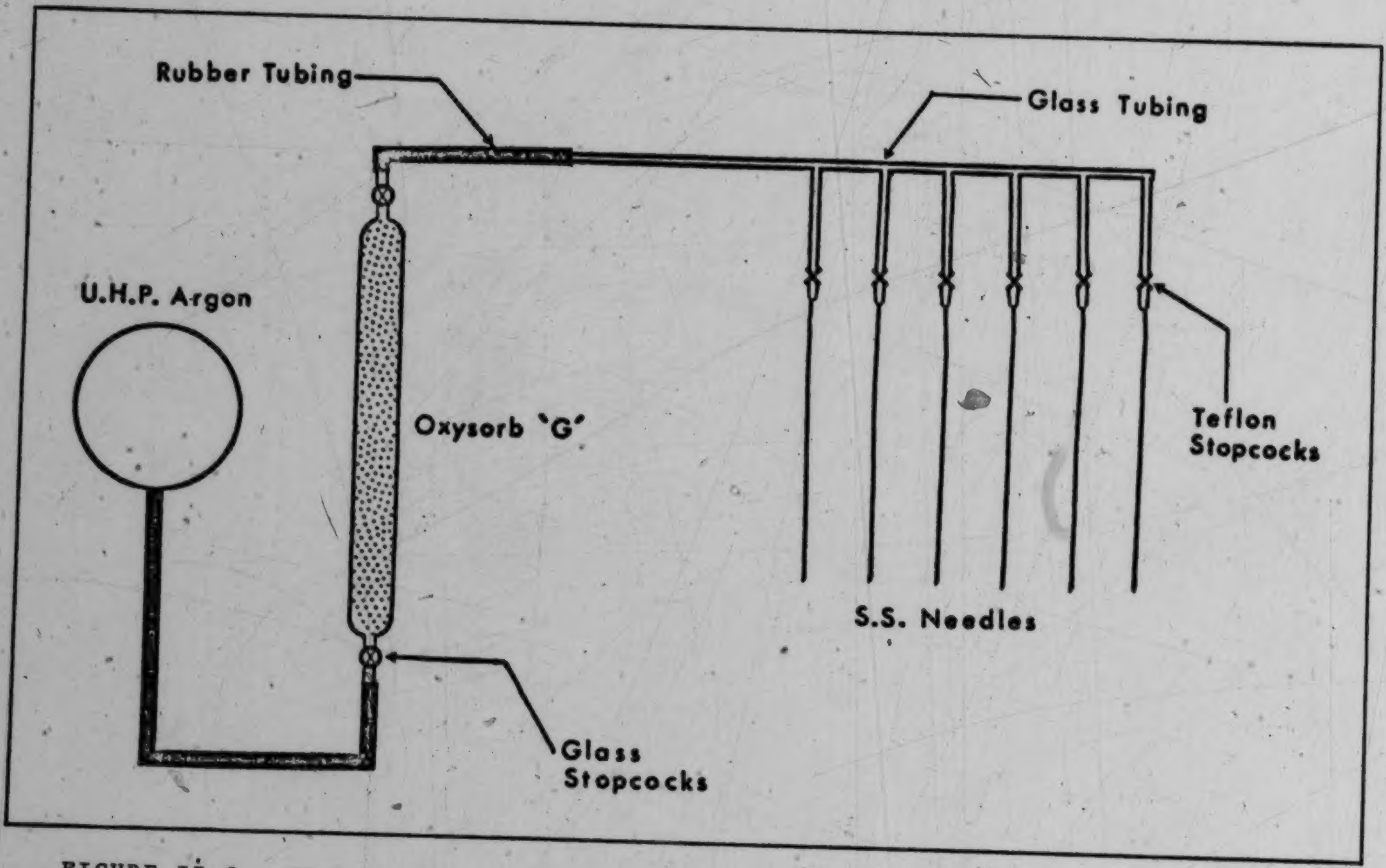
Rubber Tubing
Glass Tubing
U.H.P. Argon
Oxysorb 'G'
Teflon Stopcocks
S.S. Needles
Glass Stopcocks

FIGURE II-2. The Sample Bubbler Manifold for Use with Quartz Cells

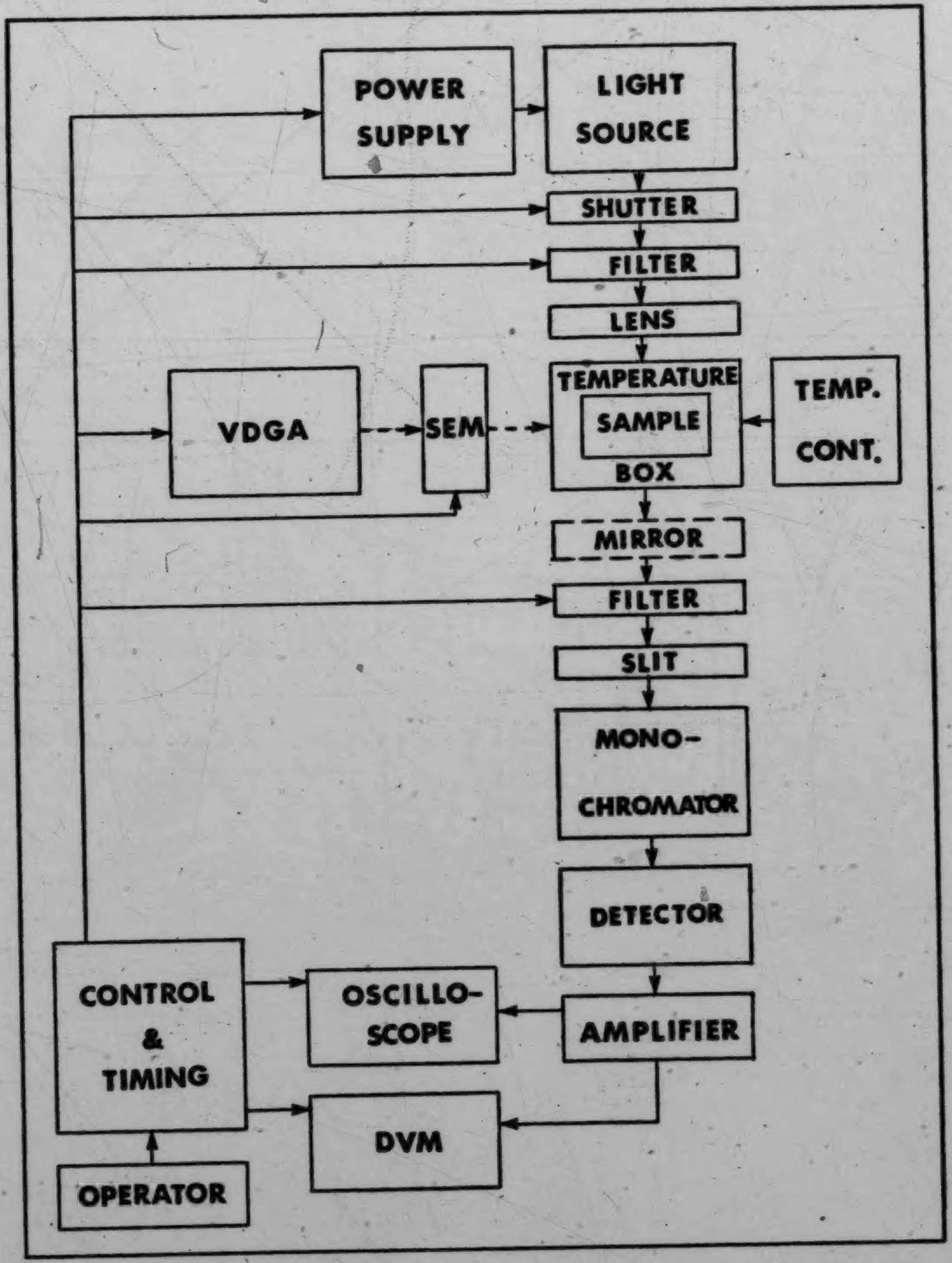
POWER SUPPLY
LIGHT SOURCE
SHUTTER
FILTER
LENS
VDGA
SEM
TEMPERATURE
SAMPLE
BOX
TEMP. CONT.
MIRROR
FILTER
SLIT
MONO-CHROMATOR
DETECTOR
CONTROL & TIMING
OSCILLO-SCOPE
AMPLIFIER
DVM
OPERATOR

FIGURE II-3. The Block Diagram of Optical Detection System.

(a) The van de Graaff Accelerator (VDGA)

The source of high energy electrons was a Type AK-60 2.0 MeV van de Graaff Accelerator (VDGA) manufactured by High Voltage Engineering Corporation. The maximum peak current delivered during pulsed operation was 130 mA. Pulse lengths of 3, 10, 30, 100 nanoseconds (ns) and 1.0 microsecond (μs) were available, but only the two longest pulses provided useful doses.

The entrance from the control room to the accelerator and target rooms was shielded by a concrete maze. Closing and locking the iron gate at the control room end of the maze sounded a warning buzzer for 15 seconds (s). Accelerator operation was possible only after cessation of the buzzer. Opening of the iron gate resulted in immediate shut-down of the VDGA.

Several methods could be used to monitor the steering and focussing of the electron beam. The method commonly used was to fix a piece of phosphorescent paper to the end of the accelerator beam pipe. The paper could be viewed on closed circuit television. Each pulse of electrons caused a visible glow where it struck the phosphor, enabling accurate steering and focussing by adjustment of current to electromagnets. When equipment blocked visual observation, the beam could be steered by maximizing either the secondary emission monitor (SEM) dose (see next section) or the absorption from a dummy sample.

Typical beam diameter at the electron window (see part b of this section) was 2.5 cm, with the most intense portion confined to an area of about 1 cm^2.

(b) The Secondary Emission Monitor (SEM)

The relative dose for each electron pulse was indicated by a SEM (267). The SEM consisted of three thin metal foils placed inside the accelerator beam pipe perpendicular to the path of the high energy electrons. As shown in Figure II-4, the SEM was positioned as near as possible to the beam pipe electron window, because of beam scattering at the foils.

Aluminum (0.001" thick) was originally used for the foils. However, the emission characteristics changed with time, probably due to slow surface oxidation of the foils. The secondary emission was also found to depend on beam current density.

Use of Havar, a cobalt base high strength alloy, overcame these problems. It was obtained in very thin (0.0001") sheets from the Hamilton Watch Company, Precision Metal Division. The low average atomic number (At. No. about 27) of this material made it superior to gold (At. No. 79) because of less beam attenuation through electron scattering.

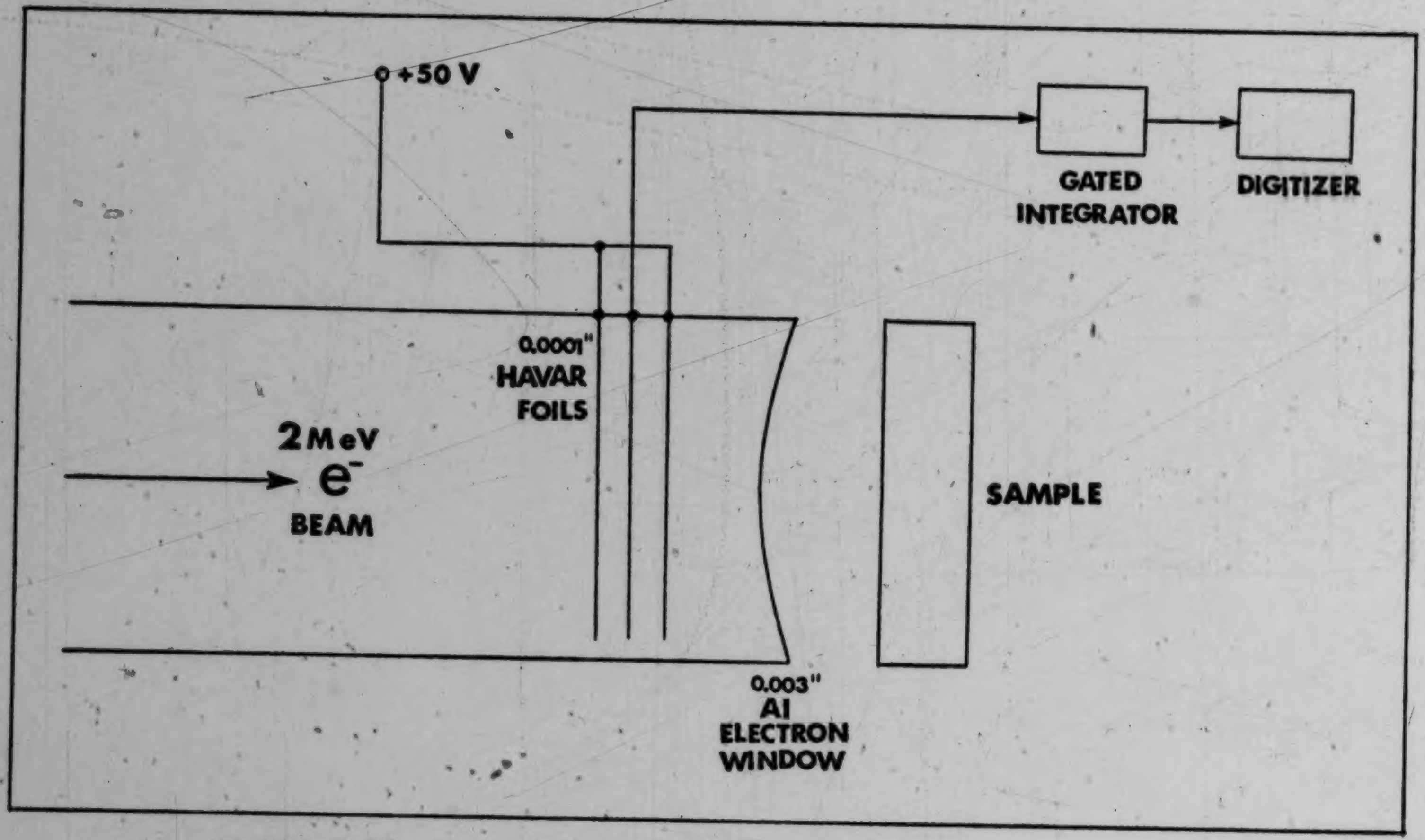
+50 V
GATED INTEGRATOR
DIGITIZER
0.0001" HAVAR FOILS
2 MeV
e⁻
BEAM
SAMPLE
0.003" Al ELECTRON WINDOW

FIGURE II-4 The Secondary Emission Monitor (SEM)

The 2" diameter foils were separated by 0.5 cm. The outer two were maintained at a potential of +50 V. Passage of an electron pulse generated secondary electrons. The electrons ejected from the centre foil were collected by the outer foils, the net result being a current flow from the centre foil.

Current flow occurred only during a high energy electron pulse and was measured and held by a gated integrator, digitized and displayed by a digital readout.

The SEM dose for 1.0 and 0.1 μs electron pulses was 4.4% of the primary electron dose measured as a current from a gold target fixed to the beam pipe electron window. The ratio of SEM to target dose could be varied ± 7% by changing beam steering and/or focussing.

Actinometry in situ was used to calibrate the SEM as a secondary dosimeter as explained in Section D Part b.

(c) The Temperature Control System

Temperatures from 296K to 150K could be achieved by boiling liquid nitrogen at a controlled rate from a 50 liter, wide necked steel Dewar vessel (Sulfrian Cryogenics Inc.). A poly-vinyl chloride (PVC) pipe (2.5" i.d.) extended to the bottom of the Dewar. It was notched at the base to allow liquid nitrogen to flow in, and it was fixed to a lid which fit snugly into the neck of the Dewar. The system could be filled with liquid nitrogen while in use through a hole in the lid. A 1000 W nichrome wire coil was attached inside the PVC pipe about 7 cm from the bottom.

Cold nitrogen gas was transported to the sample box through one meter of brass pipe (0.5" i.d.). The pipe was insulated by a layer of sponge rubber tubing (0.6" i.d. x 0.5" wall thickness) and a layer of Styrofoam 3 cm thick.

Temperatures from 296K to 370K were obtained using hot air from a modified laboratory heat gun (Master Appliance Corporation, Model AH0751). Current to the heating coil and the fan motor could be individually controlled. The fan speed was powered from a normal 60 cycle outlet. Hot air travelled 45 cm through uninsulated glass tubing (0.5" i.d.) to the sample box.

Current to the nichrome element in the Dewar and heat gun element was provided by an Ohmite 'V.I.' Variac (0-120 V, 25 A) from Ohmite Manufacturing Company. It was controlled by a two mode controller from API Instrument Company. The voltage setting on the Variac depended on the temperature desired. Too high a setting would result in rapid cooling. The controller could not then respond fast enough, resulting in over cooling. Equilibration at a desired temperature could be achieved more rapidly with gradual cooling.

Optical cells were held snugly on three sides by a one piece blackened-brass holder. A steel spring which assured accurate cell position formed the fourth side of the holder. An adjustable slit, usually set at 0.3 x 2.5 cm^2, was attached to the side of the holder.

For low temperature studies, the holder was fixed in a Styrofoam box (SB) of 12 x 12 x 27 cm^3 outside and 7 x 7 x 17 cm^3 inside dimensions. To minimize spreading of the electron beam, the Styrofoam was thinned from the outside directly in front of the cell for the temperature box electron window.

In high temperature studies, the holder was fixed in an Asbestos box (AB) of 12 x 12 x 27 cm^3 outside and 11 x 11 x 17 cm^3 inside dimensions. The electron windows were 3 cm and 2 mm thick for SB and AB, respectively.

The optical windows were Suprasil quartz plates for the latter and were Suprasil quartz cylinders for the former. Analyzing light entered and left either the AB or the SB. At temperatures below 240K, it was necessary to blow dry air on the outsides of the electron and optical windows to keep them frost free.

Cooling (heating) gas entered at the bottom of the SB (AB) and was deflected to force it to circulate before leaving through a 30 cm high insulated chimney in the lid.

Temperature measurements were made using copper-constantan thermocouples (268). Initially they were calibrated in slush (269) baths at:

113K (isopentane);
175K (methanol);
210K (chloroform);
250K (carbon-tetrachloride);
273K (ice-water);
and 371K (boiling water).

Later, because of their reliability, thermocouples were only checked against each other at room temperature and 273K.

Two (three) thermocouples were attached to the brass cell holder in SB (AB), and one to the cell. Miniature thermocouple connectors (Thermo Electric (Canada) Ltd.) were used to connect the thermocouple to the voltage measurement system. The temperature was measured by Fluke Digital Thermometer Model 2100A.

Temperature equilibrium in the system was assumed to exist when all three (four) thermocouples indicated the same temperature (±1 K) for a period of five minutes. Once equilibrium was achieved, the temperature could be maintained through the whole experiment.

(d) Optical Detection System

(i) The Light Source

A schematic diagram of the path of the analyzing light is given in Figure II-5. The source was an Osram XBO 450 W xenon arc lamp contained in an Oriel Optics Corporation lamp housing (Model c-60-50). A Pyrex filter was usually placed in the lamp housing to filter out ultra-violet (UV) light with $\lambda < 320$ nm. This prevented ozone formation in the room. The lamp was run at 650 W and pulsed to 15 KW for 2 ms when an absorption measurement was desired. The pulsing circuit is shown in Figure II-6. A light shutter protected the sample from unnecessary exposure. This was important for low temperature samples, to prevent warming. The shutter was opened for 1.2 seconds per pulse.

A quartz lens was used to focus the light beam at the center of the irradiation cell. Front surface aluminum mirrors coated with silicone monoxide were used to direct the light beam and to render it parallel. In this way, the light was transported from the irradiation room through a hole in the 1.2 meter thick concrete wall. Total path length of the optical system was 12 meters. The final concave mirror was used to focus the light on the monochromator housing.

Optical slits were placed just before and just after the cell such that the light beam passed close

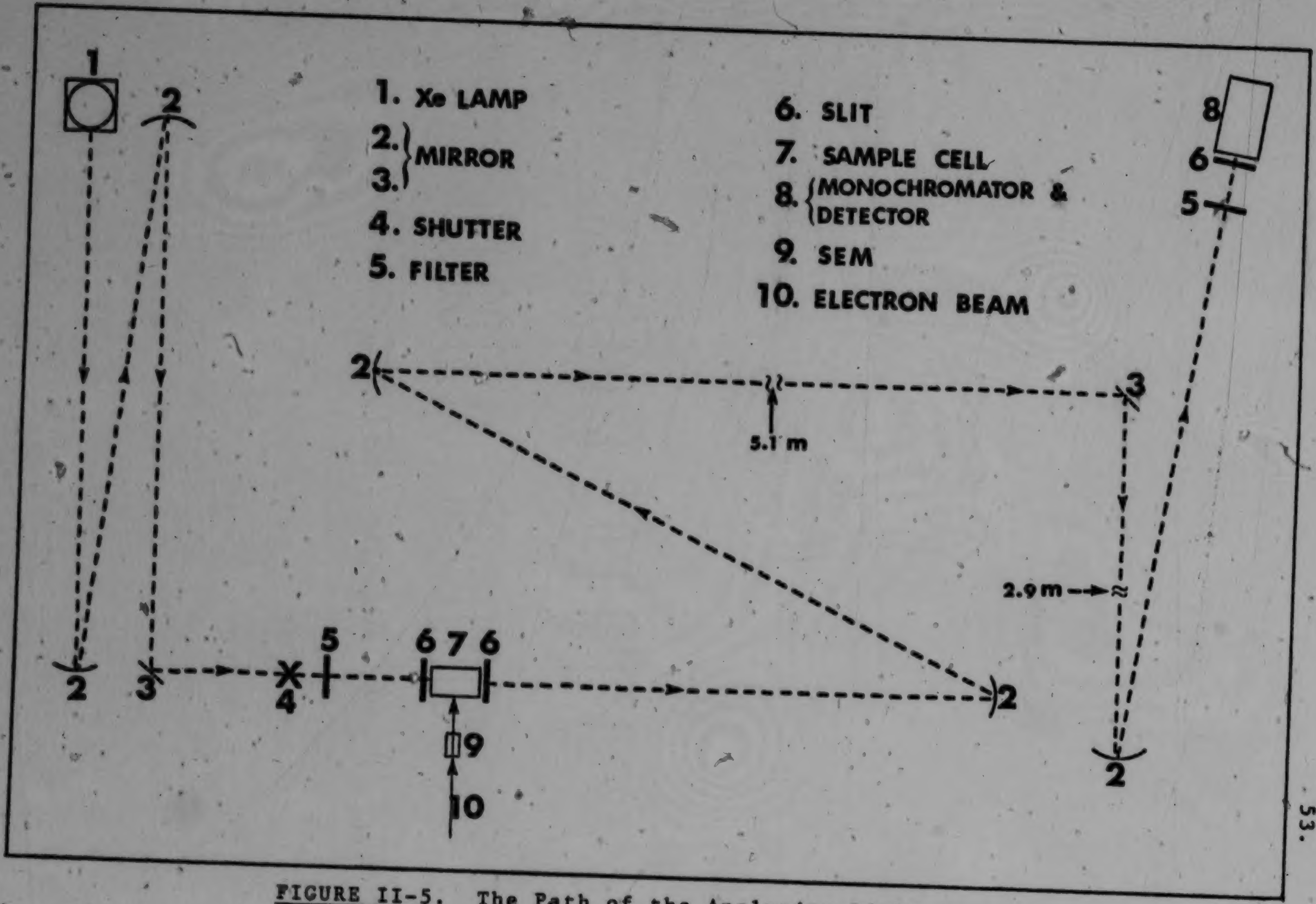
1. Xe LAMP
2. } MIRROR
3. }
4. SHUTTER
5. FILTER
6. SLIT
7. SAMPLE CELL
8. {MONOCHROMATOR & DETECTOR
9. SEM
10. ELECTRON BEAM
1
2
2
3
4
5
6 7 6
9
10
2
2
3
2
5.1 m
2.9 m
8
6
5

FIGURE II-5. The Path of the Analyzing Light

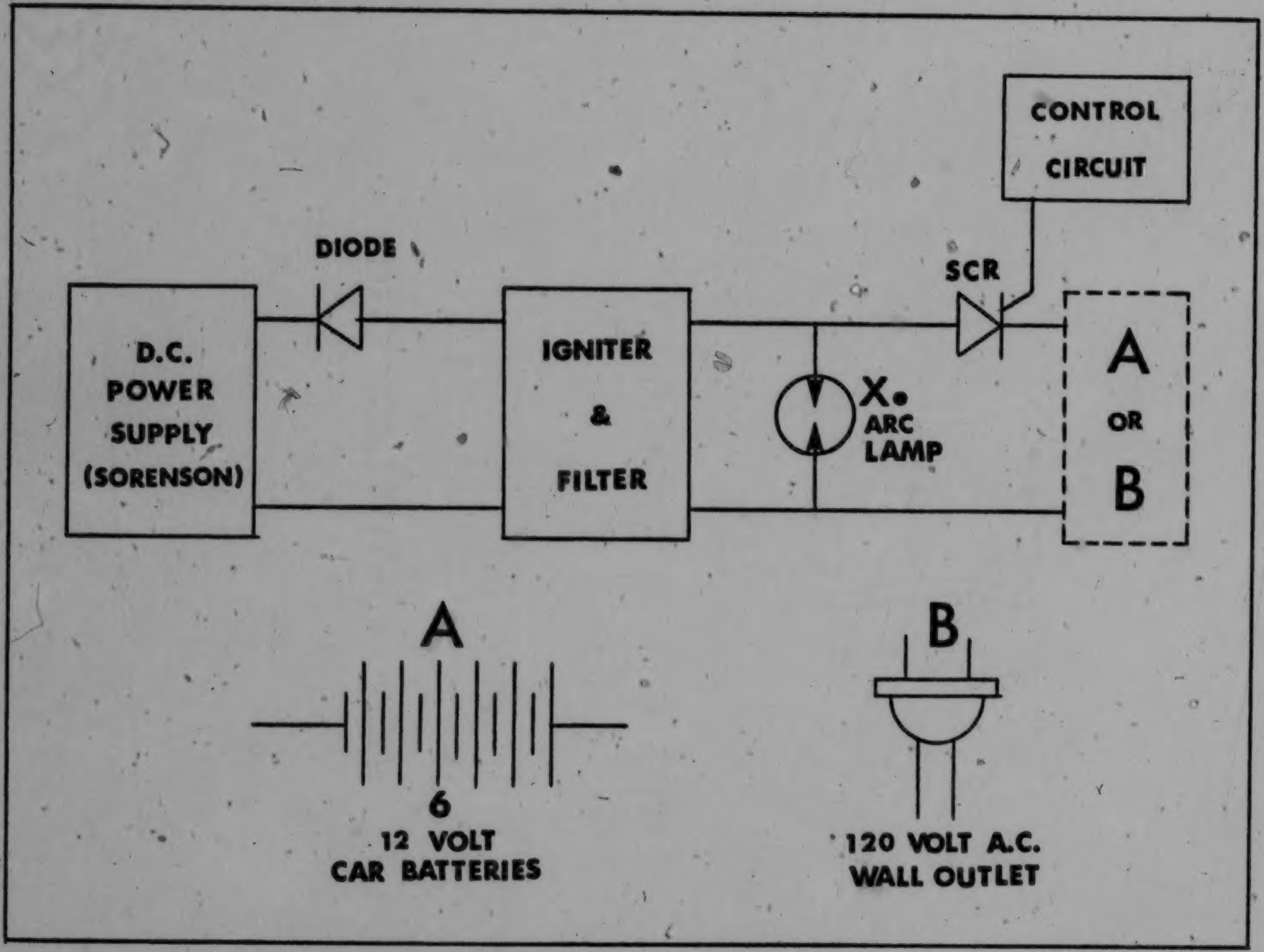
D.C.
POWER
SUPPLY
(SORENSON)
DIODE
IGNITER
&
FILTER
Xe
ARC
LAMP
SCR
CONTROL
CIRCUIT
A
OR
B
A
6
12 VOLT
CAR BATTERIES
B
120 VOLT A.C.
WALL OUTLET

FIGURE II-6. Circuit for Pulsing the Xe Lamp

to the window but did not reflect from it. They were adjusted so that the transmitted beam excluded light that had penetrated the irradiated front face of the cell.

(ii) The Monochromator, Grating and Filters

After passing through the sample, a swing concave mirror was used to focus the light on either of two Bauch and Lomb monochromator housings of type 33-86-25. They were used with three different gratings, types 33-86-02 (400 - 800 nm) and -03 (700 - 1200 nm) for visible; -78 (1100 - 2300 nm) for infrared (IR); -07 (200 - 700 nm) for UV, respectively. The grating scale was calibrated with a He-Ne gas laser (University Laboratories, Model 240) using

$$\lambda = N \times 632.8 \text{ (nm)}, \quad N = 1, 2, 3 \qquad [1]$$

and the Xe lamp spectrum (peaks from 450 to 2100 nm).

The light intensity reaching the detector was controlled by adjusting the slits on the monochromator. The band pass was:

4 ± 1 nm for -2 and -3 gratings;

40 ± 10 nm for -78 grating;

and

7 ± 1 nm for -7 grating,

respectively.

Appropriate Corning filters were mounted on a remote-controlled rotating wheel which was placed in front of the optical cell. Another filter(s), which narrowed the light band pass further, was(were) placed before the monochromator.

For IR measurements, a Corning CS-7-56 was always placed on the remote-controlled wheel. The filter placed in front of the monochromator was CS-7-56 for (1000 - 1500) nm. For wavelengths longer than 1500 nm, two filters were used, i.e., CS-7-56 along with:

CS-4-67 for (1500 - 1800) nm;
CS-4-71 for (1800 - 1900) nm;
CS-4-97 for (1900 - 2000) nm;
CS-4-72 for (2000 - 2250) nm.

For visible light, there was no filter on the remote controlled wheel but a filter was always placed in front of the monochromator. It was:

CS-4-97 for (400 - 500) nm;
CS-3-72 for (480 - 700) nm;
CS-2-64 for (700 - 1100) nm.

For UV measurements, the arrangement was similar to the visible case, except the filters placed in front of the monochromator were:

CS-9-54 for (250 - 260) nm;

CS-7-54 for (260 - 350) nm;
CS-7-59 for (350 - 410) nm;
CS-4-97 for (410 - 510) nm.

(iii) Detectors and Amplifiers

Figure II-7 shows a block diagram of detectors and amplfiers for IR, visible, and UV measurements.

The IR photocell was a Barnes Engineering A-10D/D10S InSb diode. It was cooled to 77K in a Dewar having side view sapphire windows. The detector was used over the wavelength range (800 - 2300) nm. The amplifier (Figure II-8) had a gain of 2700 Ohm/V, with a 40 ns rise time (10 - 90%) and a linear dynamic output range from 0 to 10 V.

At each wavelength setting, the incident light intensity was offset by a Tektronix 7A13 plug-in so that the output signal could be displayed on a Tektronix 7623 oscilloscope. The combined cell and amplifier rise time for 3 to 97% response was measured by Čerenkov emission from n-pentane to be 600 ns, independent of wavelength (125).

The silicon visible light detector covered the wavelength (400 - 1100) nm. It was an SGD-444-2 photodiode from EG & G Incorporated. Maximum spectral response occurred at 900 nm where the sensitivity was typically 0.5 μA/μW.

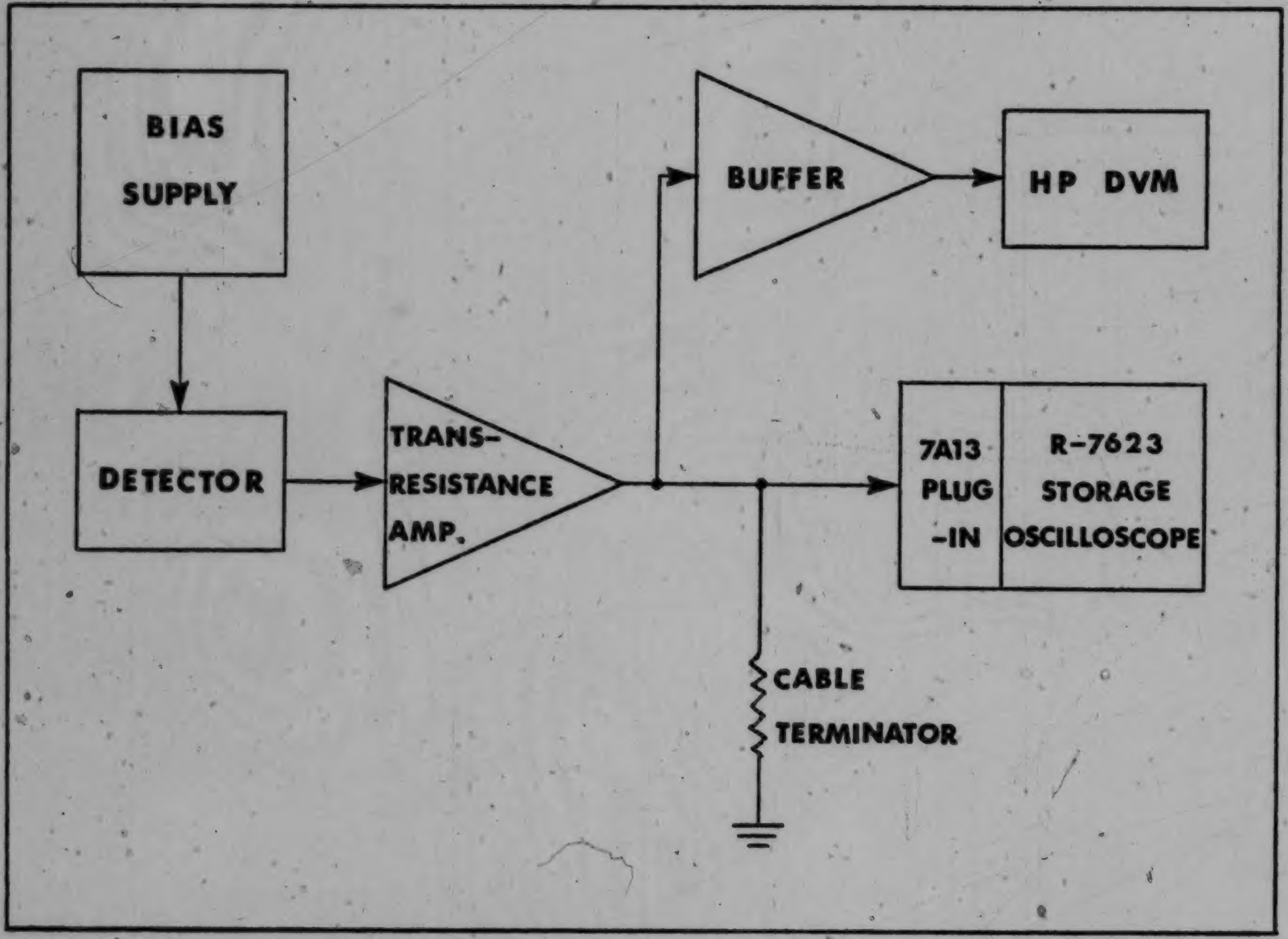
BIAS SUPPLY
DETECTOR
TRANS-RESISTANCE AMP.
BUFFER
HP DVM
7A13 PLUG -IN
R-7623 STORAGE OSCILLOSCOPE
CABLE TERMINATOR

FIGURE II-7. Block Diagram of the Detectors and the Amplifiers for IR, Visible, and UV Measurements.

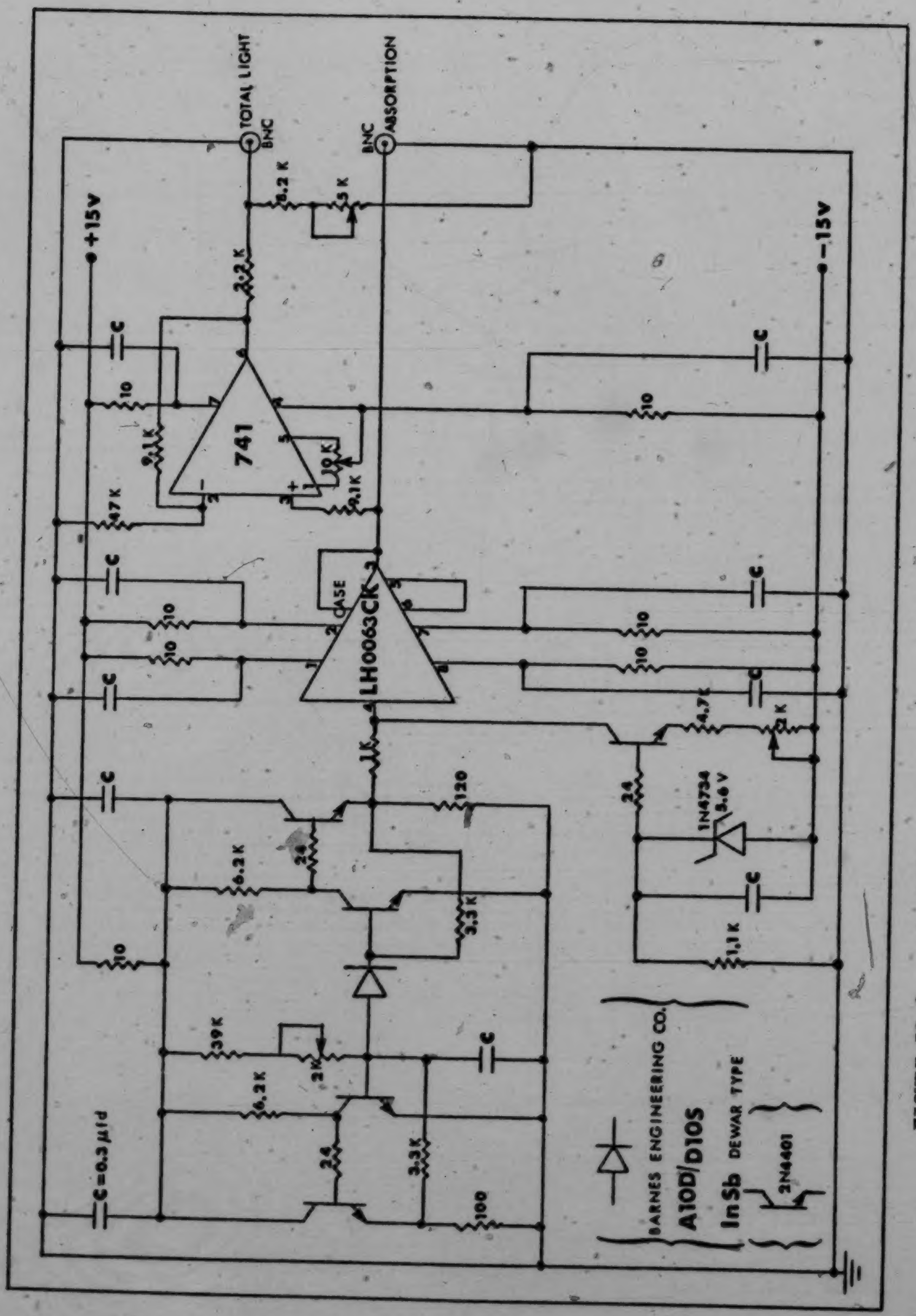
TOTAL LIGHT
BNC
BNC
ABSORPTION
+15V
-15V
8.2 K
5 K
2.2 K
C
10
9.1 K
47 K
741
10 K
9.1 K
CASE
LH0063CK
10
10
C
C
1 K
4.7 K
2 K
24
1N4734
5.6 V
120
6.2 K
24
3.3 K
10
1.1 K
39 K
2 K
6.2 K
C
24
3.3 K
100
C=0.3 μfd
BARNES ENGINEERING CO.
A10D/D10S
InSb DEWAR TYPE
2N4401

FIGURE II-8. Amplifier Circuit for the IR Light Detector

Response was linear over seven decades of incident power. The amplifier to accommodate the rapid increase of incident light from the pulsed lamp is shown in Figure II-9. The overall rise and fall times for 3 to 97% response of the detector, amplifier, and 7623 oscilloscope was 90 ns with 5 MHz bandwidth in the 7A-13 plug-in. The amplifier had a gain of 2700 Ohm/V, and a linear dynamic output range from 0 to 10 V.

The UV detector was an RCA 1P28 photomultiplier. The amplifier circuit is shown in Figure II-10. The first six dinodes, followed by an amplifier with 150 Ohms gain, were used. The power supply (Fluke 412B High Voltage Power Supply) for the 1P28 was gated on-off with the lamp shutter, which opened for an interval of one second. The power supply was set to 650-800 V, depending on the light intensity.

The amplifier was connected by a 93 (50) Ohms coaxial cable to the Tektronix 7623 oscilloscope, for UV (IR and visible) measurement(s), respectively.

(iv) Digital Voltmeter (DVM) and Oscilloscope

Incident light was recorded as a voltage on a Hewlett-Packard (HP) Model 3440A digital voltmeter (DVM).

Absorption signals were recorded as voltages on

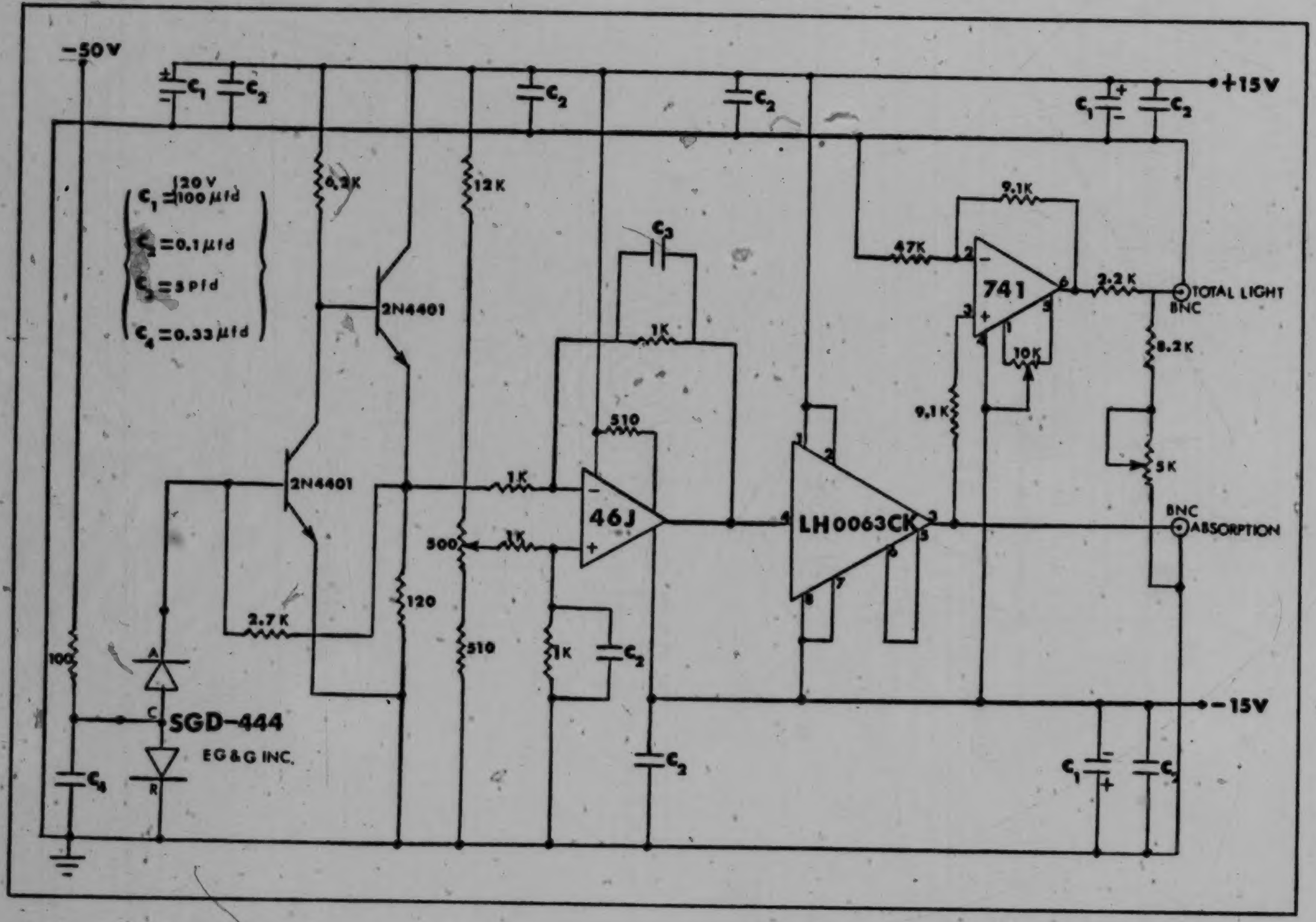
-50V
+15V
-15V
C1
C2
C3
C4
C1 = 120 V 100 μfd
C2 = 0.1 μfd
C3 = 3 pfd
C4 = 0.33 μfd
6.2K
12K
2N4401
2N4401
2.7K
120
510
500
1K
1K
510
1K
1K
46J
LH0063CK
741
47K
9.1K
9.1K
10K
2.2K
8.2K
5K
TOTAL LIGHT BNC
BNC ABSORPTION
100
A
C
R
SGD-444
EG&G INC.

FIGURE II-9. Amplifier Circuit for the Visible Light Detector

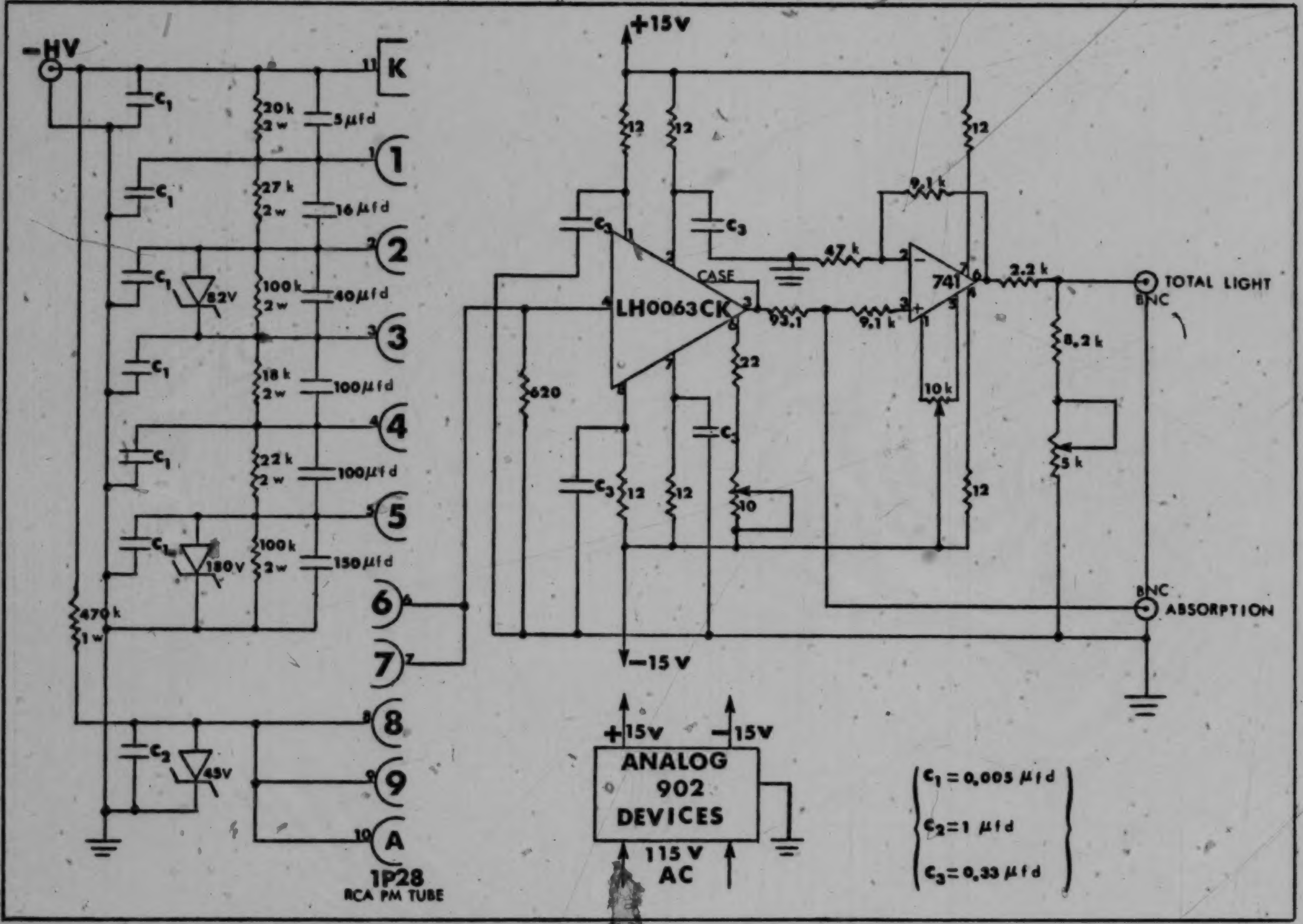
-HV
K
1
2
3
4
5
6
7
8
9
A
1P28
RCA PM TUBE
C1
C2
20k 2w
27k 2w
100k 2w
18k 2w
22k 2w
100k 2w
470k 1w
5μfd
16μfd
40μfd
100μfd
100μfd
150μfd
82V
180V
45V
+15V
-15V
LH0063CK
CASE
C3
12
620
22
10
93.1
47k
9.1k
10k
741
2.2k
8.2k
5k
TOTAL LIGHT
BNC
ABSORPTION
ANALOG
902
DEVICES
115 V
AC
+15V
-15V
C1 = 0.005 μfd
C2 = 1 μfd
C3 = 0.33 μfd

FIGURE II-10. Amplifier Circuit for the UV Light Detector.

an oscilloscope cathode ray tube (CRT). A Tektronix 7623 oscilloscope equipped with the appropriate plug-ins was used. Each CRT trace was photographed for later analysis using a Polaroid Model C12 camera and type 47 or 410 Polaroid Land film.

(e) The Timing and Control System

Several coordinated measurements were necessary to conduct a successful fast absorption experiment. The electronic system evolved to the point where a properly prepared experiment could be conducted by pushing one button. The timing of events initiated by this button is illustrated in Figure II-11. Since the duration of events differ by up to six orders of magnitude, their widths in the figure could not be drawn to scale.

Assuming all preparation was complete, including setting on the Tektronix 7623 fast storage oscilloscope, an experiment proceeded as follows. Initially, the remote erase cleared the oscilloscope CRT and Channel A of the Transistor Specialties Incorporation (TSI) Counter Model 1535. The electron pulse count total was registered on a HP 5245L Electronic Counter.

After 1.2 seconds, at point A on the figure, the main sweep was enabled. To improve reproducibility, the main gate always triggered from a point on the power line signal which had positive level and positive

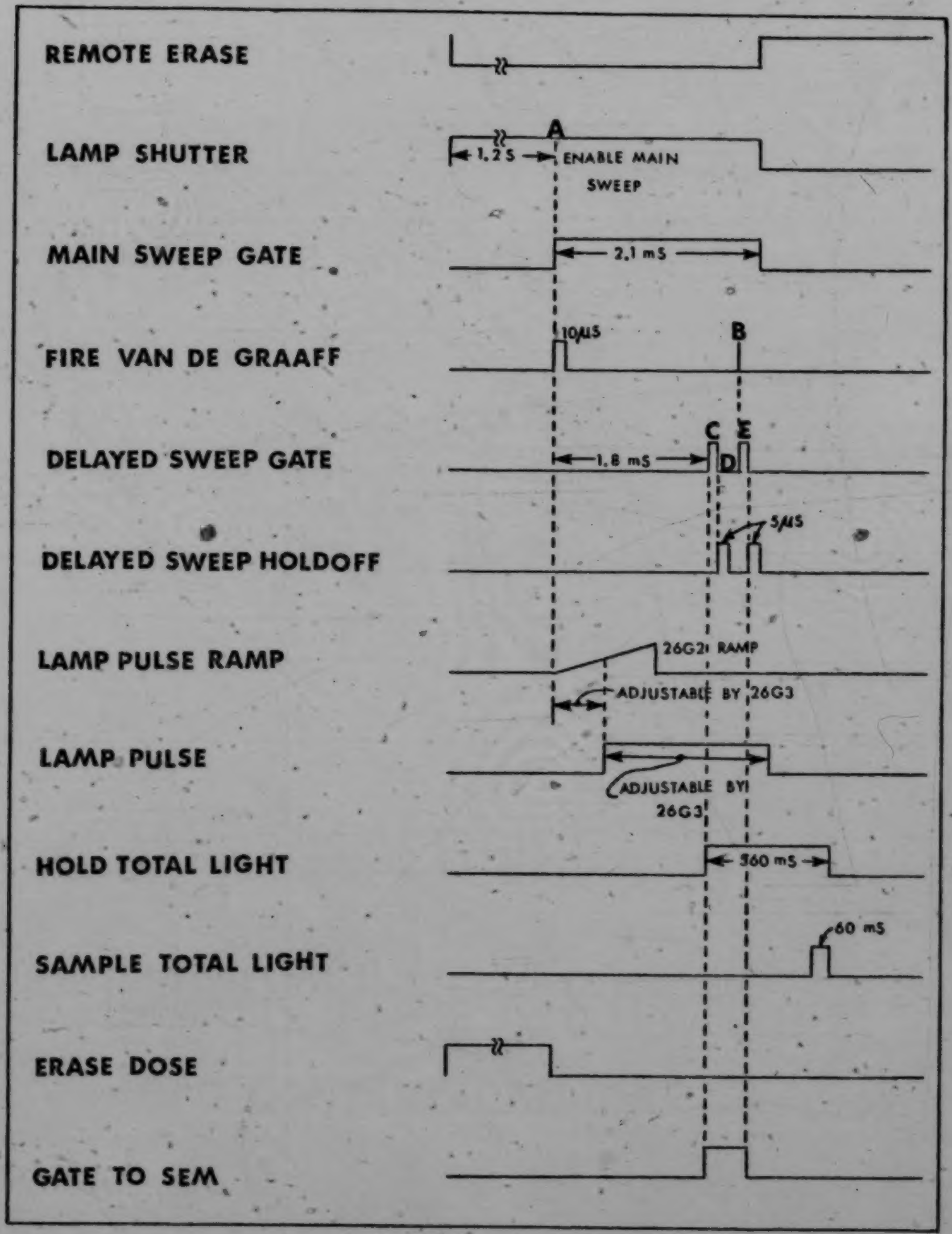
REMOTE ERASE
LAMP SHUTTER
A
1.2 S
ENABLE MAIN SWEEP
MAIN SWEEP GATE
2.1 mS
FIRE VAN DE GRAAFF
10µS
B
DELAYED SWEEP GATE
C
E
D
1.8 mS
DELAYED SWEEP HOLDOFF
5µS
LAMP PULSE RAMP
26G2 RAMP
ADJUSTABLE BY 26G3
LAMP PULSE
ADJUSTABLE BY 26G3
HOLD TOTAL LIGHT
360 mS
SAMPLE TOTAL LIGHT
60 mS
ERASE DOSE
GATE TO SEM

FIGURE II-11. The Time Sequence of an Absorption Experiment.

slope. This point was chosen to obtain the longest possible low light-noise region for the experiment. Reasons for the importance of the analyzing light amplitude remaining constant during an experiment are given later.

The first event in the main sweep was a 10 μs pulse to fire the VDGA. A high energy electron pulse, indicated by B, occurred about 1.8 ms later. There was an uncertainty (of 10 - 50 μs) in the time a beam pulse would occur. This was called beam "jitter" and was caused by the uncertainty in closing time of a relay.

The signal required to sweep the baseline for the absorption trace came from the delayed sweep gate at point C. It was swept at the same speed as set for the corresponding absorption decay curve. After sweeping the baseline, there was a 5 μs delayed sweep holdoff. This time was needed to allow the time base to settle.

Passage of the electron pulse through a toroid located part way down the accelerator beam pipe supplied a fast pulse. This pulse was used to trigger the oscilloscope sweep to record the absorption signal. Point E on the figure represents this sweep. Again, as for C, it was followed by a 5 μs delayed sweep holdoff.

The SEM was monitored from the beginning of a baseline sweep up to the end of the absorption sweep. Thus, any current from the SEM due to passage of high energy electrons was measured during the entire experiment and recorded.

The incident analyzing light was sampled at the same time as a baseline was swept. It then had to be held for at least 500 ms while the HP 3440A DVM responded. Actual sampling of the incident light took a further 60 ms. This was the time required for the DVM to digitize the analog signal.

Beam "jitter" was a complicating factor, particularly in obtaining an accurate baseline. It was important to have the baseline written as close in time to the absorption as possible. This was because any change in the analyzing light amplitude between sweeps C and E would result in an erroneous baseline. Any adjustment made in the delay time preceeding sweep C was, therefore, quite critical. If the baseline was swept too early, it could be incorrect. If it was swept too late, the absorption signal would be either missed completely (if the electron pulse occurred during the delayed sweep holdoff) or it would appear during the baseline sweep. The slower the sweep speed, the greater the possibility became that there would be delay problems. The system was in fact limited to the slowest horizontal sweep of 2 μs/division.

Modification of the system would allow use of slower sweeps. This was necessary only for samples having a solvated electron half life greater than about 15 μs. The method used was to deliberately sweep the baseline late. The electron pulse would, thus, occur during sweep C, producing a short leading baseline, then the absorption trace. However, even with this technique, for speeds of 10 μs/division or slower, there was a significant chance for error due to intensity changes in analyzing light during the absorption trace, and also due to the poor low-frequency response of the amplifier. Therefore, an additional amplifier having D.C. frequency was used (see Figure II-12).

When the automatic sequence of events was complete, the manual sequence began. First, the CRT trace was photographed and the oscilloscope settings were recorded. Then the pulse number, SEM dose, incident light, temperature, monochromator wavelength and other pertinent data were recorded.

C. Techniques

1. Sample Preparation

Quartz cells and other glassware were cleaned by performing the following sequence of operations. First the vessel was rinsed twice with absolute ethanol. While the surface was still alcohol wetted, concentrated

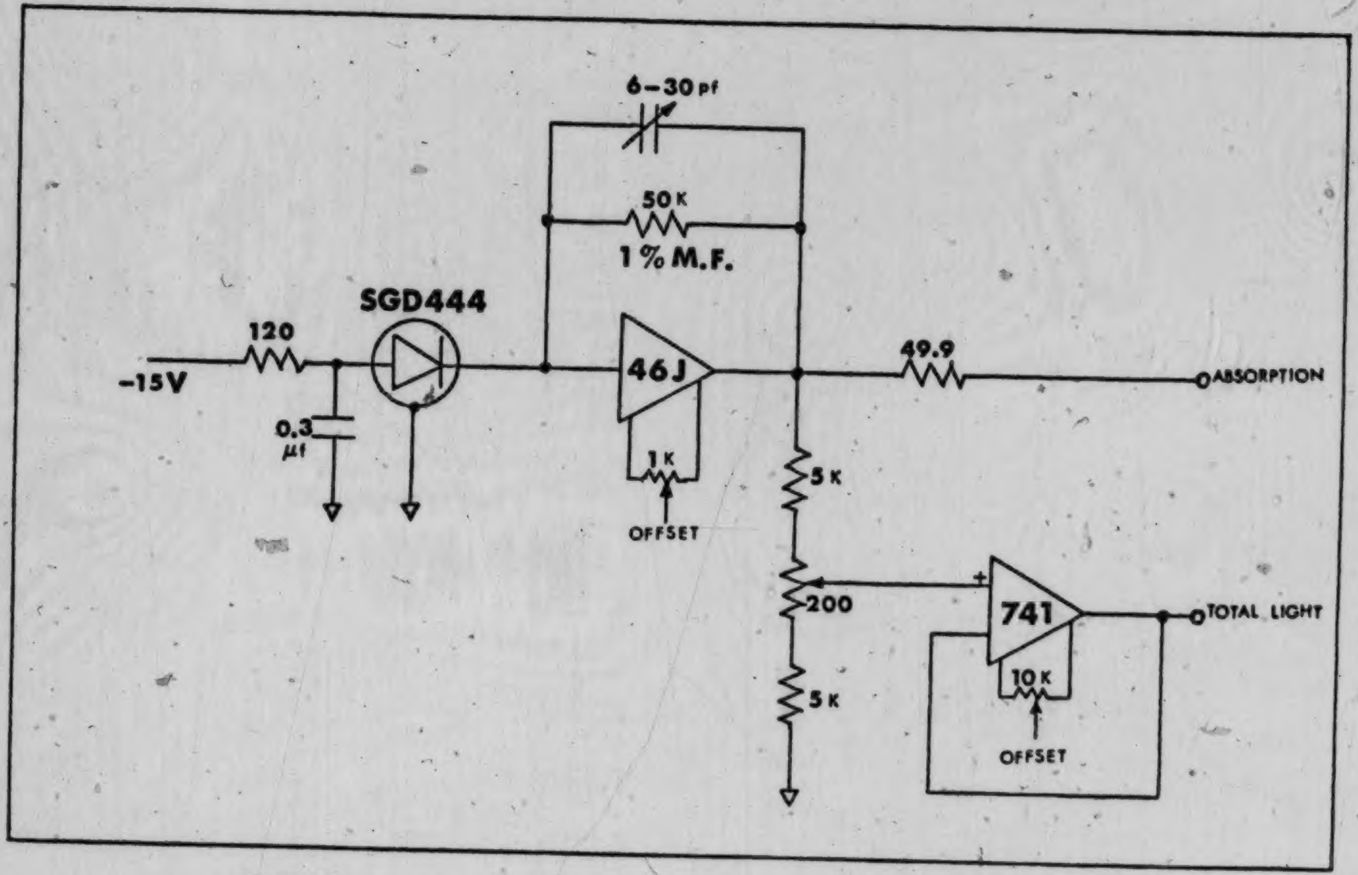
6–30 pf
50 K
1 % M.F.
SGD444
120
-15V
0.3 μf
46J
1 K
OFFSET
49.9
ABSORPTION
5 K
200
5 K
741
10 K
OFFSET
TOTAL LIGHT
+

FIGURE II-12. Direct Current Absorption Amplifier

nitric acid was added. The resulting exothermic reaction caused the acid to boil vigorously. Acid was then removed by rinsing twice with dilute sodium bicarbonate solution and many times with triply distilled water. The glassware and quartz cells were dried at 388K in a clean oven reserved for that purpose. Just before use, the vessel was rinsed twice with the appropriate solvent or solution.

Syringe needles were washed first with hexane to remove oil and grease, then with soap and hot water. They were finally rinsed many times with triply distilled water and oven dried. Before use, they were rinsed several times with the solvent or solution being used.

Stock solutions were prepared in 50 ml Pyrex volumetric flasks with the aid of syringes. Samples were prepared by syringe addition of stock solution to a clean cell, and were de-aerated by bubbling for at least one hour with UHP argon at a rate of about 20 cc per minute, and were then sealed after bubbling as illustrated in Figure II-13. Step 1 took place at room temperature. The syringe needle was then withdrawn to just above the liquid as shown in step 2 and the argon flow rate was increased somewhat. The cell was placed in a Dewar flask filled with an appropriate coolant and cooled to ~5K above its melting

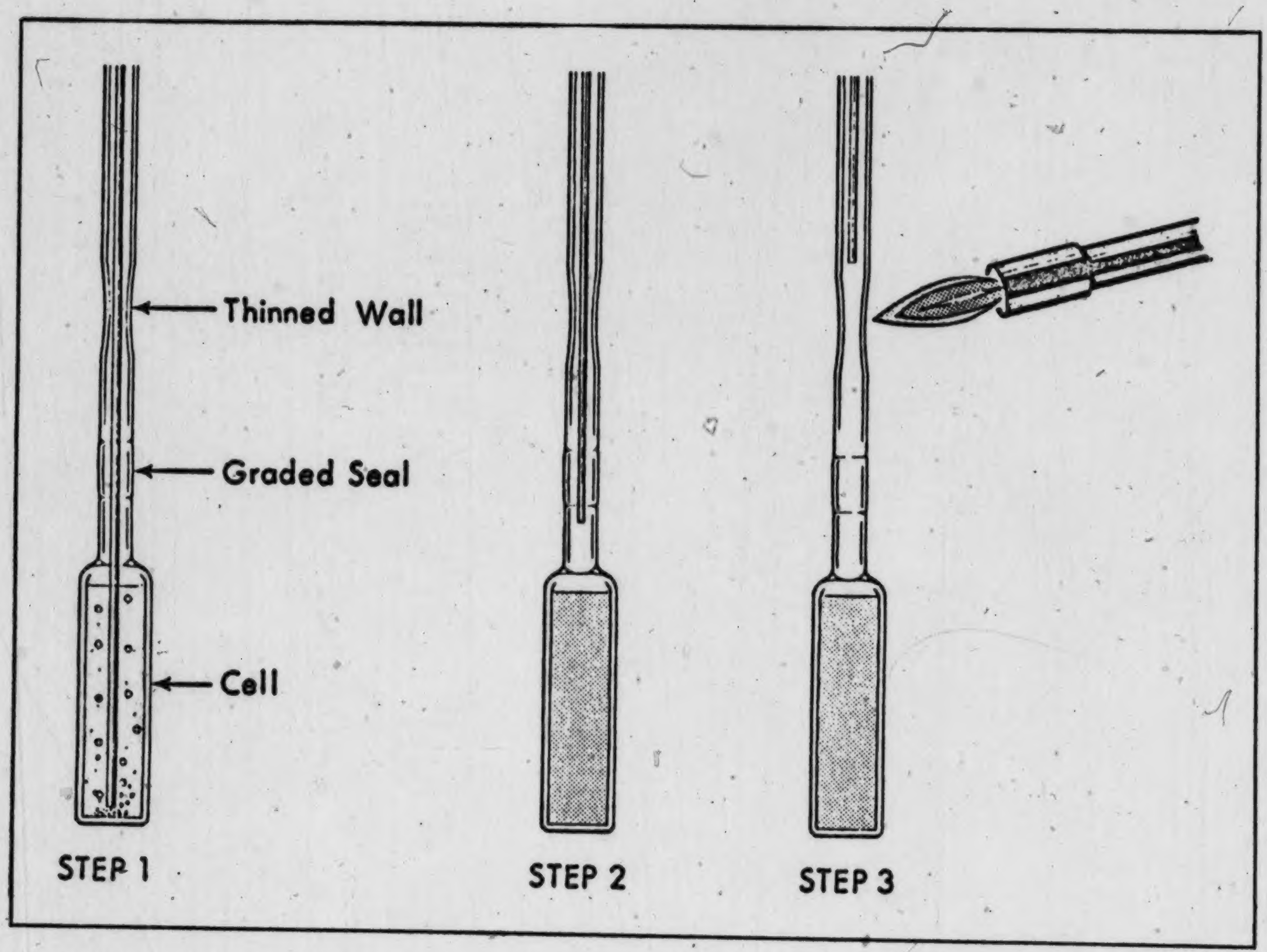
Thinned Wall
Graded Seal
Cell
STEP 1
STEP 2
STEP 3

FIGURE II-13. The Sealing Technique for Type (b) Cells.

point. Heating the thinned portion of the tubing with a flame flushed volatile substances from the glass wall. The syringe needle was then further withdrawn as shown in step 3, and the seal was made as rapidly as possible. This method was used for all samples.

2. Analysis of Polaroid Photographs

Typical photographs taken from the CRT of the Tektronix 7623 oscilloscope are shown in Figure II-14. Each picture was taken at a sweep speed (horizontal scale) of 1.0 μs/division. The vertical scale is in volts/division, and is proportional to absorbance. For 'i' and 'ii', the vertical scale is 0.05 and 0.1 volts/division, respectively.

(a). Analysis of Optical Absorption from Photograph 'i'

Photograph 'i', in Figure II-14, shows the decay curve of the solvated electron absorption at 600 nm in ethanol at 298K. A best-fit line was drawn through the noise on both the baseline and the decay curve. Using a graticle line as reference, the vertical line was then drawn through the point which represents the end of the electron pulse.

Absorbance could be determined at any time along the solvated electron curve by substitution in the following formula.

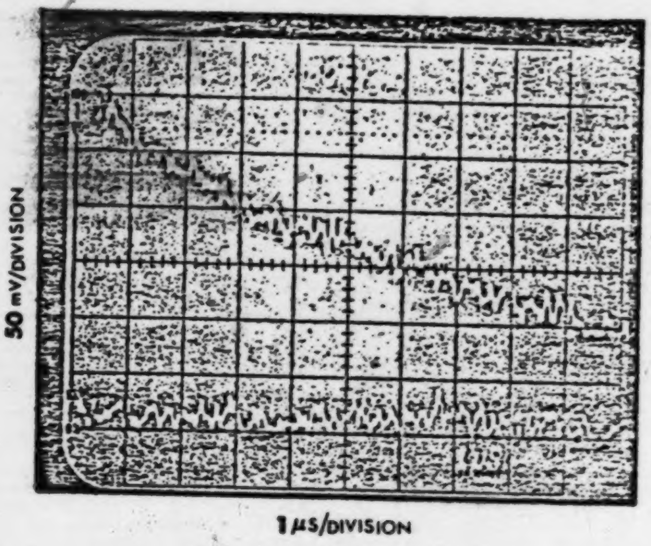

i. ETHANOL

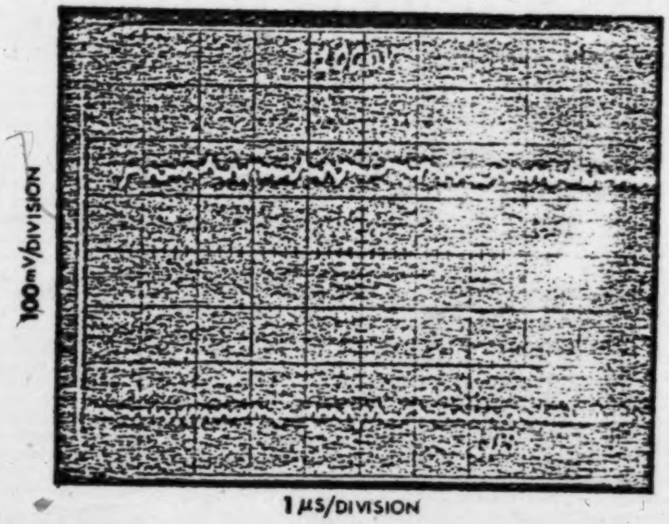

ii. AQUEOUS 5.0 mM KSCN

FIGURE II-14. Typical Oscilloscope Trace Photograph.

$$A = (D_o/D).\log\{I_o/(I_o - I_t/F)\} \qquad [2]$$

A is absorbance at time t after the beginning of the electron pulse; (D_o/D) is a dose normalization factor where D is the SEM dose and D_o is an average dose, usually chosen to be 1.0 nanocoulomb (nc) from the SEM; I_o is the incident analyzing light in volts; I_t is the absorbed light in volts at time t, and F is the amplifier factor which is the ratio of the amplification of the absorbed light to the incident analyzing light.

When the solvated electron lifetime was short, there was significant decay of electrons during the pulse. This was particularly true at temperatures higher than room temperature. A correction for this decay was applied where necessary using [3] (299)

$$A_c = A_{obs}.k.t_p/\{1-\exp(-k.t_p)\} \qquad [3]$$

A_c is the absorbance corrected for the decay during the pulse; A_{obs} is the observed absorbance at the end of the pulse; t_p is the pulse duration time, and $k = (0.693/t_{\frac{1}{2}})$ is the first order decay constant.

The correction was negligible for t_p = 100 ns and was normally <20% for t_p = 1.0 μs.

At wavelengths (λ) less than 400 nm, the half-life of the absorption increased, which indicated a contribution from species other than solvated electrons (14). The absorbance due to solvated electrons at these wavelengths was calculated from [4]

$$A_o(e^-_{solv}) = 2(A_{obs} - A_{\frac{1}{2}}) \qquad [4]$$

A_o is the absorbance corrected for other species absorption, and $A_{\frac{1}{2}}$ is the absorbance at a time equal to the solvated electron half-life measured at longer wavelengths (λ > 400 nm).

(b) Analysis of Optical Absorption from Photograph 'ii'

Photograph 'ii' in Figure II-14, is of the optical absorption at 478 nm in a 5.0 mM KSCN aqueous dosimeter solution following a 0.1 μs electron pulse. At a sweep speed of 1.0 μs/division, there is very little decay evident in the $(SCN)_2^-$ absorption.

Calipers were used to measure I_t between straight lines drawn through the noise on each trace. The absorbance was calculated using [2]. The dose received by the sample could then be calculated.

3. Analysis of Absorption Spectra

(a) Primary Parameters

After correction, each absorbance was normalized to the absorption maximum to obtain A/A_{max}. Measurements at 30 or more different wavelengths were used to obtain a spectrum. The following primary parameters were obtained from a plot of A/A_{max} against photon energy E (Figure II-15):

E_{Amax}, the energy at absorption maximum;

$W_{½}$, the band width at half-height of absorption maximum;

W_r , the part of $W_{½}$ on the red side of the absorption maximum;

W_b , the part of $W_{½}$ on the blue side of the absorption maximum.

(b) Secondary Parameters

Each spectrum was deconvoluted into overlapping Gaussian bands using equations [5] and [6] (85,86)

$$A_i = A_{i,max} . \exp\{-\ln 2((E_i - E)/g)^2\} \qquad [5]$$

$$A = \sum_i A_i + R \qquad [6]$$

where A is the experimental absorbance after correction at energy E; A_i is the absorbance of the i'th band at energy E; $A_{i,max}$ is the maximum absorbance in the i'th band; R is the residual absorbance; E_i is the energy at A_{max}; E is the photon energy associated with A, and $2g_i$ is the half-width of the i'th band. The secondary parameters $A_{i,max}$, E_i, g_i and E_o (the threshold energy of photon ionization of the solvated electron - estimated from the onset of the residue of the high energy tail) are illustrated in Figure II-16.

(c) High Energy Side of the Spectra

The high energy side of the absorption spectra were tested by using a simple exponential function (14,85, 270):

$$A/A_{max} = \text{Constant } E^{-\alpha} \qquad [7]$$

The value of α is obtained from the slope of the plot of $\ln(A/A_{max})$ vs $\ln(E)$. A representative plot is shown in Figure II-17.

(d) Area Measurements

The area under each absorption spectrum was obtained using integration in parts (Figure II-18).

The area under the low energy side, for $0.0 < A/A_{max} \leq 0.5$ was calculated with ZDHOW (a public subroutine in "APL Functions for Random Numbers and Probability") (271), using the normalized one dimensional Gaussian equation as a basic function.

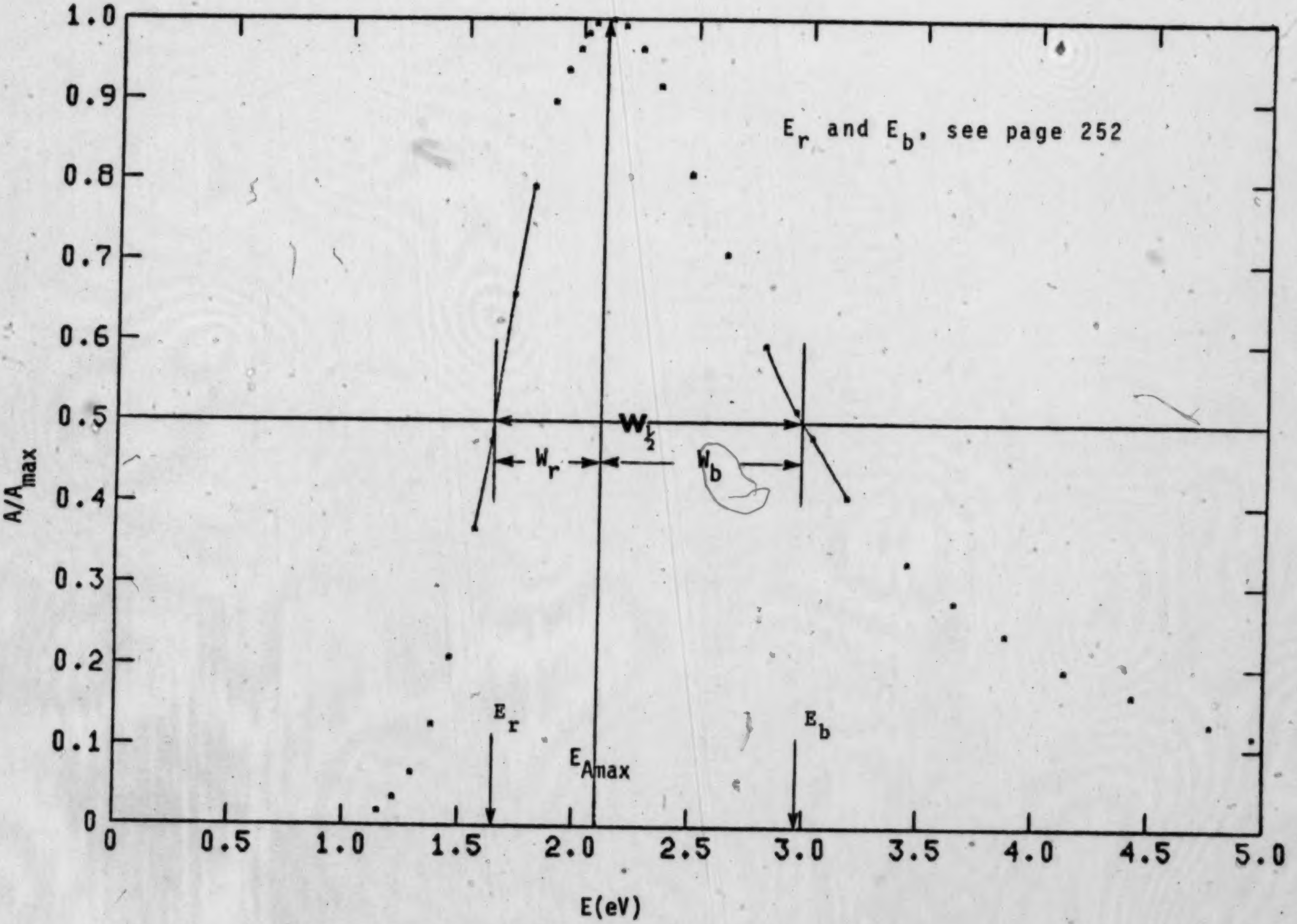

E_r and E_b, see page 252

FIGURE II-15. Graph Used to Obtain Primary Parameters

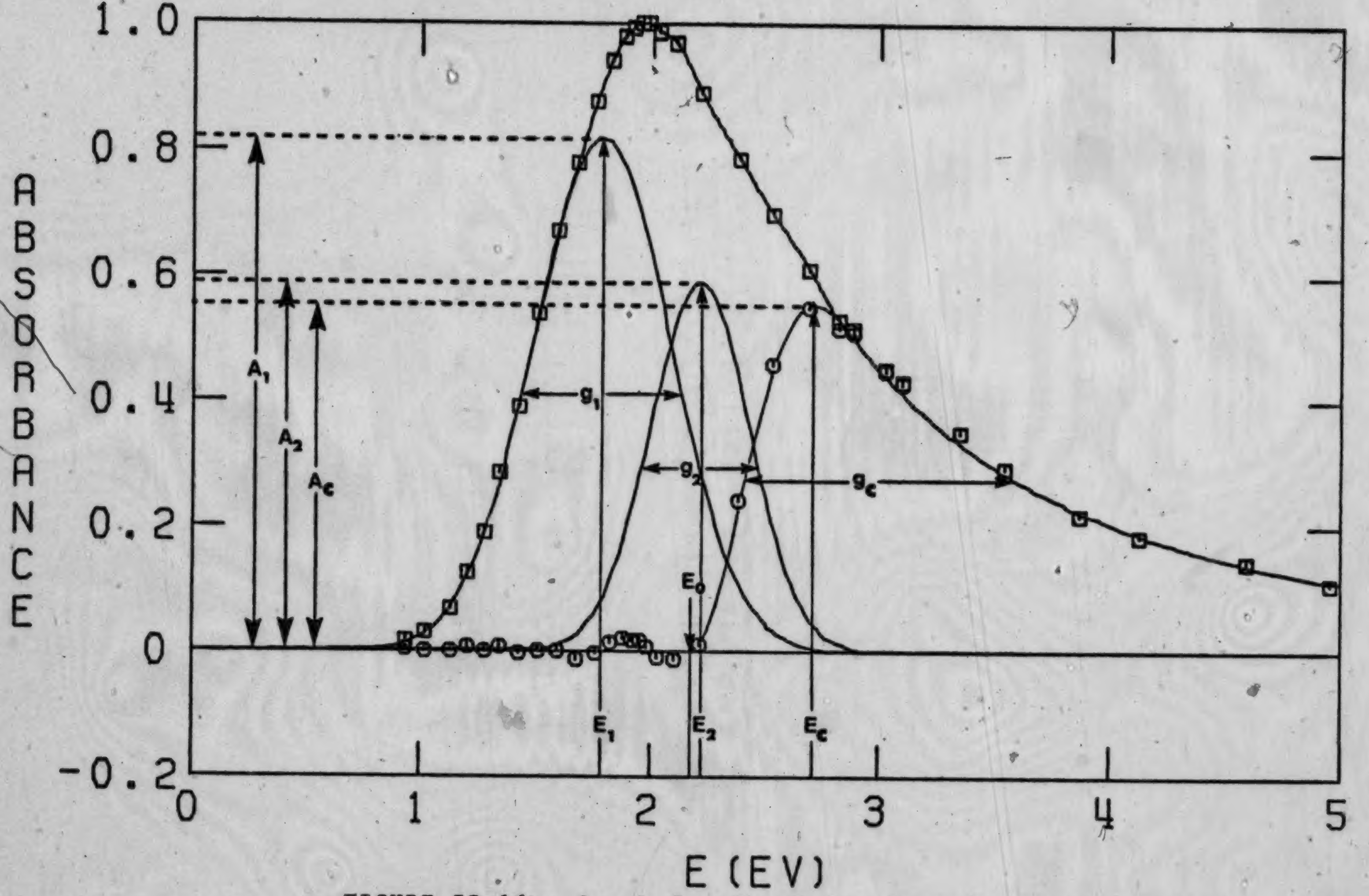

FIGURE II-16. Graph for Obtaining Secondary Parameters

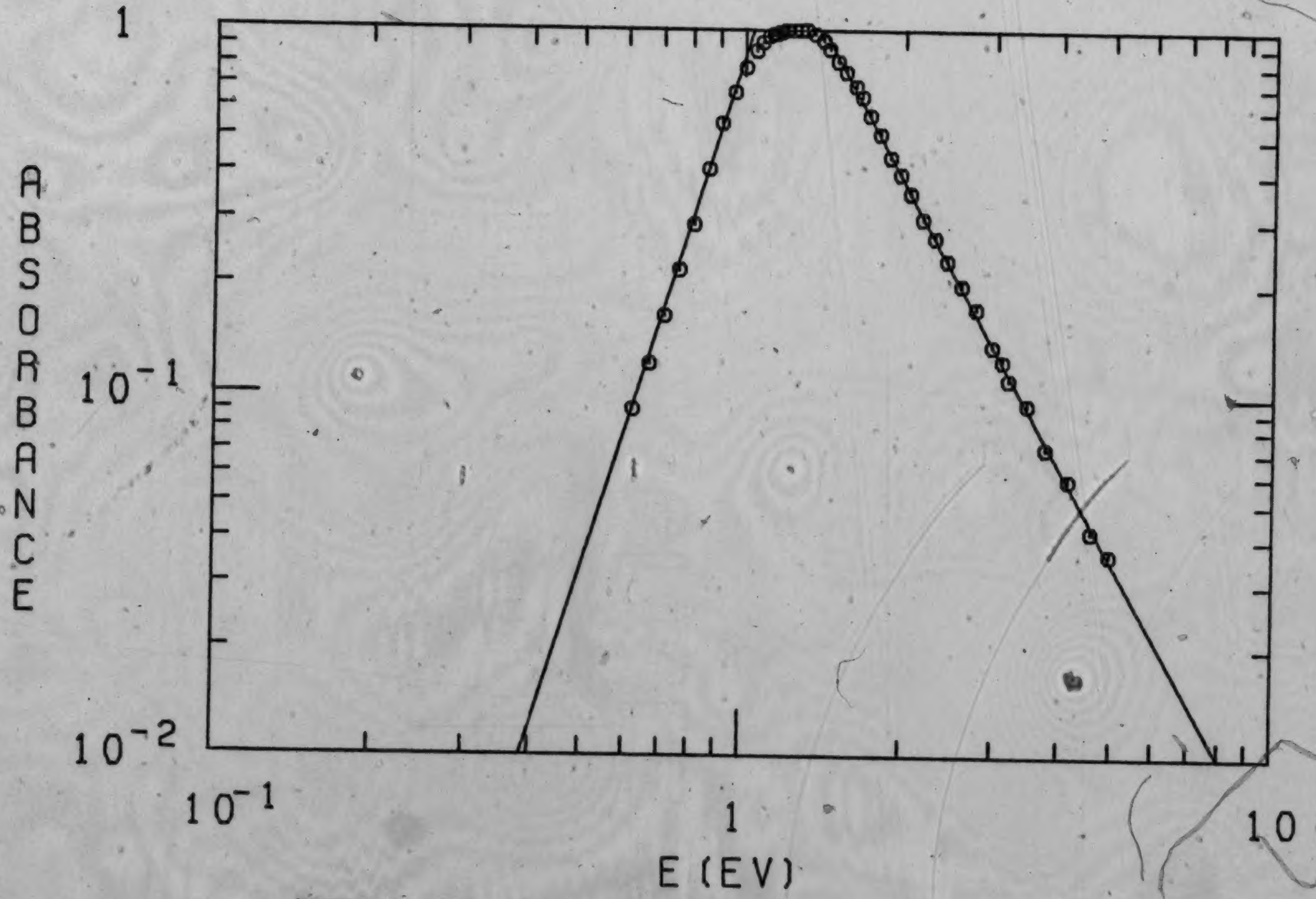

FIGURE II-17. Plot of $\ln(A/A_{max})$ vs $\ln(E)$

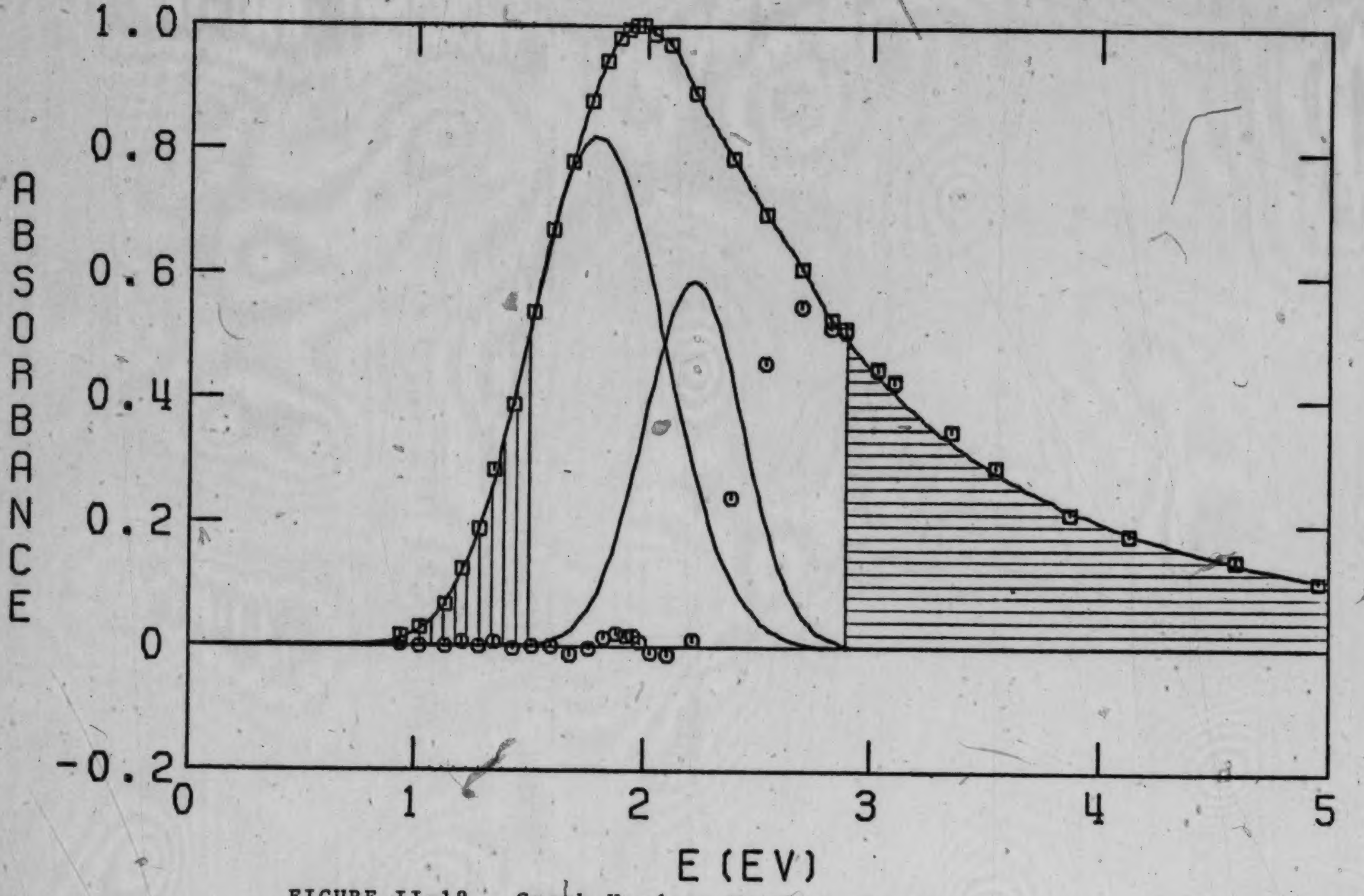

FIGURE II-18. Graph Used to Measure the Area

The area of the central part, 0.5 (low energy side) < A/A_{max} < 0.5 (high energy side), was estimated by numerical integration using the trapezoidal method. The basic function of this integration was obtained from an APL public subroutine named SPLINEHOW (272) and using a step size of 0.05 eV.

The area under the high energy side, 0.5 < A/A_{max} < ∞, was obtained by integration from E_{50} to ∞, using equation [7] as a basic function, where E_{50} is the photon energy associated with 50% A/A_{max} on the high energy side.

The area of each deconvoluted Gaussian band was calculated using equation [5] as a basic function.

D. Irradiation and Dosimetry

For irradiation of samples in quartz cells, 1.80 MeV electron pulses of 1.0 μs duration were used. These pulses normally gave doses of about 9×10^{16} eV/g (~2 nc SEM). The beam current could be adjusted to give a maximum pulse dose of about 3×10^{17} eV/g.

The dose delivered in each electron pulse was monitored by the SEM reading. The SEM was calibrated to the dose received by a sample using in situ actinometry (95).

Routine actinometry used the optical absorption produced in oxygen-saturated 5 mM KSCN aqueous solution.

The molar absorptivity, ε, (molar extinction coefficient) used was 7500/M/cm for $(SCN)_2^-$ at 478 nm (273). The wavelength of maximum absorbance ($\lambda_{max} = 478 \pm 4$ nm) and the absorbance were independent of temperature from 293 to 332K (95), and of pressure from 1 bar to 2 kbar (86). All dosimetry was done at 298K. It was assumed that G(OH) = 2.8 in the bulk solution (273,274).

The dose in eV/g was calculated from the absorbance measured from photographs of the type shown in Figure II-13-ii using [8]

$$D = (A.N)/\{\varepsilon.G(OH).b.d.10\}\text{eV/g} \qquad [8]$$

where A = absorbance; N = Avogadro's number; ε = molar absorptivity = 7500/M/cm; G(OH) = number of OH radicals scavenged by SCN^- for each 100 eV of dose absorbed; b = path length of analyzing light, and d = density of absorber.

III. RESULTS

A. Alcohol/Water Mixture, 298K

The addition of water to an alcohol shifts the optical absorption energy of solvated electrons in an irregular manner. The energy at the E_{Amax} for electrons in water mixtures with methanol, ethanol, and 1-propanol are shown in Figure III-1. The curves for ethanol and 1-propanol have a minimum at 10 mole % water. The curve for methanol does not show a minimum, although it has a greater than average slope at low water concentrations. All three curves have accentuated slopes near the pure water ends.

The behavior of $(G\varepsilon_{max})^*$ is different from that of E_{Amax}. There is a maximum in each of the $G\varepsilon_{max}$ curves at 97% water (Figure III-2). There is also an accentuated slope near the pure alcohol end of the curves.

The 90 and 2 mole % solutions were thus indicated as significant compositions for investigating optical parameters of solvated electrons. The value of E_{Amax} stayed constant for solutions between 70 and 30 mole % of each alcohol, so 50 mole % would adequately represent the behavior of E_{Amax} for the middle range of alcohol/water mixtures.

---

* see page 86 footnote

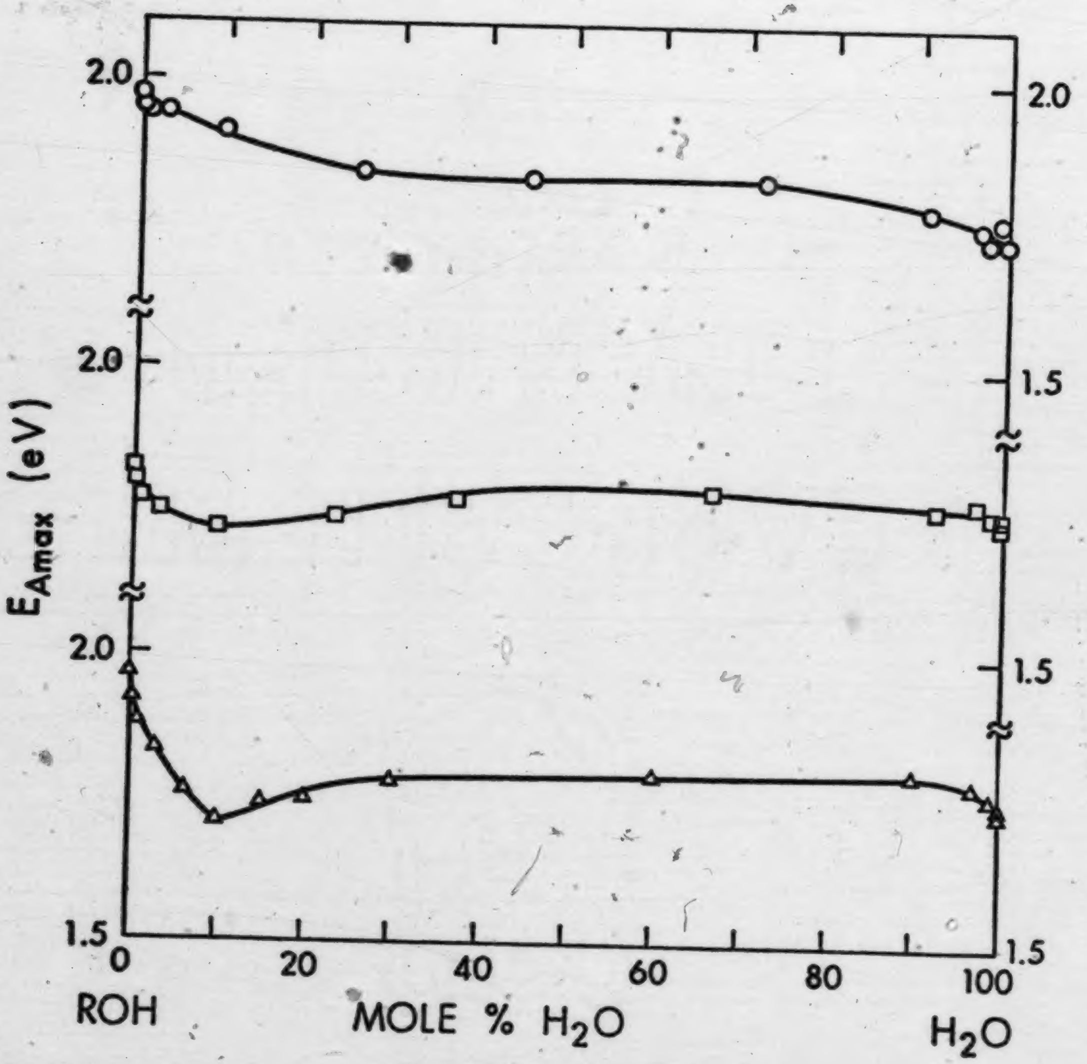

FIGURE III-1. Plot of E_{Amax} vs Composition: O, methanol; □, ethanol; △, 1-propanol The methanol and ethanol curves are unpublished results of K. N. Jha, 1974.

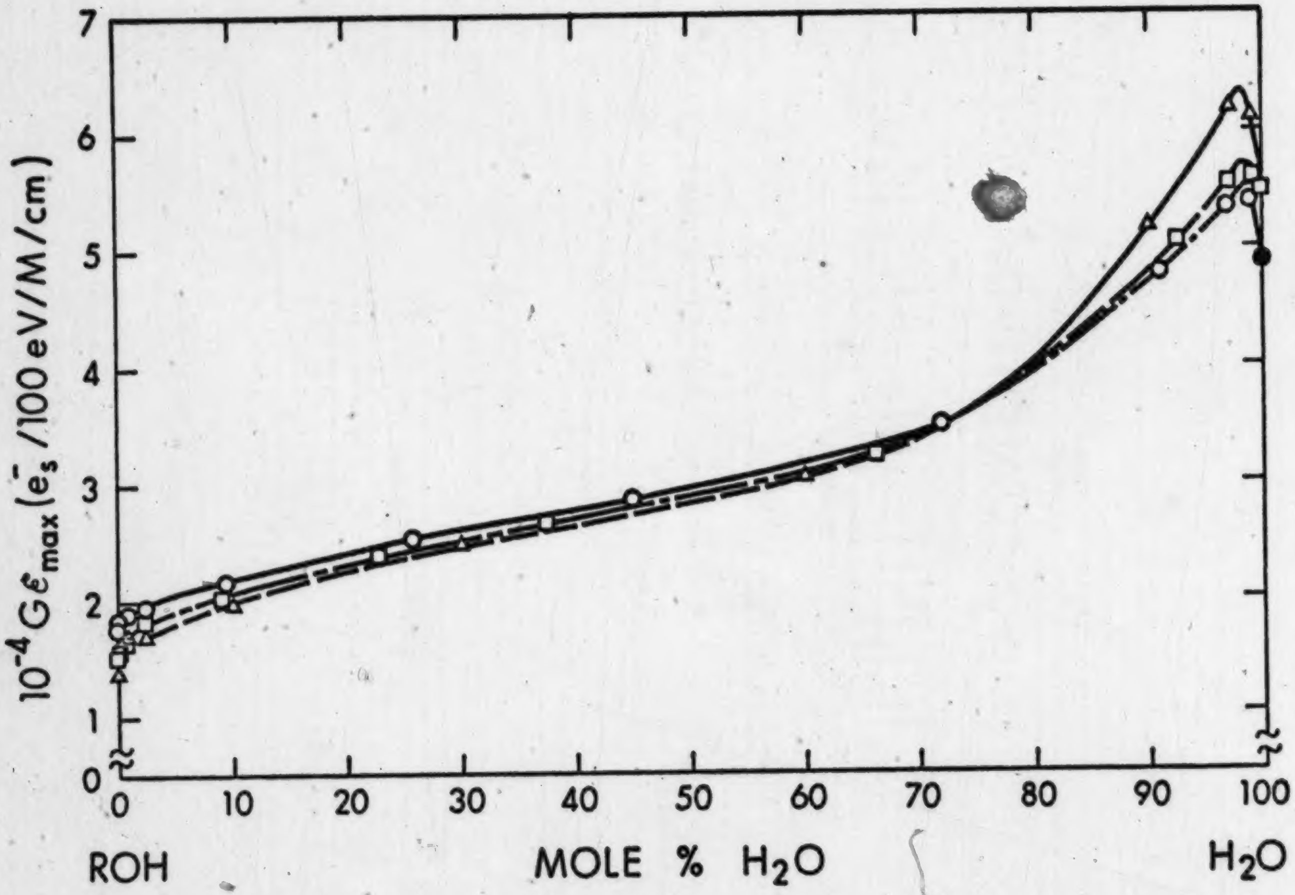

FIGURE III-2. Plot of $G\varepsilon_{max}$ vs Composition:

O, methanol; □, ethanol; △, 1-propanol.

The methanol and ethanol curves are unpublished results of K.N. Jha 1974.

The eccentricity of behavior of both E_{Amax} and $G\varepsilon_{max}$ is greater for 1-propanol than for ethanol, which is in turn greater than that for methanol (Figure III-1 and -2). To extend the study of the effect of molecular structure, measurements were made on systems containing, in most cases, 100, 90, 50, and 2 mole % of alcohols having different carbon skeletons.

---

* Footnote for Page 86

G is the number of solvated electrons observed per 100 eV of energy absorbed by the system.

ε_{max} is the molar absorptivity at absorption maximum.

B. Spectrum Shape

1. Effect of composition

(a) Methanol/Water

A variety of methanol/water mixtures have been studied. Emphasis, however, will be placed on the representative 100, 90, 50, 2 and 0 mole % alcohol compositions. Spectra obtained for solvated electrons in methanol and water mixtures of these compositions are shown in Figure III-3. The E_{Amax} of methanol falls at 1.98 eV at 298K. The main body of the band is moderately skewed towards high energy. The spectra of solvated electrons in the aqueous solutions are similar to that in methanol. The E_{Amax} occur at lower energies than in methanol and decrease as the mole % of methanol decreases.

The spectrum parameters, which are listed in Table III-1, include measurements for a variety of compositions. These are plotted against composition of methanol/water in Figure III-4, along with some literature values (105) for comparison. The $W_{\frac{1}{2}}$ constrict as the mole % of water increases. $W_{\frac{1}{2}}$ constricts sharply as mole % of water increases to 50 then levels off. The sharp constriction of $W_{\frac{1}{2}}$ is due mainly to the decreasing of W_b for the mole % of water up to 50.

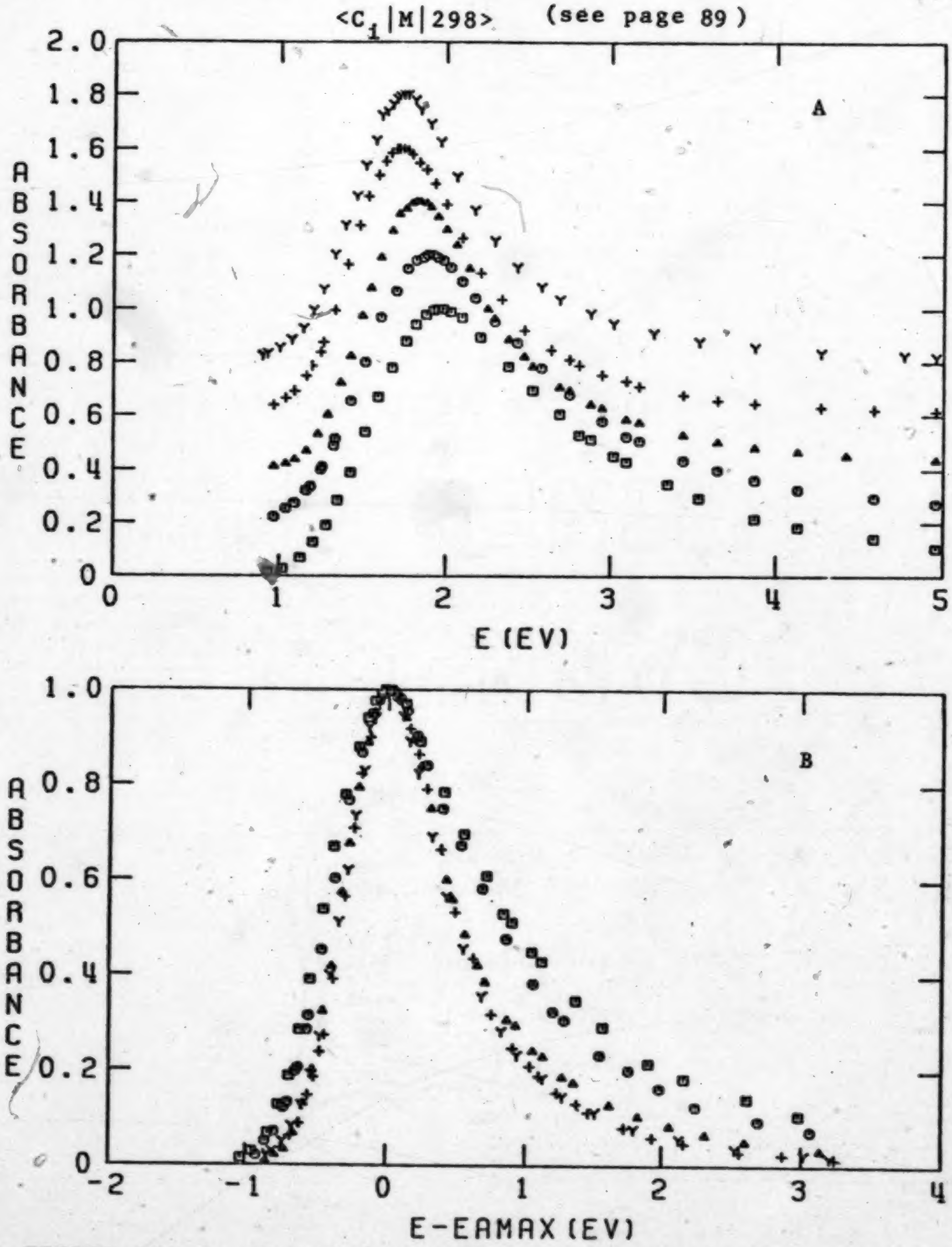

FIGURE III-3. The Optical Absorption Spectrum of Solvated Electrons in Methanol/Water at 298K and Various Compositions.

A. Successive spectra are displaced vertically by 0.2 units.

B. The spectra are normalized at E_{Amax}.

□, methanol; O, 10 mole % water; Δ, 50 mole % water; +, 98 mole % water; Y water.

TABLE III-1

Parameters of Solvated Electrons in Methanol/Water at 298K

Code No.	Composition Mole % Water	E_{Amax} eV	$W_{\frac{1}{2}}$ eV	W_r eV	W_b eV	W_b/W_r
Z1, J1	0.0	1.97	1.43	0.49	0.94	1.92
J2	0.3	1.95				
J3	1.0	1.94	1.40	0.47	0.93	1.98
J4	2.9	1.94				
J5	9.5	1.91	1.28	0.46	0.82	1.78
Z13, J6	10.0	1.90	1.26	0.45	0.81	1.80
J7	25.6	1.84				
J8	45.0	1.83	0.96	0.39	0.57	1.46
Z18, J9	50.0	1.83	0.90	0.37	0.53	1.43
J10	72.0	1.83	0.89	0.39	0.50	1.28
J11	91.2	1.78				
J12	96.9	1.75	0.85	0.35	0.50	1.43
Z22, J13	98.0	1.72	0.87	0.34	0.53	1.56
J14	99.0	1.76				
Z152, J15	100.	1.73	0.85	0.36	0.49	1.36

Z (Code) = This work

J (Code) = K. N. Jha's unpublished data, 1974.

In <C|X|T>, C represents the mol % water, X represents the alcohol and T the temperature K. The alcohols are represented by M for methanol, E for ethanol, 1P for 1-propanol, 2P for 2-propanol, 1B for 1-butanol, iB for iso-butanol, 2B for 2-butanol, and tB for t-butanol. The water is represented by W.

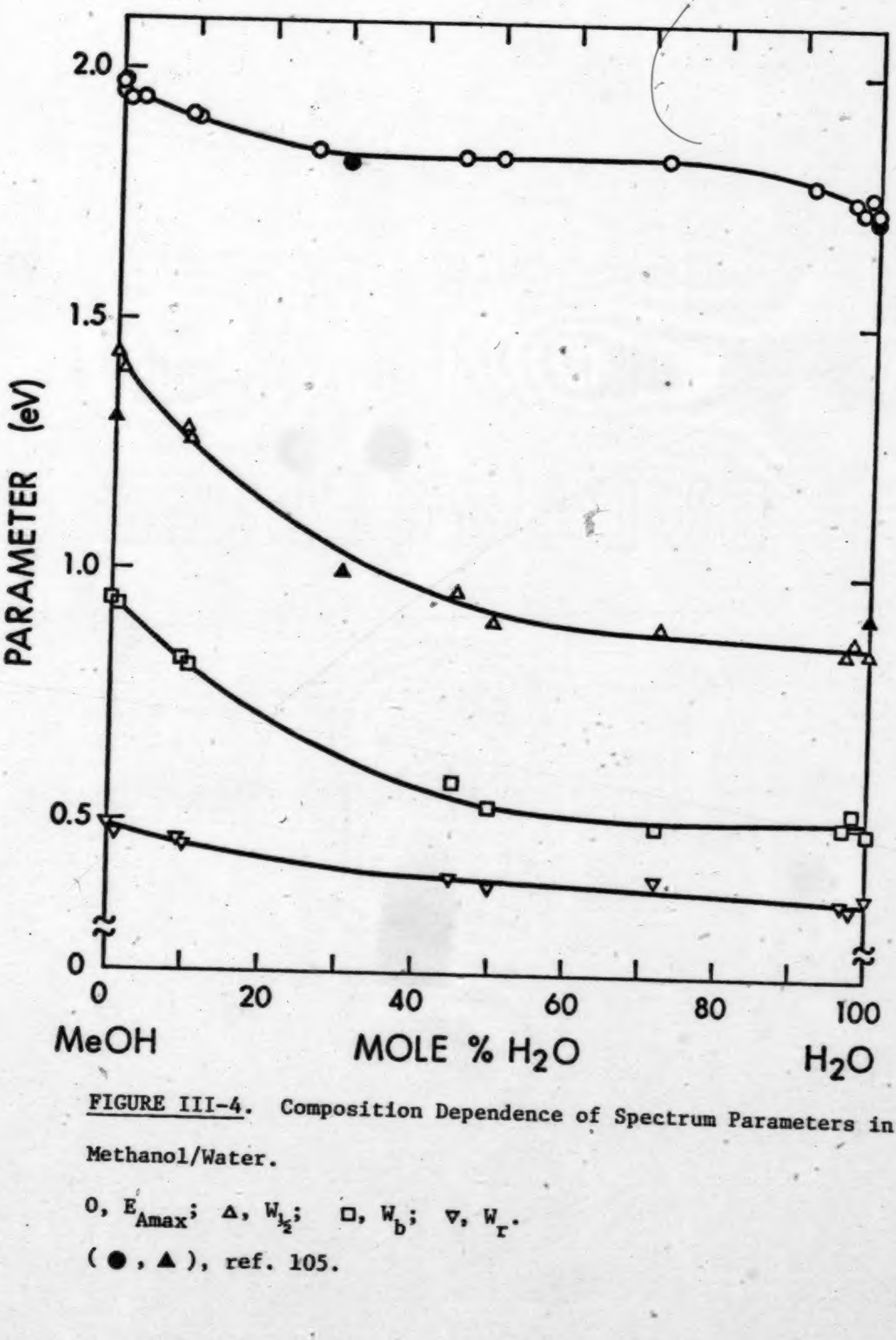

FIGURE III-4. Composition Dependence of Spectrum Parameters in Methanol/Water.

O, E_{Amax}; △, $W_{\frac{1}{2}}$; □, W_b; ▽, W_r.

(● , ▲), ref. 105.

(b) Ethanol/Water

Similar to the case of the methanol/water system, representative optical absorption spectra of solvated electrons in this system are shown in Figure III-5. The E_{Amax} of ethanol falls at 1.82 eV at 298K. The main body of the band is also moderately skewed towards high energy. Spectra obtained for its aqueous solutions are similar to that in ethanol. The E_{Amax} occur at lower energies than in ethanol, but in contrast to the case of methanol, do not decrease regularly as mole % of ethanol decreases. This irregularity is observed for 90 mole % of ethanol where E_{Amax} is the lowest.

Table III-2 shows the parameters obtained from a variety of ethanol/water mixtures which have been studied. These are plotted against composition of ethanol/water in Figure III-6, along with other values (105) from the literature for comparison. For the E_{Amax}, a trough is observed between 100 and 60 mole % of ethanol, in contrast to the curve for methanol/water. The behavior of $W_{\frac{1}{2}}$ as a function of composition is similar to the results in methanol/water mixtures, i.e., the constriction of $W_{\frac{1}{2}}$ due largely to the decreasing of W_b.

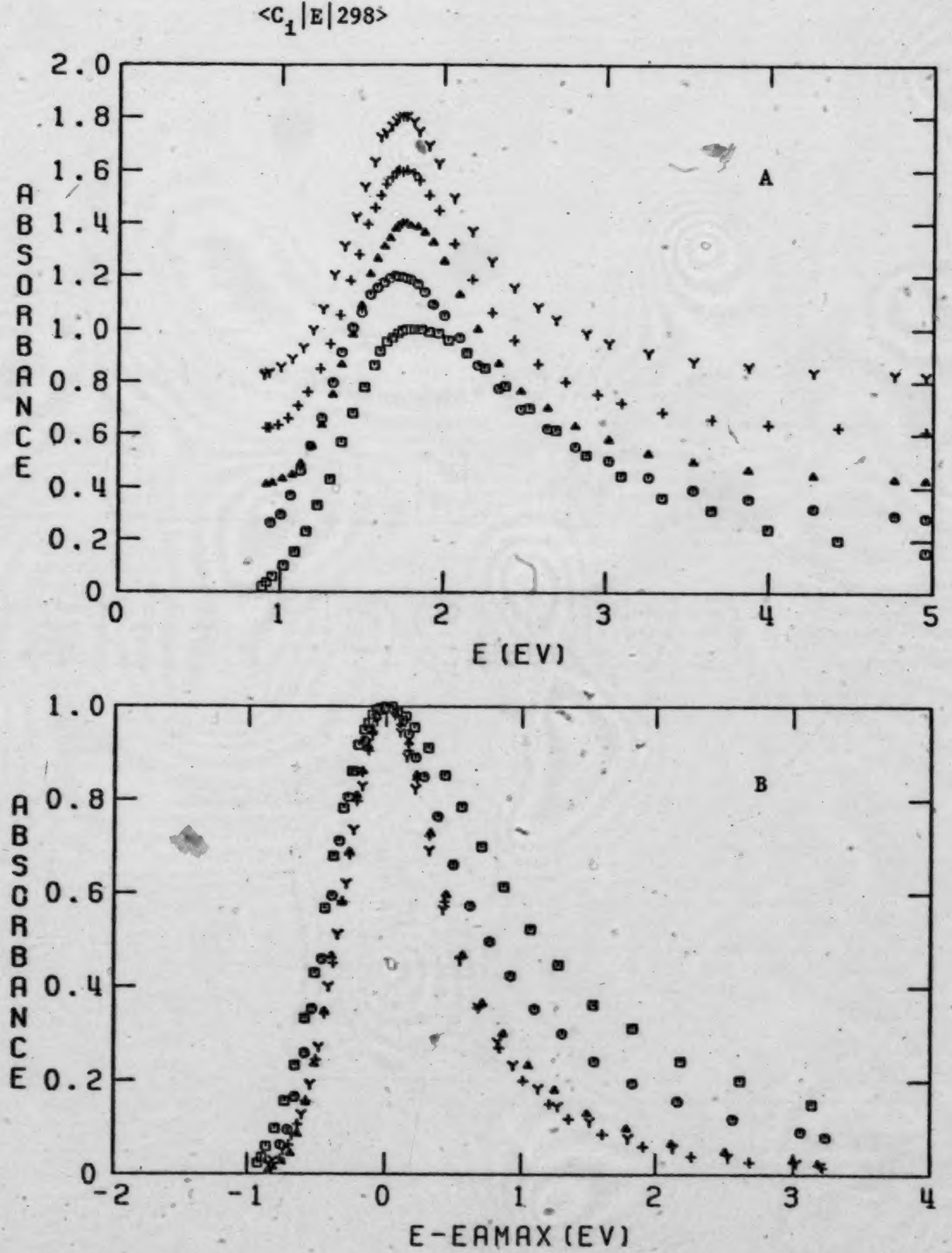

FIGURE III-5. The Optical Absorption Spectrum of Solvated Electrons in Ethanol/Water at 298K and Various Compositions.

A. Successive spectra are displaced vertically by 0.2 units.

B. The spectra are normalized at E_{Amax}. □, Ethanol; O, 10 % mole water; △, 50 mole % water; +, 98 % mole water; Y, water.

TABLE III-2

Parameters of Solvated Electrons in Ethanol/Water at 298K

	Code No.	Composition Mole % Water	E_{Amax} eV	$W_{\frac{1}{2}}$ eV	W_r eV	W_b eV	W_b/W_r
Z6,	J16	0.0	1.82	1.59	0.51	1.08	2.12
	J17	0.3	1.80				
	J18	1.0	1.77				
	J19	2.9	1.75	1.47	0.52	0.95	1.83
	J20	9.2	1.72				
Z31,		10.0	1.71	1.19	0.45	0.74	1.64
	J21	22.9	1.74				
	J22	37.3	1.77	0.94	0.40	0.54	1.35
Z36,		50.0	1.77	0.91	0.37	0.54	1.46
	J23	66.3	1.79	0.86	0.33	0.53	1.61
	J24	92.4	1.76				
	J25	97.0	1.77	0.85	0.36	0.49	1.36
Z39,	J26	98.0	1.75	0.88	0.36	0.52	1.44
	J27	99.0	1.75				
	J28	99.7	1.75				
Z152,	J15	100.	1.73	0.85	0.36	0.49	1.36

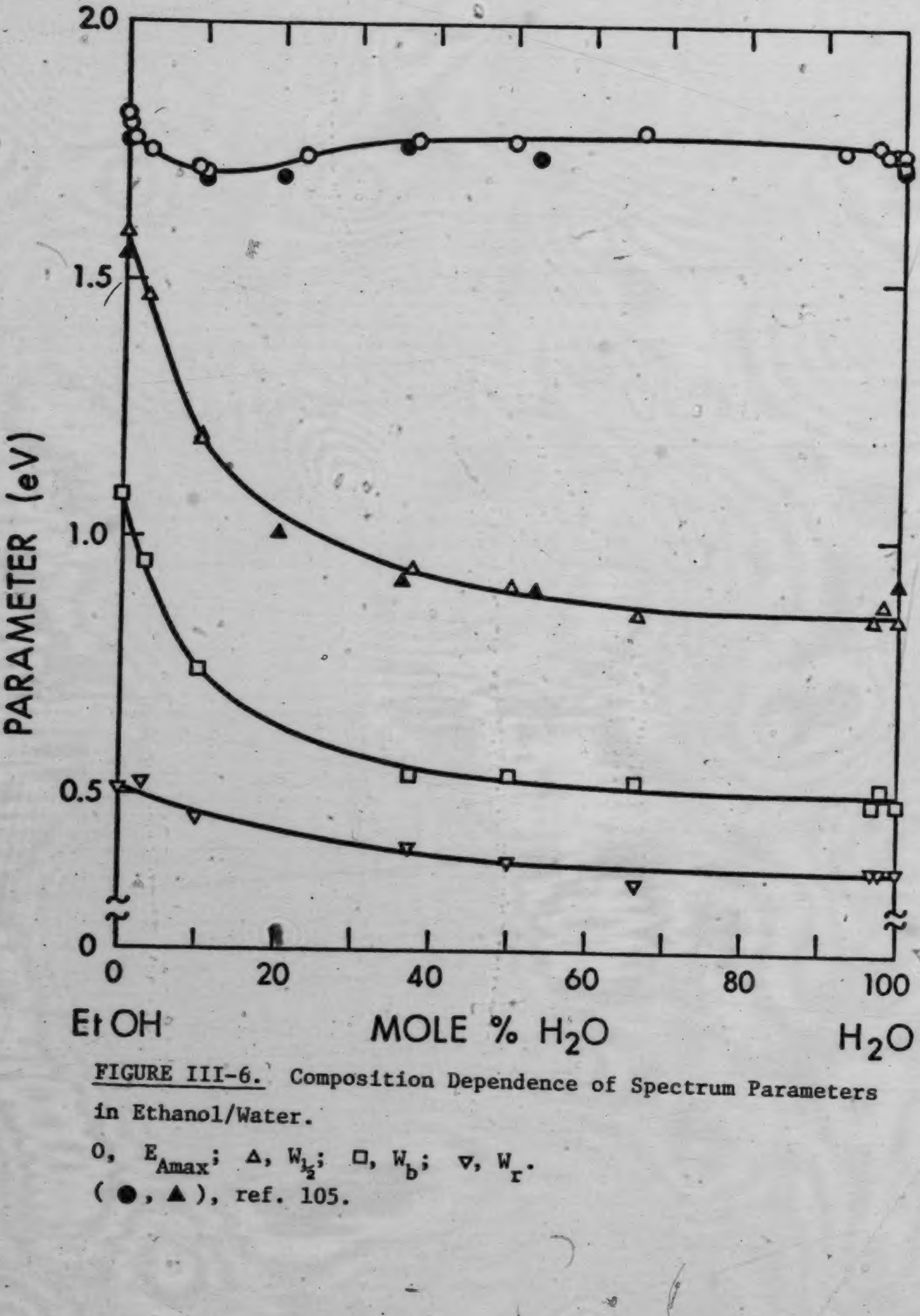

FIGURE III-6. Composition Dependence of Spectrum Parameters in Ethanol/Water.

O, E_{Amax}; △, $W_{\frac{1}{2}}$; □, W_b; ▽, W_r.

(●, ▲), ref. 105.

(c) 1-Propanol/Water

Figure III-7 shows representative optical absorption spectra of solvated electrons from a variety of studies of 1-propanol/water mixtures. The absorption maximum of 1-propanol falls at 1.95 eV at 298K. Spectra obtained for the aqueous solutions are similar to that in 1-propanol. The relation of E_{Amax} to mole % composition is similar to that found for ethanol, with the lowest E_{Amax} at 90 mole % of 1-propanol. Figure III-7-B shows that the skew in the high energy side of the spectra decreases as mole % of water increases to 50.

The parameters obtained from Figure III-7 as well as those obtained from studies of other compositions are listed in Table III-3 and plotted against composition of 1-propanol/water in Figure III-8. A trough is again observed between 100 and 60 mole % of 1-propanol. The behavior of $W_{\frac{1}{2}}$ as a function of composition is similar to the results in ethanol/water. The constriction of $W_{\frac{1}{2}}$ is also due mainly to the decreasing of W_b.

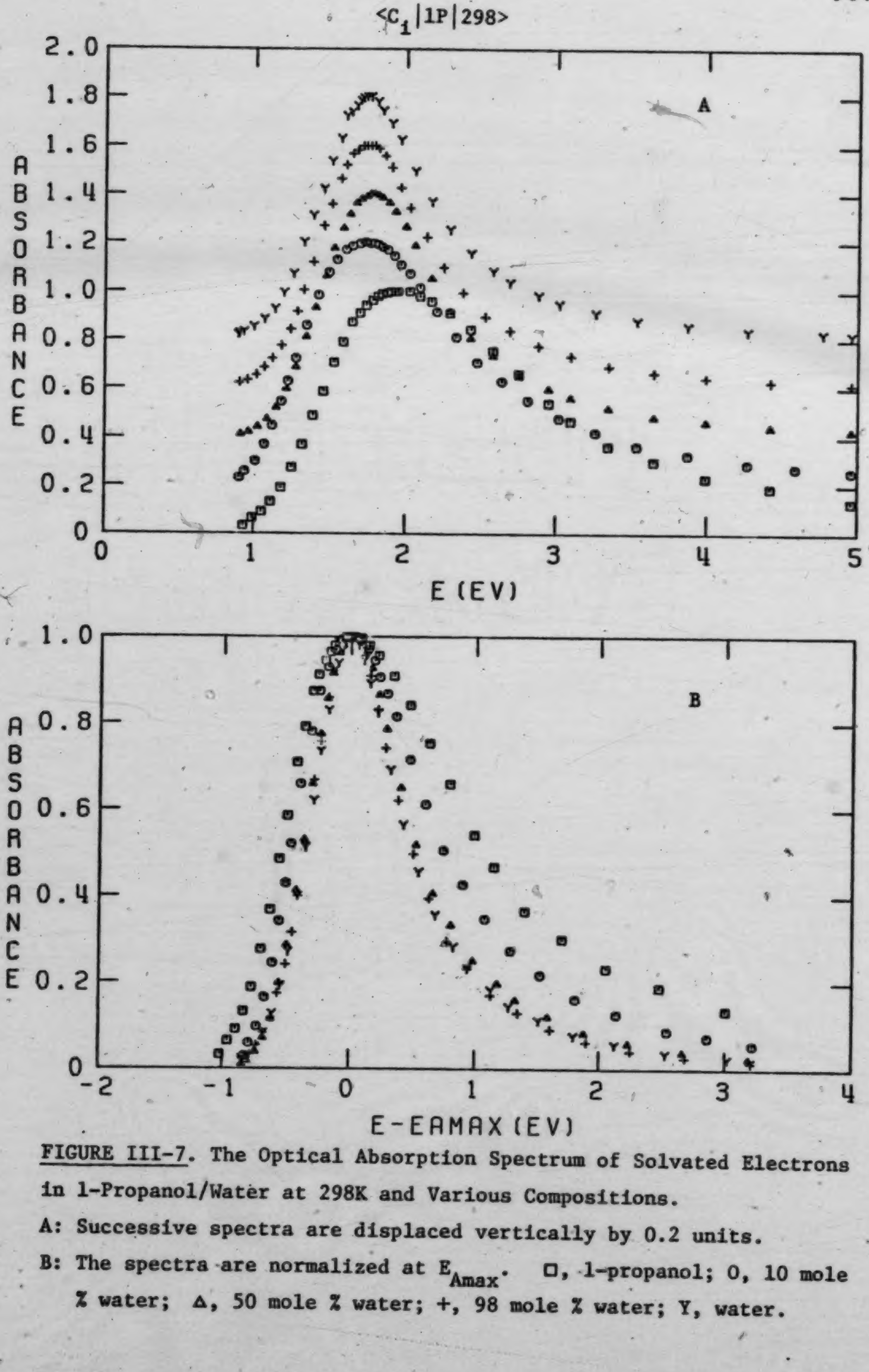

FIGURE III-7. The Optical Absorption Spectrum of Solvated Electrons in 1-Propanol/Water at 298K and Various Compositions.

A: Successive spectra are displaced vertically by 0.2 units.

B: The spectra are normalized at E_{Amax}. □, 1-propanol; O, 10 mole % water; Δ, 50 mole % water; +, 98 mole % water; Y, water.

TABLE III-3

Parameters of Solvated Electrons in 1-Propanol/Water at 298K

Code No.	Composition Mole % Water	E_{Amax} eV	$W_{\frac{1}{2}}$ eV	W_r eV	W_b eV	W_b/W_r
Z7, L1	0.0	1.95	1.63	0.52	1.11	2.13
L2	0.3	1.92	1.55	0.50	1.05	2.10
L3	1.0	1.88	1.53	0.50	1.03	2.06
Z75, L4	3.0	1.83	1.46	0.49	0.97	1.98
Z76	6.0	1.76	1.37	0.45	0.92	2.04
Z59, L5	10.0	1.71	1.24	0.46	0.78	1.70
Z78	15.0	1.74	1.15	0.44	0.71	1.61
Z79	20.0	1.75	1.11	0.44	0.67	1.52
Z80, L6	30.0	1.78	1.03	0.42	0.61	1.45
Z51	50.0	1.77	0.92	0.38	0.54	1.42
L7	60.0	1.79	0.88	0.35	0.53	1.51
L8	90.0	1.80	0.84	0.37	0.47	1.27
L9	97.0	1.78	0.85	0.38	0.47	1.24
Z57	98.0	1.75	0.87	0.37	0.50	1.35
L10	99.0	1.76	0.84	0.36	0.48	1.33
Z152, L11	100.	1.73	0.85	0.36	0.49	1.36

L(code) = Preliminary data for 1-propanol only.

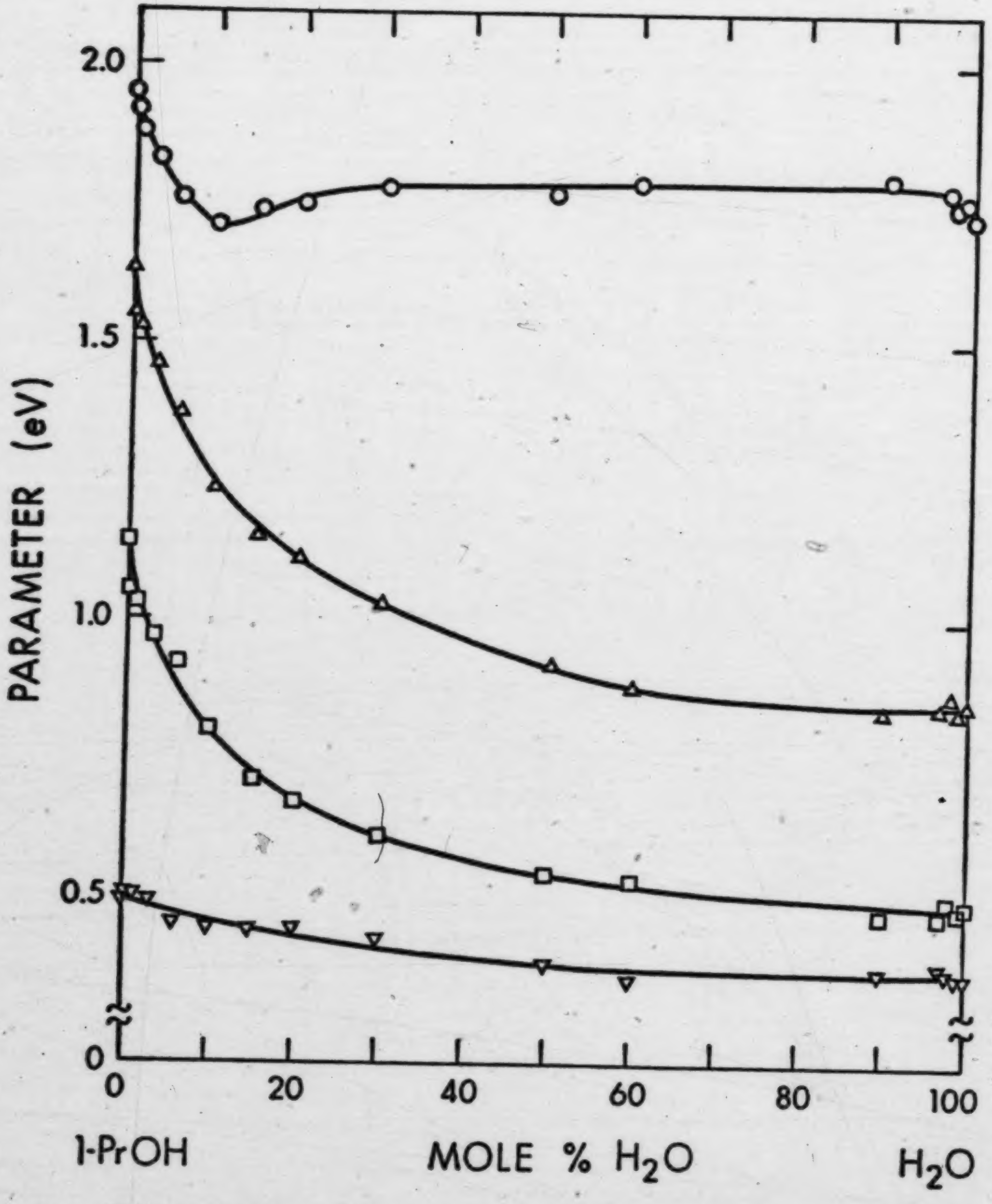

FIGURE III-8. Composition Dependence of Spectrum Parameters in 1-Propanol/Water.

O, E_{Amax}; △, $W_{\frac{1}{2}}$; □, W_b; ▽, W_r.

(d) 2-Propanol/Water

In light of the above three cases, representative optical absorption spectra of solvated electrons in 2-propanol and its aqueous solutions are shown in Figure III-9. The E_{Amax} of 2-propanol falls at 1.54 eV at 298K. Spectra obtained for its water mixtures are similar to that in 2-propanol. The E_{Amax} occur at higher energies than in 2-propanol, in contrast to the methanol, ethanol and 1-propanol systems. There is another contrast in the low energy side of the spectra, revealed in Figure III-9-B. The low energy sides line up almost exactly. The high energy sides again show a decrease in skewness as mole % of 2-propanol decreases, but with a more pronounced change between pure alcohol and the 90 mole % solution.

Parameters obtained from the study of various compositions of this system are listed in Table III-4. These are plotted against composition of 2-propanol/water in Figure III-10. Values (105) from the literature are included in the Figure. The E_{Amax} increases gradually as mole % water increases to 50 then levels off. Although the $W_{\frac{1}{2}}$ again constricts as mole % of water increases, the constriction now occurs very sharply as mole % of water increases to 10, then gradually as mole % increases from 10 to 50. However, the constriction of $W_{\frac{1}{2}}$ is similar to those in the other systems and is again due mainly to the decreasing of W_b.

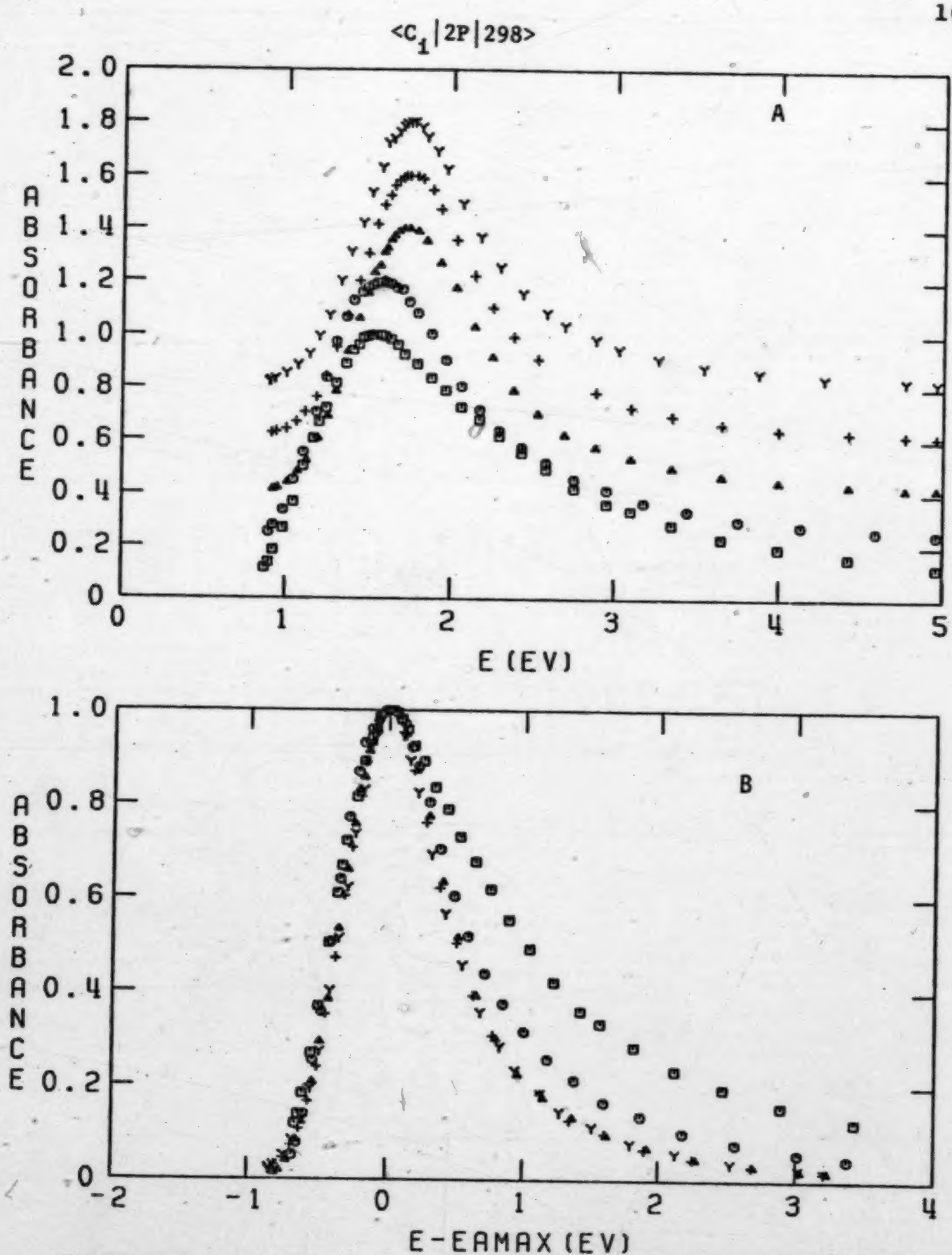

FIGURE III-9. The Optical Absorption Spectrum of Solvated Electrons in 2-Propanol/Water at 298K and Various Compositions.

A: Successive spectra are displaced vertically by 0.2 units.

B: The spectra are normalized at E_{Amax}.

□, 2-propanol; O, 10 mole % water; Δ, 50 mole % water; +, 98 mole % water; Y, water.

TABLE III-4

Parameters of Solvated Electrons in 2-Propanol/Water at 298K

Code No.	Composition Mole % Water	E_{Amax} eV	$W_{\frac{1}{2}}$ eV	W_r eV	W_b eV	W_b/W_r
Z8	0.0	1.52	1.45	0.44	1.01	2.30
Z81	3.0	1.54	1.12	0.42	0.70	1.67
Z82	6.0	1.56	1.04	0.40	0.64	1.60
Z65, Z83	10.0	1.58	1.00	0.40	0.60	1.50
Z84	15.0	1.61	0.99	0.39	0.60	1.54
Z85	20.0	1.64	0.96	0.40	0.56	1.40
Z86	30.0	1.68	0.95	0.39	0.56	1.44
Z67	50.0	1.73	0.91	0.37	0.54	1.46
Z72	98.0	1.75	0.86	0.36	0.50	1.39
Z152	100.	1.73	0.85	0.36	0.49	1.36

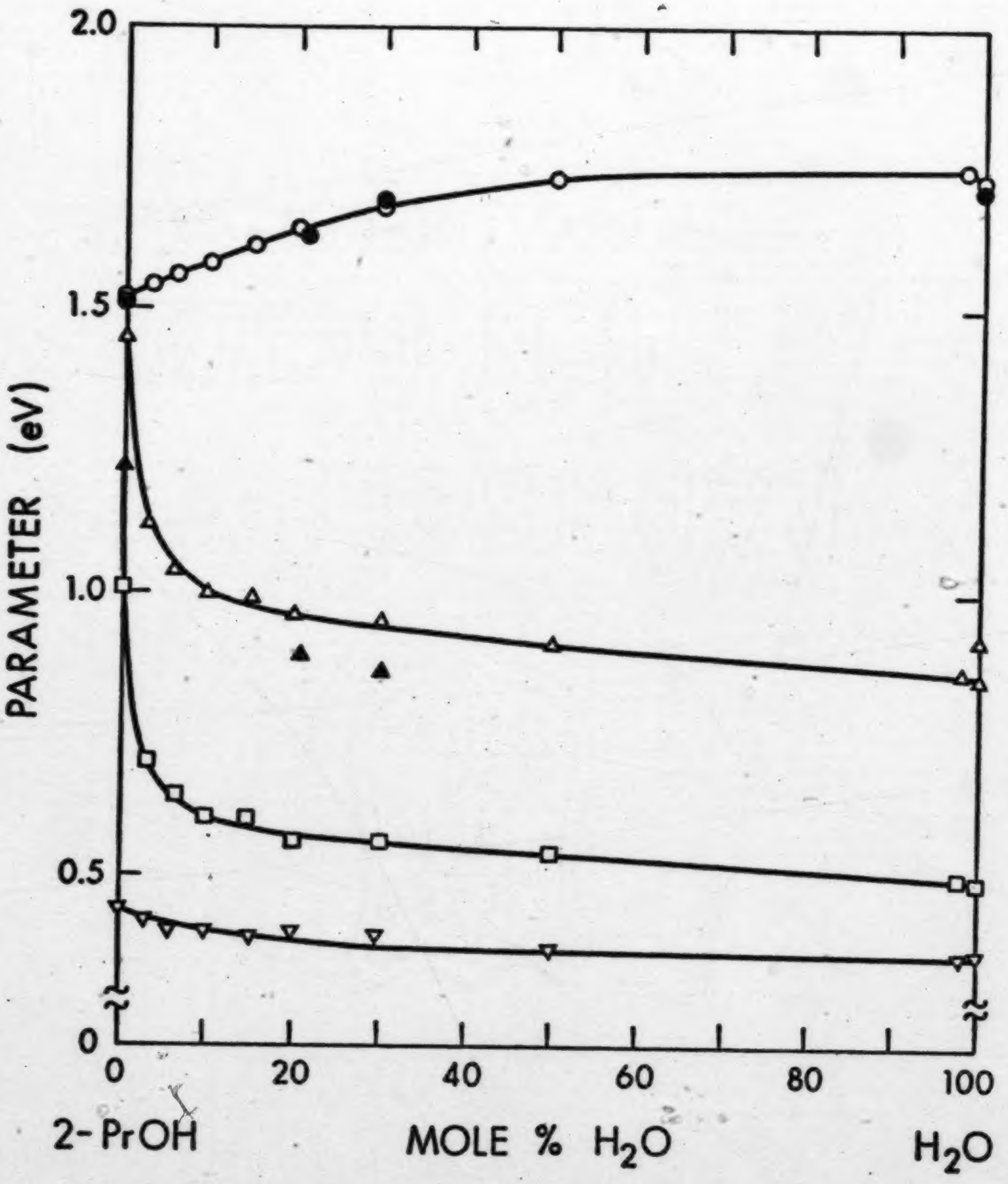

FIGURE III-10. Composition Dependence of Spectrum Parameters in 2-Propanol/Water.

O, E_{Amax}; △, $W_{\frac{1}{2}}$; □, W_b; ▽, W_r.

(●, ▲), ref. 105.

(e) 1-Butanol/water

Spectra obtained for solvated electrons in 1-butanol and its water mixtures are shown in Figure III-11. The E_{Amax} of 1-butanol falls at 1.98 eV at 298K. The spectra of solvated electrons in the aqueous solutions are similar to that in 1-butanol. The values of E_{Amax} are lower than in 1-butanol. The relation of E_{Amax} to mole % composition is similar to that found for ethanol, and 1-propanol, with the lowest E_{Amax} observed for 90 mole % of 1-butanol. Figure III-11-B shows that the skew in the high energy side of the spectra decreases as mole % water increases to 50. On the low energy side the shapes are quite similar.

The parameters obtained from Figure III-11 are listed in Table III-5 and are plotted against composition of 1-butanol/water in Figure III-12. A trough is again observed between 100 and 60 mole % of 1-butanol. The behavior of $W_{\frac{1}{2}}$ as a function of composition is similar to the results in ethanol (1-propanol)/water. The constriction of $W_{\frac{1}{2}}$ is again due mainly to the decreasing of W_b.

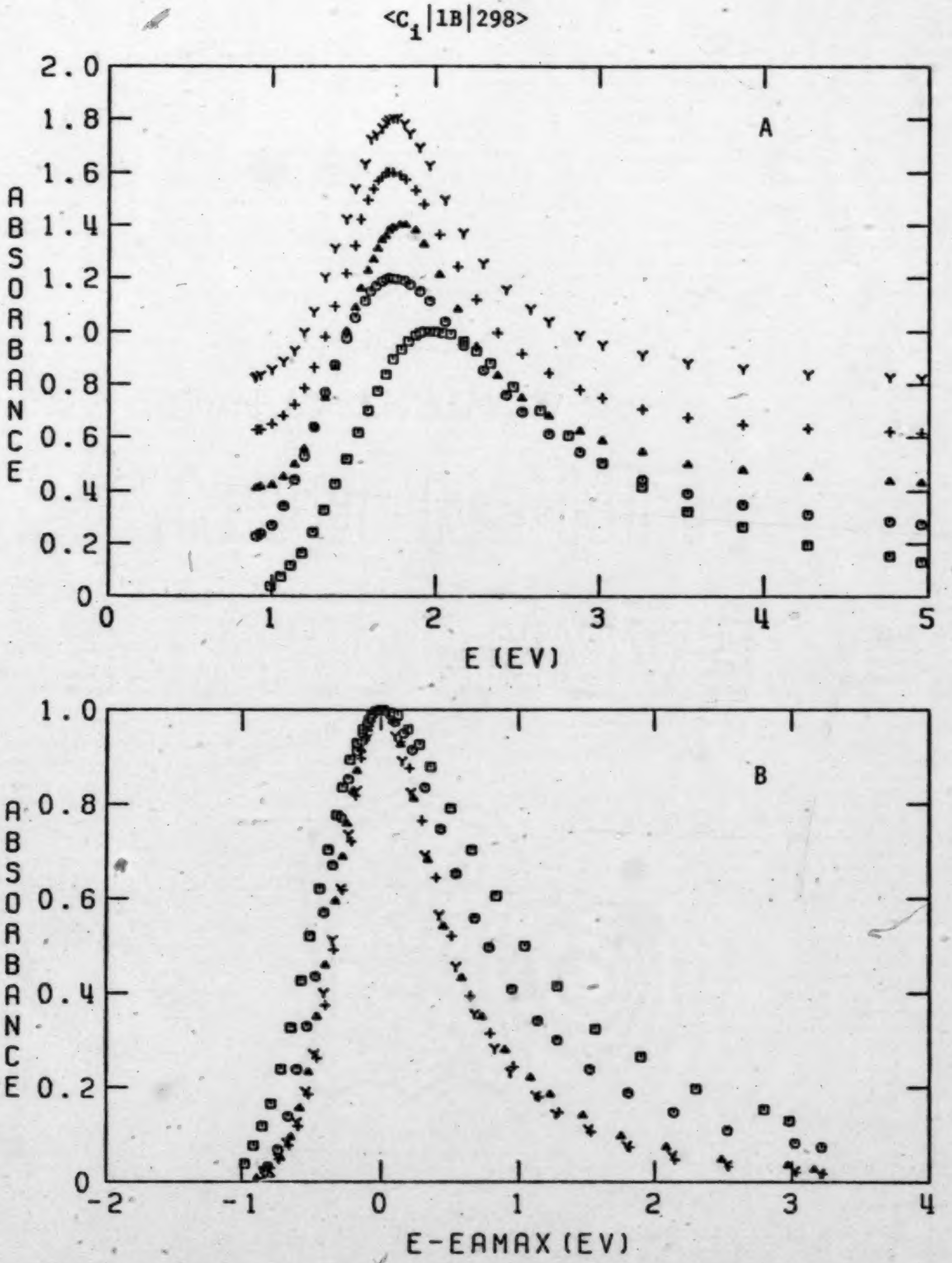

FIGURE III-11. The Optical Absorption Spectrum of Solvated Electrons in 1-Butanol/Water at 298K and Various Compositions.

A: Successive spectra are displaced vertically by 0.2 units

B: The spectra are normalized at E_{Amax}. □, 1-Butanol, O, 10 mole % water; △, 50 mole % water; +, 98 mole % water; Y, water.

TABLE III-5

Parameters of Solvated Electrons in 1-Butanol/Water at 298K

Code No.	Composition Mole % Water	E_{Amax} eV	$W_{\frac{1}{2}}$ eV	W_r eV	W_b eV	W_b/W_r
Z9	0.0	1.98	1.57	0.53	1.04	1.96
Z126	10.0	1.73	1.23	0.45	0.78	1.73
Z148	50.0	1.79	0.88	0.36	0.52	1.44
Z122	98.0	1.74	0.88	0.36	0.52	1.44
Z 152	100.	1.73	0.85	0.36	0.49	1.36

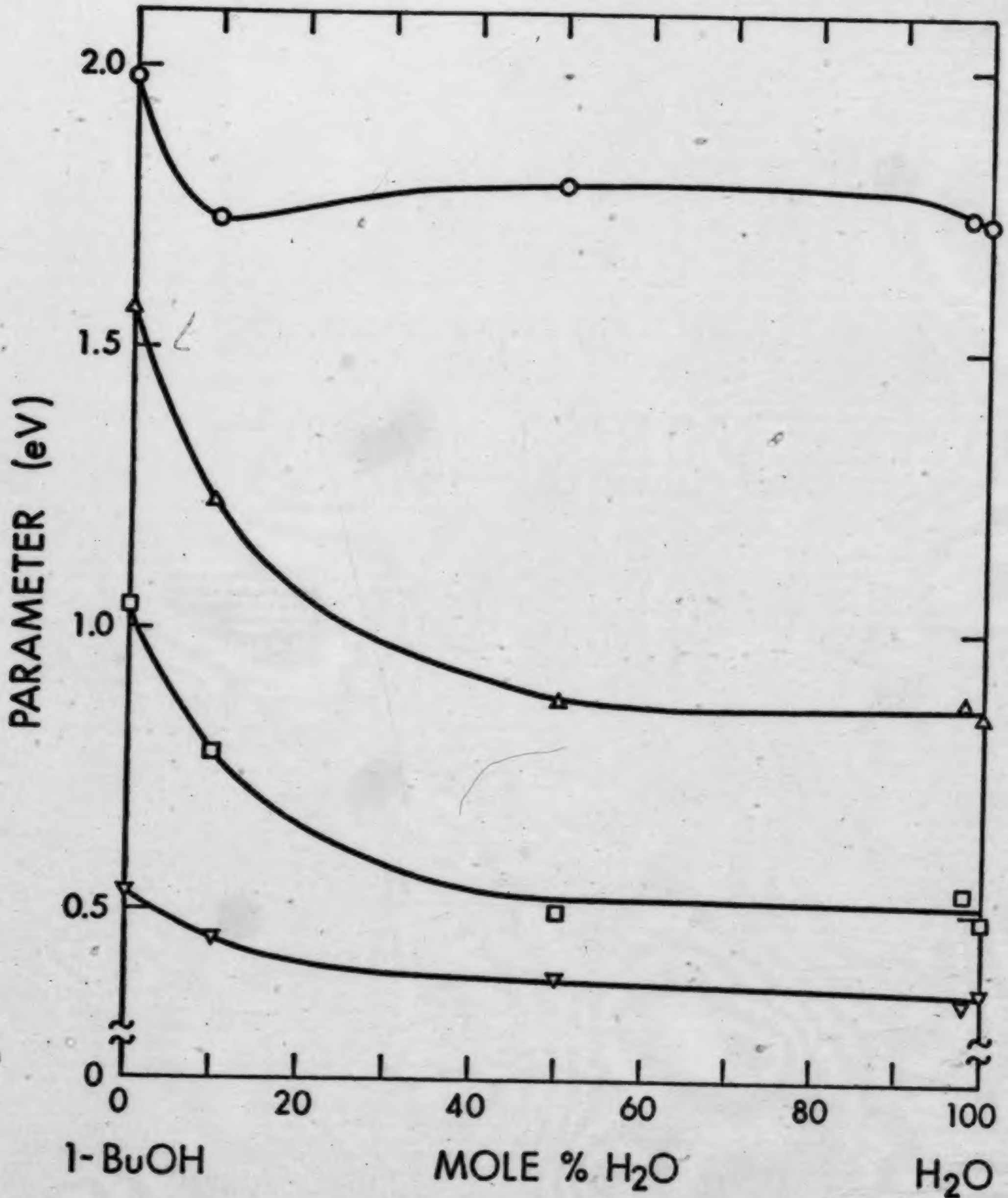

FIGURE III-12. Composition Dependence of Spectrum Parameters in 1-Butanol/Water.

O, E_{Amax}; △, $W_{½}$; □, W_b; ▽, W_r.

(f) Iso-Butanol (2-Methyl-1-propanol)/Water

The optical absorption spectra of solvated electrons in iso-butanol and its water mixtures are shown in Figure III-13. The E_{Amax} of iso-butanol falls at 1.97 eV at 298K. Spectra obtained for its aqueous solutions are similar to that in iso-butanol. The E_{Amax} occur at lower energies than in iso-butanol. The relation of E_{Amax} to mole % composition is similar to the ethanol, 1-propanol, and 1-butanol systems, with the lowest E_{Amax} observed for 90 mole % of iso-butanol. Figure III-13-B shows that the skew in the high energy side of the spectra decreases as mole % water increases to 50. On the low energy side the shapes are quite similar.

The parameters obtained from Figure III-13, which are listed in Table III-6, are plotted against composition of iso-butanol/water in Figure III-14. A trough is again observed between 100 and 60 mole % of iso-butanol. The behavior of $W_{\frac{1}{2}}$ as a function of composition is similar to the results in ethanol (1-propanol, 1-butanol)/water. The constriction of $W_{\frac{1}{2}}$ is again due mainly to the decreasing of W_b.

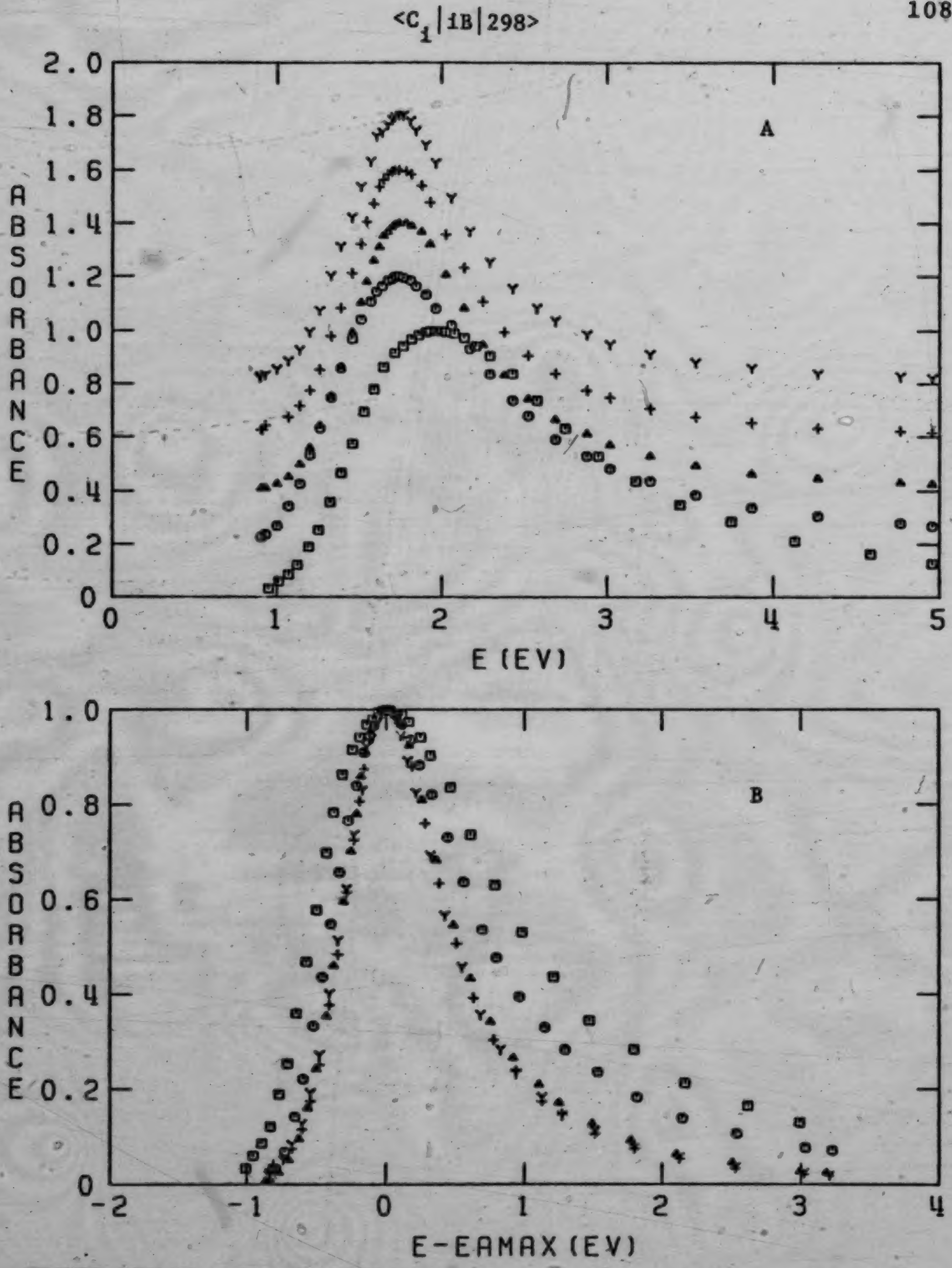

FIGURE III-13. The Optical Absorption Spectrum of Solvated Electrons in iso-Butanol/Water at 298K and Various Compositions.

A: Successive spectra are displaced vertically by 0.2 units.

B: The spectra are normalized at E_{Amax}. □, iso-Butanol; O, 10 mole % water; △, 50 mole % water; +, 98 mole % water; Y, water.

TABLE III-6

Parameters of Solvated Electrons in iso-Butanol/Water at 298K

Code No.	Composition Mole % Water	E_{Amax} eV	$W_{1/2}$ eV	W_r eV	W_b eV	W_b/W_r
Z10	0.0	1.97	1.61	0.57	1.04	1.82
Z131	10.0	1.73	1.18	0.43	0.75	1.74
Z145	50.0	1.78	0.89	0.36	0.53	1.47
Z118	98.0	1.75	0.86	0.35	0.51	1.46
Z152	100.	1.73	0.85	0.36	0.49	1.36

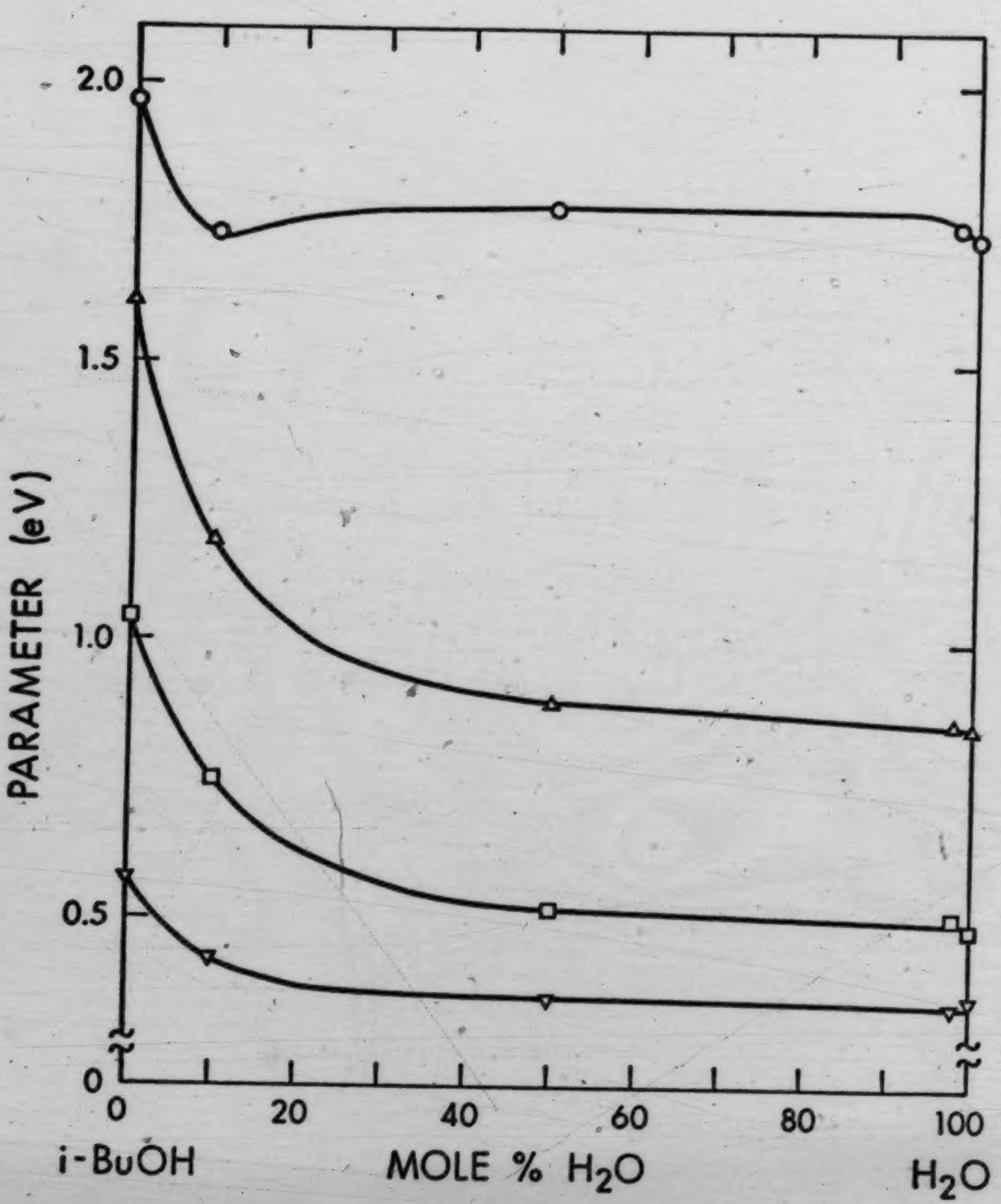

FIGURE III-14. Composition Dependence of Spectrum Parameters in iso-Butanol/Water.

O, E_{Amax}; △, $W_{½}$; □, W_b; ▽, W_r.

(g) 2-Butanol (sec-Butyl Alcohol)/Water

Spectra obtained for solvated electrons in 2-butanol and its water mixtures are shown in Figure III-15. The E_{Amax} of 2-butanol falls at 1.59 eV at 298K. The spectra of solvated electrons in the aqueous solutions are similar to that in 2-butanol. The E_{Amax} occur at higher energies than in 2-butanol. This is similar to that found for 2-propanol, but differs from the case of either methanol/water or ethanol (1-propanol, 1-butanol, isobutanol)/water. From Figure III-15-B, it can be seen that the shapes of low energy side spectra line up almost exactly and that the high energy sides again show a decrease in skewness as mole % 2-butanol decreases, but with a more pronounced change between pure alcohol and the 90 mole % solution. This is again similar to 2-propanol and again differs from others.

The parameters obtained from Figure III-15, which are listed in Table III-7, are plotted against composition of 2-butanol/water in Figure III-16. The E_{Amax} increases gradually as mole % water increases to 50, then levels off. This behavior is similar to that found for 2-propanol. Although the $W_{\frac{1}{2}}$ again constricts as mole % water increases, the constriction now occurs very sharply as mole % of water increases to 10, then gradually as mole % increases from 10 to 50. However, the constriction of $W_{\frac{1}{2}}$ is again mainly due to the decreasing of W_b.

<C$_i$|2B|298>

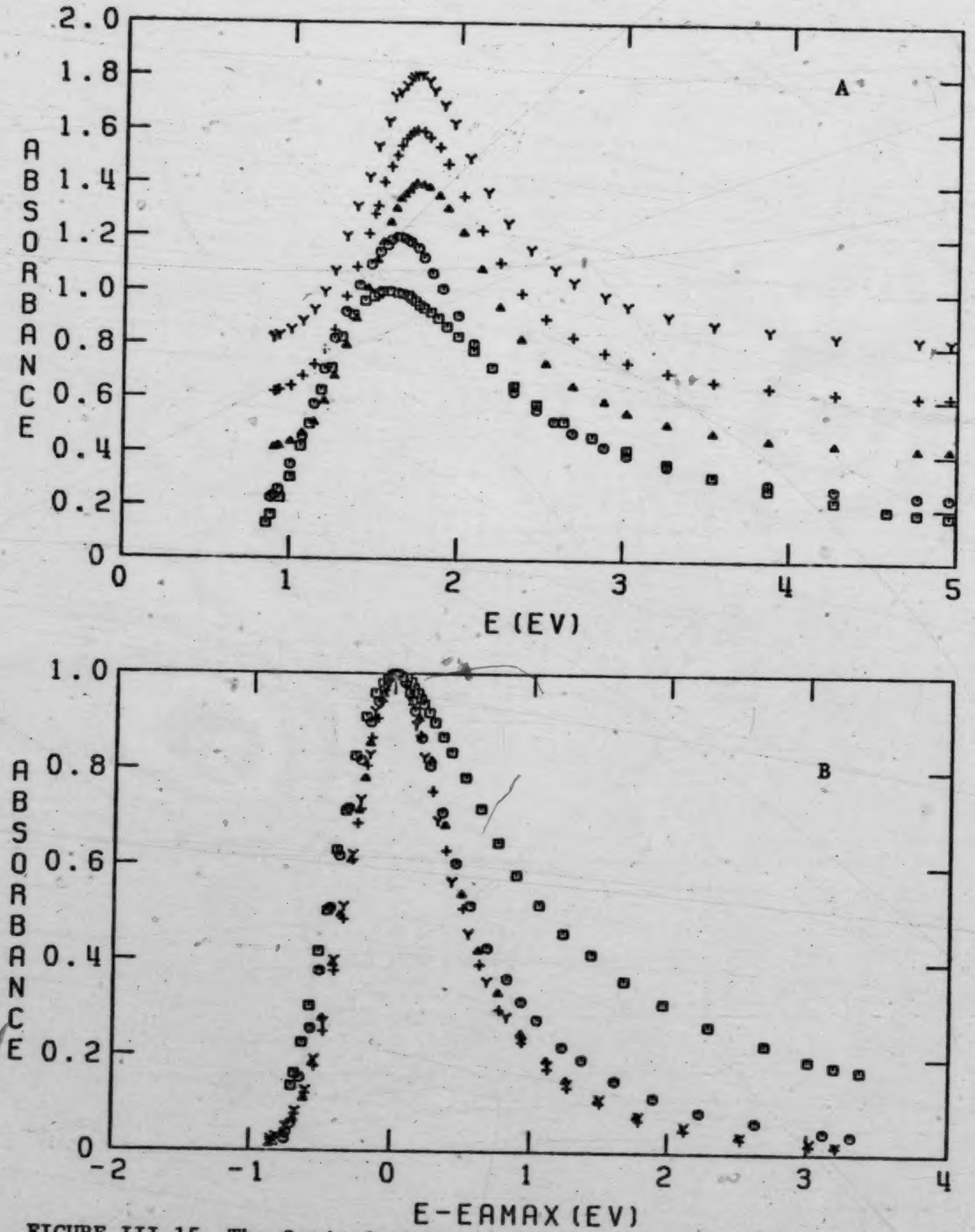

FIGURE III-15. The Optical Absorption Spectrum of Solvated Electrons in 2-Butanol/Water at 298K and Various Compositions.

A: Successive spectra are displaced vertically by 0.2 units.

B: The spectra are normalized at E_{Amax}. □, 2-Butanol; O, 10 mole % water; △, 50 mole % water; + 98 mole % water; Y, water.

TABLE III-7

Parameters of Solvated Electrons in 2-Butanol/Water at 298K

Code No.	Composition Mole % Water	E_{Amax} eV	$W_{1/2}$ eV	W_r eV	W_b eV	W_b/W_r
Z156	0.0	1.59	1.57	0.47	1.10	2.34
Z136	10.0	1.65	1.04	0.46	0.58	1.26
Z140	50.0	1.76	0.89	0.36	0.53	1.47
Z114	98.0	1.75	0.86	0.35	0.51	1.46
Z152	100.	1.73	0.85	0.36	0.49	1.36

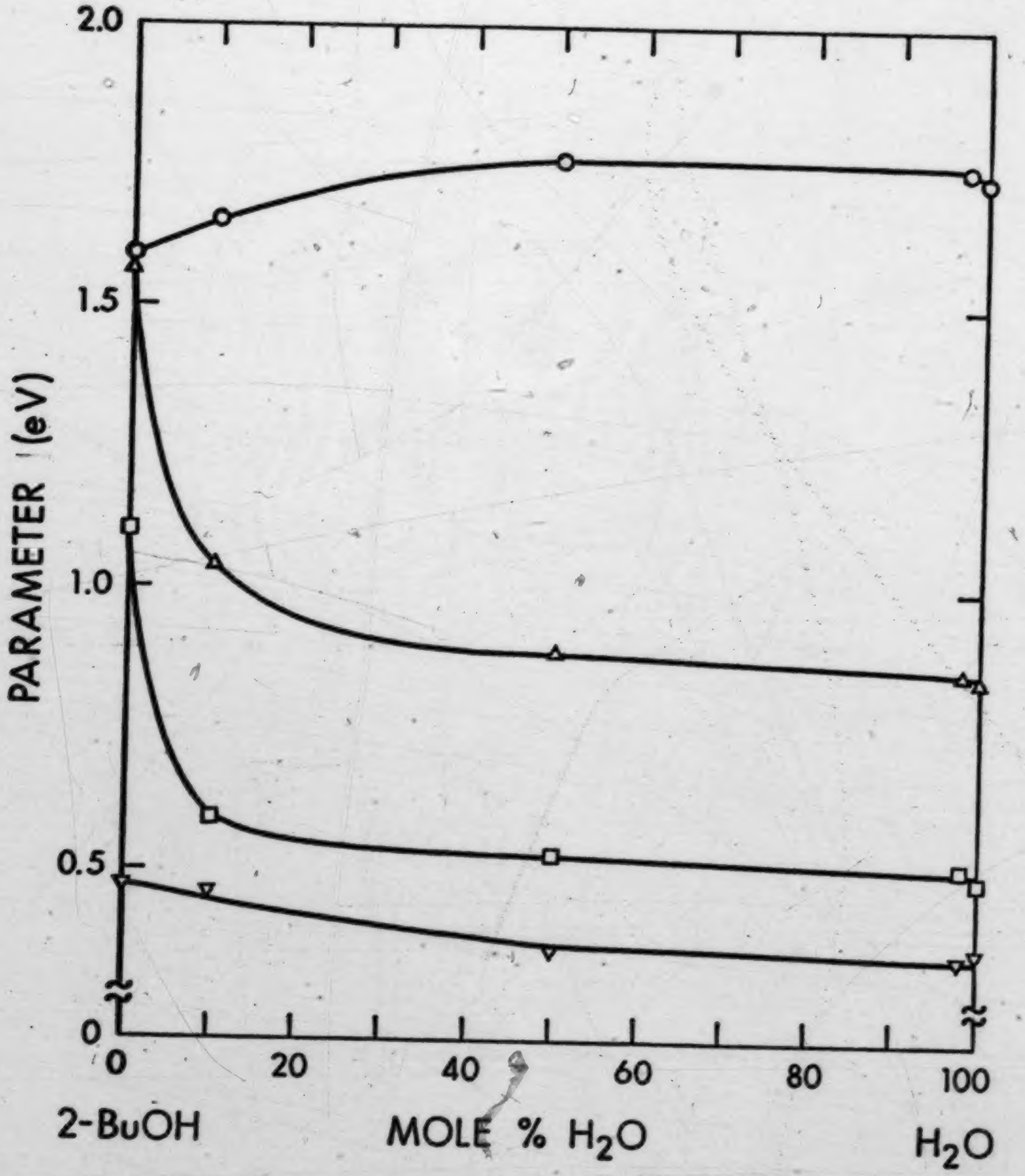

FIGURE III-16. Composition Dependence of Spectrum Parameters in 2-Butanol/Water.

O, E_{Amax}; △, $W_{\frac{1}{2}}$; □, W_b; ▽, W_r.

(h) tert-Butanol (2-Methyl-2-propanol)/Water

The optical absorption spectra for solvated electrons in tert-butanol and its aqueous solutions are shown in Figure III-17. The E_{Amax} of tert-butanol falls at 1.20 eV at 298K. The band is less skewed than are those for the primary alcohols. Spectra obtained for its water mixtures are similar to that in tert-butanol. The E_{Amax} occur at higher energies than in tert-butanol. This is similar to that found for 2-propanol (2-butanol), but differs from others. From Figure III-17-B, it can be seen that the shapes of both low energy side and high energy side spectra line up almost exactly. This differs entirely from either the secondary or the primary alcohols.

The parameters obtained from Figure III-17 are listed in Table III-8 and are plotted against composition of tert-butanol/water in Figure III-18. The E_{Amax} increases sharply as mole % water increases to 50 and gradually to 100. The $W_{\frac{1}{2}}$ constricts very slightly as mole % water increases. These behaviors differ from all other alcohols in this study.

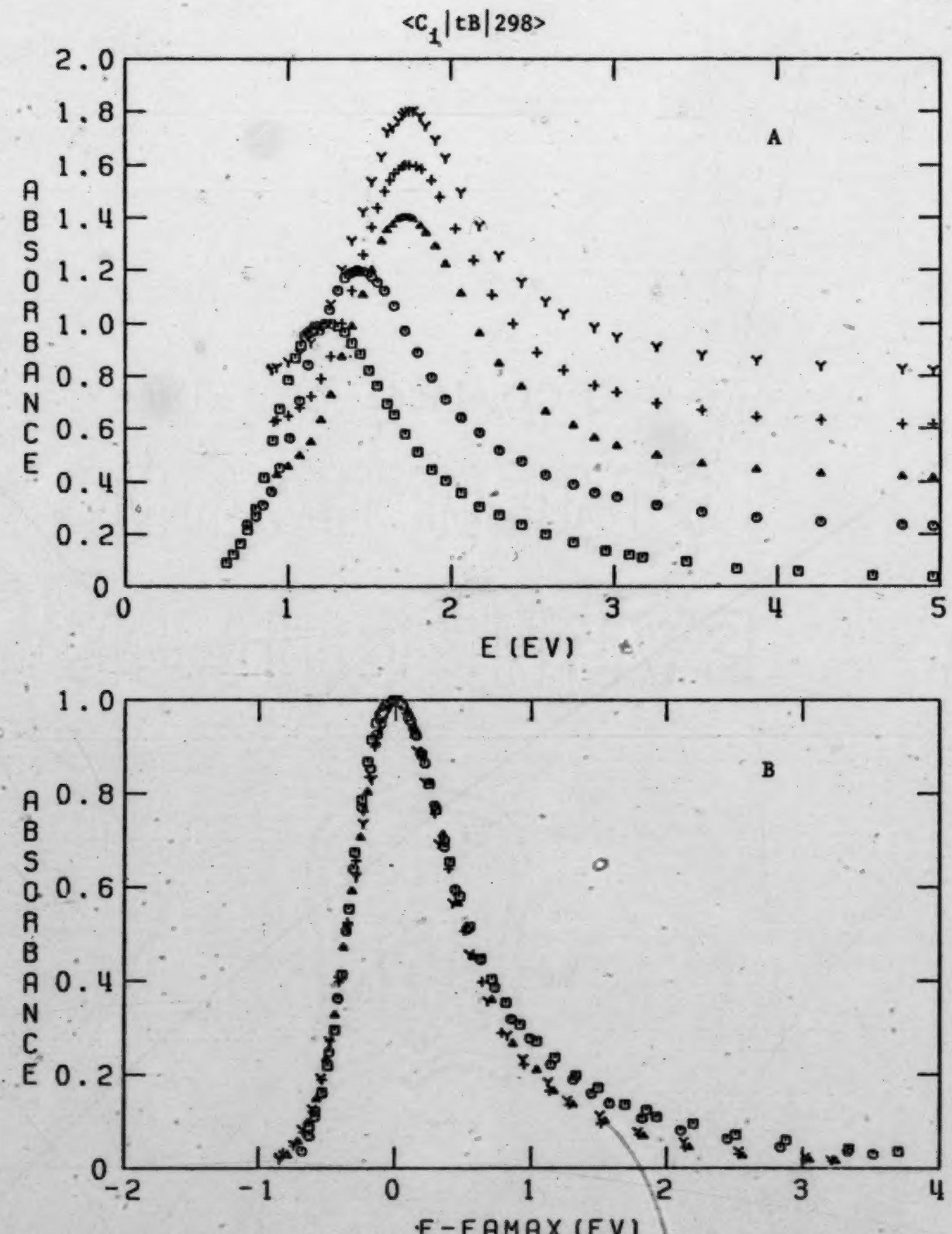

FIGURE III-17. The Optical Absorption Spectrum of Solvated Electrons in tert-Butanol/Water at 298K and Various Compositions.

A: Successive spectra are displaced vertically by 0.2 units.

B: The spectra are normalized at E_{Amax}. □, t-Butanol; O, 10 mole % water; △, 50 mole % water; +, 98 mole % water; Y, water.

TABLE III-8

Parameters of Solvated Electrons in t-Butanol/Water at 298K

Code No.	Composition Mole % Water	E_{Amax} eV	$W_{1/2}$ eV	W_r eV	W_b eV	W_b/W_r
Z157	0.0	1.20	0.93	0.37	0.56	1.51
Z103	10.0	1.44	0.94	0.37	0.57	1.54
Z158	50.0	1.71	0.89	0.37	0.52	1.41
Z110	98.0	1.75	0.88	0.36	0.52	1.44
Z152	100.	1.73	0.85	0.36	0.49	1.36

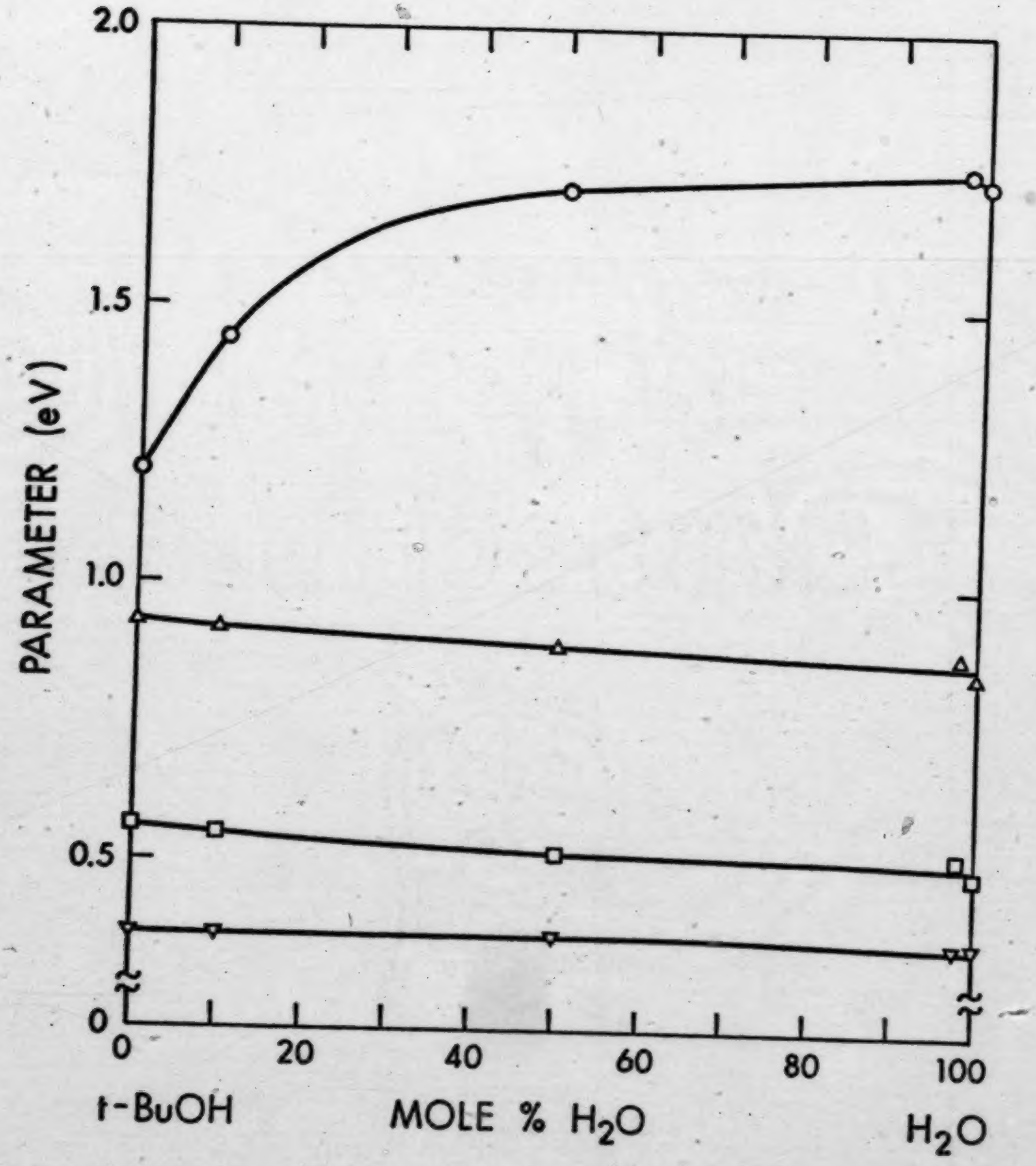

FIGURE III-18. Composition Dependence of Spectrum Parameters in t-Butanol/Water.

O, E_{Amax}; Δ, $W_{½}$; □, W_b; ▽, W_r.

Summary

The optical absorption spectra for solvated electrons in alcohol/water mixtures are skewed towards high energy. The skew decreases as the mole % of water increases.

Three types of curve were observed for the relation of E_{Amax} to composition (Figure III-19):

(i) For methanol, E_{Amax} decreases gradually as mole % water increases to 50, and is approximately constant until 95, then decreases again;

(ii) For the primary alcohols (ethanol, 1-propanol, 1-butanol, iso-butanol), E_{Amax} decreases rapidly to a minimum at around 10 mole % water, then increases rapidly to around 30 mole % water, followed by a gradual increase until 50 mole %. After 50 mole % water, it behaves as in (i);

(iii) For the case of secondary (2-propanol, 2-butanol) and tertiary (tert-butanol) alcohols, E_{Amax} is at its lowest for pure alcohol, then increases sharply as mole % water increases to 50, and gradually until 95 where it again behaves as in (i). In the region of 0 to 50 mole % water, however, the increase is more pronounced for tertiary than for secondary alcohol.

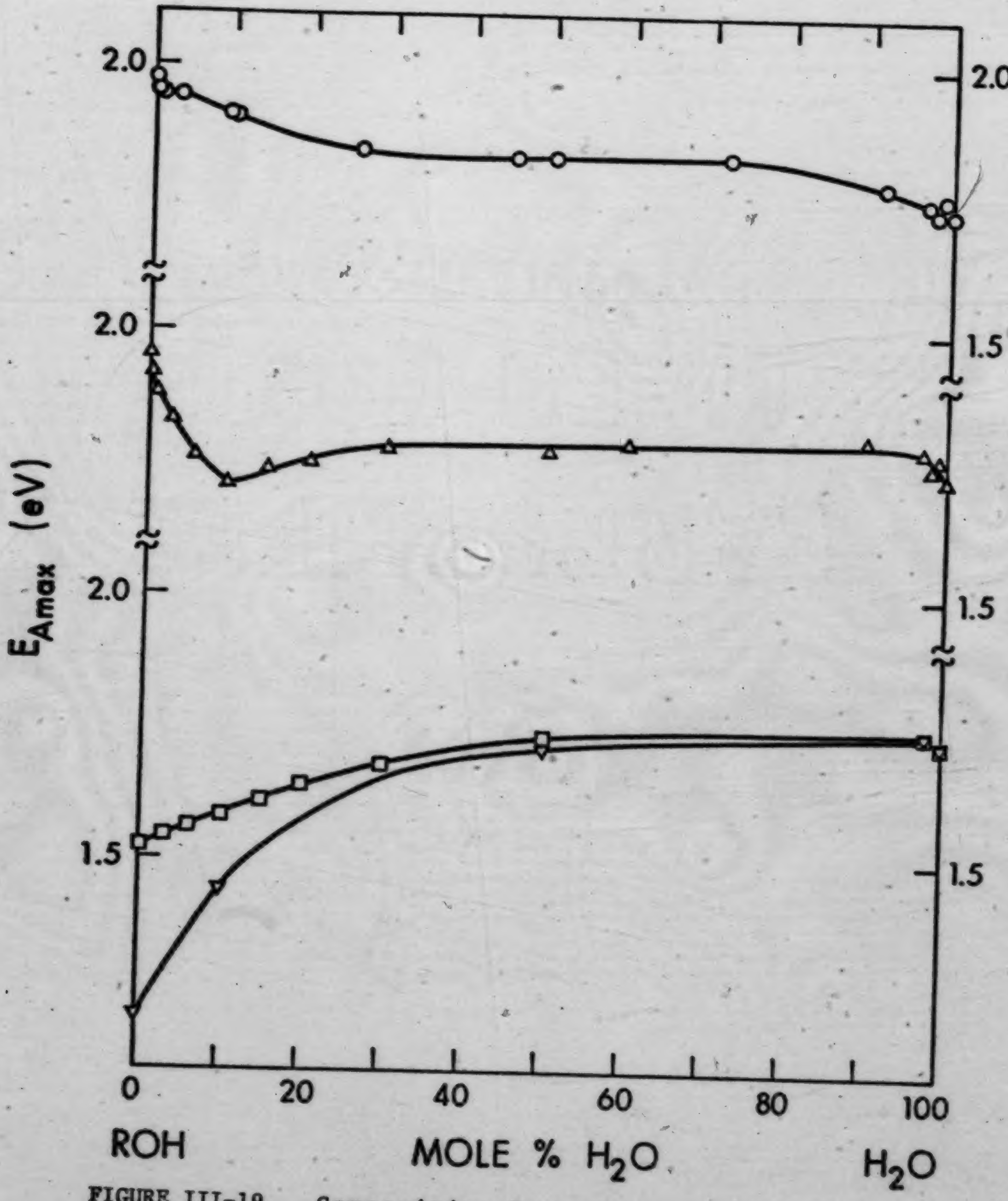

FIGURE III-19. Composition Dependence of E_{Amax} for Alcohol/Water Mixtures at 298K.

○, Methanol; △, 1-Propanol; □, 2-Propanol; ▽, t-Butanol. Shapes for other primary and secondary alcohols are similar to that for △ and □, respectively.

The curves obtained for the relation of $W_{\frac{1}{2}}$ to composition, except for tert-butanol, all show a region of sharp decrease in $W_{\frac{1}{2}}$ as mole % water increases to a certain point, then a very gradual decrease or levelling off for the remainder of the curve (Figure III-20):

(i) For methanol and the primary alcohols, most of the decrease occurs up to 50 mole % water, and then gradually levels off;

(ii) For secondary alcohols, most of the decrease occurs up to 10~15 mole % water with only a slight change up to 50 and then behaves as in (i);

(iii) For the tertiary alcohol, $W_{\frac{1}{2}}$ is independent of composition.

From Figure III-21, it can be seen that in the case of (i) and (ii), the sharp decrease in $W_{\frac{1}{2}}$ is largely accounted for by the decrease of W_b, as W_r decreases only slightly as mole % water increases.

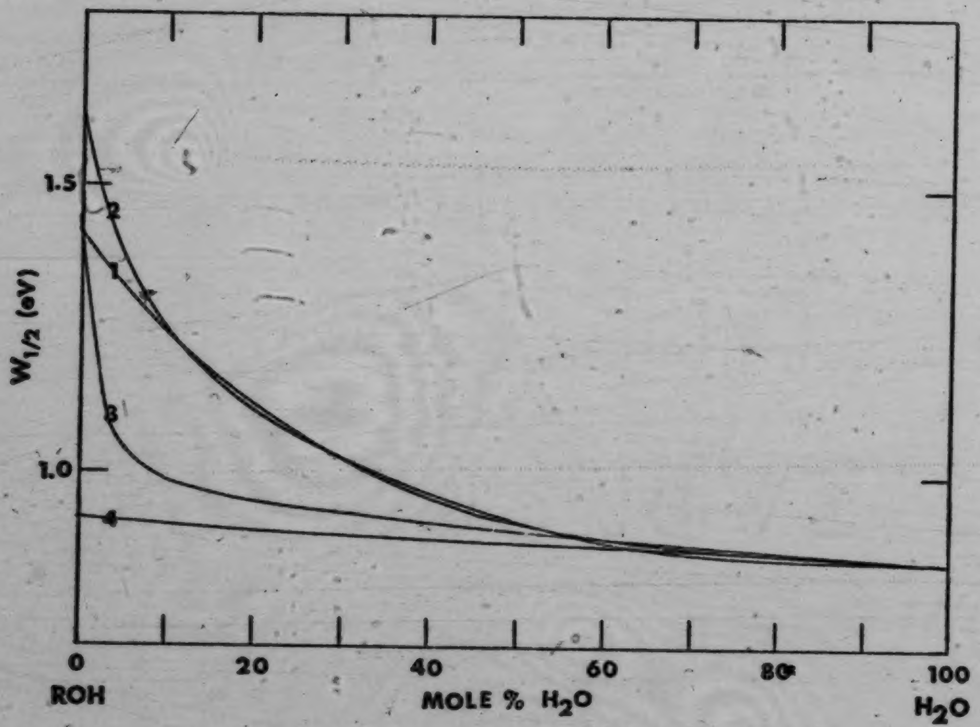

FIGURE III-20 Composition Dependence of $W_{\frac{1}{2}}$ for Alcohol/Water Mixtures at 298K.

1, Methanol; 2, n-Propanol; 3, iso-Propanol; 4, t-Butanol. Shapes for other primary and secondary alcohols are similar to that for 2, and for 3, respectively.

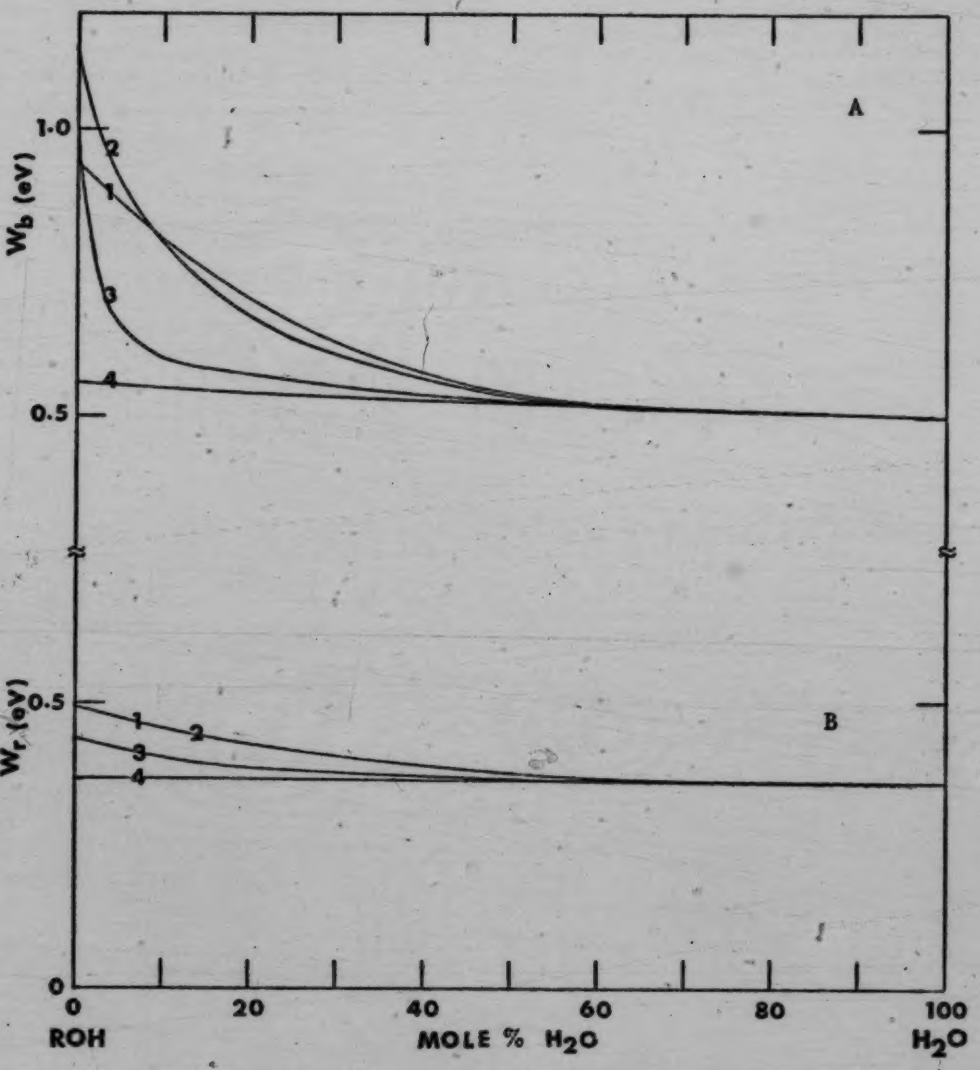

FIGURE III-21. Composition Dependence of W_b (part A) and W_r (part B) for Alcohol/Water Mixtures at 298K.

1, Methanol; 2, n-Propanol; 3, iso-Propanol; 4, t-Butanol. Shapes for other primary and secondary alcohols are similar to that for 2, and for 3, respectively.

2. Effect of Temperature

In order to study the effect of temperature upon the optical spectrum parameters of solvated electrons, measurements were made on the 0, 10, 50, 98 and 100 mole % water solutions of eight alcohols at temperatures from near the freezing point to near the boiling point of each. The results for each alcohol, including the temperature coefficient for the parameters, are summarized in Table III-10 to -17. The results for water are listed in Table III-9. For each alcohol/water solution, three figures are used to illustrate the finds. The first figure contains the entire spectrum for each temperature, showing the change in E_{Amax}. The second figure contains these spectra normalized at E_{Amax}, allowing comparison of spectrum shape and of $W_{\frac{1}{2}}$. The final figure for each solution contains a plot of the parameters against temperature. The first and second figures are presented in the same page. These figures are shown in Figure III-22 to -87.

TABLE III-9

Parameters of Solvent Electrons in Water at Different Temperatures

$\langle 100\vert W\vert T_i\rangle$	Code No.	Z155	Z152	Z153	Z154	(dX/dT)*
	Unit					meV/K
T	K	273	298	350	373	
E_{Amax}	eV	1.80	1.73	1.61	1.57	-2.42
$W_{\frac{1}{2}}$	eV	0.84	0.85	0.89	0.90	0.68
W_r	eV	0.35	0.36	0.39	0.41	0.57
W_b	eV	0.49	0.49	0.50	0.50	0.11
W_b/W_r		1.40	1.36	1.28	1.22	

---

[*] The temperature coefficient of X, where X represents the parameters E_{Amax}, $W_{\frac{1}{2}}$, W_r and W_b, respectively.

TABLE III-10

Parameters of Solvated Electrons in Methanol/Water at Different Temperatures

$\langle 0\|M\|T_i\rangle$	Code No. Unit	Z5	Z4	Z3	Z1	Z2	dX/dT meV/K
T	K	180	200	250	298	350	
E_{Amax}	eV	2.26	2.21	2.10	1.98	1.78	-2.71
$W_{\frac{1}{2}}$	eV	1.24	1.23	1.33	1.43	1.44	1.32
W_r	eV	0.41	0.41	0.46	0.50	0.45	0.35
W_b	eV	0.83	0.82	0.87	0.93	0.99	0.97
W_b/W_r		2.02	2.00	1.89	1.86	2.20	
$\langle 10\|M\|T_i\rangle$	Code No.	Z16	Z15	Z14	Z13	Z17	
T	K	180	200	250	298	350	
E_{Amax}	eV	2.27	2.24	2.10	1.90	1.71	-3.39
$W_{\frac{1}{2}}$	eV	1.10	1.11	1.23	1.26	1.26	1.04
W_r	eV	0.37	0.41	0.45	0.45	0.45	0.42
W_b	eV	0.73	0.70	0.78	0.81	0.81	0.63
W_b/W_r		1.97	1.71	1.73	1.80	1.80	

(continued)

TABLE 10 (continued)

$<50\|M\|T_i>$	Code No.	Z20	Z19	Z18	Z21	
T	K	200	250	298	350	
E_{Amax}	eV	2.11	1.98	1.83	1.67	-2.95
$W_{½}$	eV	0.84	0.86	0.90	0.94	0.67
W_r	eV	0.29	0.33	0.37	0.38	0.65
W_b	eV	0.55	0.53	0.53	0.56	0.02
W_b/W_r		1.90	1.61	1.43	1.47	

$<98\|M\|T_i>$	Code No.	Z23	Z22	Z24	Z25	
T	K	273	298	350	370	
E_{Amax}	eV	1.80	1.72	1.60	1.56	-2.47
$W_{½}$	eV	0.81	0.87	0.86	0.90	0.70
W_r	eV	0.32	0.34	0.35	0.39	0.60
W_b	eV	0.49	0.53	0.51	0.51	0.10
W_b/W_r		1.53	1.56	1.46	1.31	

TABLE III-11

Parameters of Solvated Electrons in Ethanol/Water at Different Temperatures

$\langle 0\|E\|T_i\rangle$	Code No. Unit	Z28	Z27	Z26	Z6	Z29	dX/dT meV/K
T	K	160	200	250	298	350	
E_{Amax}	eV	2.25	2.12	1.98	1.82	1.65	-3.13
$W_{\frac{1}{2}}$	eV	1.50	1.53	1.56	1.60	1.56	0.36
W_r	eV	0.46	0.46	0.46	0.48	0.49	0.16
W_b	eV	1.04	1.07	1.10	1.12	1.07	0.20
W_b/W_r		2.26	2.33	2.39	2.33	2.24	
$\langle 10\|E\|T_i\rangle$	Code No.	Z34	Z33	Z32	Z31	Z30	
T	K	160	200	250	298	350	
E_{Amax}	eV	2.31	2.14	1.93	1.71	1.55	-4.04
$W_{\frac{1}{2}}$	eV	1.41	1.37	1.33	1.19	1.15	-1.47
W_r	eV	0.49	0.45	0.45	0.45	0.44	-0.23
W_b	eV	0.92	0.92	0.88	0.74	0.71	-1.24
W_b/W_r		1.87	2.04	1.95	1.64	1.61	

(continued)

TABLE III-11 (continued)

5

$\langle 50\vert E\vert T_1\rangle$	Code No.	Z38	Z37	Z36	Z35	
T	K	222	250	298	350	
E_{Amax}	eV	2.04	1.94	1.77	1.61	-3.37
$W_{\frac{1}{2}}$	eV	0.88	0.89	0.91	0.90	0.16
W_r	eV	0.36	0.36	0.37	0.38	0.14
W_b	eV	0.52	0.53	0.54	0.52	0.02
W_b/W_r		1.44	1.47	1.46	1.31	
$\langle 98\vert E\vert T_1\rangle$	Code No.	Z40	Z39	Z41	Z42	
T	K	273	298	350	366	
E_{Amax}	eV	1.80	1.75	1.61	1.58	-2.49
$W_{\frac{1}{2}}$	eV	0.83	0.88	0.88	0.90	0.68
W_r	eV	0.32	0.36	0.37	0.39	0.59
W_b	eV	0.51	0.52	0.51	0.51	0.08
W_b/W_r		1.59	1.44	1.38	1.31	

TABLE III-12

Parameters of Solvated Electrons in 1-Propanol/Water at Different Temperatures

$\langle 0 \vert 1P \vert T_i \rangle$	Code No. Unit	Z47	Z46	Z45	Z7	Z43	Z44	dX/dT meV/K
T	K	150	200	250	298	350	369	
E_{Amax}	eV	2.41	2.30	2.14	1.95	1.78	1.71	-3.28
$W_{\frac{1}{2}}$	eV	1.51	1.56	1.60	1.63	1.69	1.70	0.85
W_r	eV	0.55	0.57	0.57	0.53	0.59	0.62	0.26
W_b	eV	0.96	0.99	1.03	1.10	1.10	1.08	0.59
W_b/W_r		1.75	1.74	1.81	2.08	1.86	1.74	
$\langle 10 \vert 1P \vert T_i \rangle$	Code No.		Z61	Z60	Z59	Z62		
T	K		200	250	298	350		
E_{Amax}	eV		2.20	1.98	1.72	1.57		-4.22
$W_{\frac{1}{2}}$	eV		1.37	1.33	1.24	1.14		-1.59
W_r	eV		0.50	0.50	0.47	0.44		-0.42
W_b	eV		0.87	0.83	0.72	0.70		-1.17
W_b/W_r			1.74	1.66	1.63	1.59		

(continued)

TABLE III-12 (continued)

$\langle 50\|1P\|T_i\rangle$	Code No.	Z52	Z 51	Z53	Z54	
T	K	260	298	350	360	
E_{Amax}	eV	1.91	1.77	1.61	1.58	-3.28
$W_{\frac{1}{2}}$	eV	0.91	0.92	0.91	0.90	-0.06
W_r	eV	0.38	0.38	0.37	0.36	-0.14
W_b	eV	0.53	0.54	0.54	0.54	0.08
W_b/W_r		1.39	1.42	1.46	1.50	

$\langle 98\|1P\|T_i\rangle$	Code No.	Z58	Z57	Z55	Z56	
T	K	273	298	350	363	
E_{Amax}	eV	1.81	1.75	1.61	1.59	-2.55
$W_{\frac{1}{2}}$	eV	0.85	0.87	0.87	0.90	0.67
W_r	eV	0.34	0.37	0.37	0.39	0.63
W_b	eV	0.51	0.50	0.50	0.51	0.04
W_b/W_r		1.50	1.35	1.35	1.31	

TABLE III-13

Parameters of Solvated Electrons in 2-Propanol/Water at Different Temperatures

$<0\vert 2P\vert T_i>$	Code No. Unit	Z49	Z48	Z8	Z50	dX/dT meV/K
T	K	200	250	298	350	
E_{Amax}	eV	1.97	1.76	1.52	1.28	-4.42
$W_{\frac{1}{2}}$	eV	1.47	1.43	1.45	1.39	-1.93
W_r	eV	0.44	0.42	0.44	0.42	-0.12
W_b	eV	1.03	1.01	1.01	0.97	-0.47
W_b/W_r		2.34	2.40	2.30	2.31	
$<10\vert 2P\vert T_i>$	Code No.	Z64	Z63	Z65	Z66	
T	K	200	250	298	350	
E_{Amax}	eV	1.91	1.72	1.58	1.42	-3.53
$W_{\frac{1}{2}}$	eV	1.16	1.09	1.00	0.97	-1.30
W_r	eV	0.43	0.44	0.40	0.38	-0.36
W_b	eV	0.73	0.65	0.60	0.59	-0.94
W_b/W_r		1.70	1.48	1.50	1.55	

(continued)

TABLE III-13 (continued)

$\langle 50\vert 2P\vert T_i\rangle$	Code No.	Z70	Z67	Z68	Z69	
T	K	250	298	339	352	
E_{Amax}	eV	1.93	1.73	1.65	1.57	-3.44
$W_{½}$	eV	0.89	0.91	0.89	0.89	-0.07
W_r	eV	0.39	0.37	0.39	0.38	-0.08
W_b	eV	0.50	0.54	0.51	0.51	0.01
W_b/W_r		1.28	1.46	1.31	1.34	

$\langle 98\vert 2P\vert T_i\rangle$	Code No.	Z71	Z72	Z73	Z74	
T	K	273	298	339	360	
E_{Amax}	eV	1.81	1.75	1.65	1.59	-2.63
$W_{½}$	eV	0.84	0.86	0.87	0.88	0.49
W_r	eV	0.34	0.36	0.35	0.39	0.42
W_b	eV	0.50	0.50	0.52	0.49	0.07
W_b/W_r		1.47	1.39	1.49	1.26	

TABLE III-14

Parameters of Solvated Electrons in 1-Butanol/Water at Different Temperatures

$<0\|1B\|T_i>$	Code No. Unit	Z87	Z88	Z9	Z89	Z90	dX/dT meV/K
T	K	200	250	298	350	388	
E_{Amax}	eV	2.30	2.14	1.98	1.79	1.64	-3.49
$W_{½}$	eV	1.49	1.58	1.57	1.69	1.64	0.90
W_r	eV	0.55	0.57	0.53	0.58	0.63	0.39
W_b	eV	0.94	1.01	1.04	1.11	1.01	0.51
W_b/W_r		1.71	1.77	1.96	1.91	1.60	

$<10\|1B\|T_i>$	Code No.	Z130	Z129	Z126	Z127	Z128	
T	K	200	250	298	350	373	
E_{Amax}	eV	2.22	1.99	1.73	1.56	1.49	-4.26
$W_{½}$	eV	1.37	1.35	1.23	1.13	1.10	-1.71
W_r	eV	0.48	0.52	0.45	0.42	0.42	-0.49
W_b	eV	0.89	0.83	0.78	0.71	0.68	-1.23
W_b/W_r		1.85	1.60	1.73	1.69	1.62	

(continued)

TABLE III-14 (continued)

	Code No.	Z148	Z149	Z150	Z151	
$\langle 50 \vert 1B \vert T_i \rangle$						
T	K	298	325	350	364	
E_{Amax}	eV	1.79	1.69	1.62	1.57	-3.35
$W_{1/2}$	eV	0.88	0.89	0.93	0.91	0.60
W_r	eV	0.36	0.36	0.39	0.39	0.53
W_b	eV	0.52	0.53	0.54	0.52	0.06
W_b/W_r		1.44	1.47	1.38	1.33	

	Code No.	Z123	Z122	Z124	Z125	
$\langle 98 \vert 1B \vert T_i \rangle$						
T	K	273	298	350	363	
E_{Amax}	eV	1.79	1.74	1.60	1.56	-2.69
$W_{1/2}$	eV	0.83	0.88	0.89	0.90	0.66
W_r	eV	0.32	0.36	0.37	0.38	0.62
W_b	eV	0.51	0.52	0.52	0.52	0.04
W_b/W_r		1.59	1.44	1.41	1.37	

TABLE III-15

Parameters of Solvated Electrons in iso-Butanol/Water at Different Temperatures

$\langle 0\|iB\|T_1\rangle$	Code No.	Z95	Z94	Z93	Z10	Z91	Z92	dX/dT meV/K
	Unit							
T	K	170	200	250	298	350	378	
E_{Amax}	eV	2.42	2.36	2.17	1.97	1.79	1.60	-3.86
$W_{\frac{1}{2}}$	eV	1.56	1.48	1.57	1.61	1.64	1.66	0.68
W_r	eV	0.63	0.55	0.56	0.57	0.61	0.65	0.20
W_b	eV	0.93	0.93	1.01	1.04	1.03	1.01	0.47
W_b/W_r		1.48	1.69	1.80	1.82	1.69	1.55	

$\langle 10\|iB\|T_1\rangle$	Code No.	Z135	Z134	Z131	Z132	Z133	
T	K	200	250	298	350	365	
E_{Amax}	eV	2.22	1.96	1.73	1.55	1.49	-4.37
$W_{\frac{1}{2}}$	eV	1.44	1.25	1.18	1.13	1.08	-1.96
W_r	eV	0.48	0.48	0.43	0.42	0.41	-0.48
W_b	eV	0.96	0.77	0.75	0.71	0.67	-1.48
W_b/W_r		2.00	1.60	1.74	1.69	1.63	

(continued)

TABLE III-15 (continued)

$<50\vert iB\vert T_1>$	Code No.	Z144	Z145	Z146	Z147	
T	K	286	298	325	350	
E_{Amax}	eV	1.82	1.78	1.68	1.60	-3.55
$W_{½}$	eV	0.91	0.89	0.89	0.89	-0.23
W_r	eV	0.38	0.36	0.36	0.36	-0.21
W_b	eV	0.53	0.53	0.53	0.53	0.
W_b/W_r		1.39	1.47	1.47	1.47	

$<98\vert iB\vert T_1>$	Code No.	Z119	Z118	Z120	Z121	
T	K	273	298	350	363	
E_{Amax}	eV	1.81	1.75	1.61	1.57	-2.70
$W_{½}$	eV	0.84	0.86	0.90	0.89	0.57
W_r	eV	0.33	0.35	0.39	0.37	0.51
W_b	eV	0.51	0.51	0.51	0.52	0.06
W_b/W_r		1.55	1.46	1.31	1.41	

TABLE III-16

Parameters of Solvated Electrons in 2-Butanol/Water at Different Temperatures

$\langle 0\vert 2B\vert T_i\rangle$	Code No.	Z100	Z99	Z98	Z156	Z96	Z97	dX/dT meV/K
	Unit							
T	K	163	200	250	298	350	370	
E_{Amax}	eV	2.23	2.05	1.87	1.59	1.39	1.28	-4.45
$W_{\frac{1}{2}}$	eV	1.88	1.86	1.72	1.57	1.48	1.42	-2.34
W_r	eV	0.61	0.61	0.51	0.47	0.50	0.48	-0.66
W_b	eV	1.27	1.25	1.21	1.10	0.98	0.94	-1.68
W_b/W_r		2.08	2.05	2.37	2.34	1.96	1.96	

$\langle 10\vert 2B\vert T_i\rangle$	Code No.	Z139	Z138	Z136	Z137	
T	K	200	250	298	350	
E_{Amax}	eV	2.01	1.81	1.65	1.44	-3.76
$W_{\frac{1}{2}}$	eV	1.16	1.04	1.04	0.94	-1.33
W_r	eV	0.50	0.45	0.46	0.34	-0.90
W_b	eV	0.66	0.59	0.58	0.60	-0.43
W_b/W_r		1.32	1.31	1.26	1.76	

(continued)

TABLE III-16 (continued)

$<50|2B|T_1>$

Code No.		Z143	Z140	Z141	Z142	
T	K	273	298	325	350	
E_{Amax}	eV	1.84	1.76	1.62	1.57	-3.40
$W_{\frac{1}{2}}$	eV	0.89	0.89	0.88	0.88	-0.10
W_r	eV	0.36	0.36	0.34	0.35	-0.11
W_b	eV	0.53	0.53	0.54	0.53	0.01
W_b/W_r		1.47	1.47	1.59	1.51	

$<98|2B|T_1>$

Code No.		Z115	Z114	Z116	Z117	
T	K	273	298	350	370	
E_{Amax}	eV	1.82	1.75	1.59	1.55	-2.75
$W_{\frac{1}{2}}$	eV	0.83	0.86	0.88	0.89	0.50
W_r	eV	0.34	0.35	0.37	0.38	0.39
W_b	eV	0.49	0.51	0.51	0.51	0.11
W_b/W_r		1.44	1.46	1.38	1.34	

TABLE III-17

Parameters of Solvated Electrons in tert-Butanol/Water at Different Temperatures

$\langle 0 \vert tB \vert T_i \rangle$	Code No.	Z157	Z101	Z102	dX/dT meV/K
	Unit				
T	K	298	325	350	
E_{Amax}	eV	1.20	1.10	0.99	-4.80
$W_{1/2}$	eV	0.93	0.97	0.82	-2.30
W_r	eV	0.37	0.35	0.31	-0.98
W_b	eV	0.56	0.62	0.51	-1.32
W_b/W_r		1.51	1.77	1.65	

$\langle 10 \vert tB \vert T_i \rangle$	Code No.	Z103	Z104	Z105	
T	K	298	325	350	
E_{Amax}	eV	1.44	1.33	1.24	-3.84
$W_{1/2}$	eV	0.94	0.93	0.91	-0.70
W_r	eV	0.37	0.34	0.36	-0.32
W_b	eV	0.57	0.59	0.55	-0.38
W_b/W_r		1.54	1.74	1.53	

(continued)

TABLE III-17 (continued)

	Code No.	Z109	Z158	Z107	Z108	
$\langle 50 \vert tB \vert T_i \rangle$						
T	K	273	298	350	368	
E_{Amax}	eV	1.82	1.71	1.55	1.48	-3.47
$W_{½}$	eV	0.86	0.89	0.87	0.87	0.05
W_r	eV	0.36	0.37	0.36	0.38	0.09
W_b	eV	0.50	0.52	0.51	0.49	-0.04
W_b/W_r		1.39	1.41	1.42	1.29	

	Code No.	Z113	Z110	Z111	Z112	
$\langle 98 \vert tB \vert T_i \rangle$						
T	K	273	298	350	370	
E_{Amax}	eV	1.82	1.75	1.59	1.54	-2.89
$W_{½}$	eV	0.83	0.88	0.83	0.89	0.31
W_r	eV	0.34	0.36	0.34	0.38	0.20
W_b	eV	0.49	0.52	0.49	0.51	0.11
W_b/W_r		1.44	1.44	1.44	1.34	

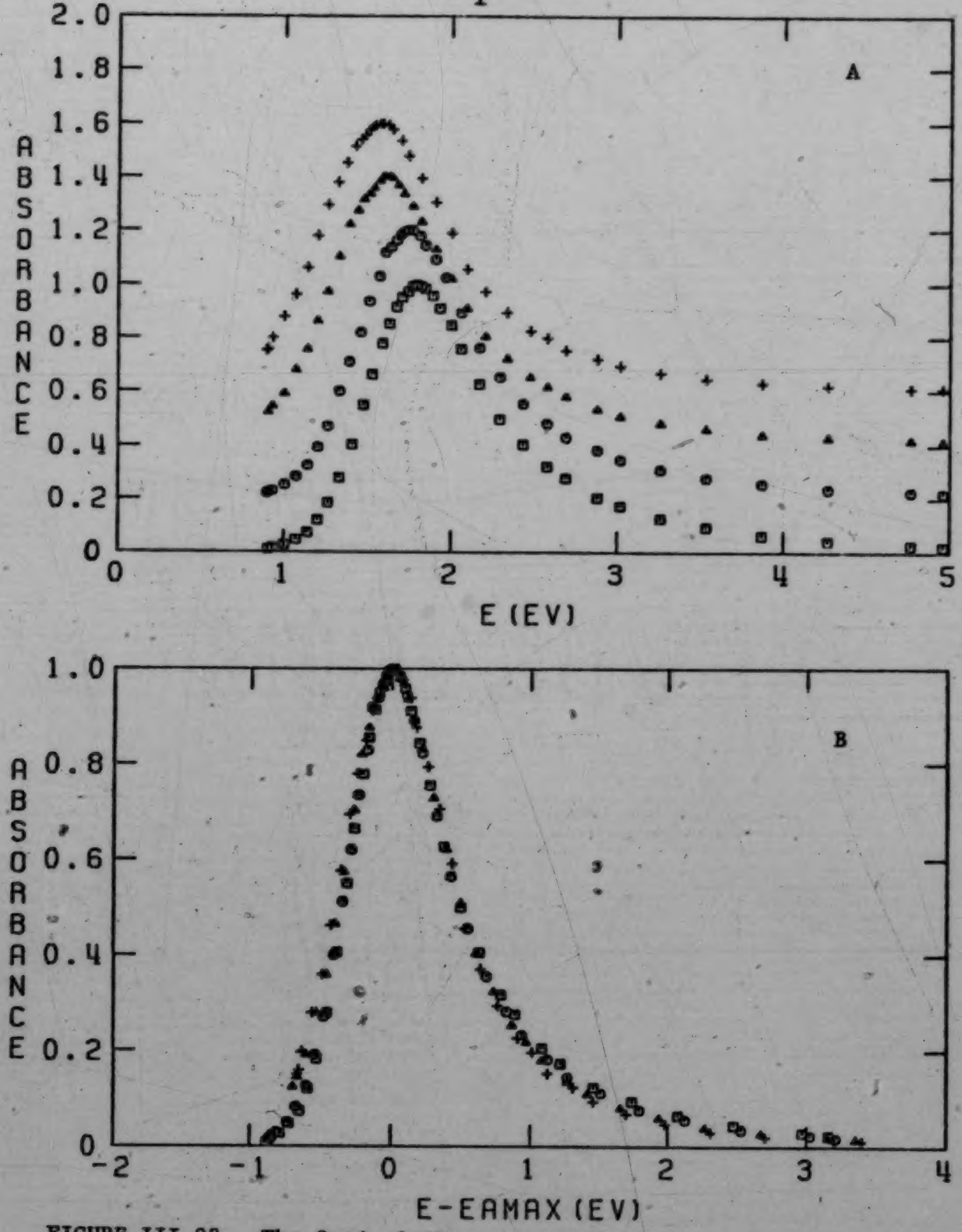

FIGURE III-22. The Optical Absorption Spectrum of Solvated Electrons in Water at Different Temperatures.

A: Successive spectra are displaced vertically by 0.2 units.

B: The spectra are normalized at E_{Amax}. □, 273K; O, 298K; △, 350K; +, 373K.

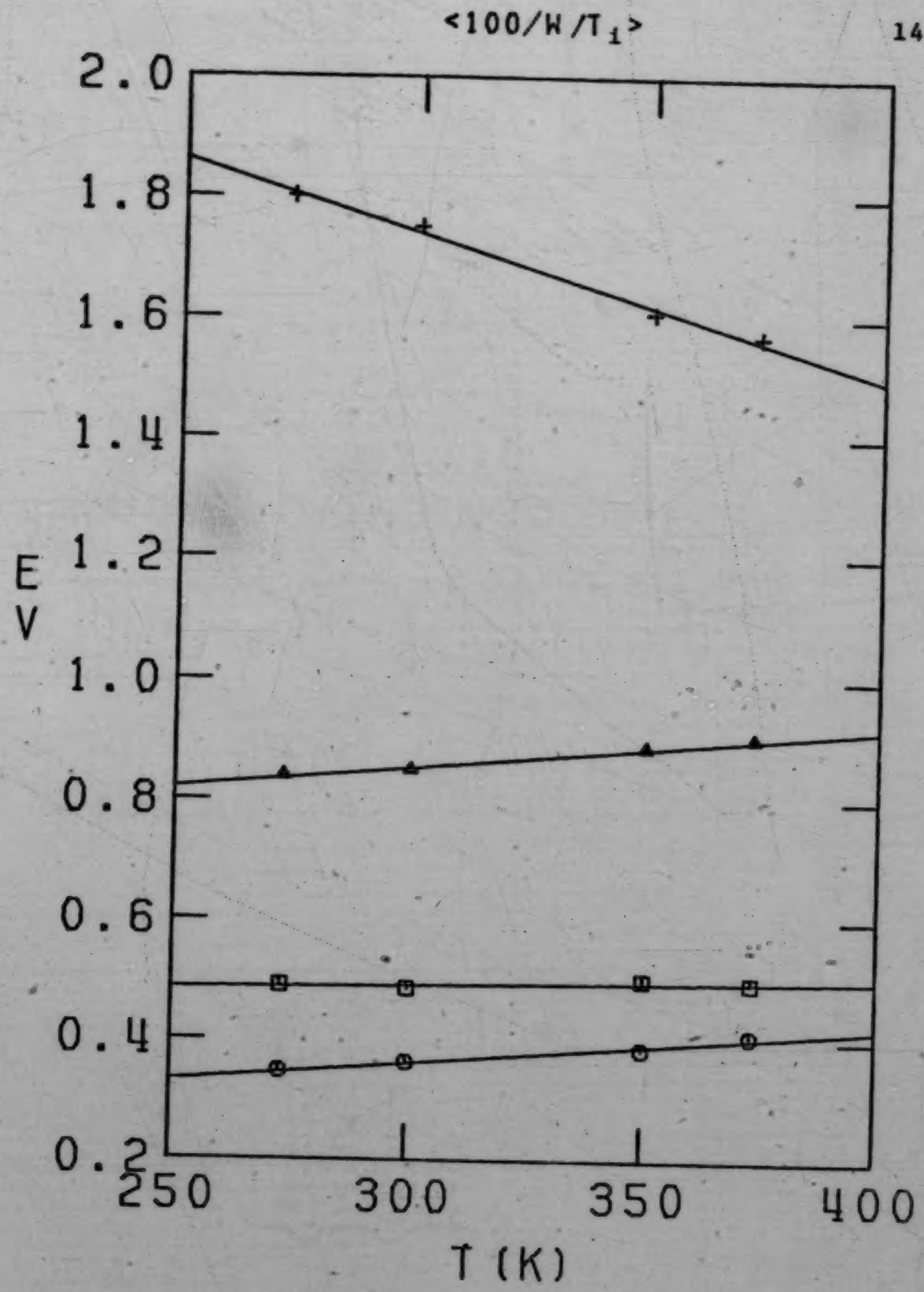

FIGURE III-23. Temperature Dependence of Spectrum Parameters in Water.

+, E_{Amax}; Δ, $W_{\frac{1}{2}}$; O, W_r; □, W_b.

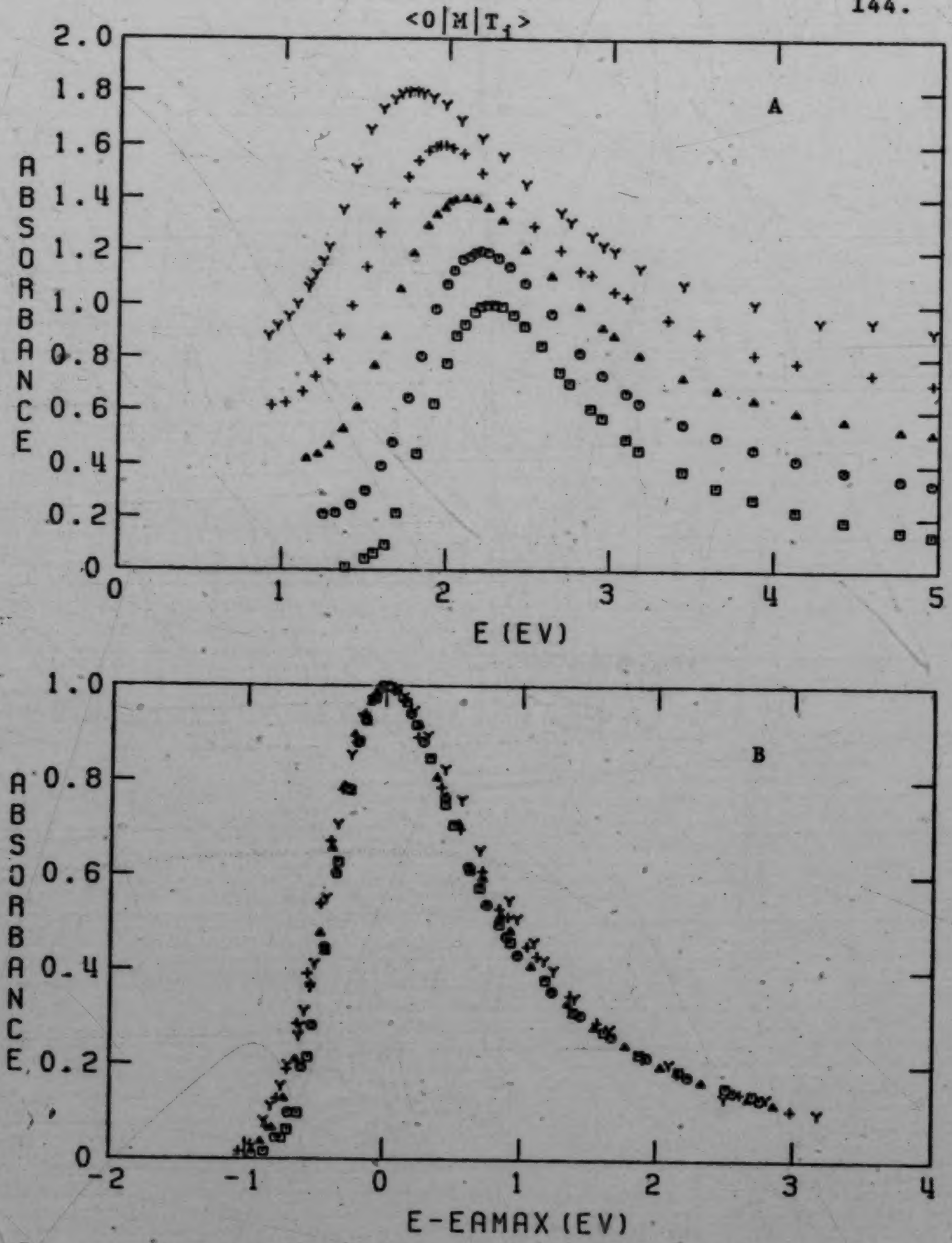

FIGURE III-24. The Optical Absorption Spectrum of Solvated Electrons in Methanol at Different Temperatures.

A: Successive spectra are displaced vertically by 0.2 units.

B: The spectra are normalized at E_{Amax}. □, 180K; O, 200K; △, 250K; +, 298K; Y, 350K.

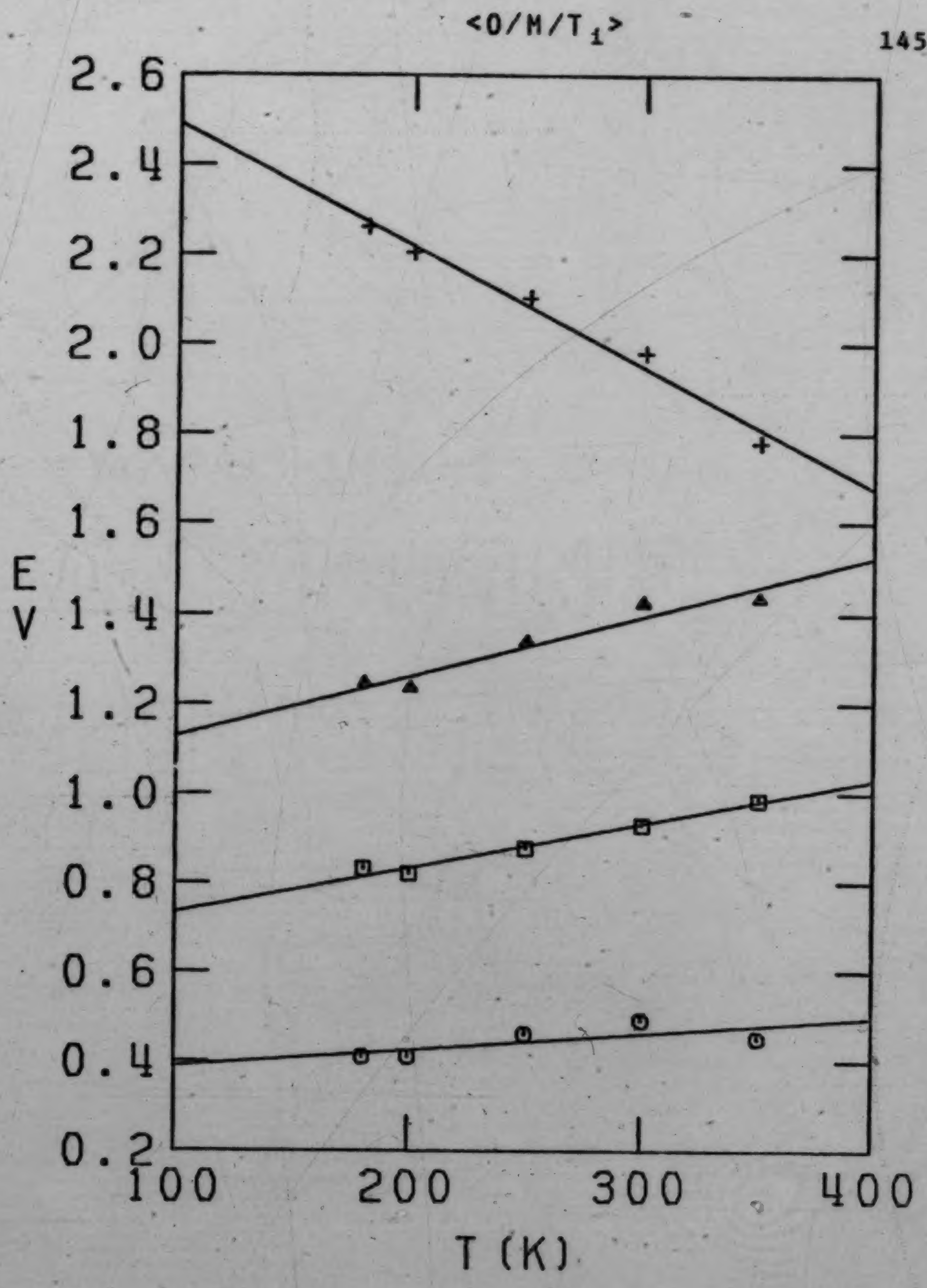

FIGURE III-25. Temperature Dependence of Spectrum Parameters in Methanol.

+, E_{Amax}; △, $W_{\frac{1}{2}}$; O, W_r; □, W_b.

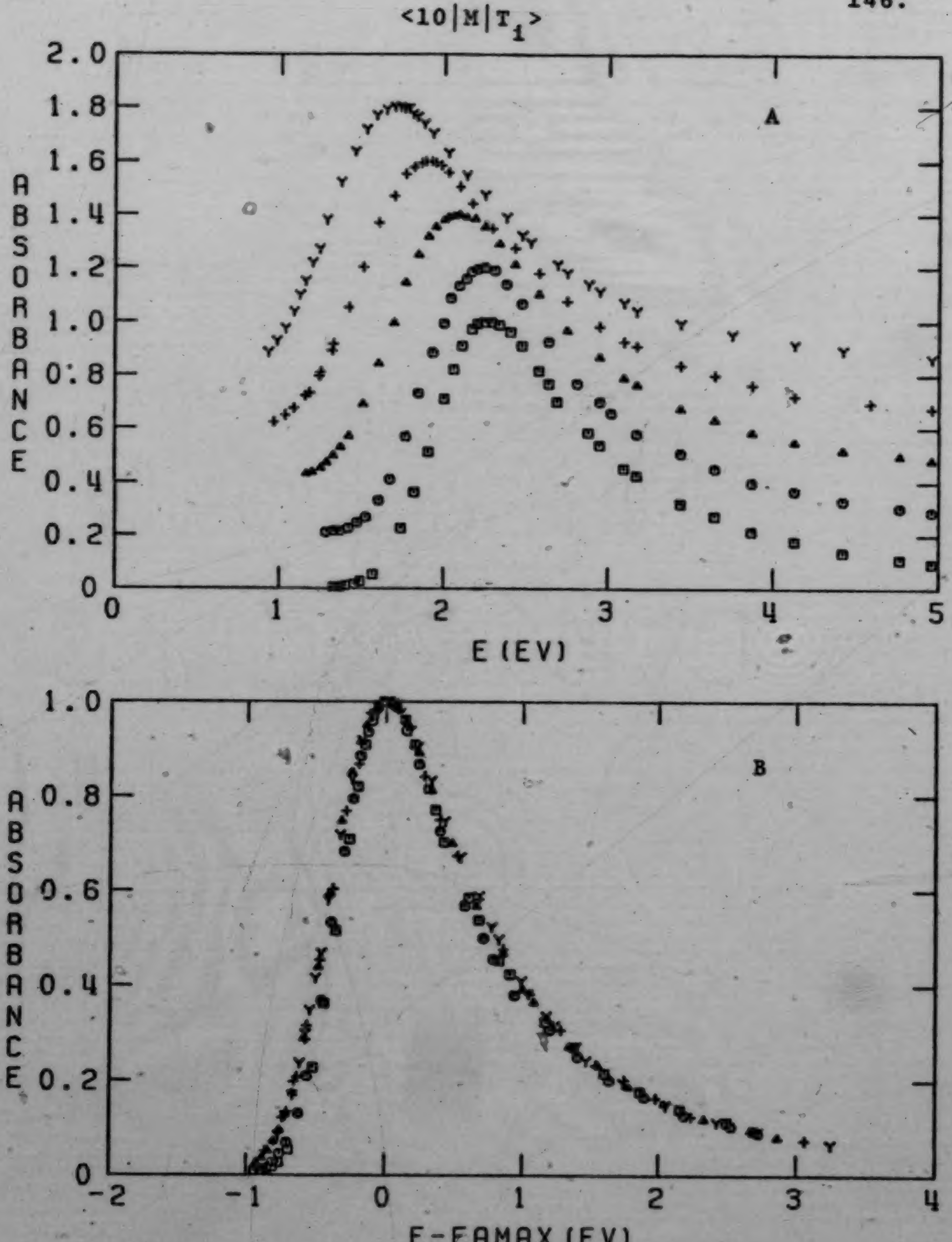

FIGURE III-26. The Optical Absorption Spectrum of Solvated Electrons in a Solution of 10 Mole % Water in Methanol at Different Temperatures.

A: Successive spectra are displaced vertically by 0.2 units.

B: The spectra are normalized at E_{Amax}. □, 180K; O, 200K; △, 250K; +, 298K; Y, 350K.

<10/M/T$_1$>

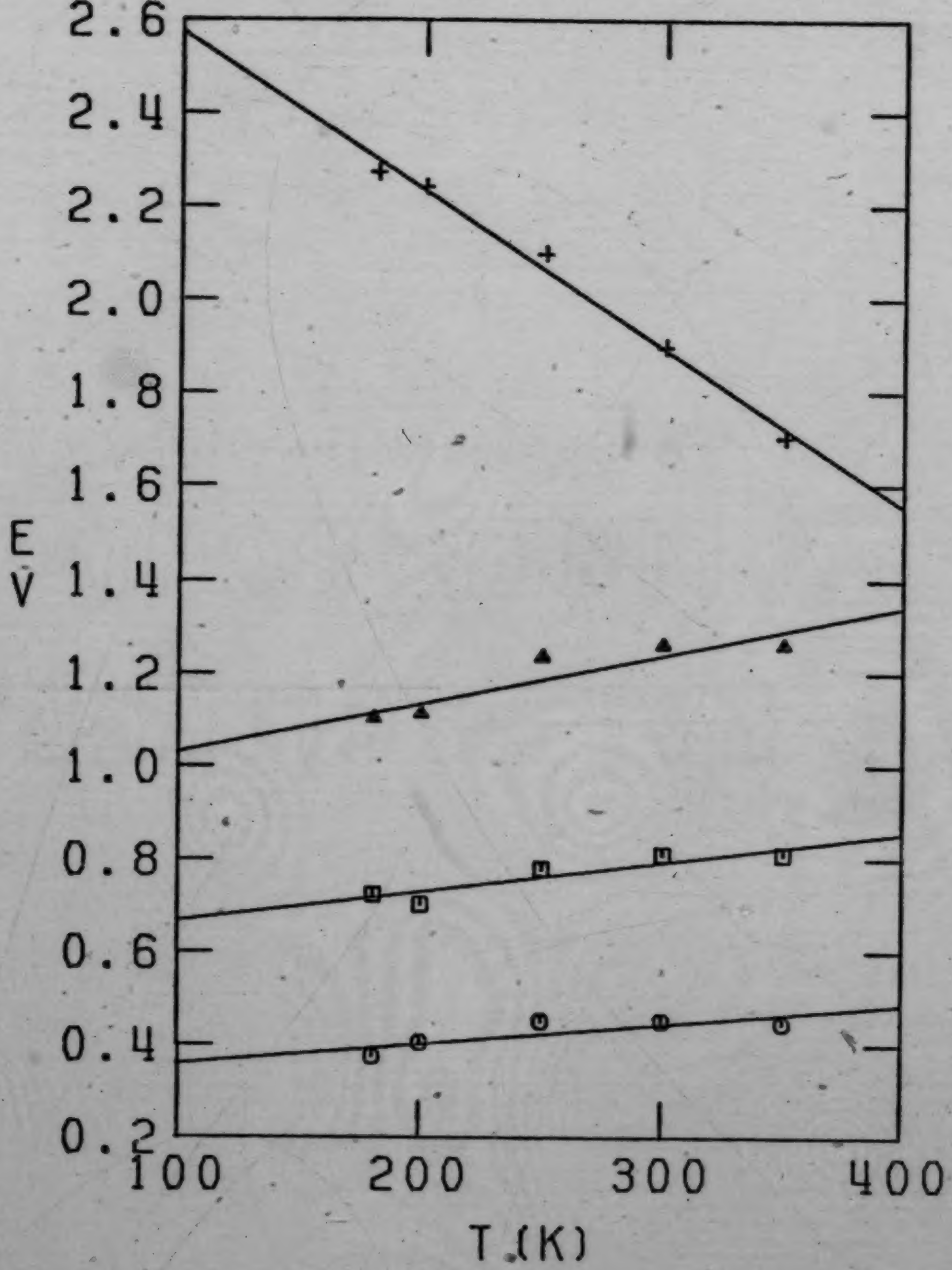

FIGURE III-27. Temperature Dependence of Spectrum Parameters in a Solution of 10 Mole % Water in Methanol.

+, E_{Amax}; △, $W_{\frac{1}{2}}$; O, W_r; □, W_b.

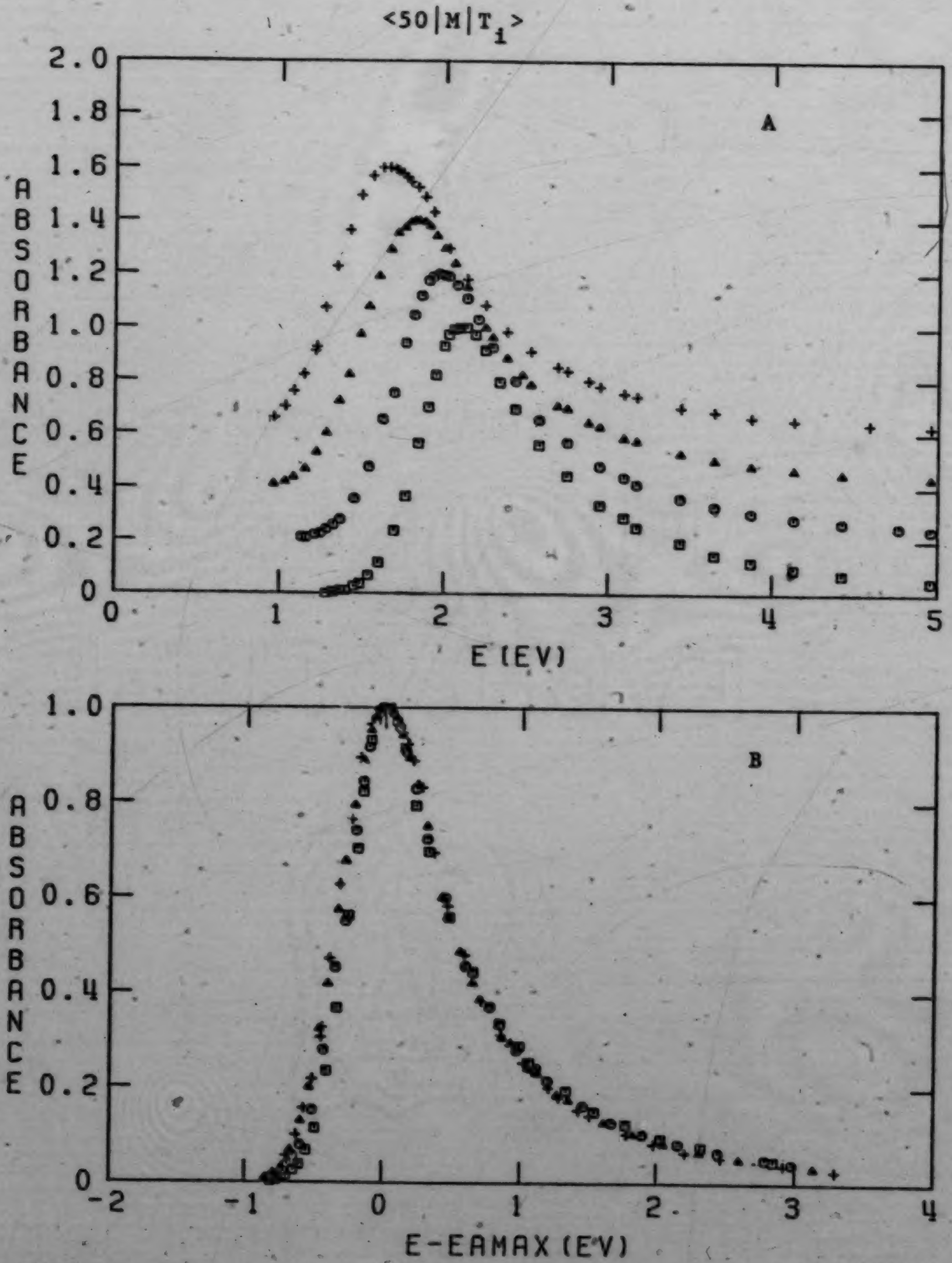

__FIGURE III-28__. The Optical Absorption Spectrum of Solvated Electrons in a Solution of 50 Mole % Water in Methanol at Different Temperatures.

A: Successive spectra are displaced vertically by 0.2 units.

B: The spectra are normalized at E_{Amax}. □, 200K; O, 250K; △, 298K; +, 350K.

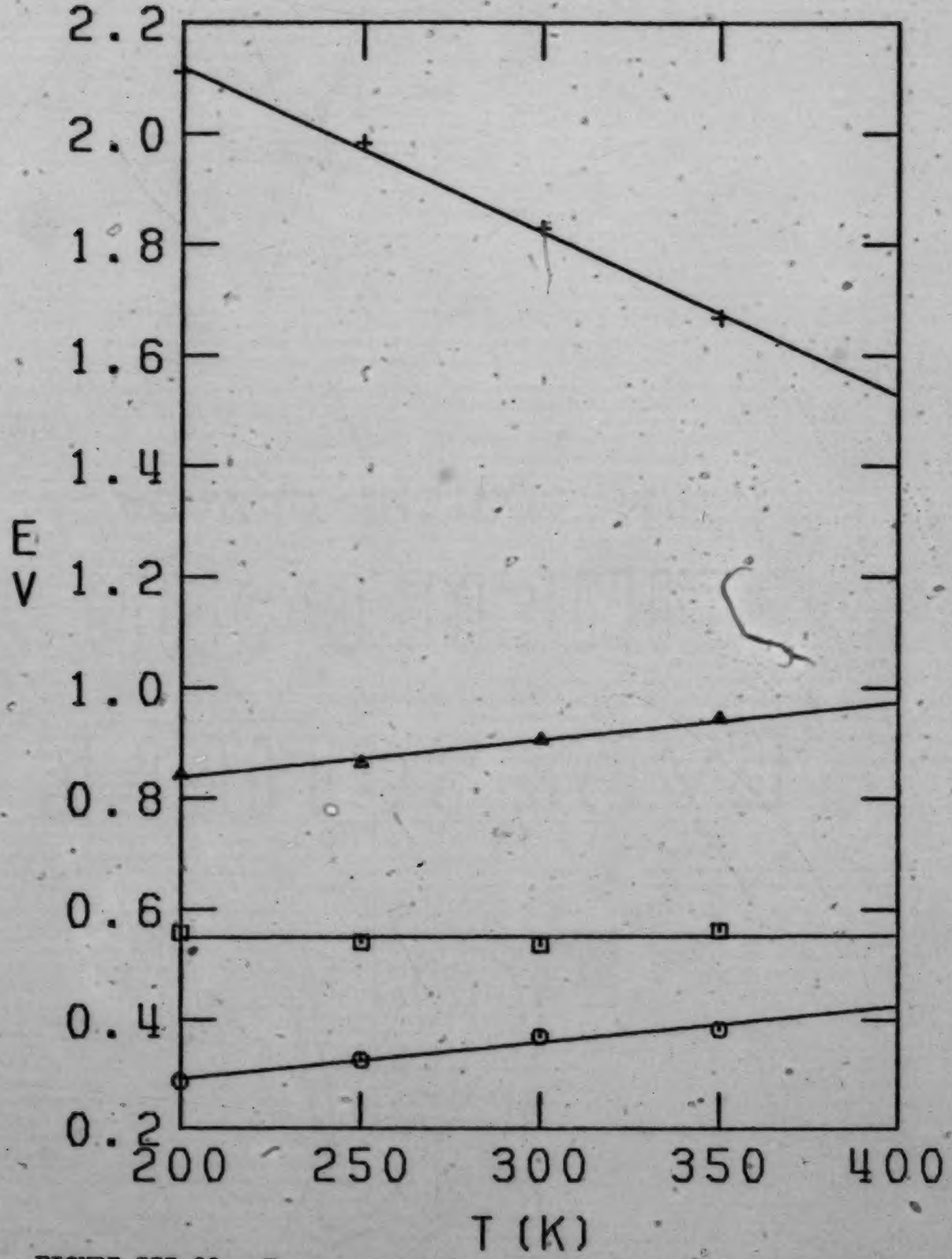

FIGURE III-29. Temperature Dependence of Spectrum Parameters in a Solution of 50 Mole % Water in Methanol.

+, E_{Amax}; Δ, $W_{\frac{1}{2}}$; O, W_r; □, W_b

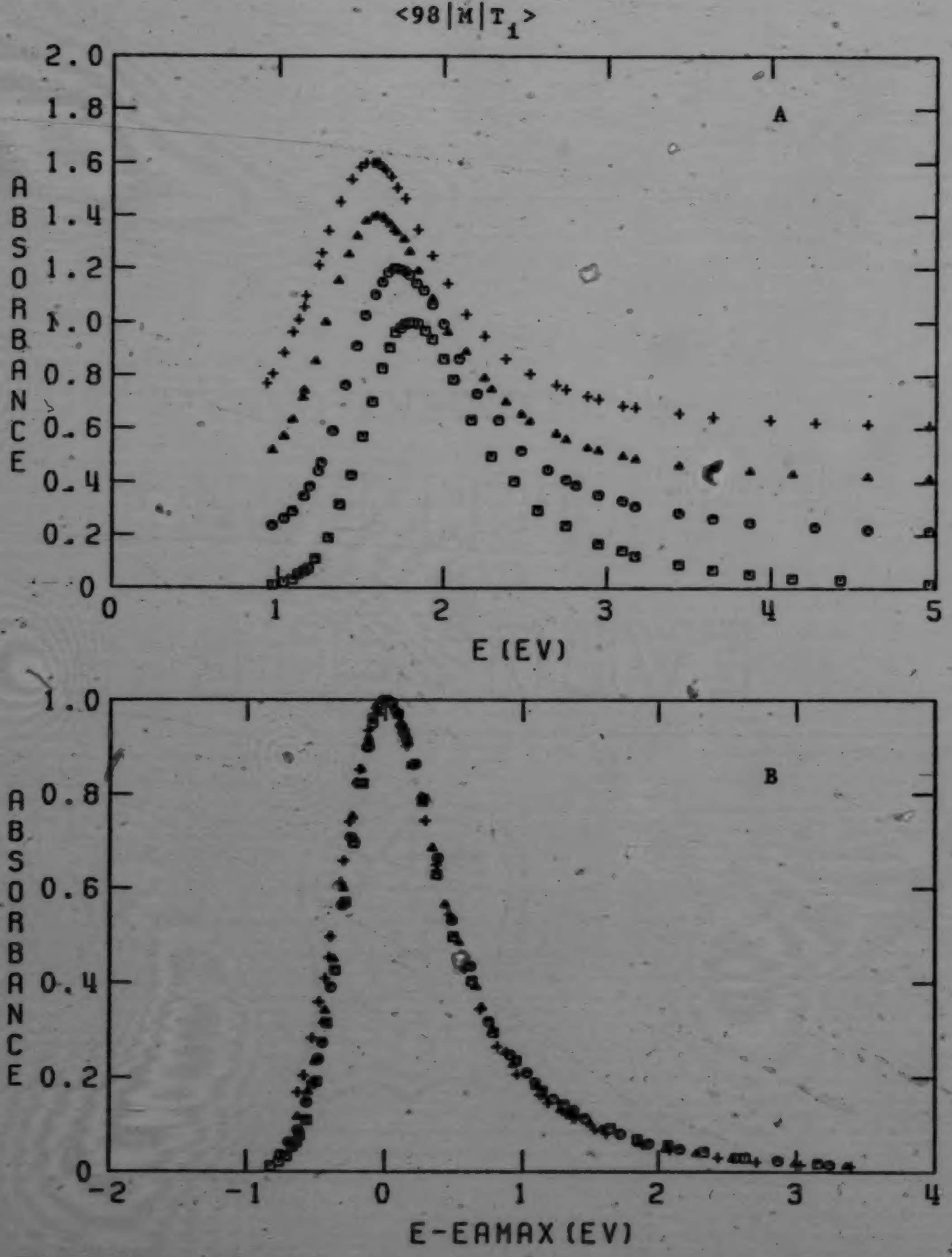

FIGURE III-30. The Optical Absorption Spectrum of Solvated Electrons in a Solution of 98 Mole % Water in Methanol at Different Temperatures.

A: Successive spectra are displaced vertically by 0.2 units.

B: The spectra are normalized at E_{Amax}. □, 273K; O, 298K; △, 350K; +, 370K.

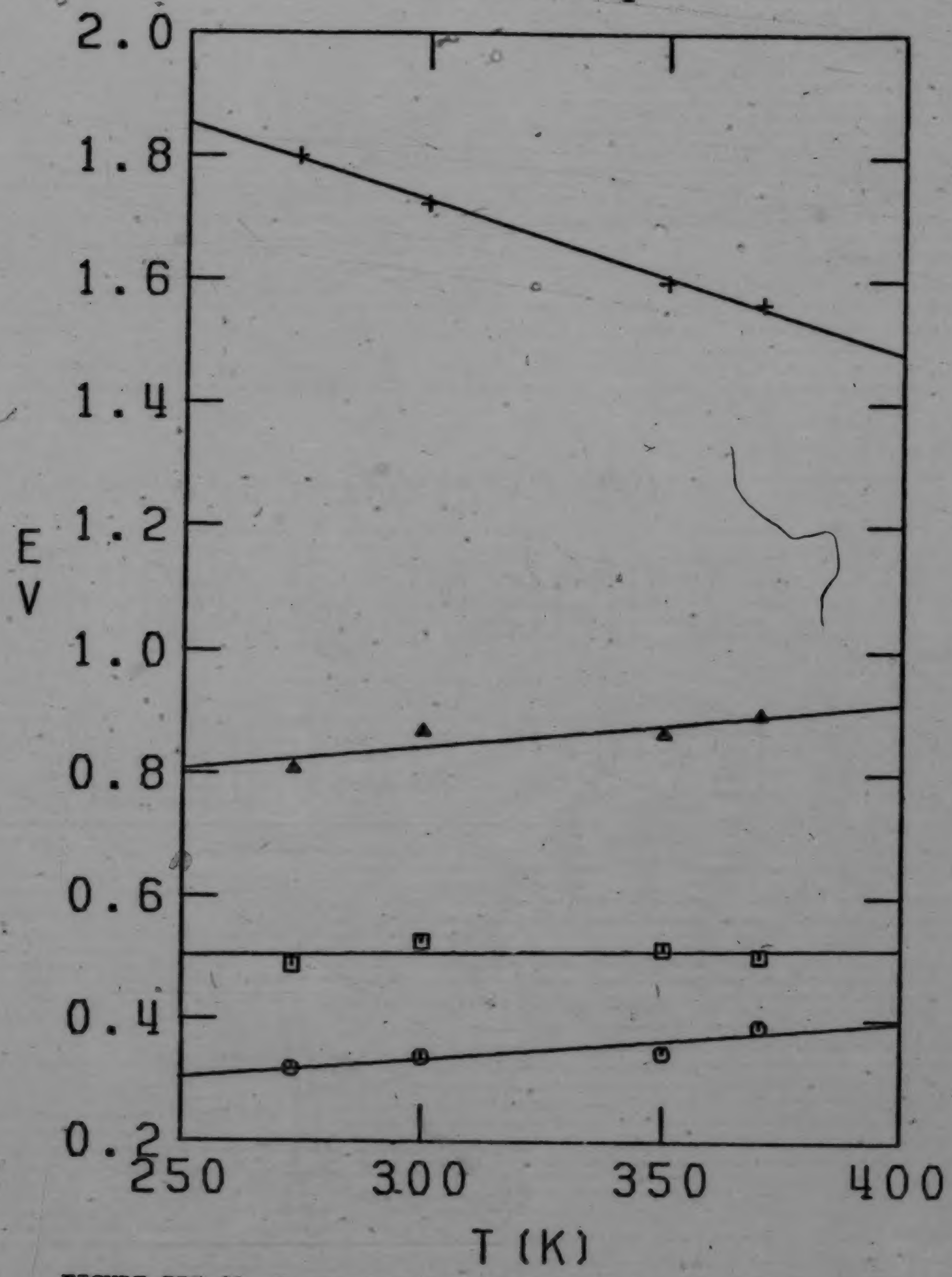

FIGURE III-31. Temperature Dependence of Spectrum Parameters in a Solution of 98 Mole % Water in Methanol.

+, E_{Amax}; △, $W_{\frac{1}{2}}$; O, W_r; □, W_b.

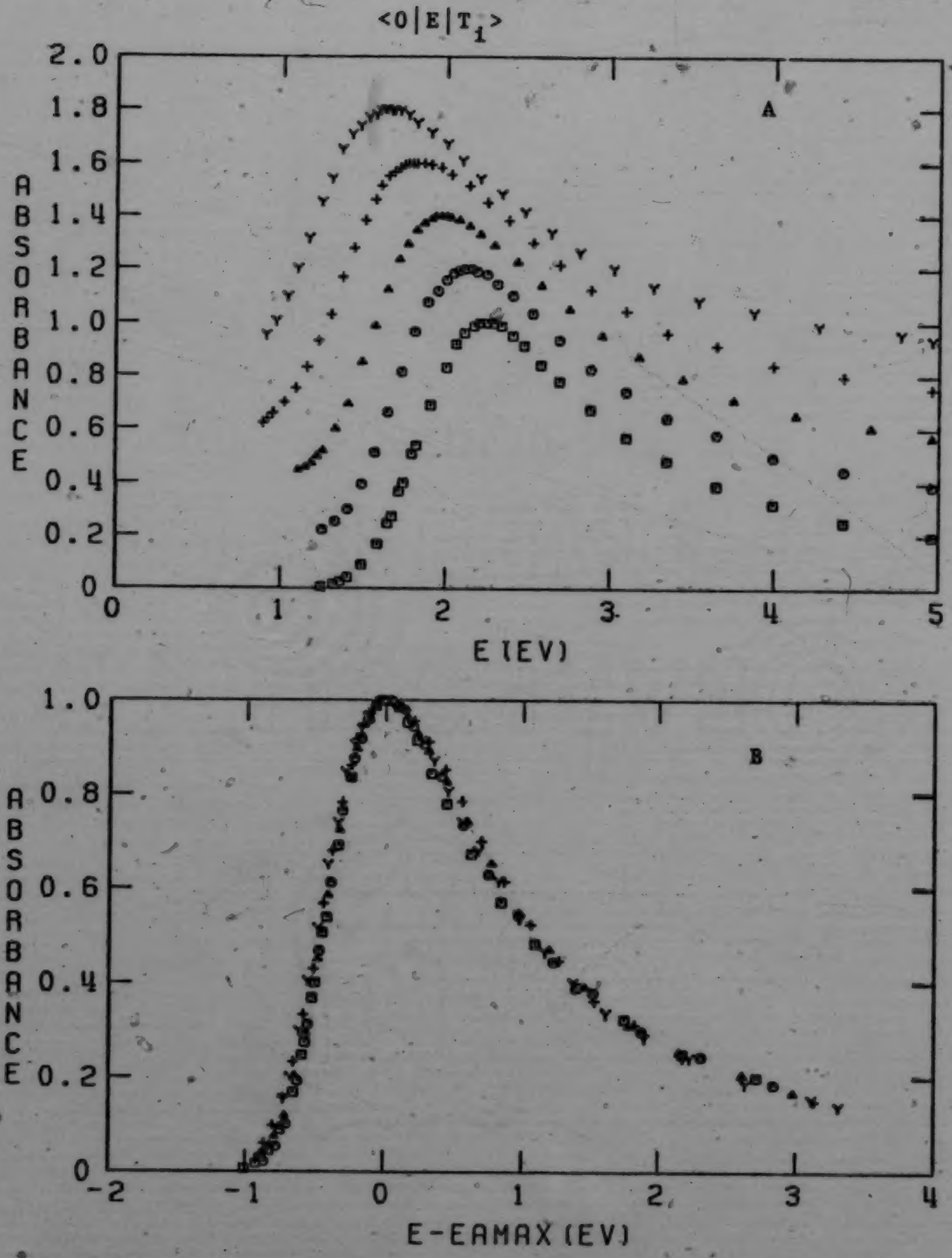

FIGURE III-32: The Optical Absorption Spectrum of Solvated Electrons in Ethanol at Different Temperatures.

A: Successive spectra are displaced vertically by 0.2 units.

B: The spectra are normalized at E_{Amax}. □, 160K; O, 200K; △, 250K; +, 298K; Y, 350K.

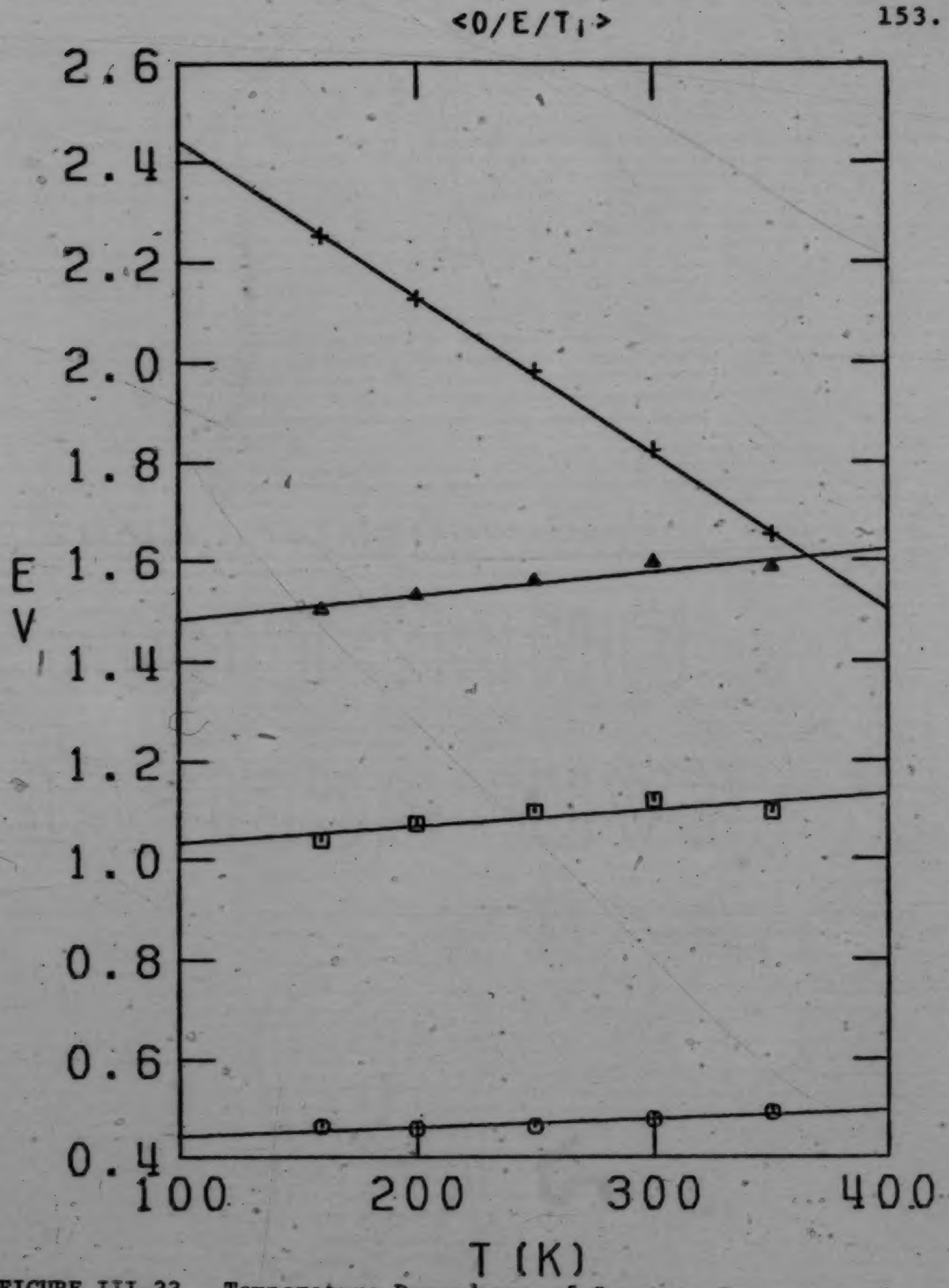

FIGURE III-33. Temperature Dependence of Spectrum Parameters in Ethanol.

+, E_{Amax}; △, $W_{\frac{1}{2}}$; O, W_r; □, W_b.

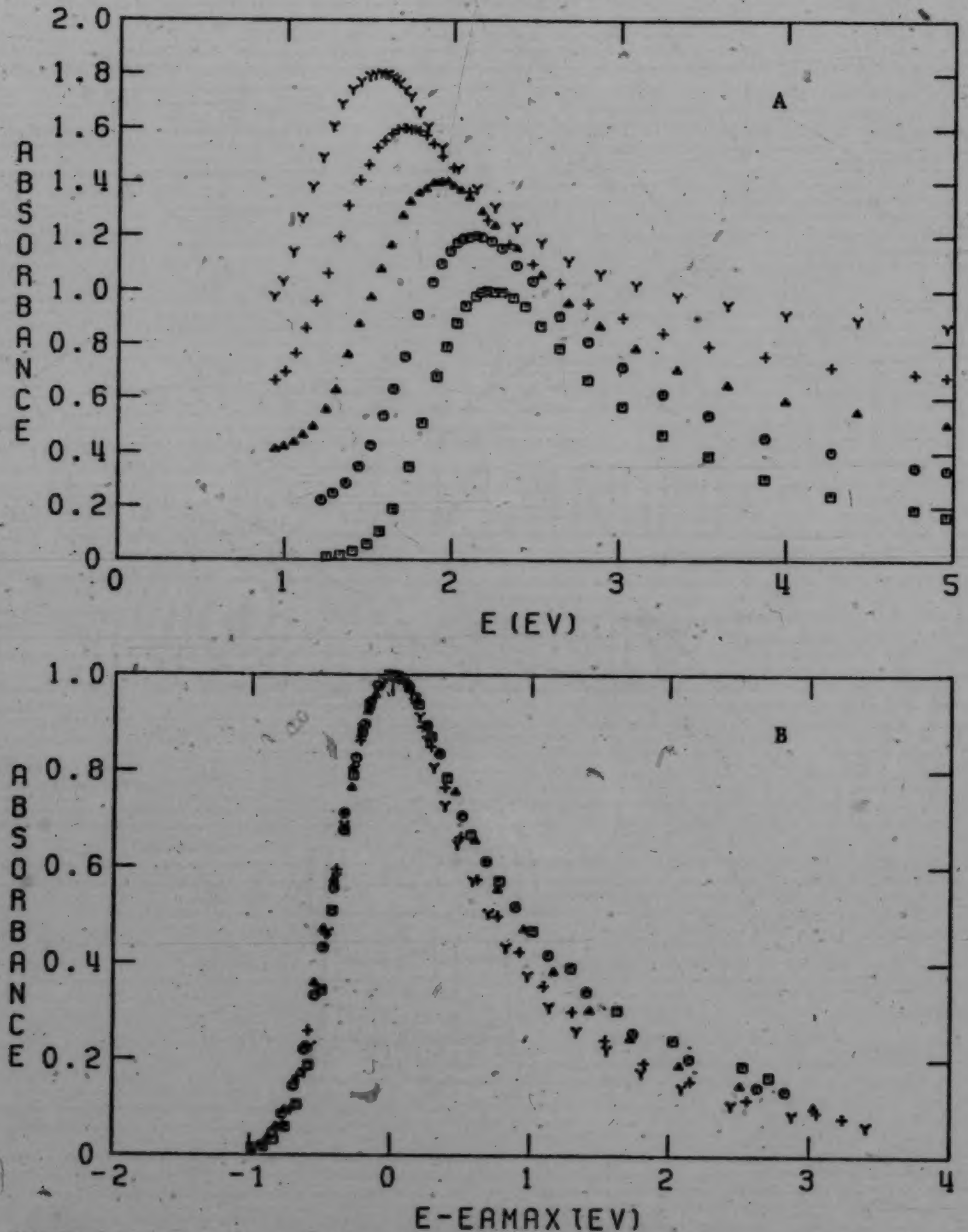

FIGURE III-34. The Optical Absorption Spectrum of Solvated Electrons in a Solution of 10 Mole % Water in Ethanol at Different Temperatures.

A: Successive spectra are displaced vertically by 0.2 units.

B: The spectra are normalized at E_{Amax}. □, 160K; ○, 200K; △, 250K; +, 298K; Y, 350K.

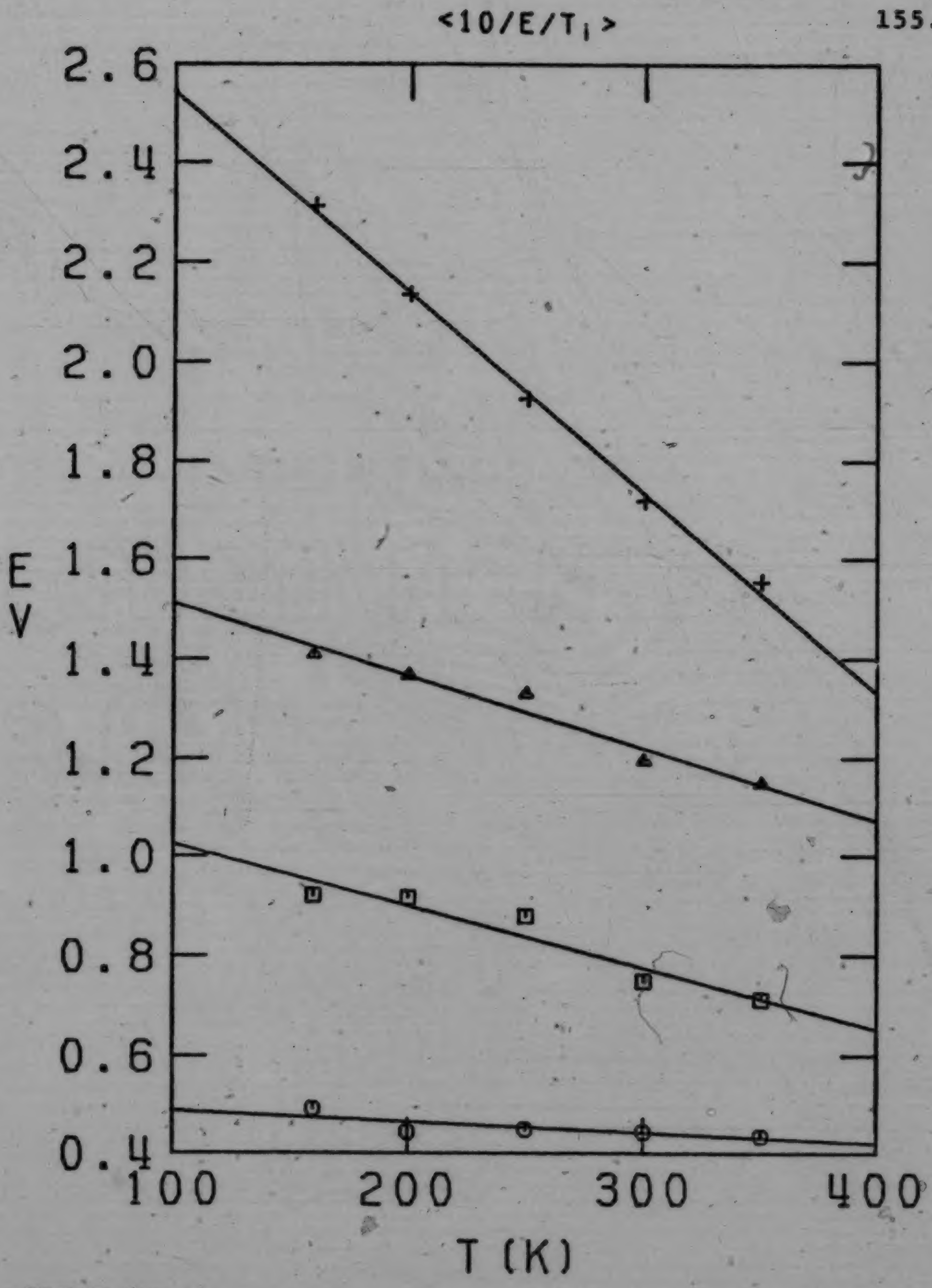

FIGURE III-35. Temperature Dependence of Spectrum Parameters in a Solution of 10 Mole % Water in Ethanol.

+, E_{Amax}; △, $W_{\frac{1}{2}}$; O, W_r; □, W_b.

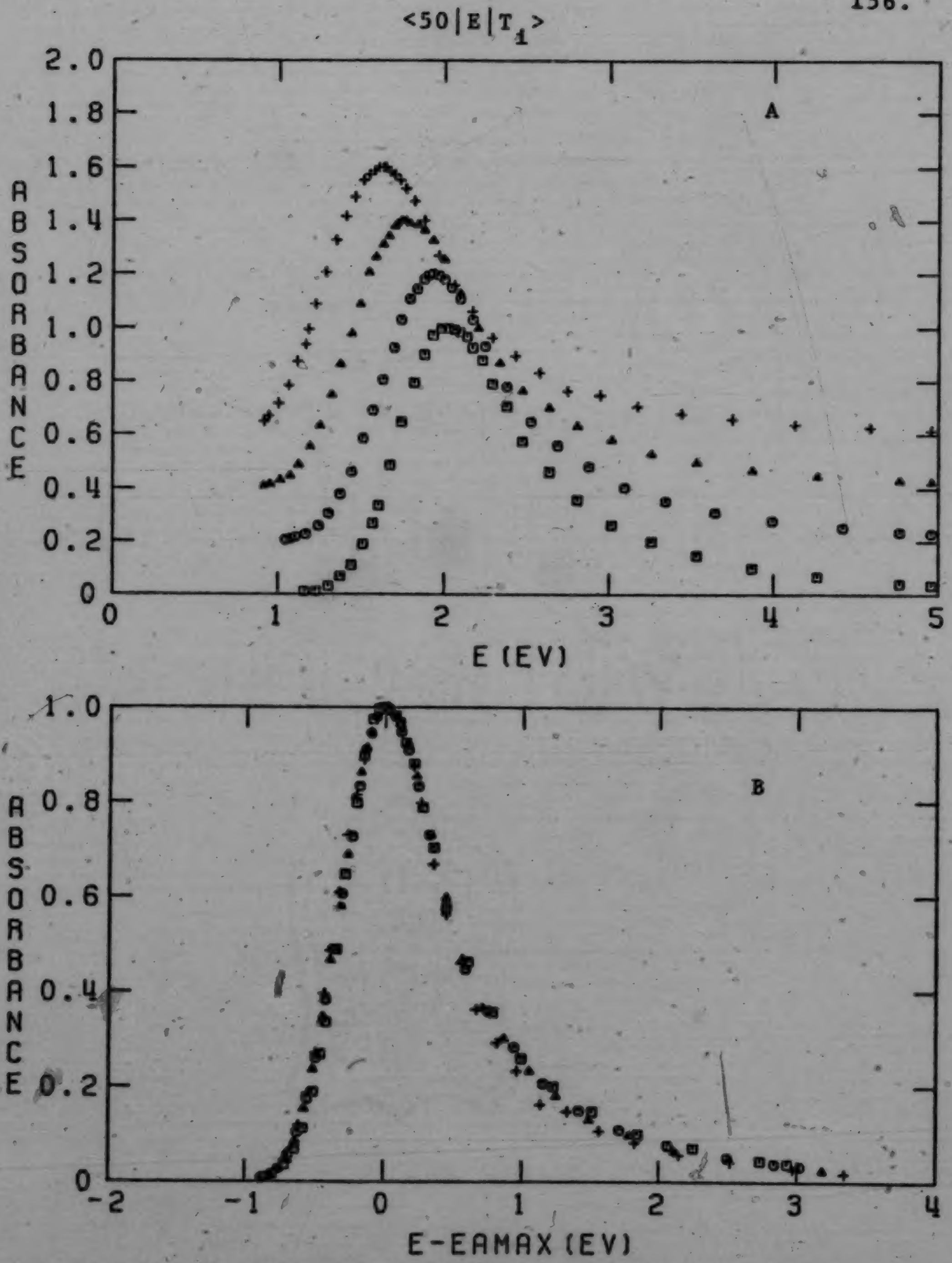

FIGURE III-36. The Optical Absorption Spectrum of Solvated Electrons in a Solution of 50 Mole % Water in Ethanol at Different Temperatures.

A: Successive spectra are displaced vertically by 0.2 units.

B: The spectra are normalized at E_{Amax}. □, 222K; O, 250K; △, 298K; +, 350K.

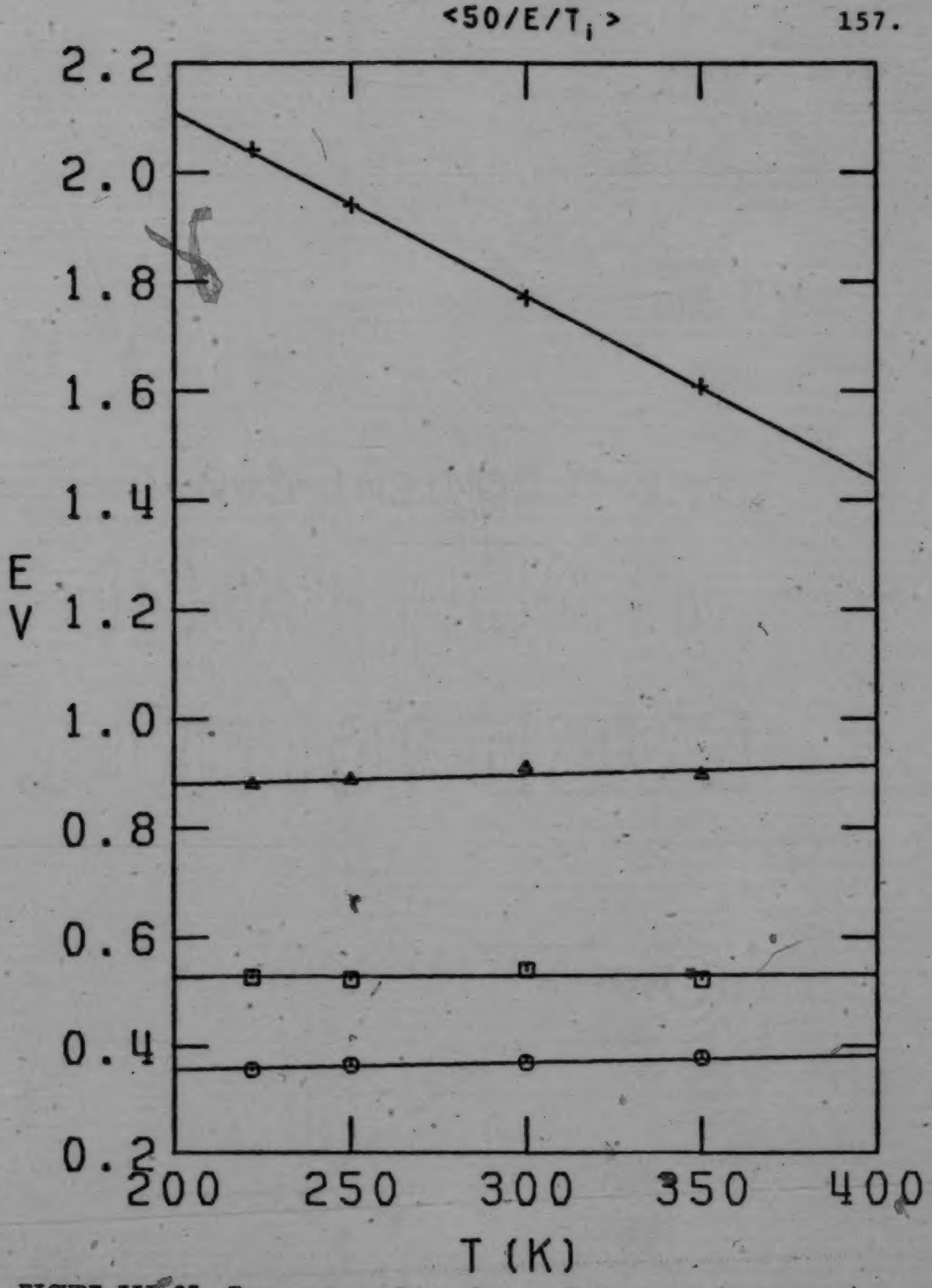

FIGURE III-37. Temperature Dependence of Spectrum Parameters in a Solution of 50 Mole % Water in Ethanol.

+, E_{Amax}; △, $W_{\frac{1}{2}}$; O, W_r; □, W_b.

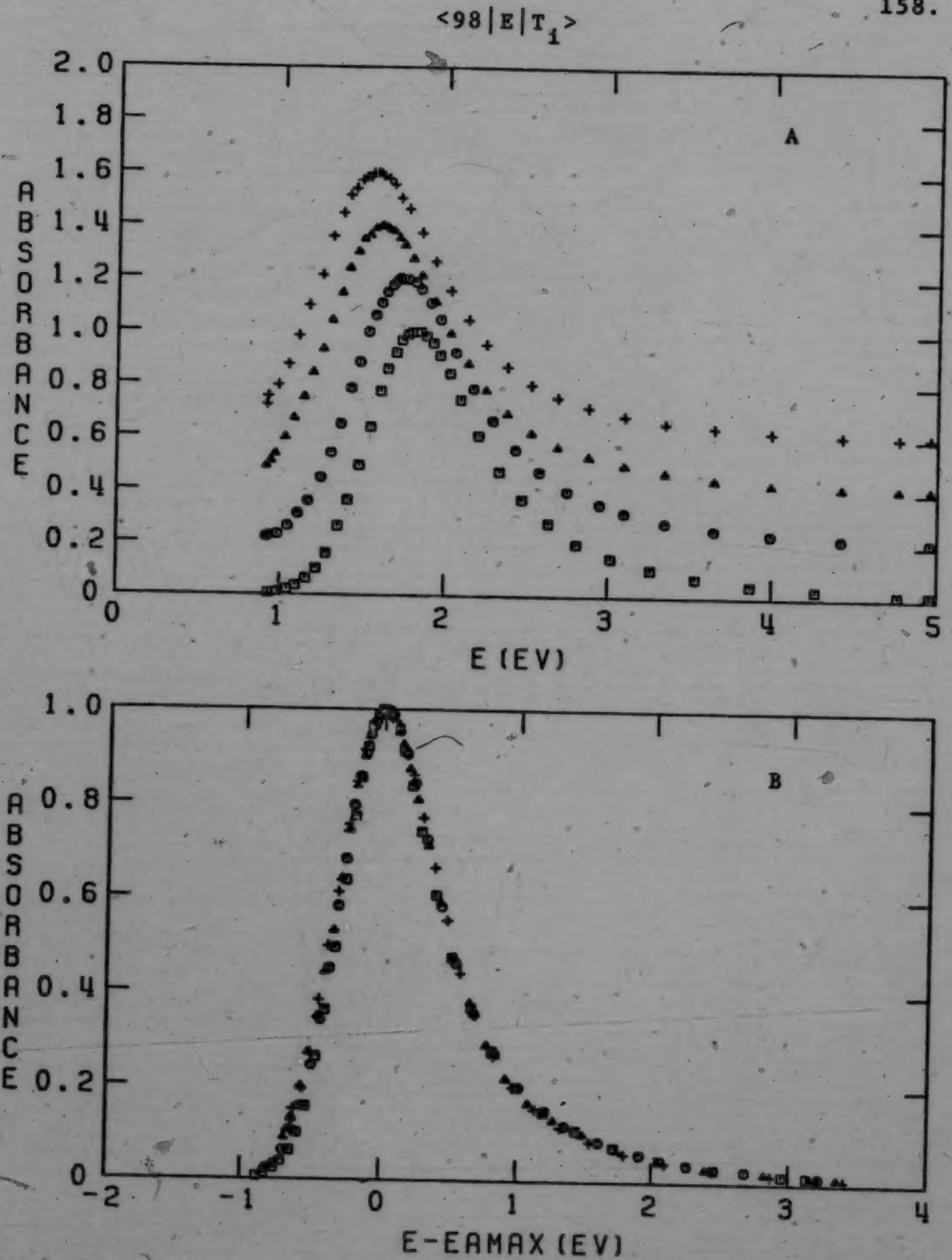

FIGURE III-38. The Optical Absorption Spectrum of Solvated Electrons in a Solution of 98 Mole % Water in Ethanol at Different Temperatures.

A: Successive spectra are displaced vertically by 0.2 units.

B: The spectra are normalized at E_{Amax}. □, 273K; O, 298K; △, 350K; +, 366K.

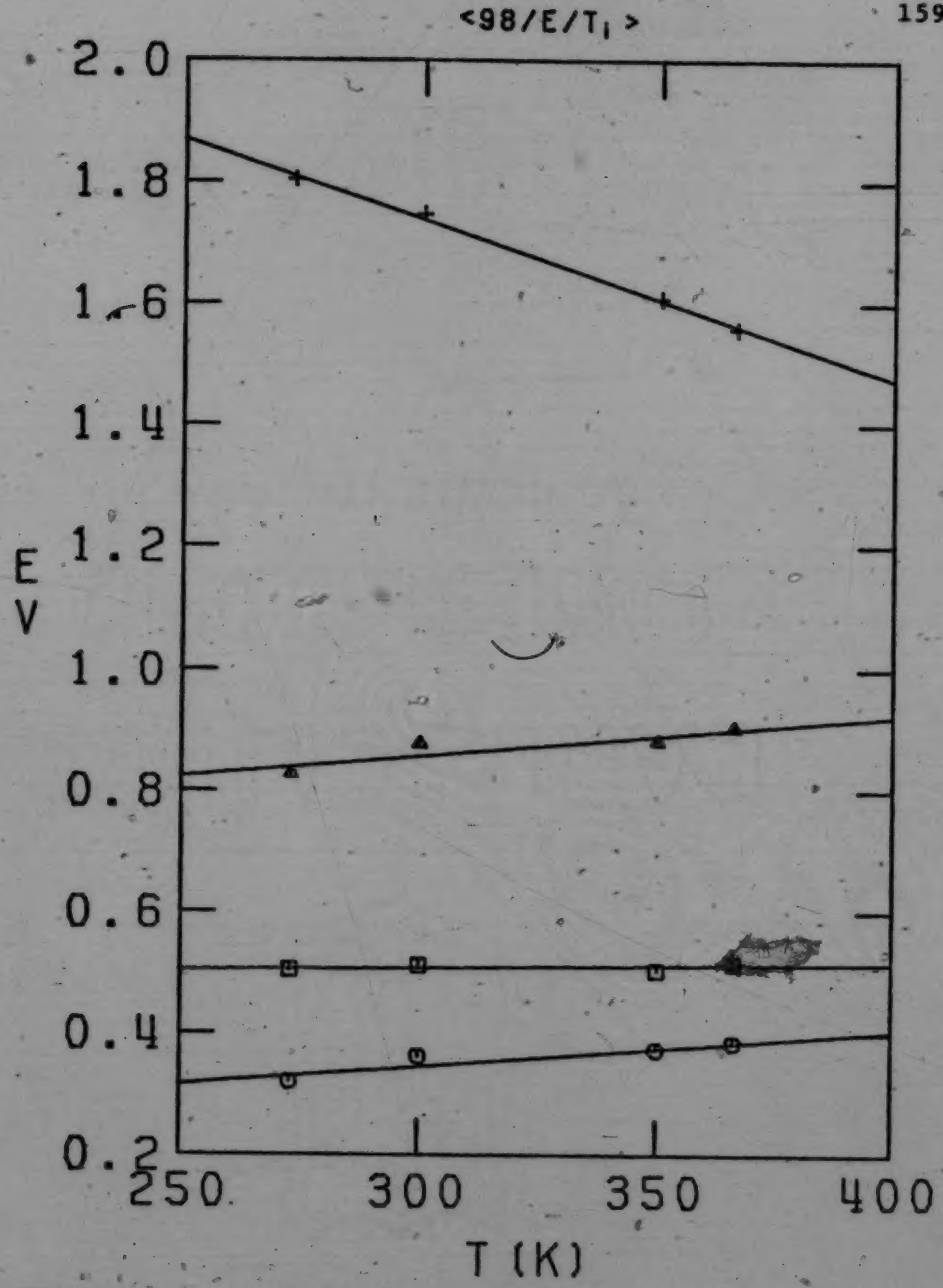

FIGURE III-39. Temperature Dependence of Spectrum Parameters in a Solution of 98 Mole % Water in Ethanol.

+, E_{Amax}; △, $W_{\frac{1}{2}}$; O, W_r; □, W_b.

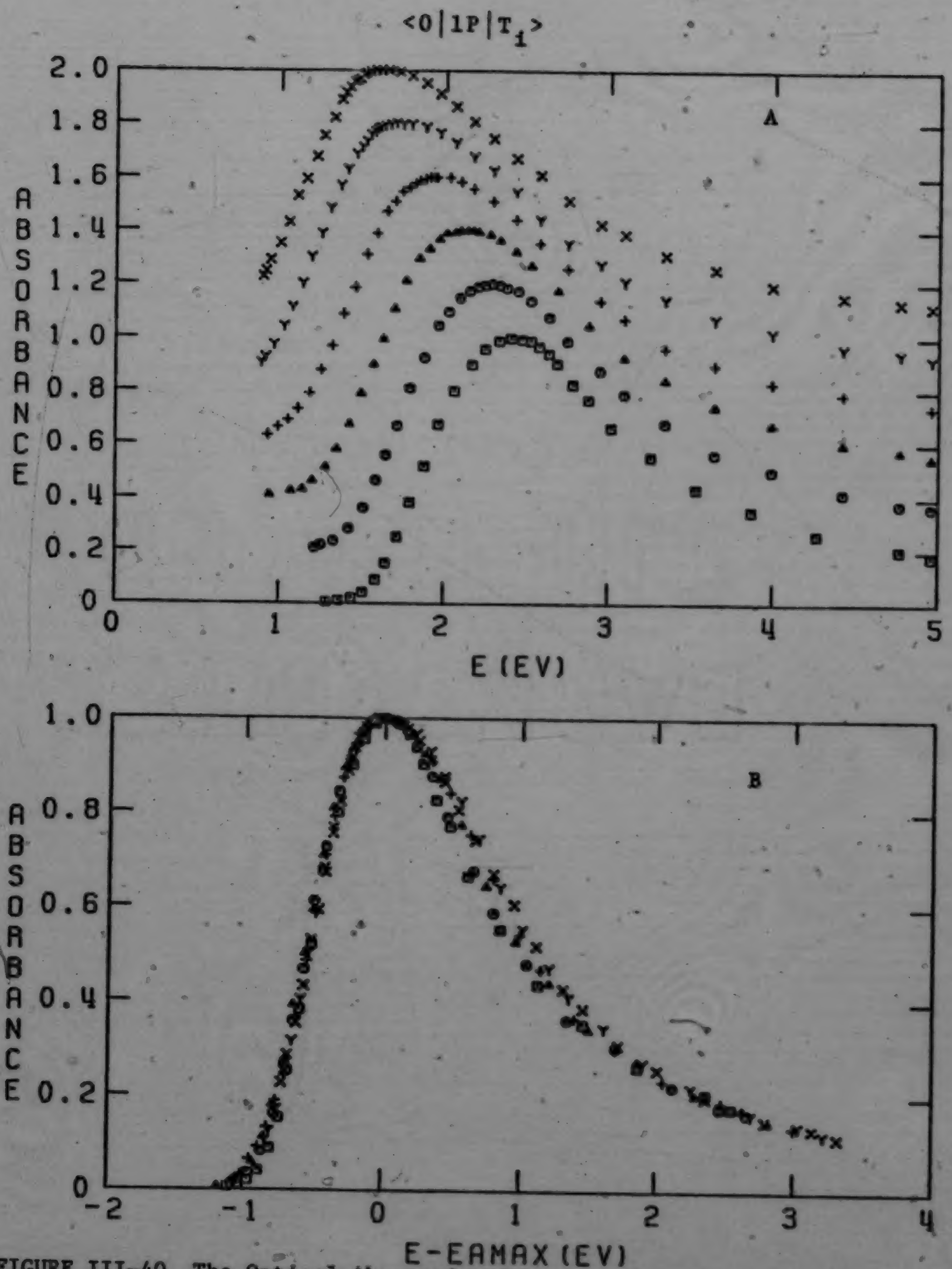
$\langle 0|1P|T_i \rangle$

FIGURE III-40. The Optical Absorption Spectrum of Solvated Electrons in 1-Propanol at Different Temperatures.

A: Successive spectra are displaced vertically by 0.2 units.

B: The spectra are normalized at E_{Amax}. □, 150K; O, 200K; △, 250K; +, 298K; Y, 350K; X, 369K.

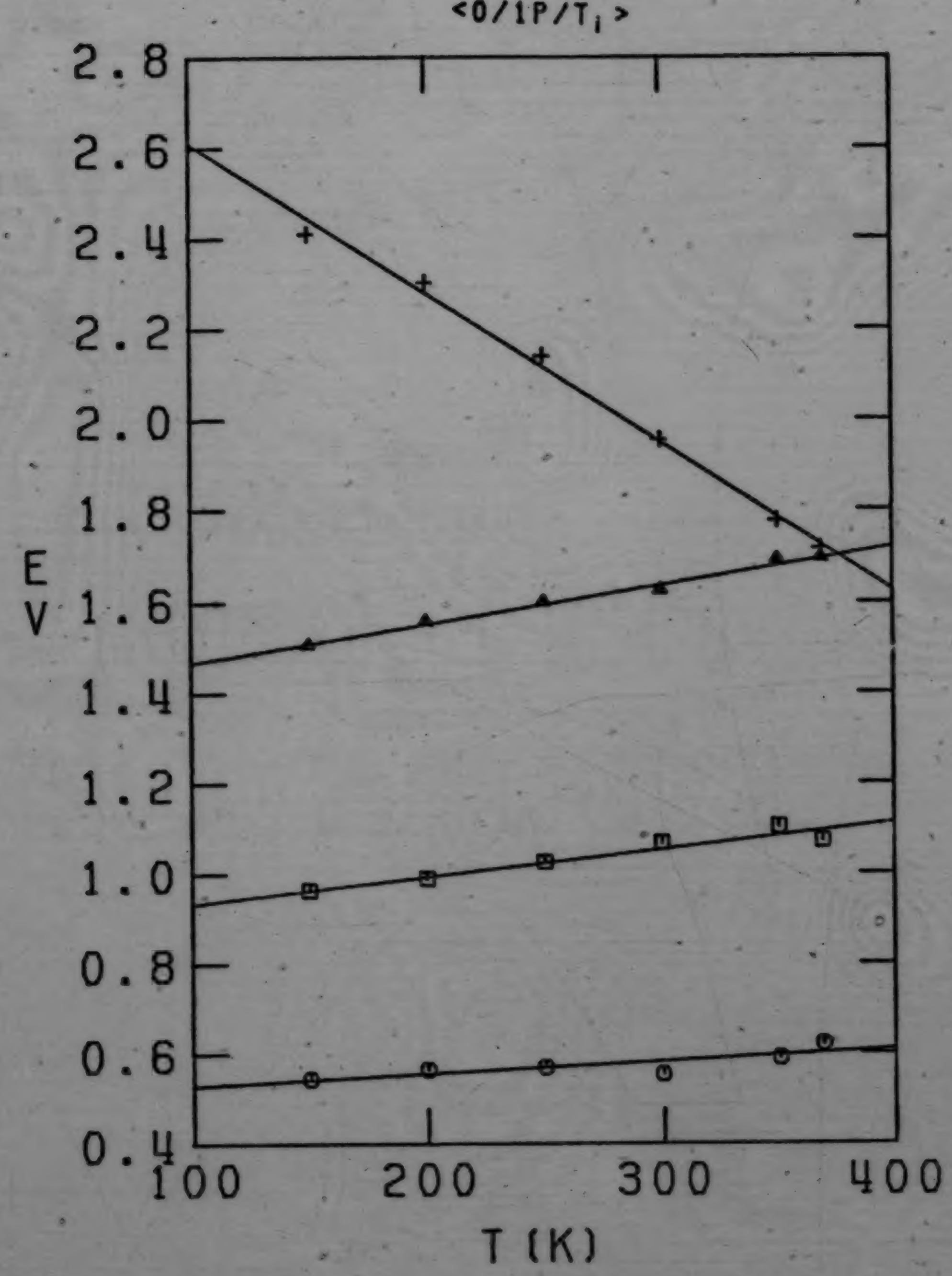

FIGURE III-41. Temperature Dependence of Spectrum Parameters in 1-Propanol.

+, E_{Amax}; Δ, $W_{\frac{1}{2}}$; O, W_r; □, W_b.

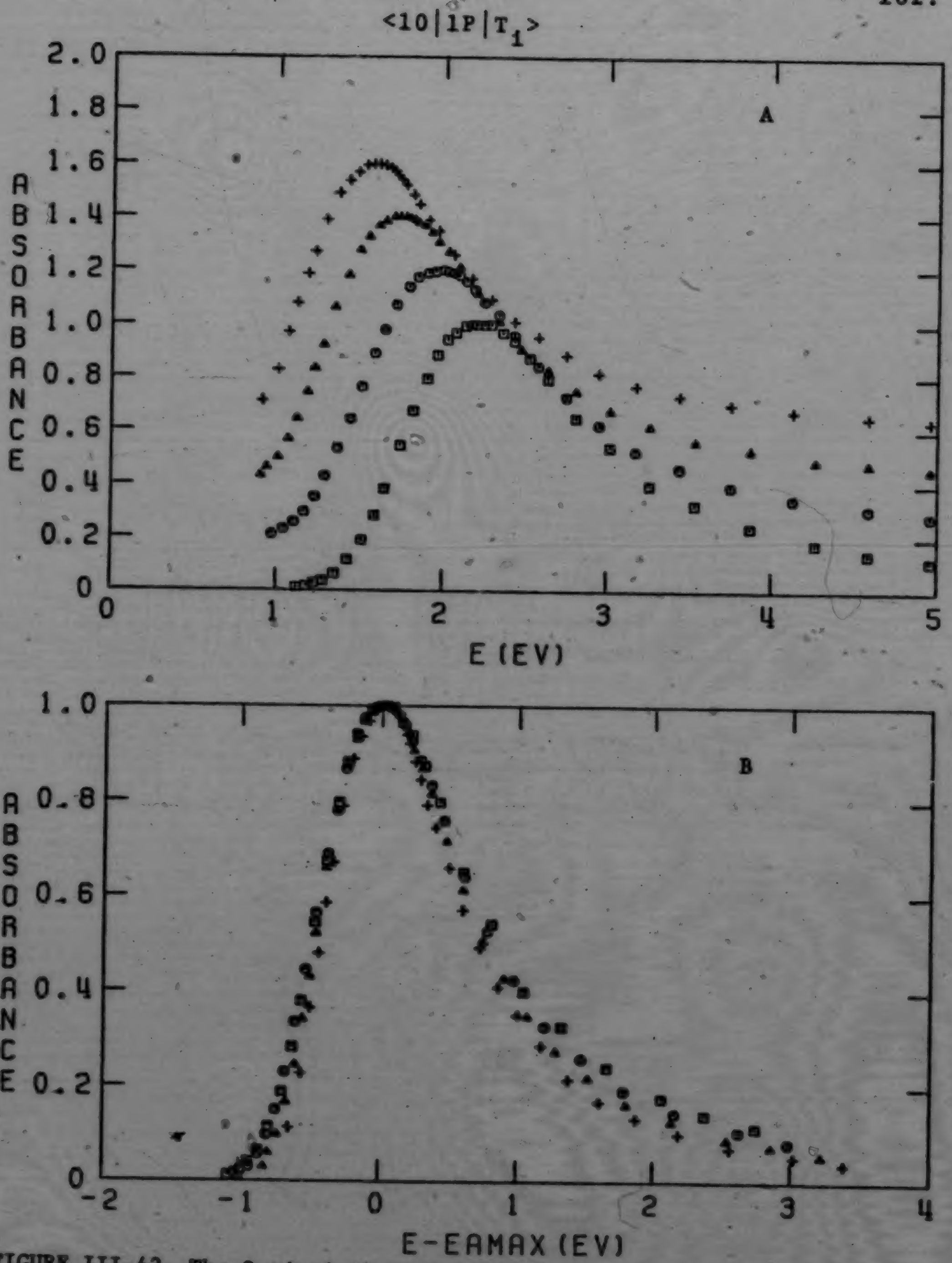

FIGURE III-42. The Optical Absorption Spectrum of Solvated Electrons in a Solution of 10 Mole % Water in 1-Propanol at Different Temperatures.

A: Successive spectra are displaced vertically by 0.2 units.

B: The spectra are normalized at E_{Amax}. □, 200K; O, 250K; △, 298K; +, 350K.

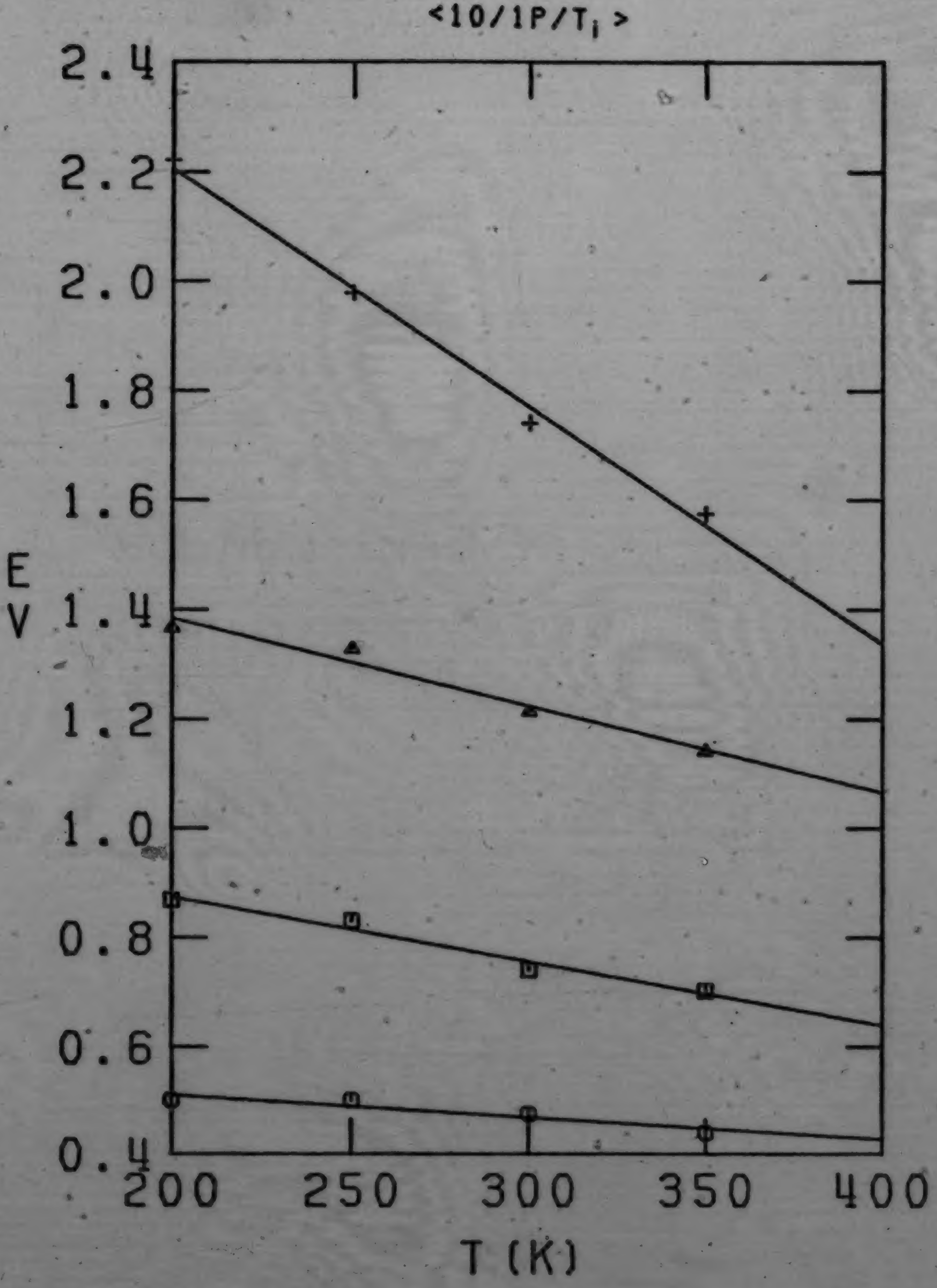

FIGURE III-43. Temperature Dependence of Spectrum Parameters in a Solution of 10 Mole % Water in 1-Propanol.

+, E_{Amax}; △, $W_{½}$; O, W_r; □, W_b.

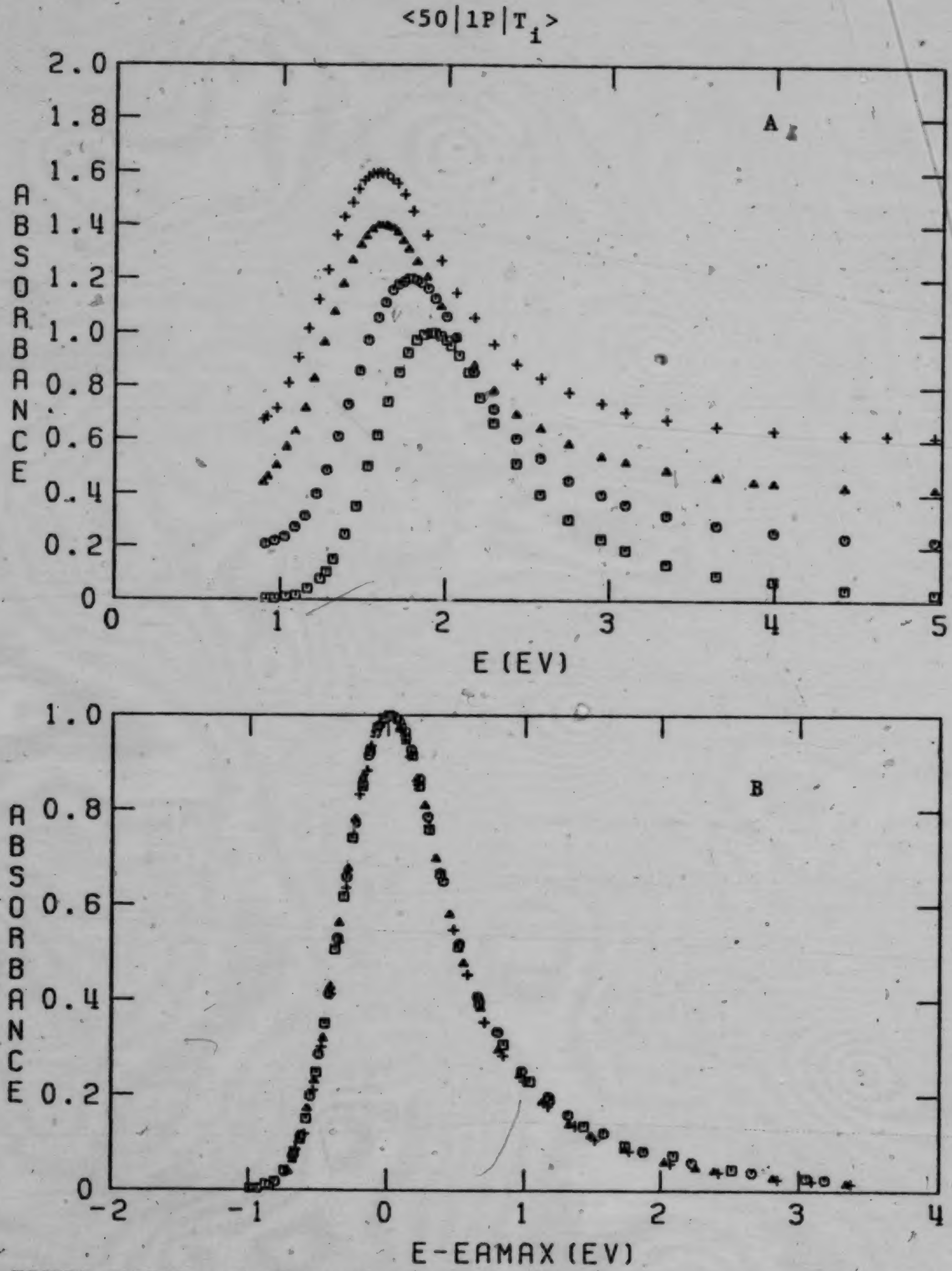

FIGURE III-44. The Optical Absorption Spectrum of Solvated Electrons in a Solution of 50 Mole % Water in 1-Propanol at Different Temperatures.

A: Successive spectra are displaced vertically by 0.2 units.

B: The spectra are normalized at E_{Amax}. □, 260K; O, 298K; △, 350K; +, 360K.

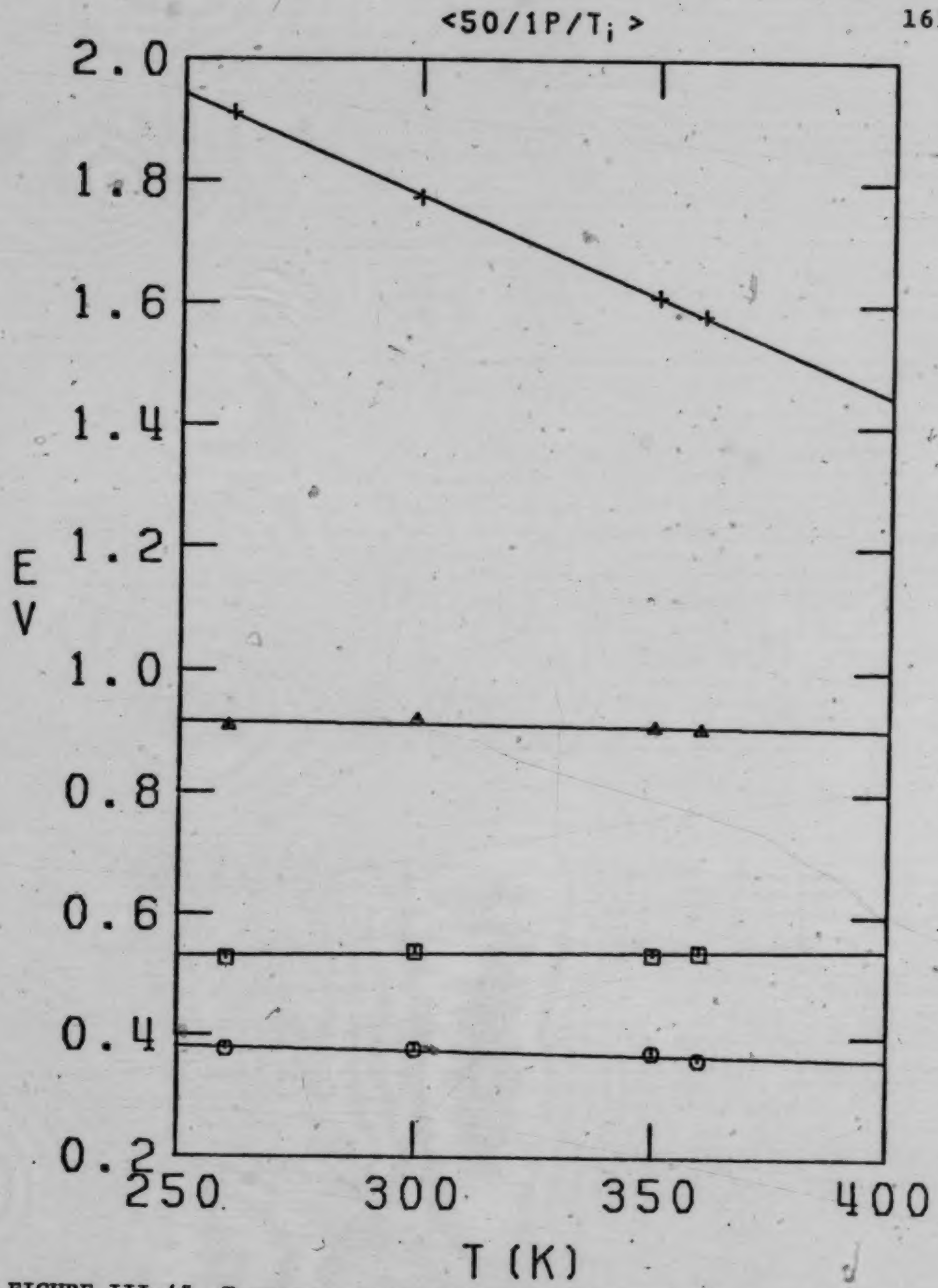

FIGURE III-45. Temperature Dependence of Spectrum Parameters in a Solution of 50 Mole % Water in 1-Propanol.

+, E_{Amax}; △, $W_{\frac{1}{2}}$; O, W_r; □, W_b.

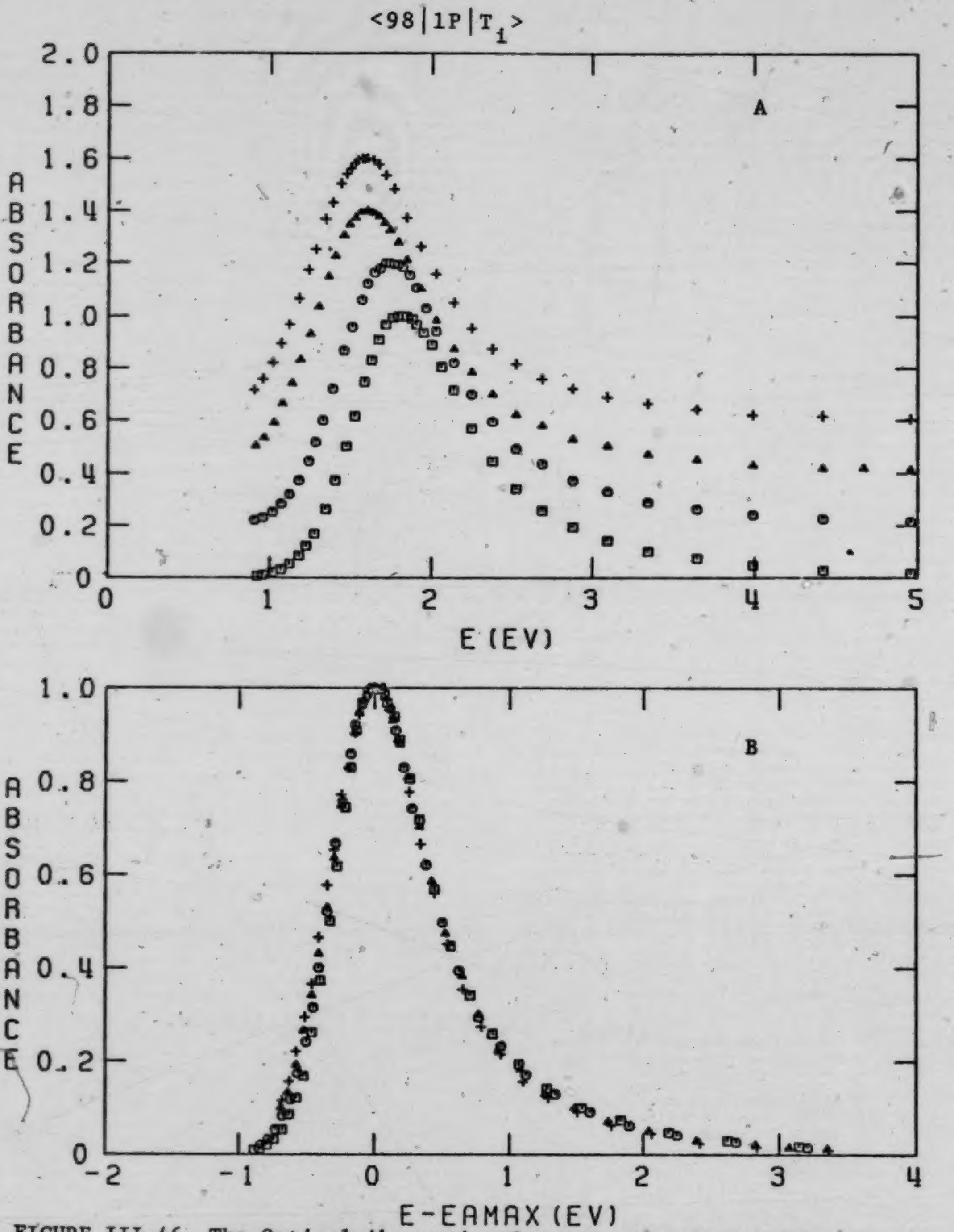

FIGURE III-46. The Optical Absorption Spectrum of Solvated Electrons in a Solution of 98 Mole % Water in 1-Propanol at Different Temperatures.

A: Successive spectra are displaced vertically by 0.2 units.

B: The spectra are normalized at E_{Amax}. □, 273K, O, 298K; △, 350K; +, 363K.

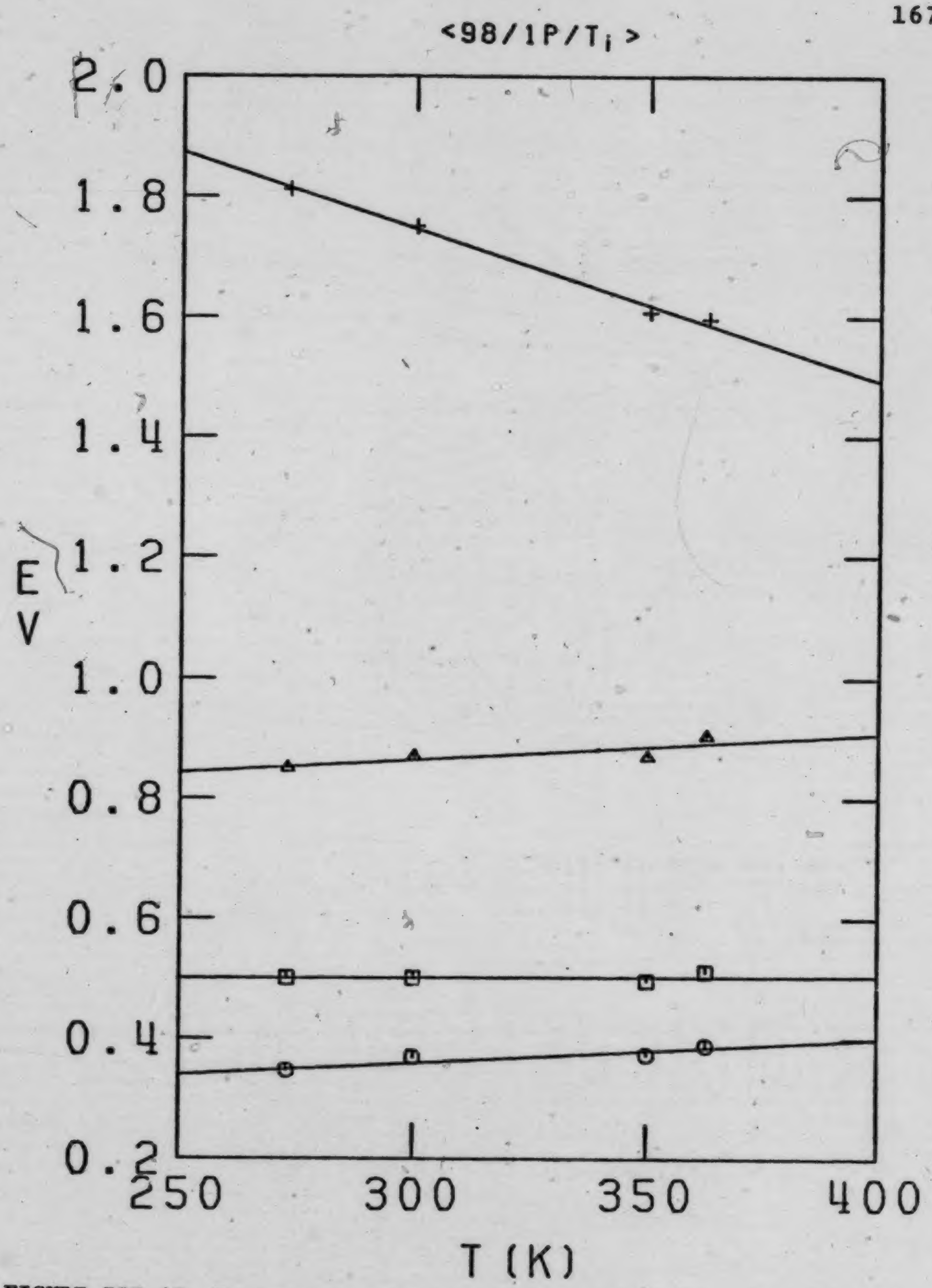

FIGURE III-47. Temperature Dependence of Spectrum Parameters in a Solution of 98 Mole % Water in 1-Propanol.

+, E_{Amax}; △, $W_{\frac{1}{2}}$; O, W_r; □, W_b.

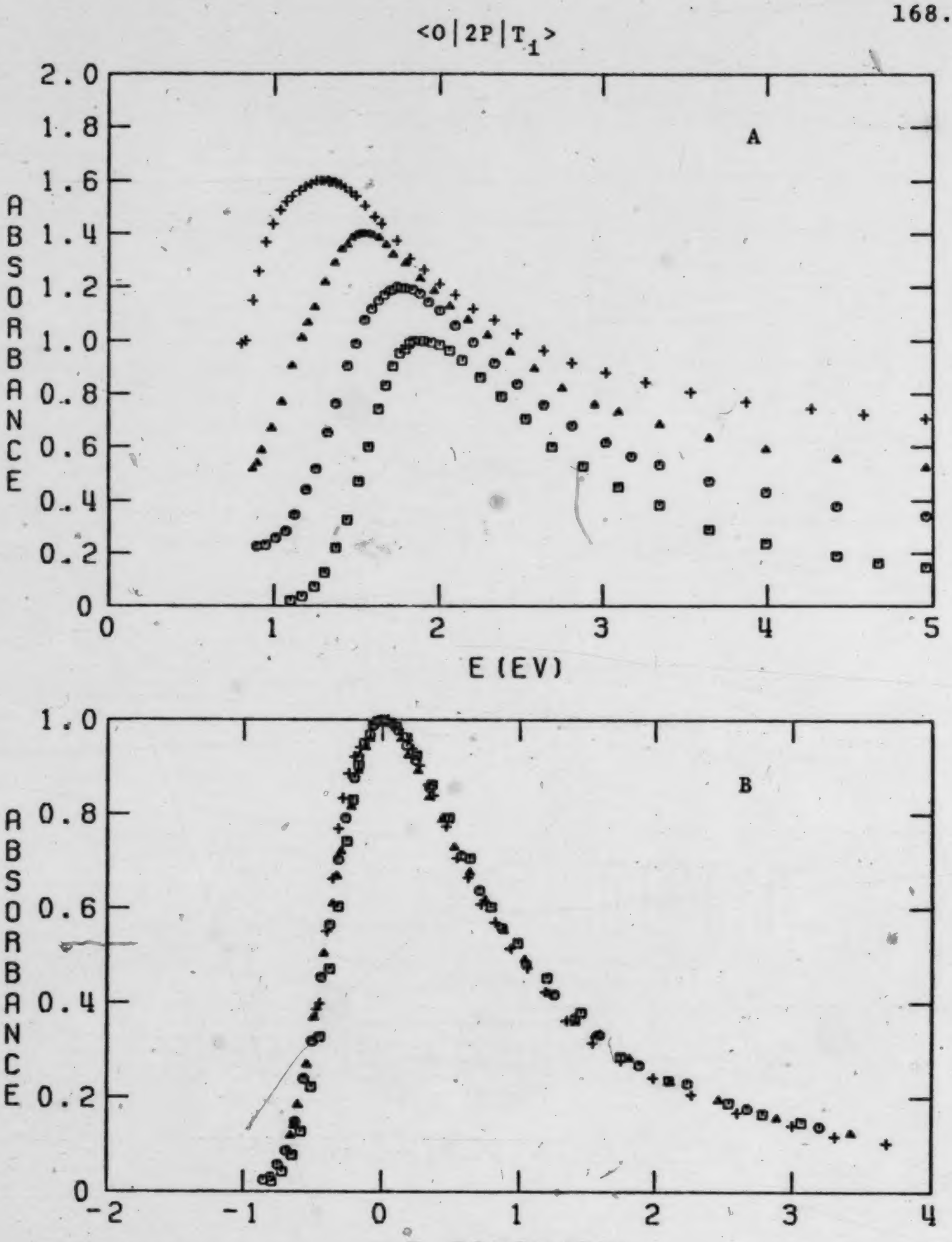

FIGURE III-48. The Optical Absorption Spectrum of Solvated Electrons in 2-Propanol at Different Temperatures.

A: Successive spectra are displaced vertically by 0.2 units.

B: The spectra are normalized at E_{Amax}. □, 200K; O, 250K; △, 298K; +, 350K.

<0/2P/T$_i$>

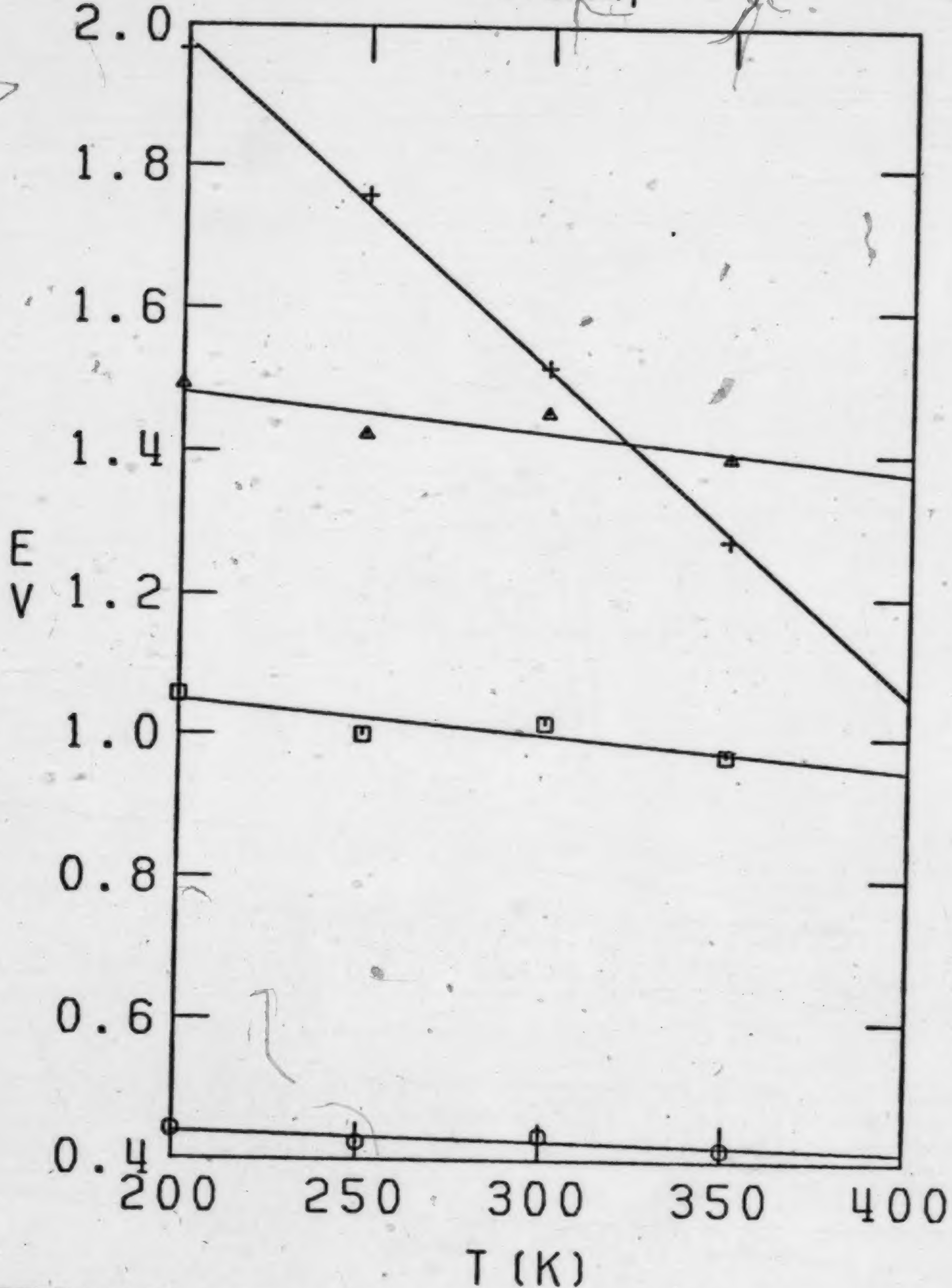

FIGURE III-49. Temperature Dependence of Spectrum Parameters in 2-Propanol.

+, E_{Amax}; △, $W_{\frac{1}{2}}$; O, W_r; □, W_b.

<10|2P|T_1>

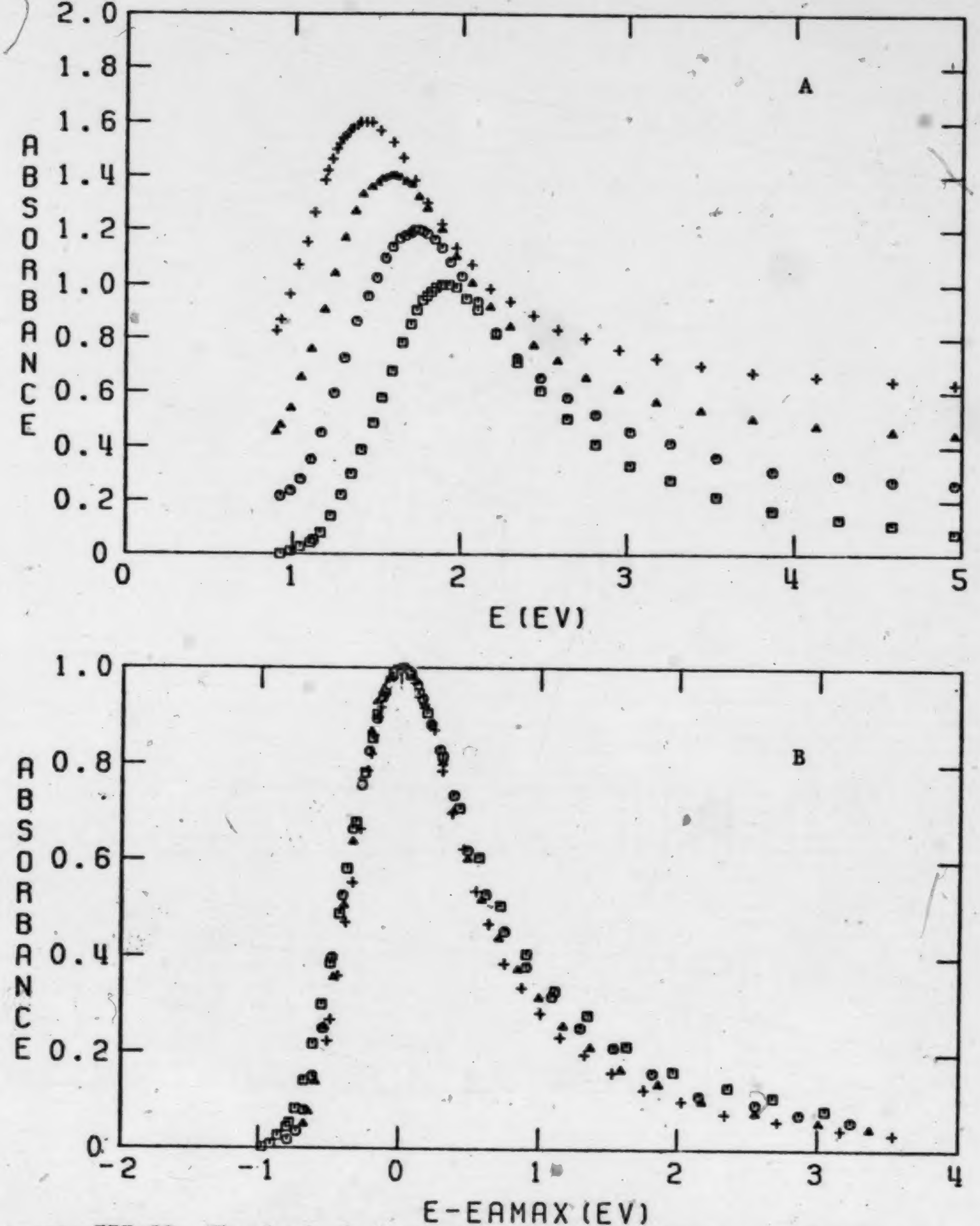

FIGURE III-50. The Optical Absorption Spectrum of Solvated Electrons in a Solution of 10 Mole % Water in 2-Propanol at Different Temperatures.

A: Successive spectra are displaced vertically by 0.2 units.

B: The spectra are normalized at E_{Amax}. □, 200K; O, 250K; △, 298K; +, 350K.

<10/2P/T$_i$>

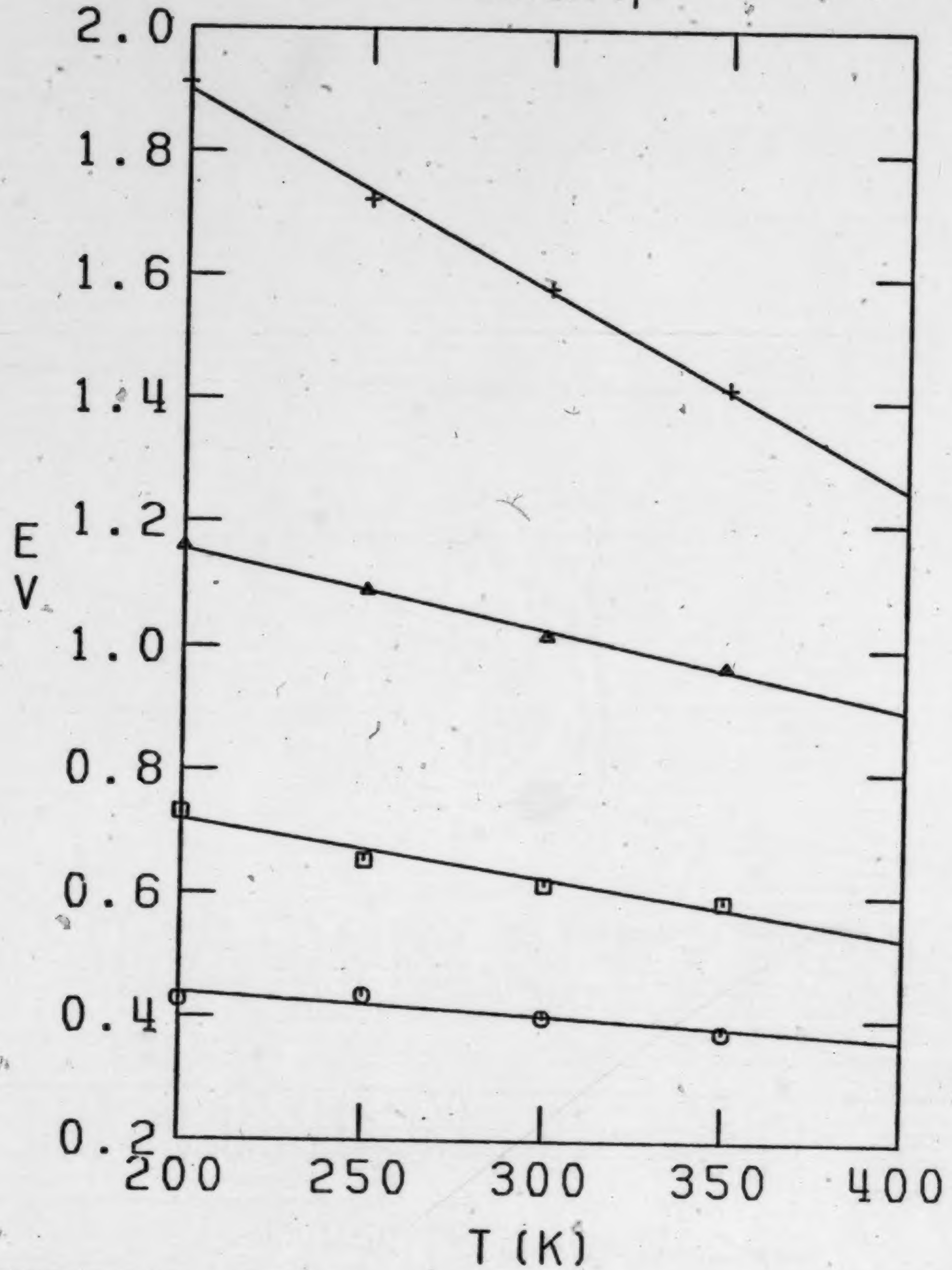

FIGURE III-51. Temperature Dependence of Spectrum Parameters in a Solution of 10 Mole % Water in 2-Propanol.

+, E_{Amax}: Δ, $W_{\frac{1}{2}}$; O, W_r; □, W_b.

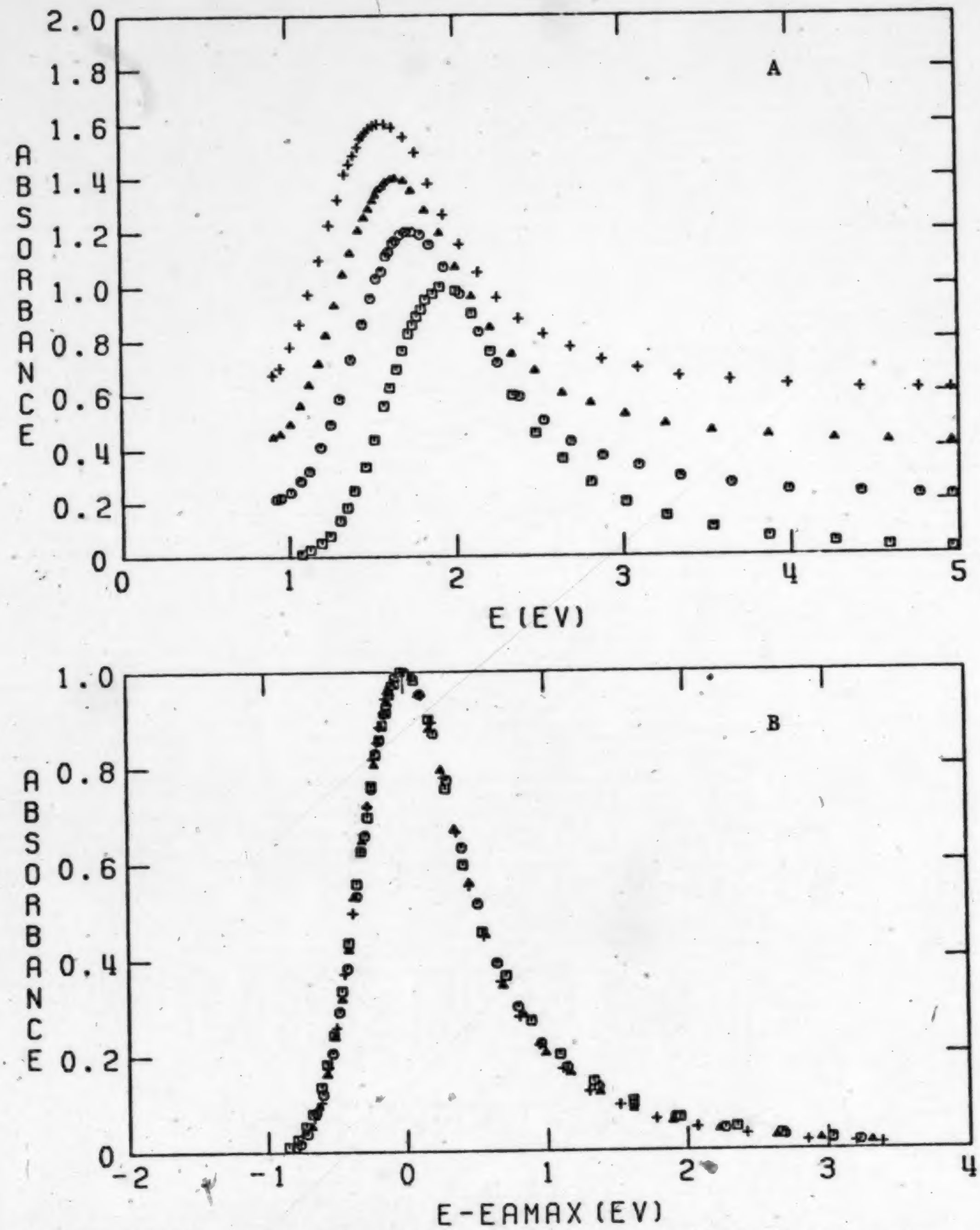

FIGURE III-52. The Optical Absorption Spectrum of Solvated Electrons in a Solution of 50 Mole % Water in 2-Propanol at Different Temperatures.

A: Successive spectra are displaced vertically by 0.2 units.

B: The spectra are normalized at E_{Amax}. □, 250K; O, 298K; △, 339K; +, 352K.

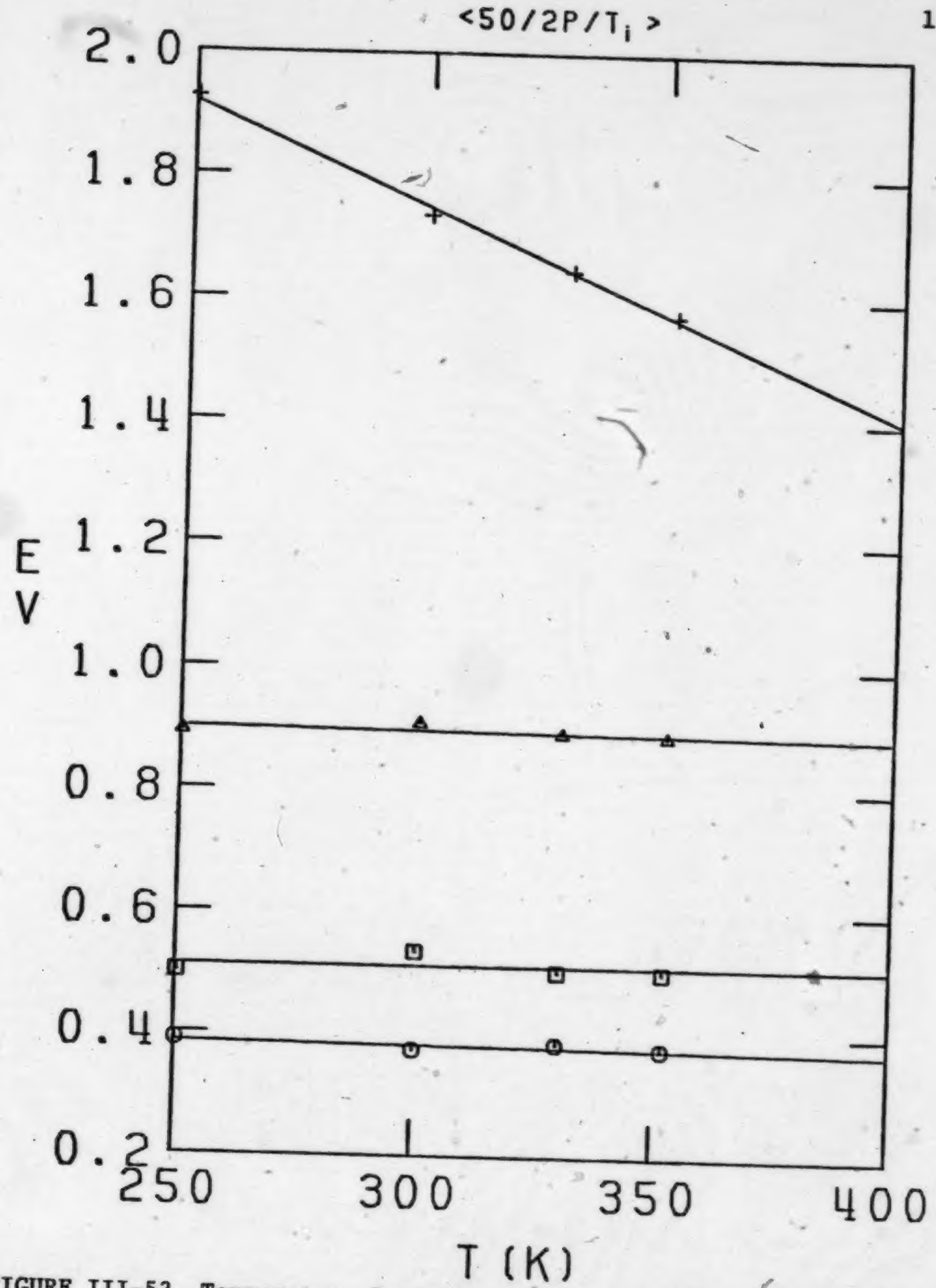

FIGURE III-53. Temperature Dependence of Spectrum Parameters in a Solution of 50 Mole % Water in 2-Propanol.

+, E_{Amax}; △, $W_{\frac{1}{2}}$; O, W_r; □, W_b.

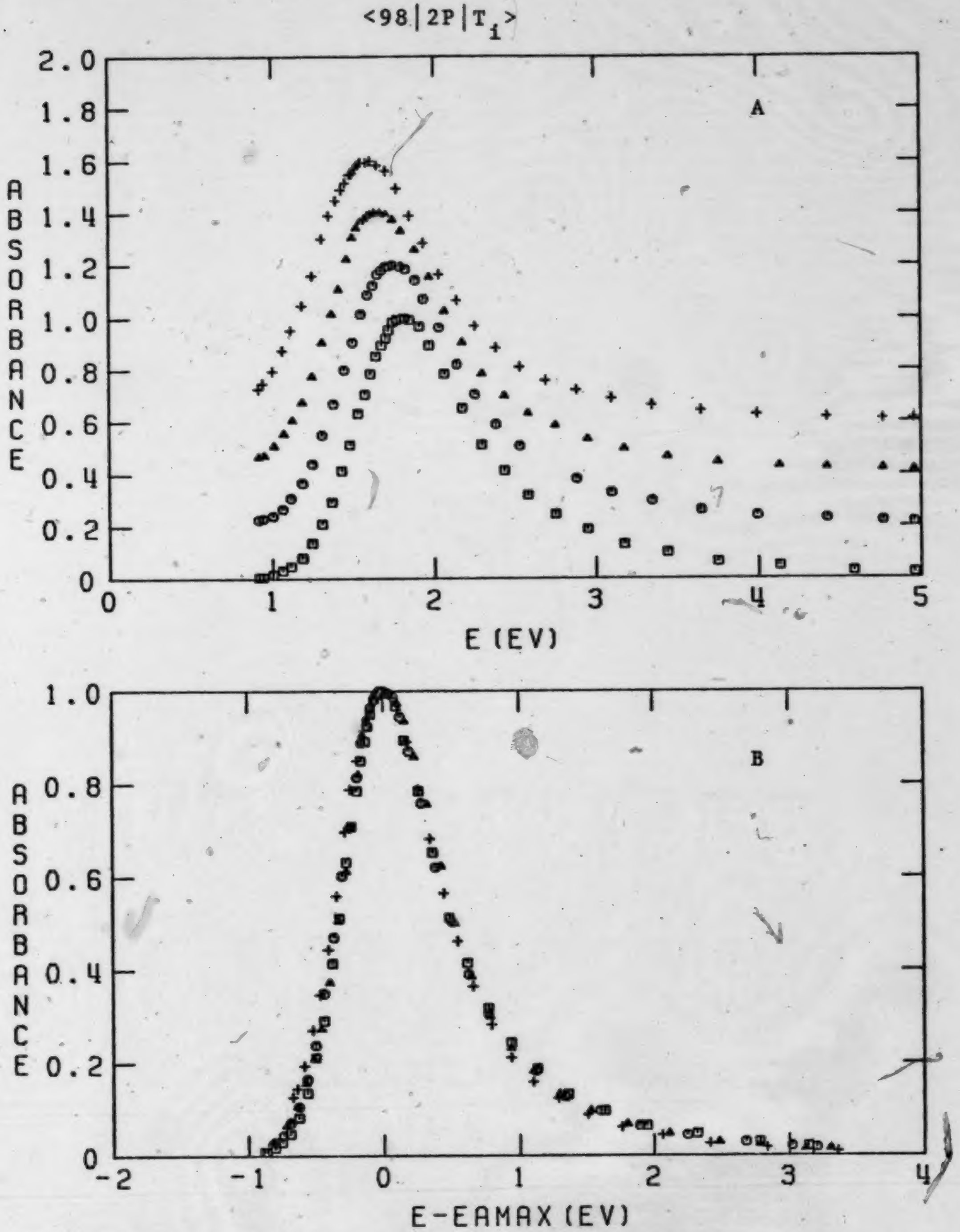

FIGURE III-54. The Optical Absorption Spectrum of Solvated Electrons in a Solution of 98 Mole % Water in 2-Propanol at Different Temperatures.

A: Successive spectra are displaced vertically by 0.2 units.

B: The spectra are normalized at E_{Amax}. □, 273K; O, 298K; Δ, 339K; +, 360K.

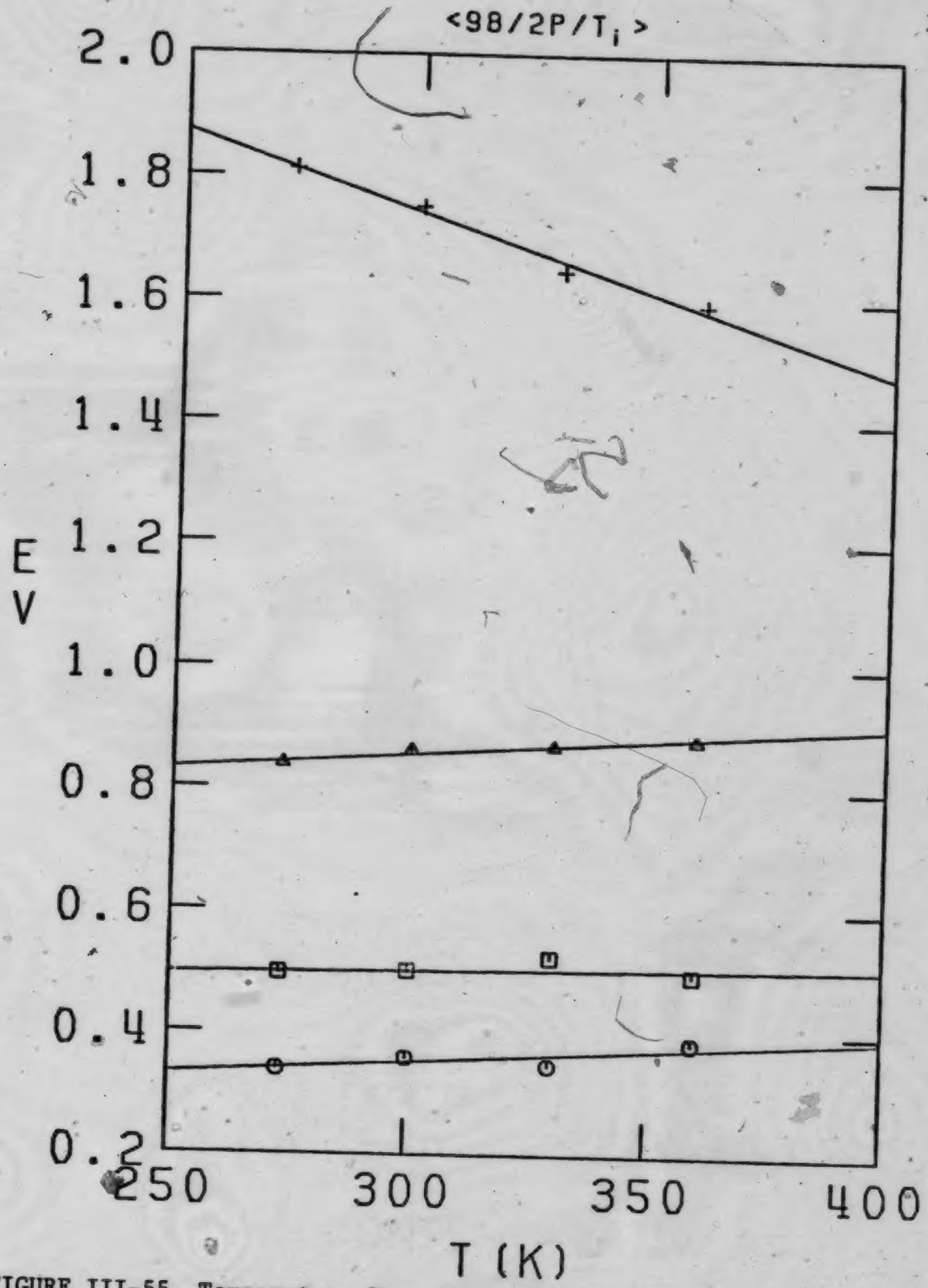

FIGURE III-55. Temperature Dependence of Spectrum Parameters in a Solution of 98 Mole % Water in 2-Propanol.

+, E_{Amax}; Δ, $W_{\frac{1}{2}}$; O, W_r; □, W_b.

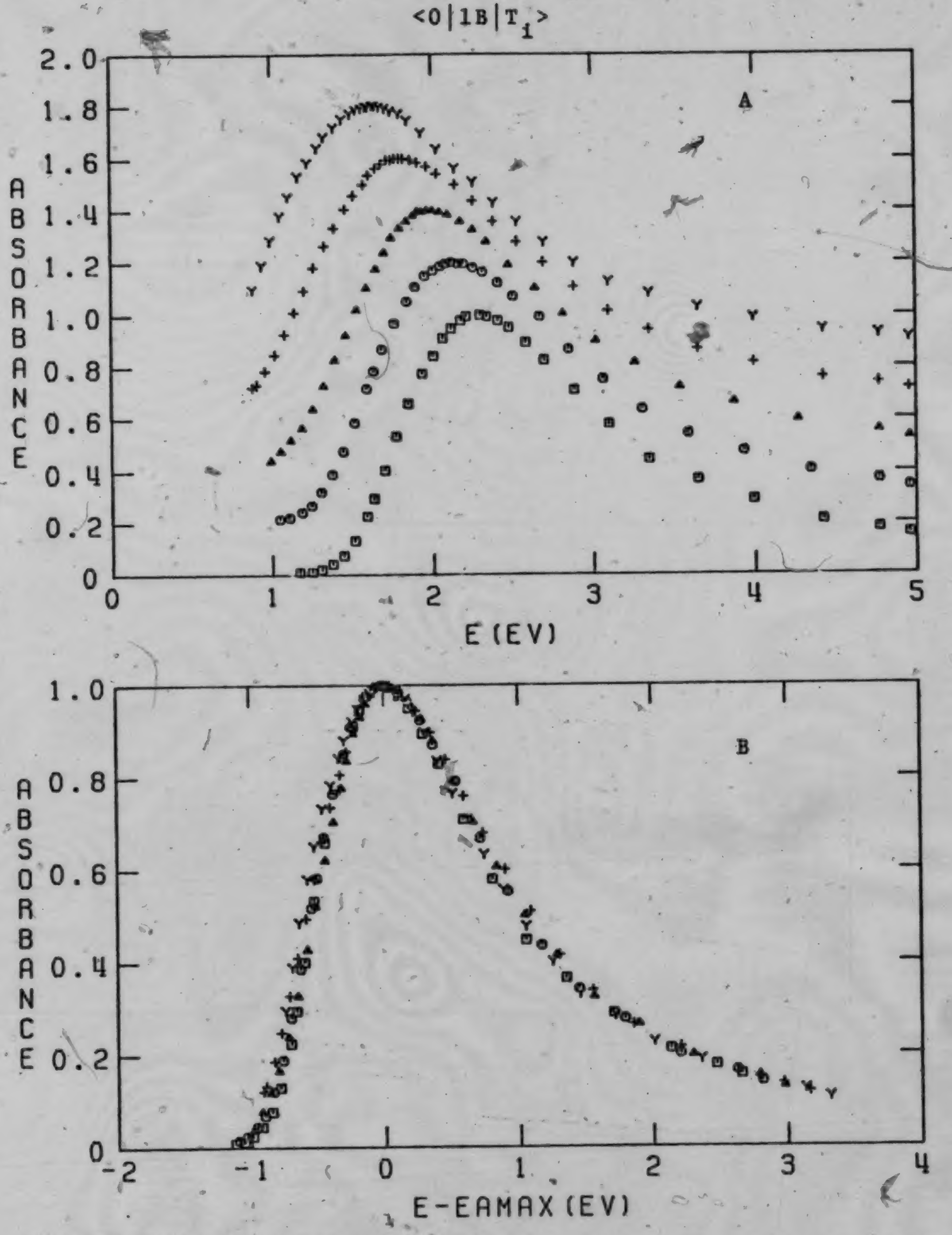

FIGURE III-56. The Optical Absorption Spectrum of Solvated Electrons in 1-Butanol at Different Temperatures.

A: Successive spectra are displaced vertically by 0.2 units.

B: The spectra are normalized at E_{Amax}. □, 200K; O, 250K: △, 298K; +, 350K; Y, 388K.

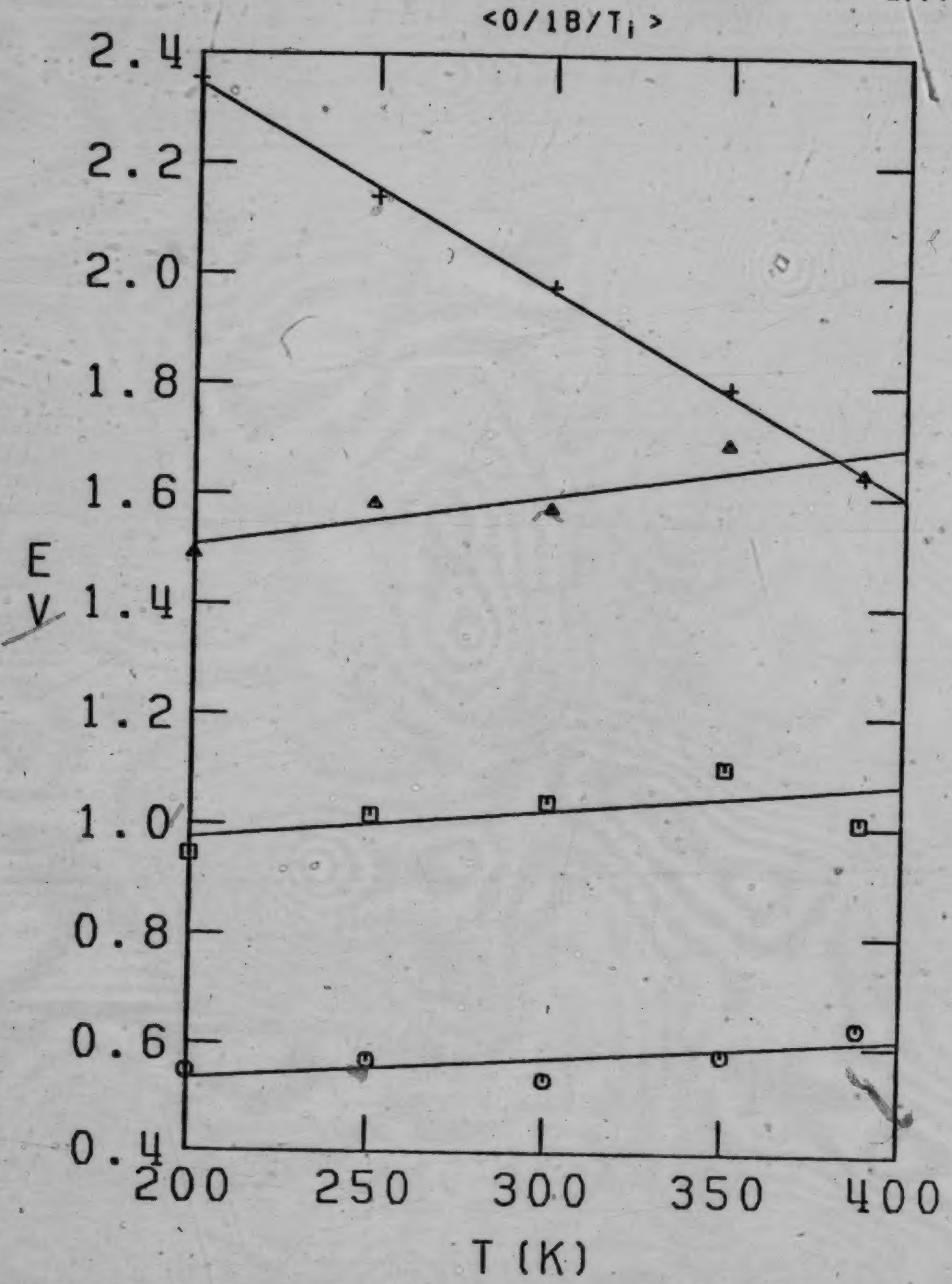

FIGURE III-57. Temperature Dependence of Spectrum Parameters in 1-Butanol.

+, E_{Amax}; △, $W_{\frac{1}{2}}$; O, W_r; □, W_b.

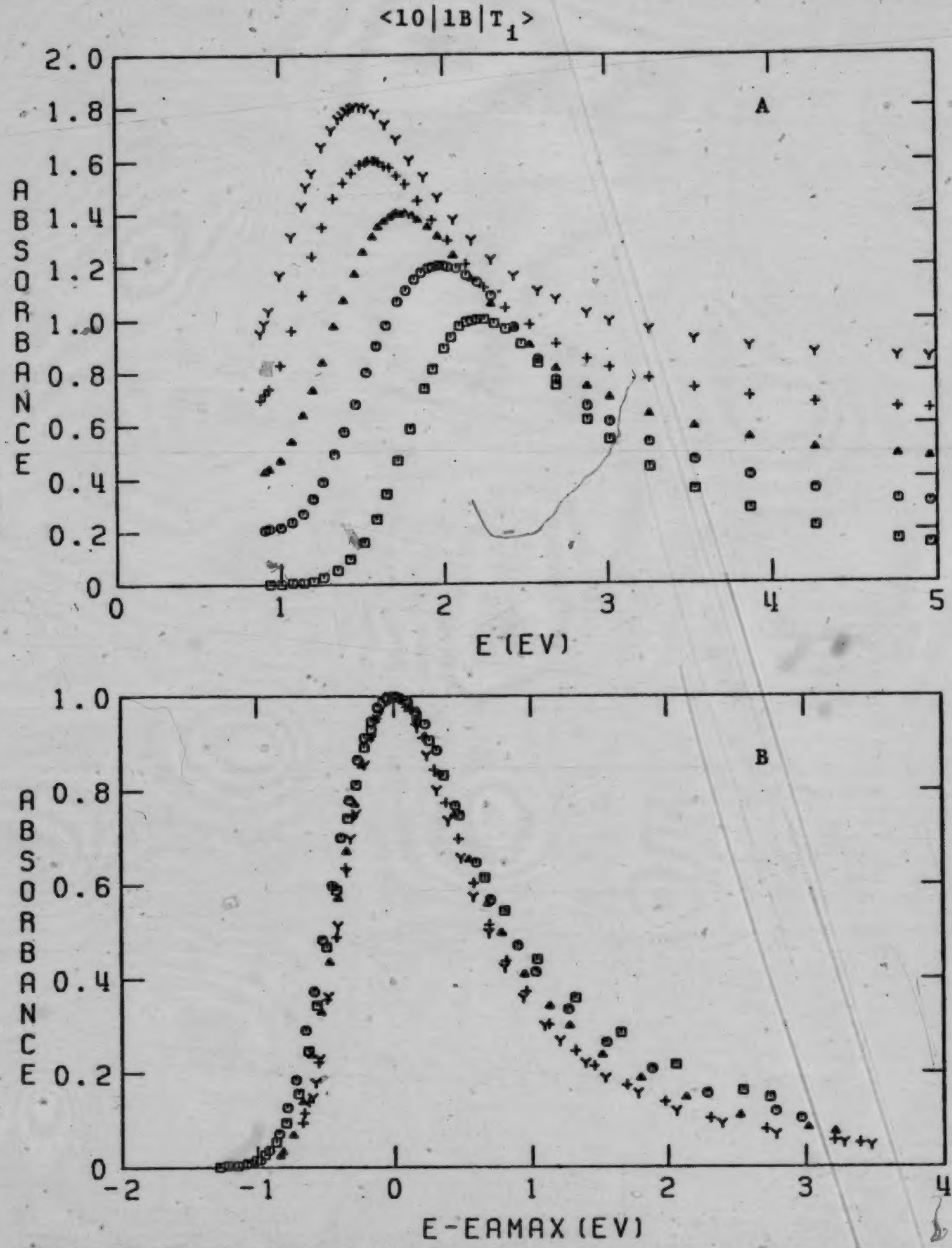

FIGURE III-58. The Optical Absorption Spectrum of Solvated Electrons in a Solution of 10 Mole % Water in 1-Butanol at Different Temperatures.

A: Successive spectra are displaced vertically by 0.2 units.

B: The spectra are normalized at E_{Amax}. □, 200K; O, 250K; △, 298K; +, 350K; Y, 373K.

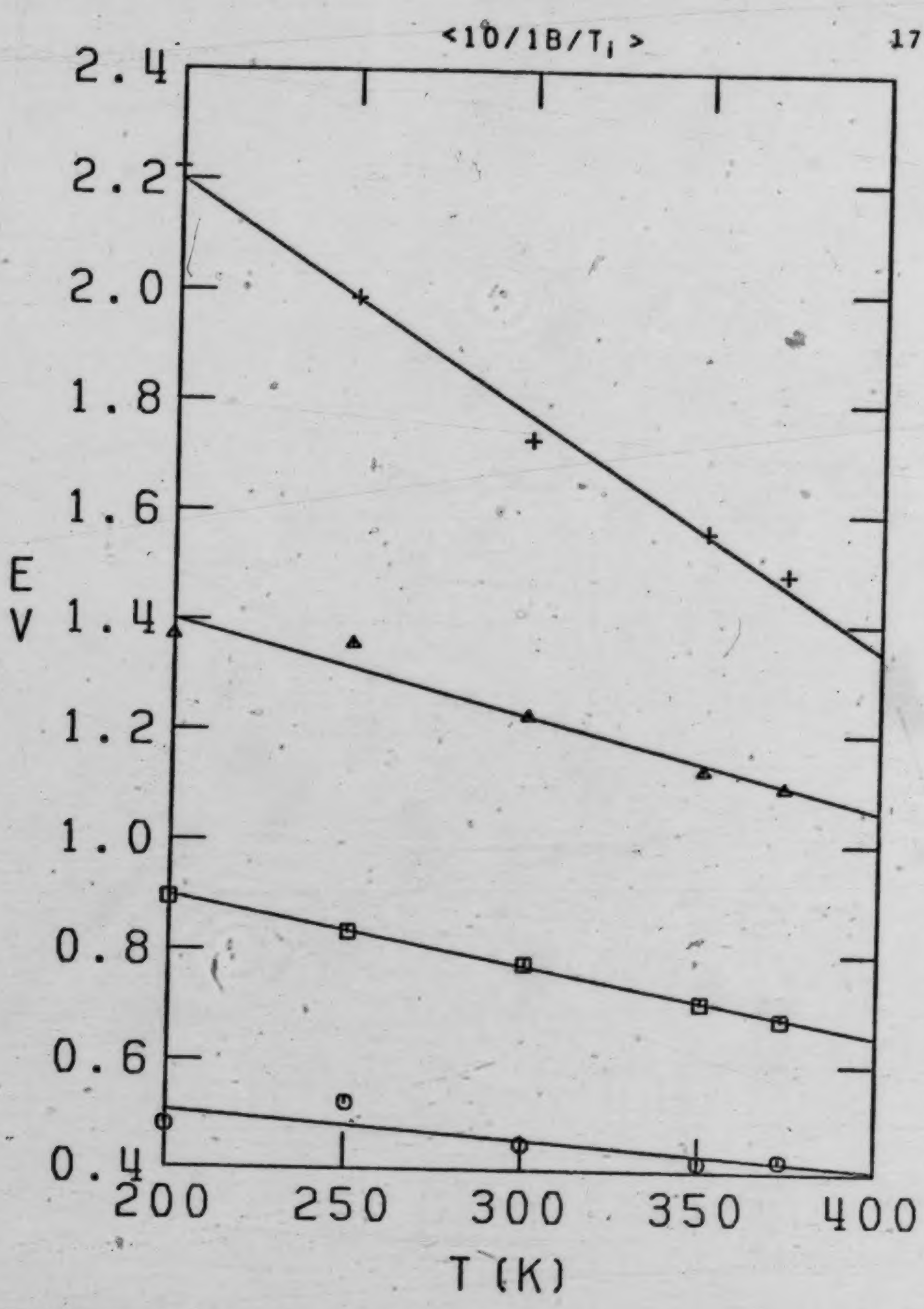

FIGURE III-59. Temperature Dependence of Spectrum Parameters in a Solution of 10 Mole % Water in 1-Butanol.

+, E_{Amax}; △, $W_{½}$; O, W_r; □, W_b.

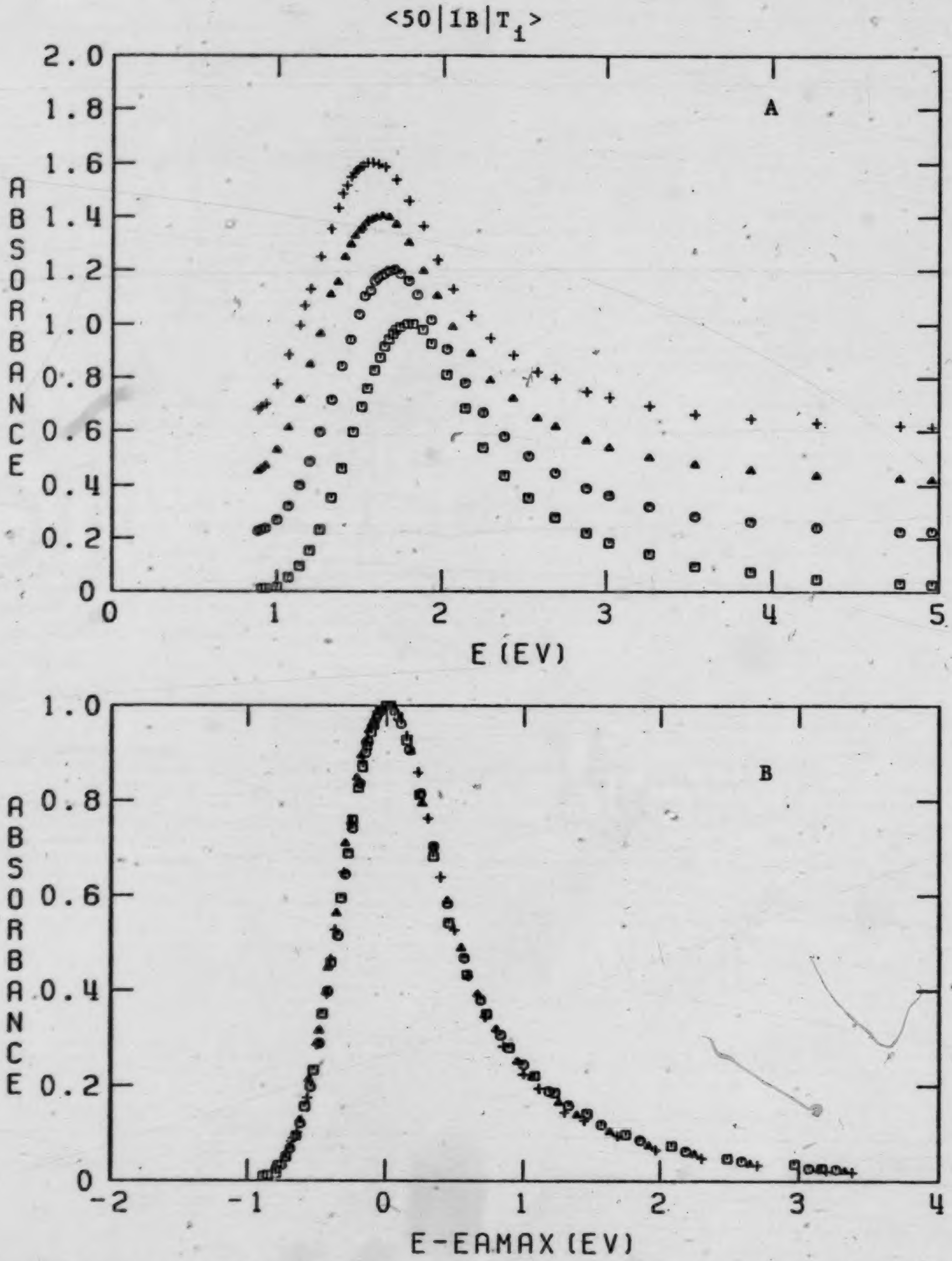

FIGURE III-60. The Optical Absorption Spectrum of Solvated Electrons in a Solution of 50 Mole % Water in 1-Butanol at Different Temperatures.

A: Successive spectra are displaced vertically by 0.2 units.

B: The spectra are normalized at E_{Amax}. □, 298K; O, 325K; △, 350K; +, 364K.

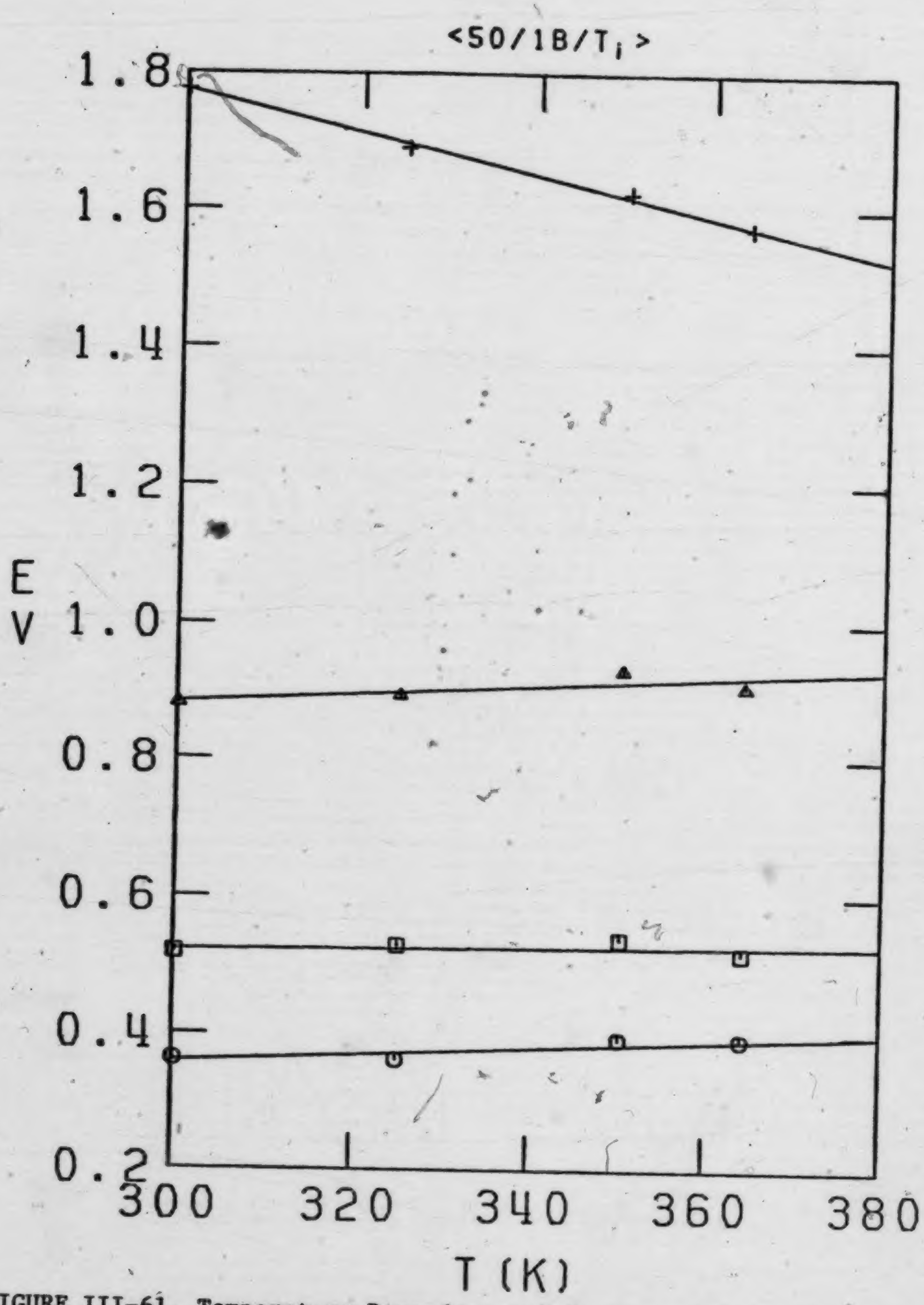

FIGURE III-61. Temperature Dependence of Spectrum Parameters in a Solution of 50 Mole % Water in 1-Butanol.

+, E_{Amax}; △, $W_{\frac{1}{2}}$; O, W_r; □, W_b.

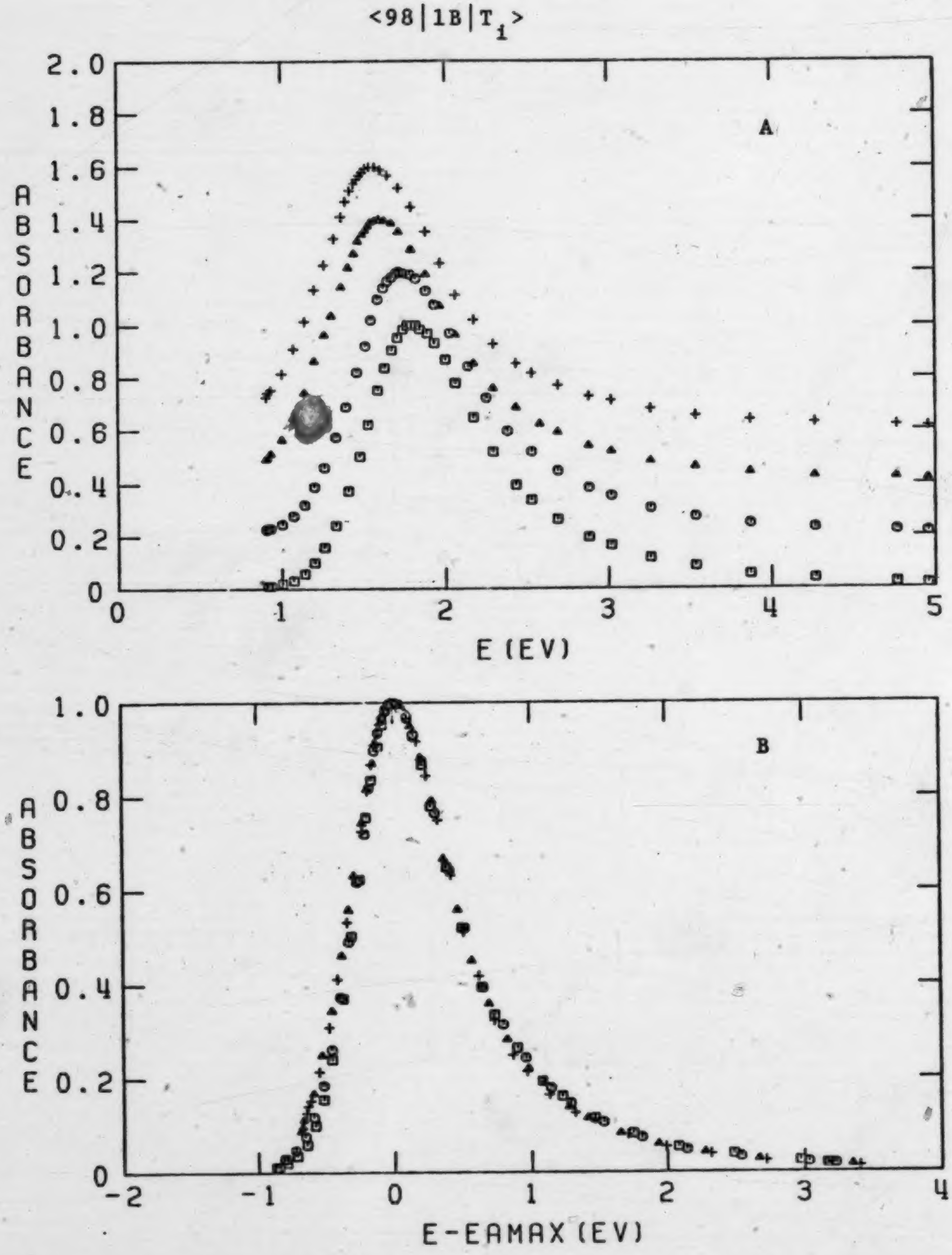

<98|1B|T$_i$>

FIGURE III-62. The Optical Absorption Spectrum of Solvated Electrons in a Solution of 98 Mole % Water in 1-Butanol at Different Temperatures.

A: Successive spectra are displaced vertically by 0.2 units.

B: The spectra are normalized at E_{Amax}. □, 273K; O, 298K; △, 350K; +, 363K.

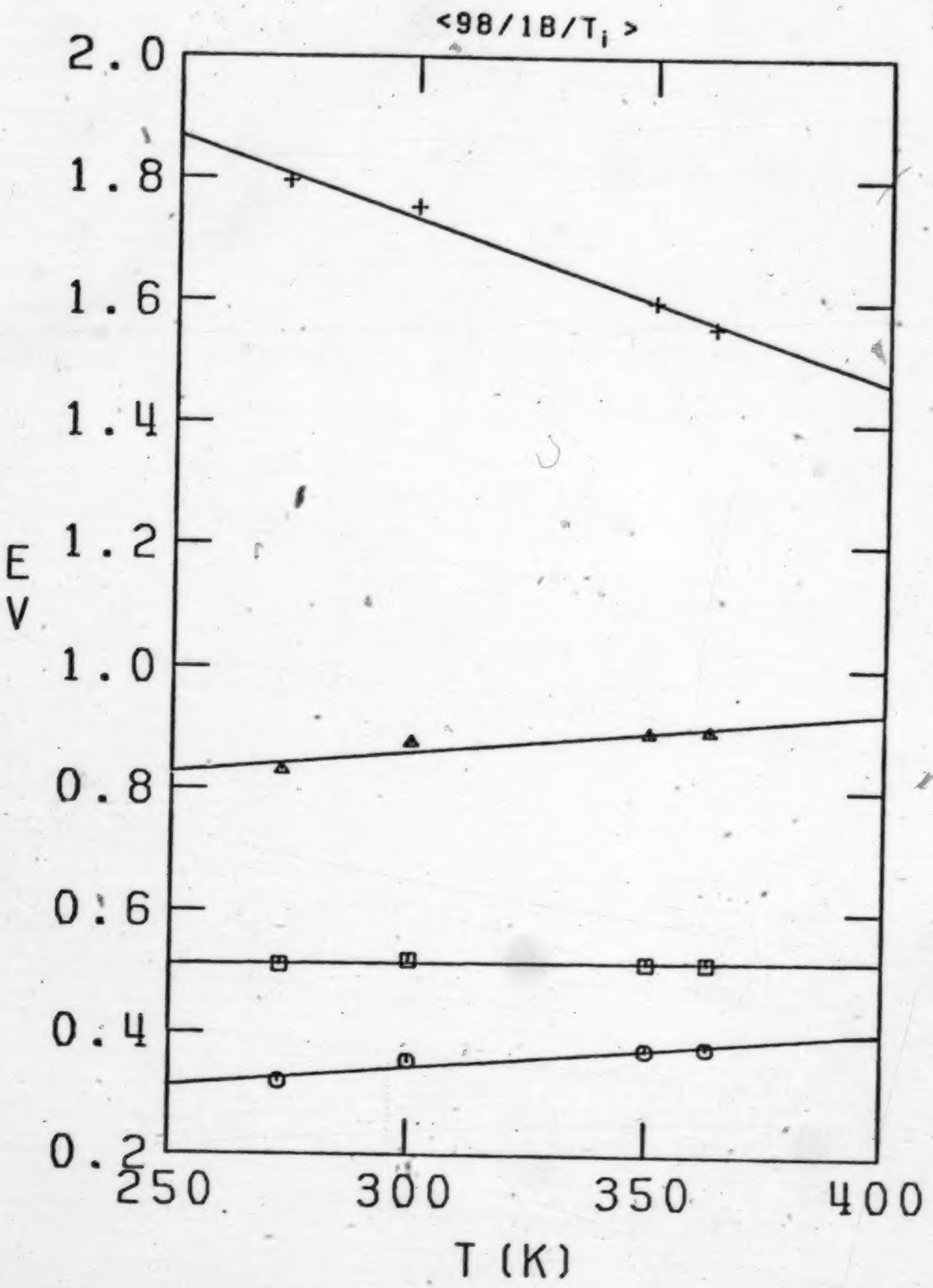

FIGURE III-63. Temperature Dependence of Spectrum Parameters in a Solution of 98 Mole % Water in 1-Butanol.

+, E_{Amax}; △, $W_{1/2}$; O, W_r; □, W_b.

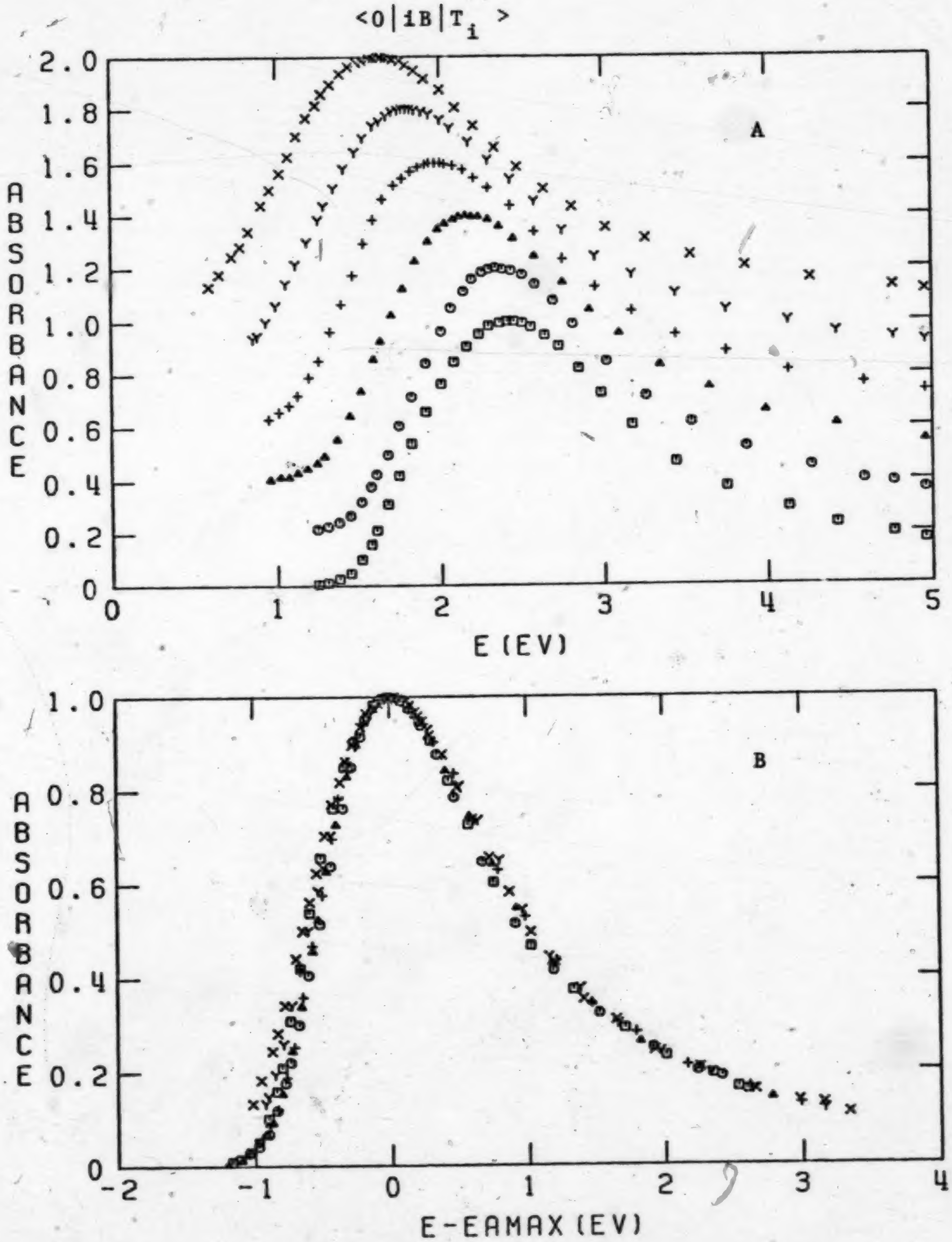

FIGURE III-64. The Optical Absorption Spectrum of Solvated Electrons in iso-Butanol at Different Temperatures.

A: Successive spectra are displaced vertically by 0.2 units.

B: The spectra are normalized at E_{Amax}. □, 170K; O, 200K; △, 250K; +, 298K; Y, 350K: X, 378K.

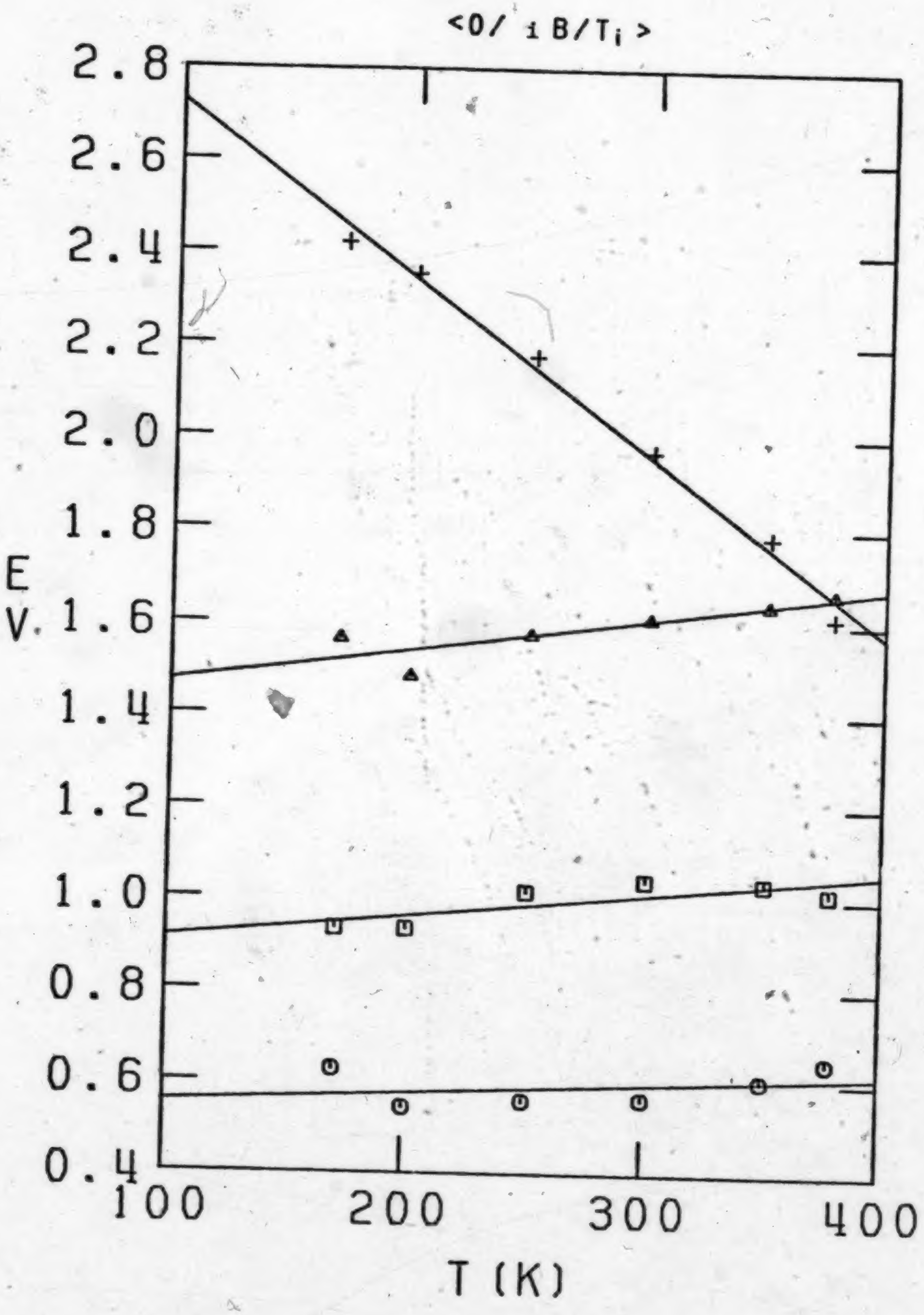

FIGURE III-65. Temperature Dependence of Spectrum Parameters in iso-Butanol.

+, E_{Amax}; △, $W_{\frac{1}{2}}$; O, W_r; □, W_b;

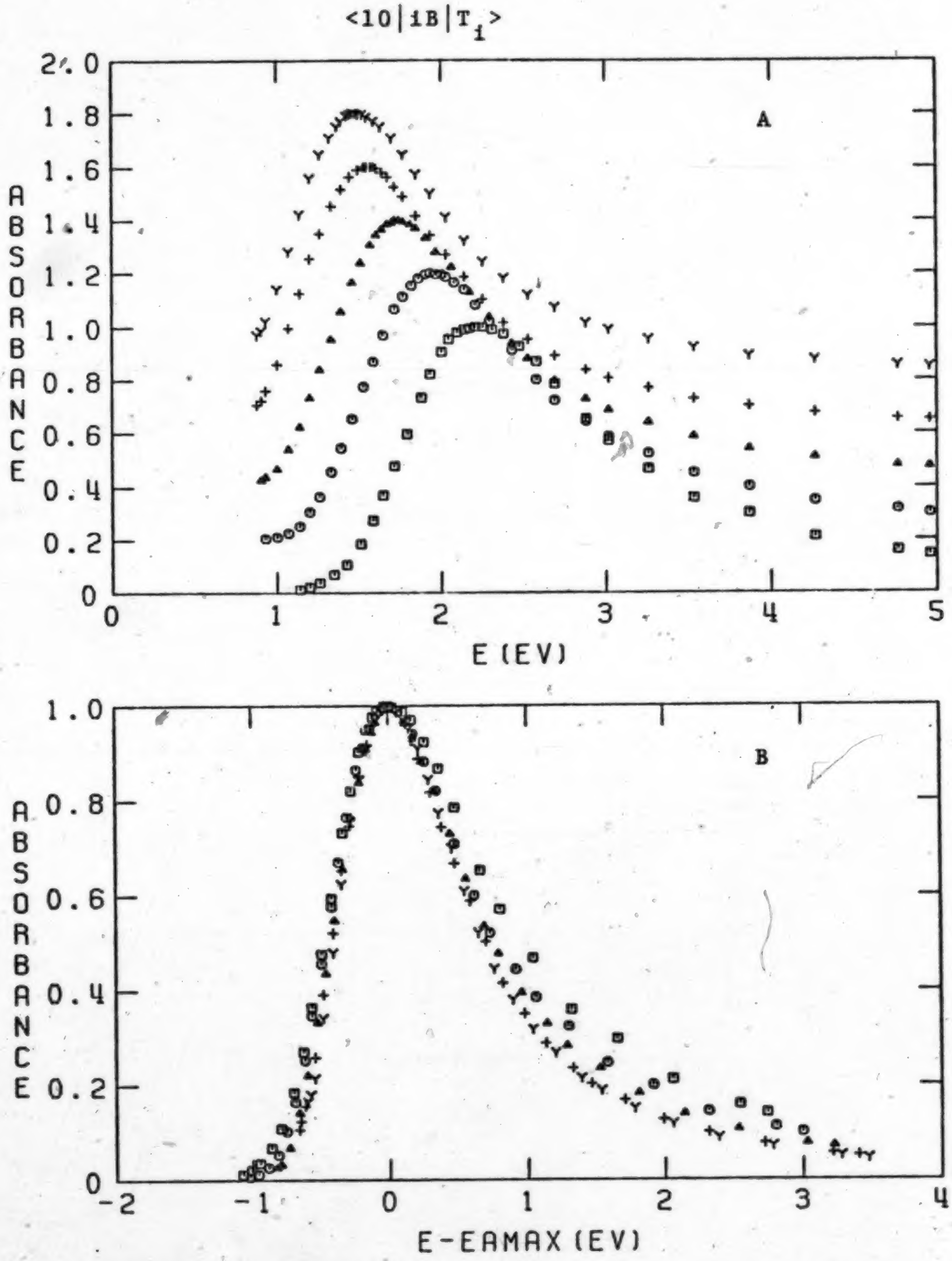

FIGURE III-66. The Optical Absorption Spectrum of Solvated Electrons in a Solution of 10 Mole % Water in iso-Butanol at Different Temperatures.

A: Successive spectra are displaced vertically by 0.2 units.

B: The spectra are normalized at E_{Amax}. □, 200K; O, 250K; △, 298K; +, 350K; Y, 365K.

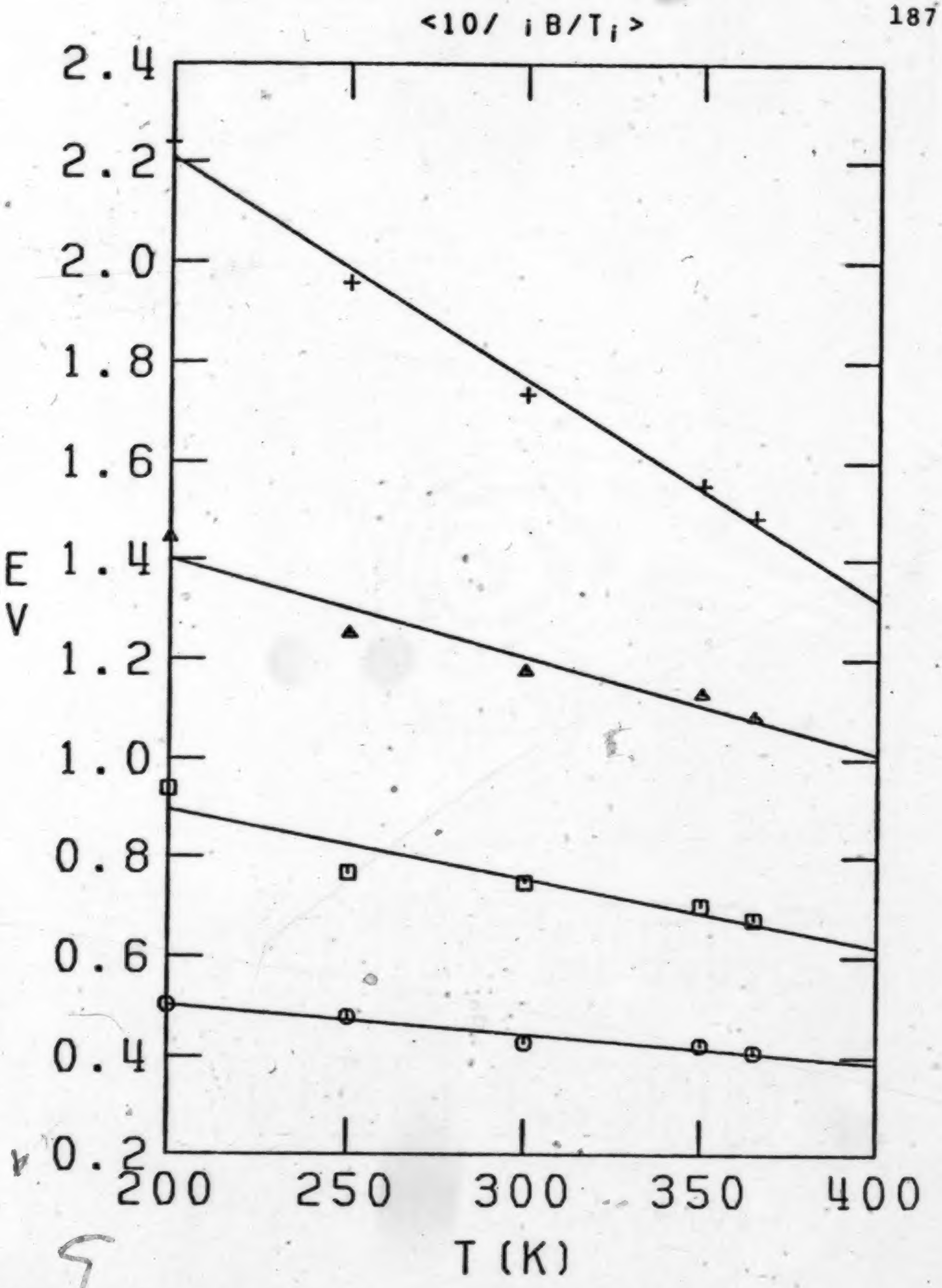

FIGURE III-67. Temperature Dependence of Spectrum Parameters in a Solution of 10 Mole % Water in iso-Butanol.
+, E_{Amax}; △, $W_{\frac{1}{2}}$; O, W_r, □, W_b.

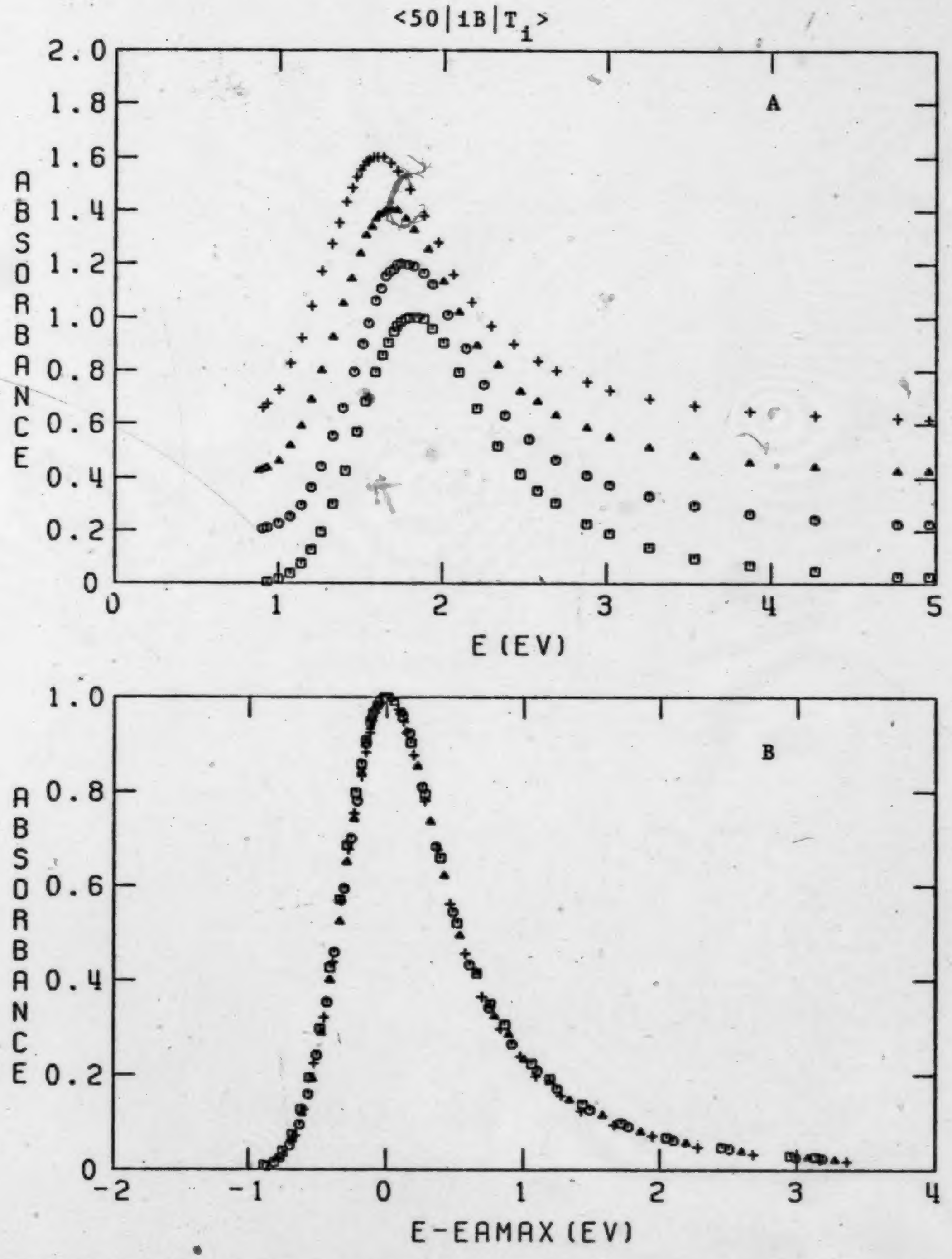

FIGURE III-68. The Optical Absorption Spectrum of Solvated Electrons in a Solution of 50 Mole % Water in iso-Butanol at Different Temperatures.

A: Successive spectra are displaced vertically by 0.2 units.

B: The spectra are normalized at E_{Amax}. □, 286K; O, 298K; △, 325K; +, 350K.

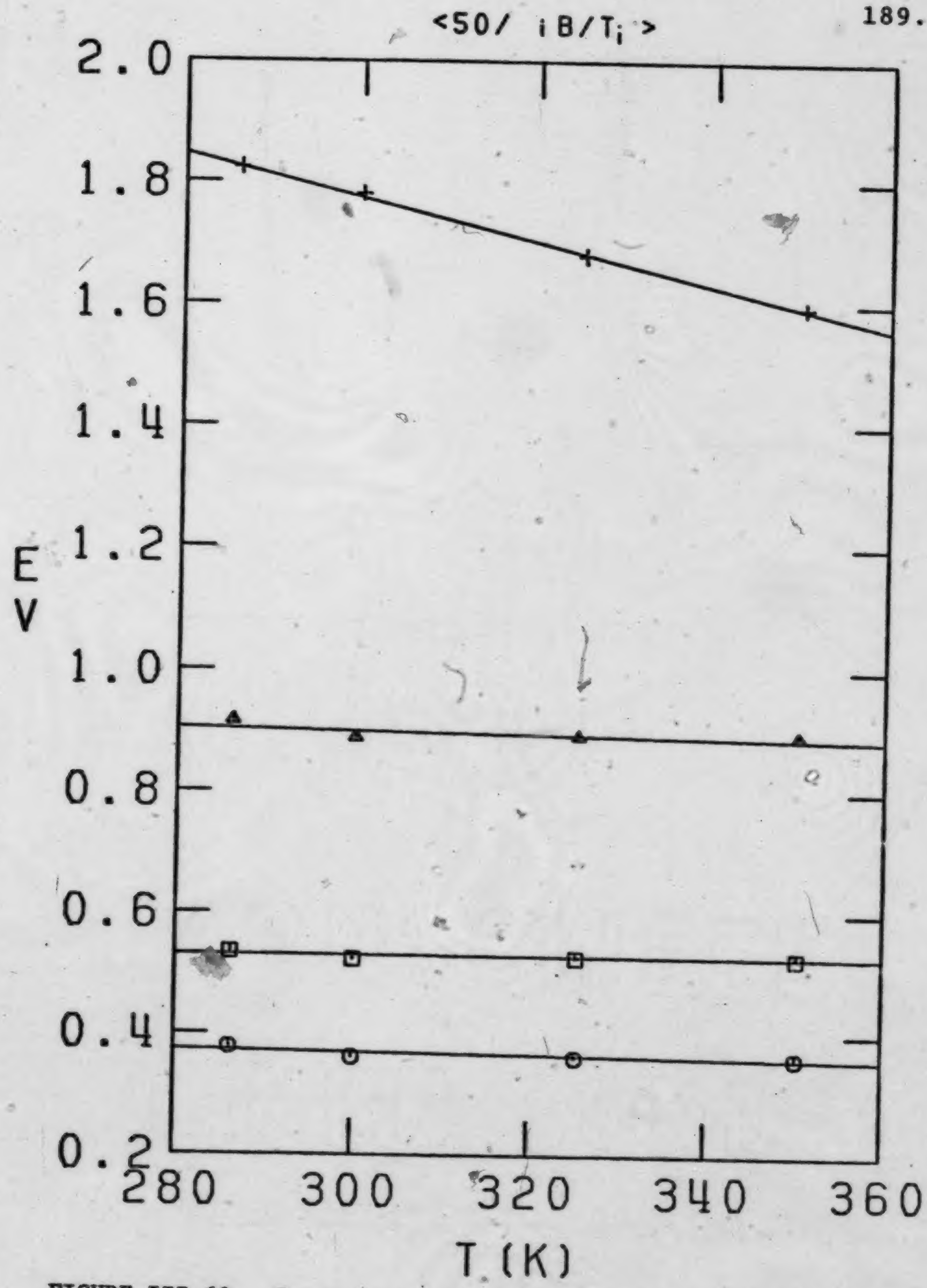

FIGURE III-69. Temperature Dependence of Spectrum Parameters in a Solution of 50 Mole % Water in iso-Butanol. +, E_{Amax}; △, $W_{\frac{1}{2}}$; O, W_r; □, W_b.

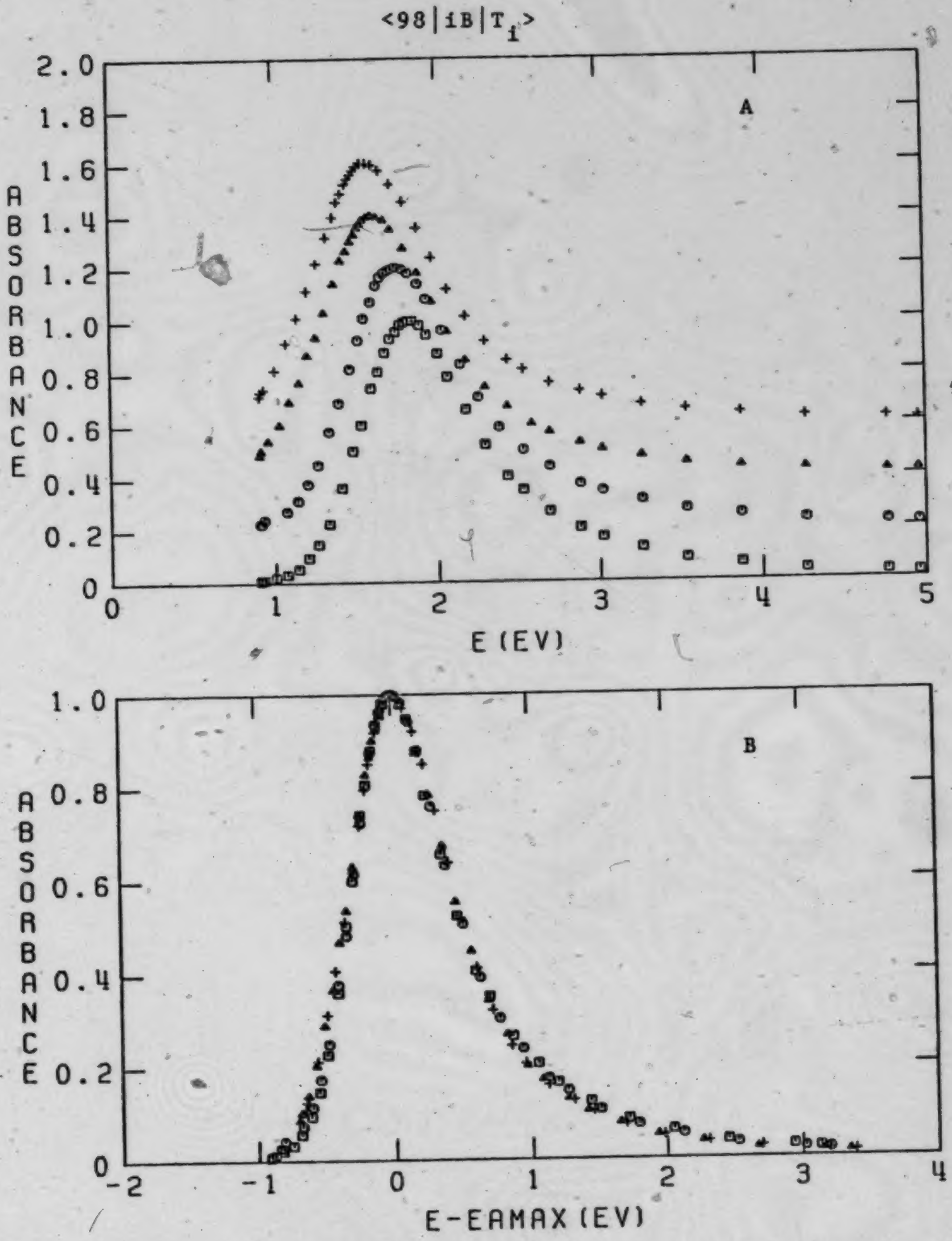

FIGURE III-70. The Optical Absorption Spectrum of Solvated Electrons in a Solution of 98 Mole % Water in iso-Butanol at Different Temperatures.

A: Successive spectra are displaced vertically by 0.2 units.

B: The spectra are normalized at E_{Amax}. □, 273K; O, 298K; △, 350K; +, 363K.

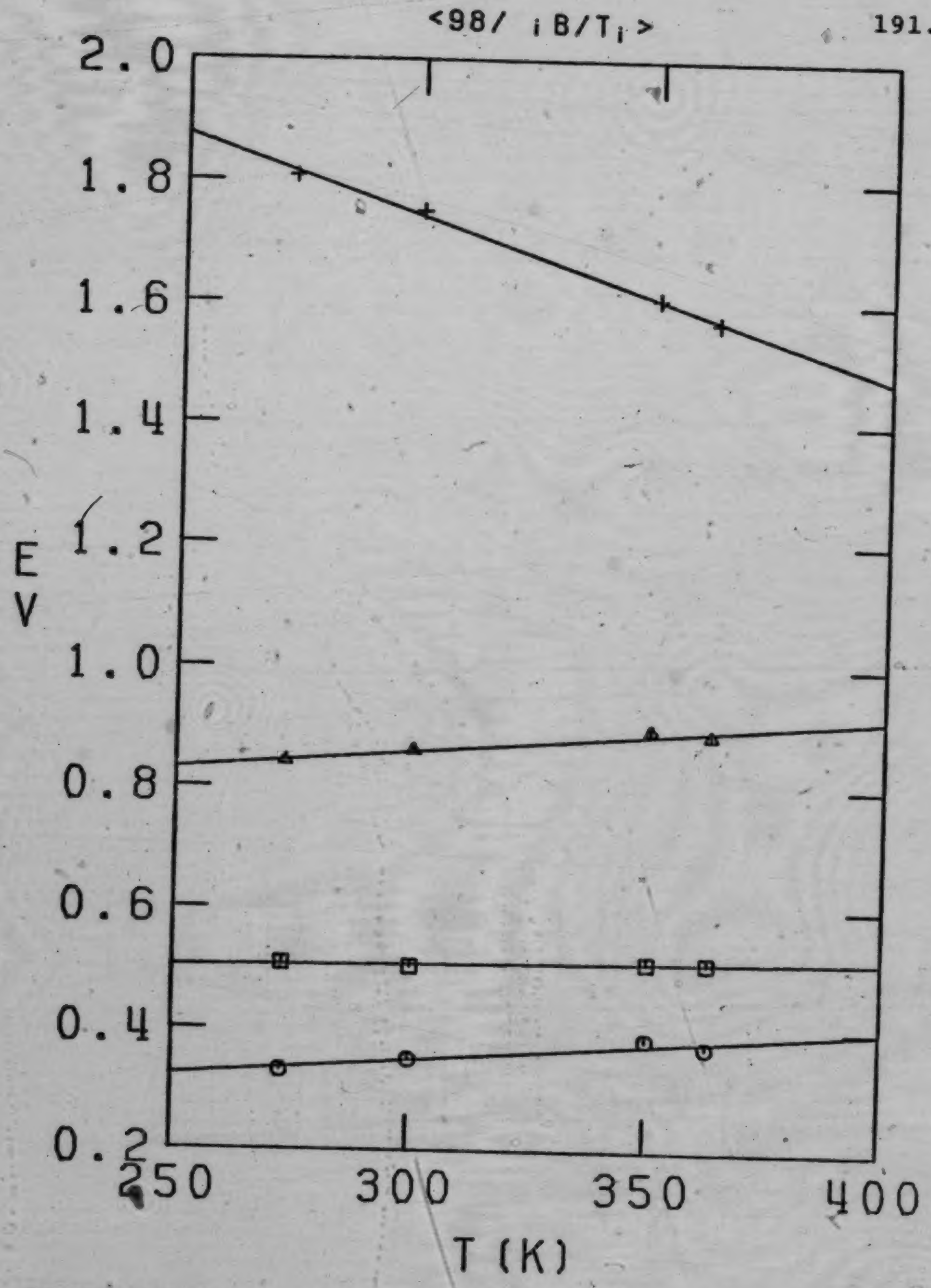

FIGURE III-71. Temperature Dependence of Spectrum Parameters in a Solution of 98 Mole % Water in iso-Butanol.

+, E_{Amax}; △, $W_{\frac{1}{2}}$; O, W_r; □, W_b.

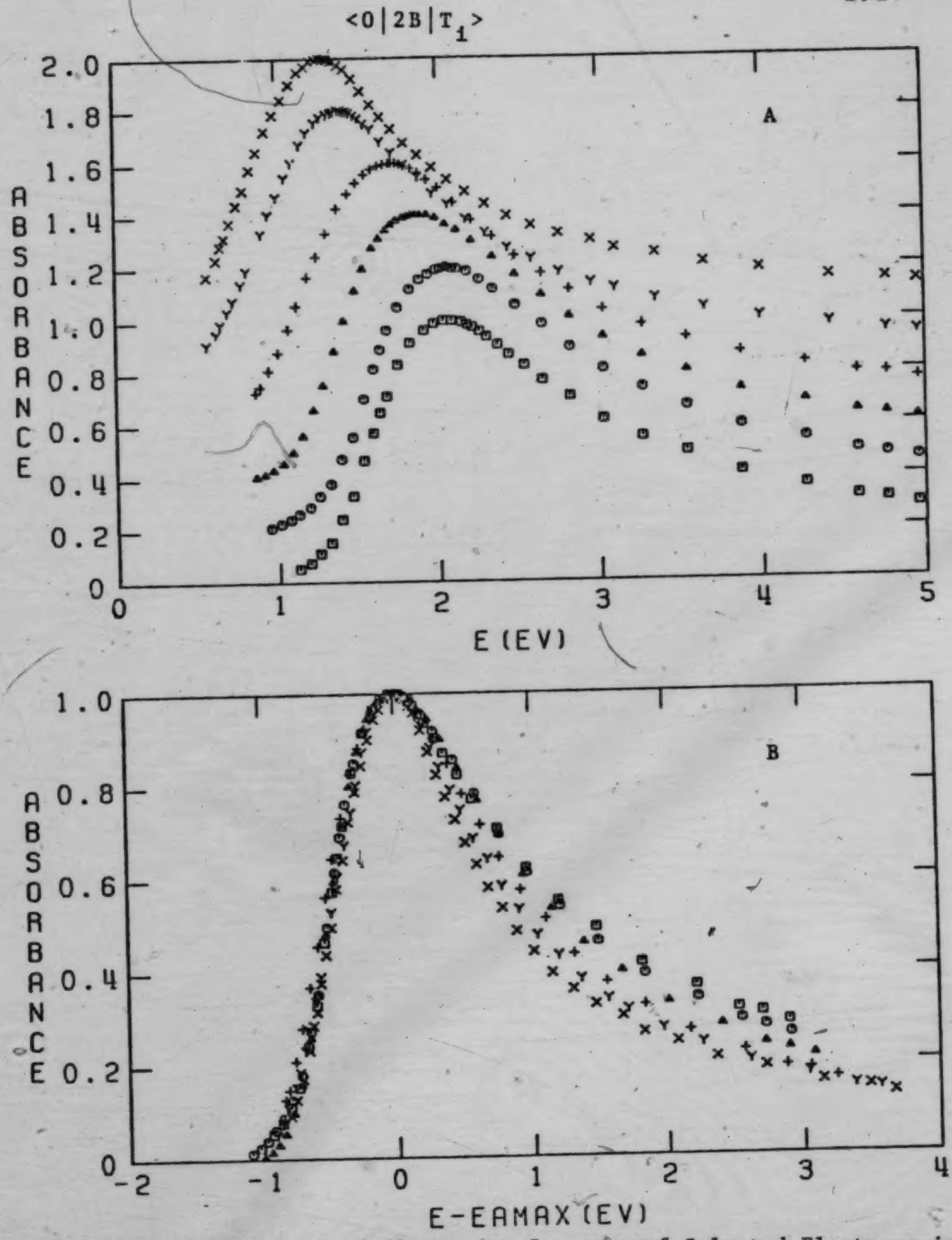

FIGURE III-72.The Optical Absorption Spectrum of Solvated Electrons in 2-Butanol at Different Temperatures.

A: Successive spectra are displaced vertically by 0.2 units.

B: The spectra are normalized at E_{Amax}. □, 163K; O, 200K; △, 250K; +, 298K; Y, 350K: X, 370K.

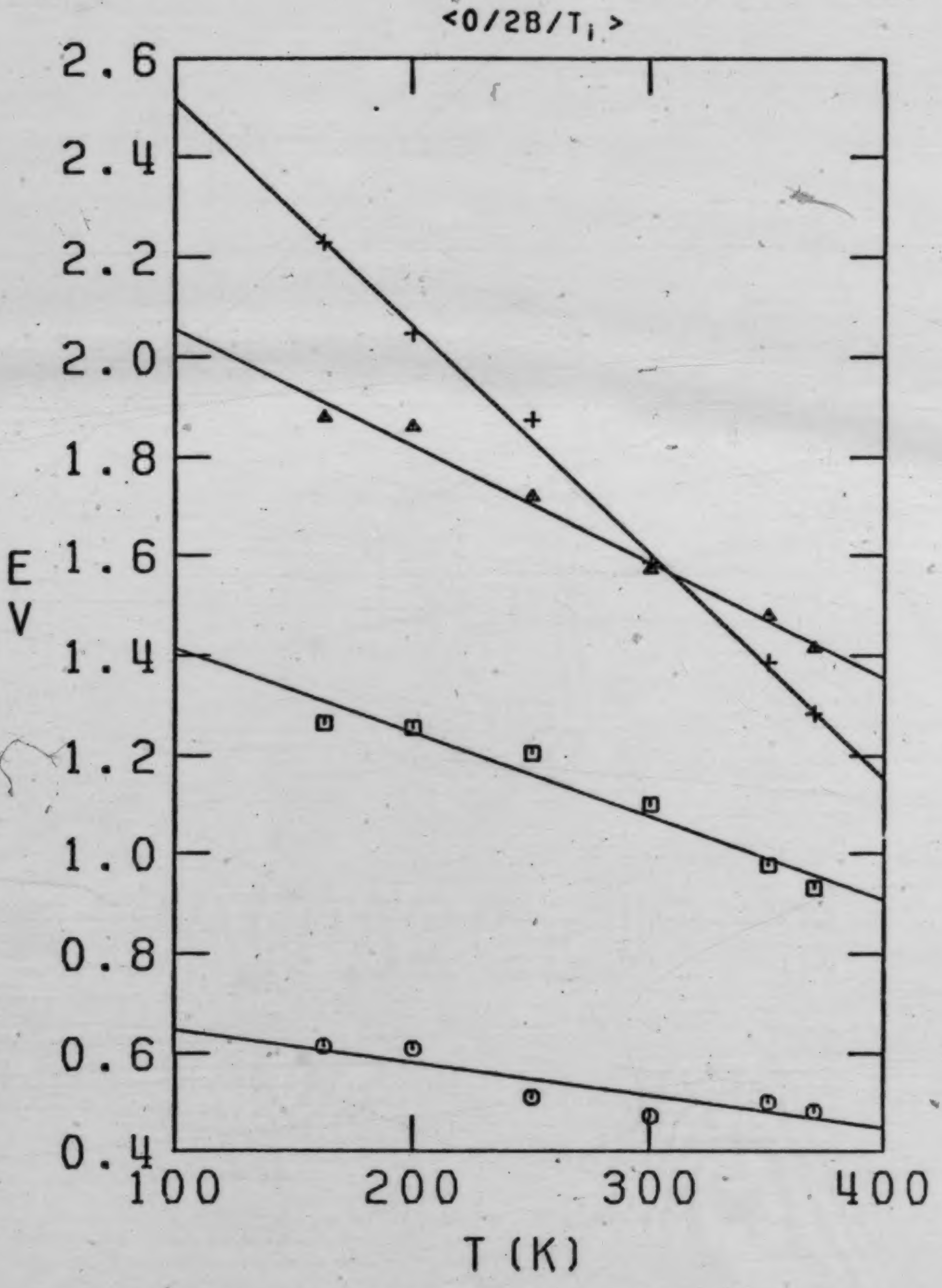

FIGURE III-73. Temperature Dependence of Spectrum Parameters in 2-Butanol.

+, E_{Amax}; △, $W_{\frac{1}{2}}$; O, W_r; □, W_b.

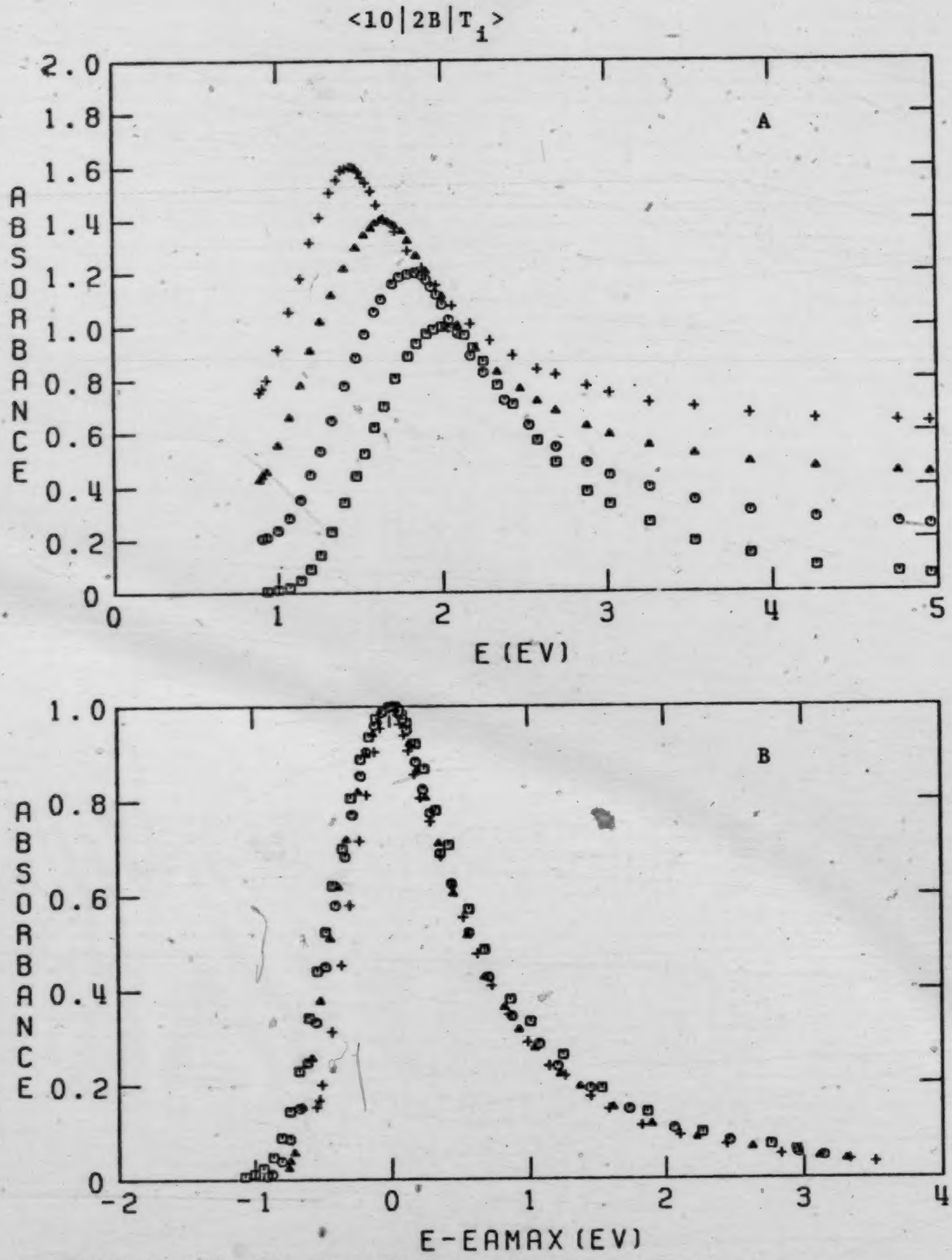

FIGURE III-74. The Optical Absorption Spectrum of Solvated Electrons in a Solution of 10 Mole % Water in 2-Butanol at Different Temperatures.

A: Successive spectra are displaced vertically by 0.2 units.

B: The spectra are normalized at E_{Amax}. □, 200K; O, 250K; △, 298K; +, 350K.

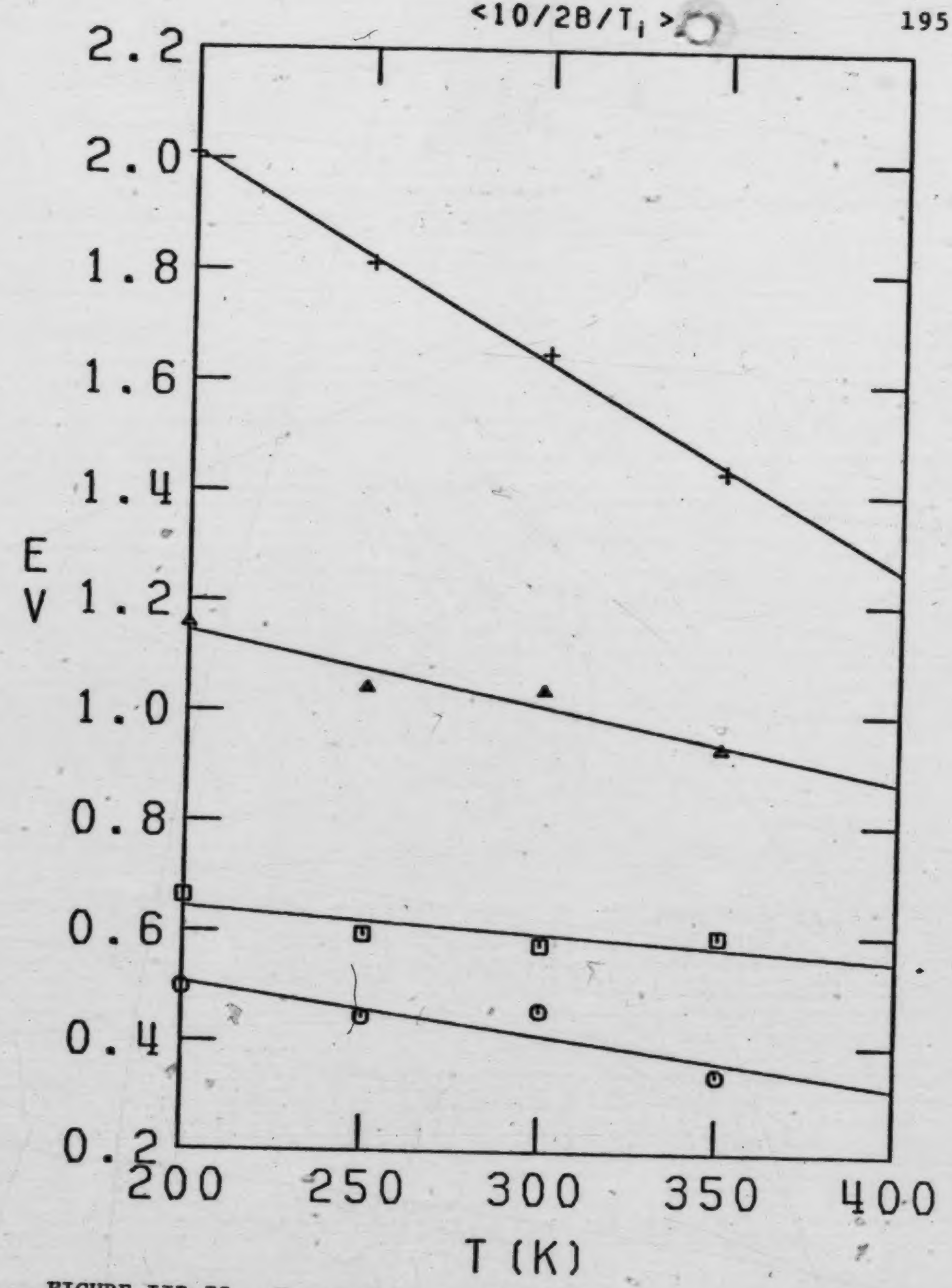

FIGURE III-75. Temperature Dependence of Spectrum Parameters in a Solution of 10 Mole % Water in 2-Butanol.
+, E_{Amax}; △, $W_{\frac{1}{2}}$; O, W_r; □, W_b.

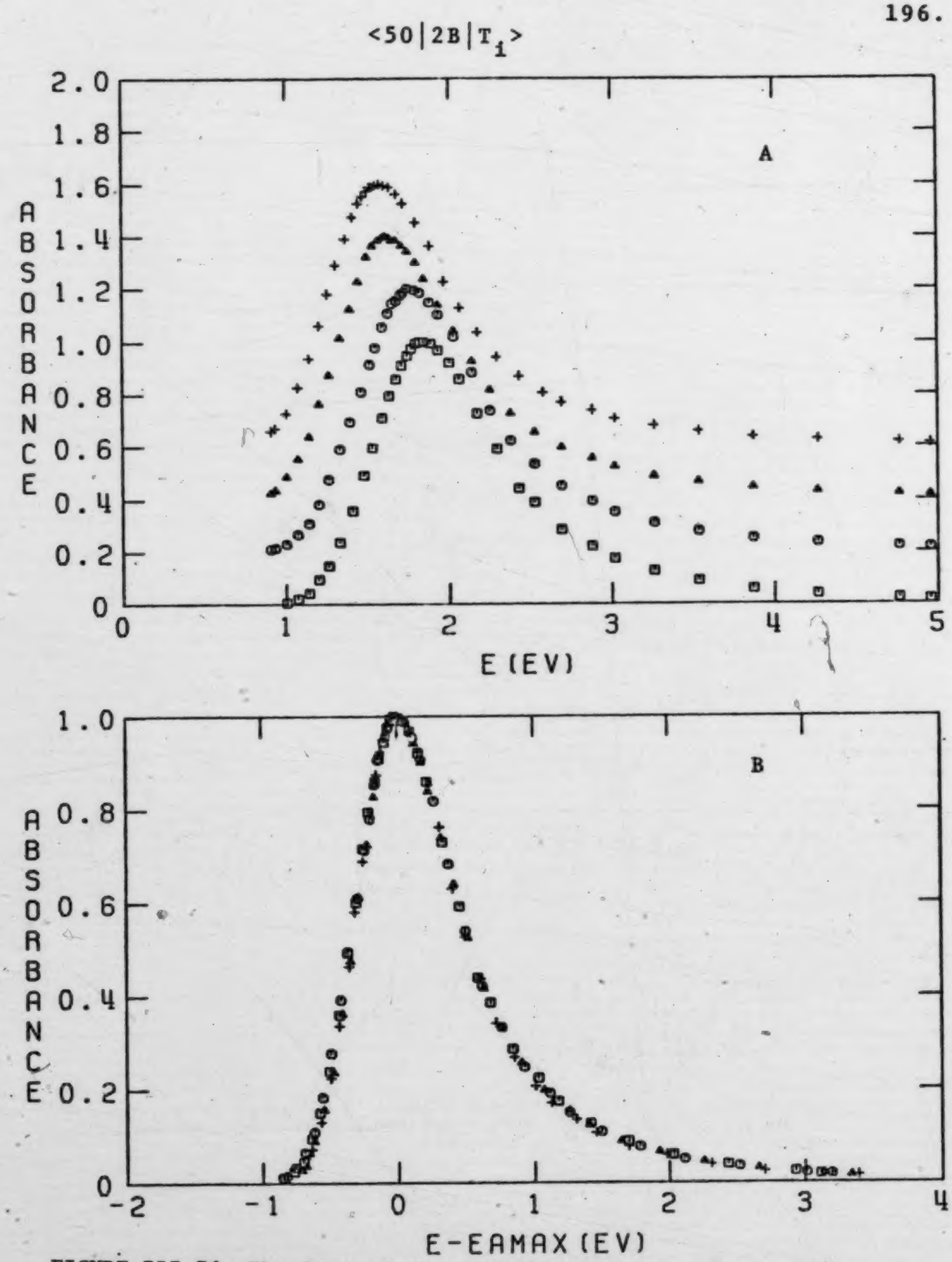

FIGURE III-76. The Optical Absorption Spectrum of Solvated Electrons in a Solution of 50 Mole % Water in 2-Butanol at Different Temperatures.

A: Successive spectra are displaced vertically by 0.2 units.

B: The spectra are normalized at E_{Amax}. □, 273K; O, 298K; △, 325K; +, 350K.

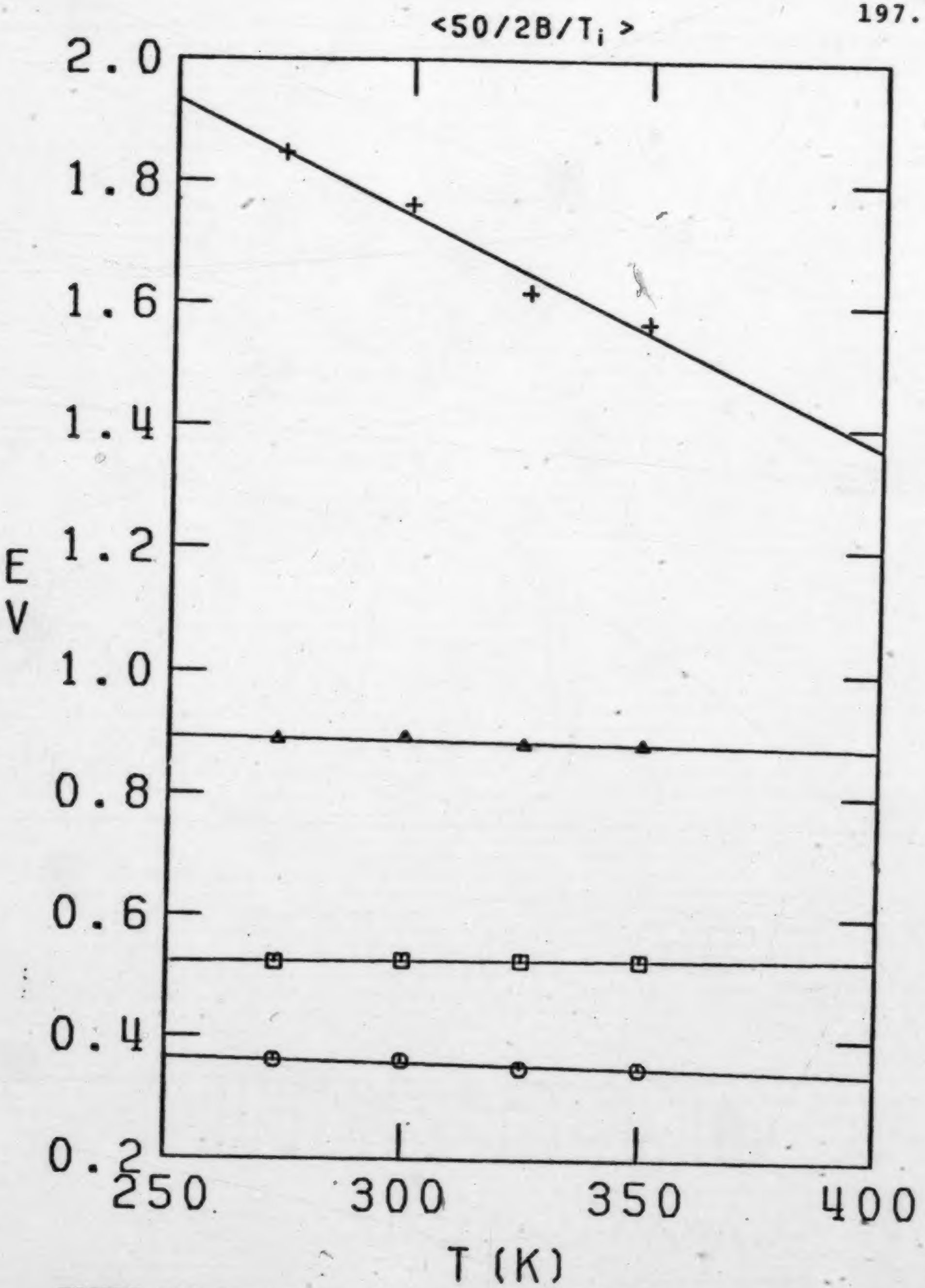

FIGURE III-77. Temperature Dependence of Spectrum Parameters in a Solution of 50 Mole % Water in 2-Butanol.

+, E_{Amax}; △, $W_{\frac{1}{2}}$; O, W_r; □, W_b.

<98|2B|T_i>

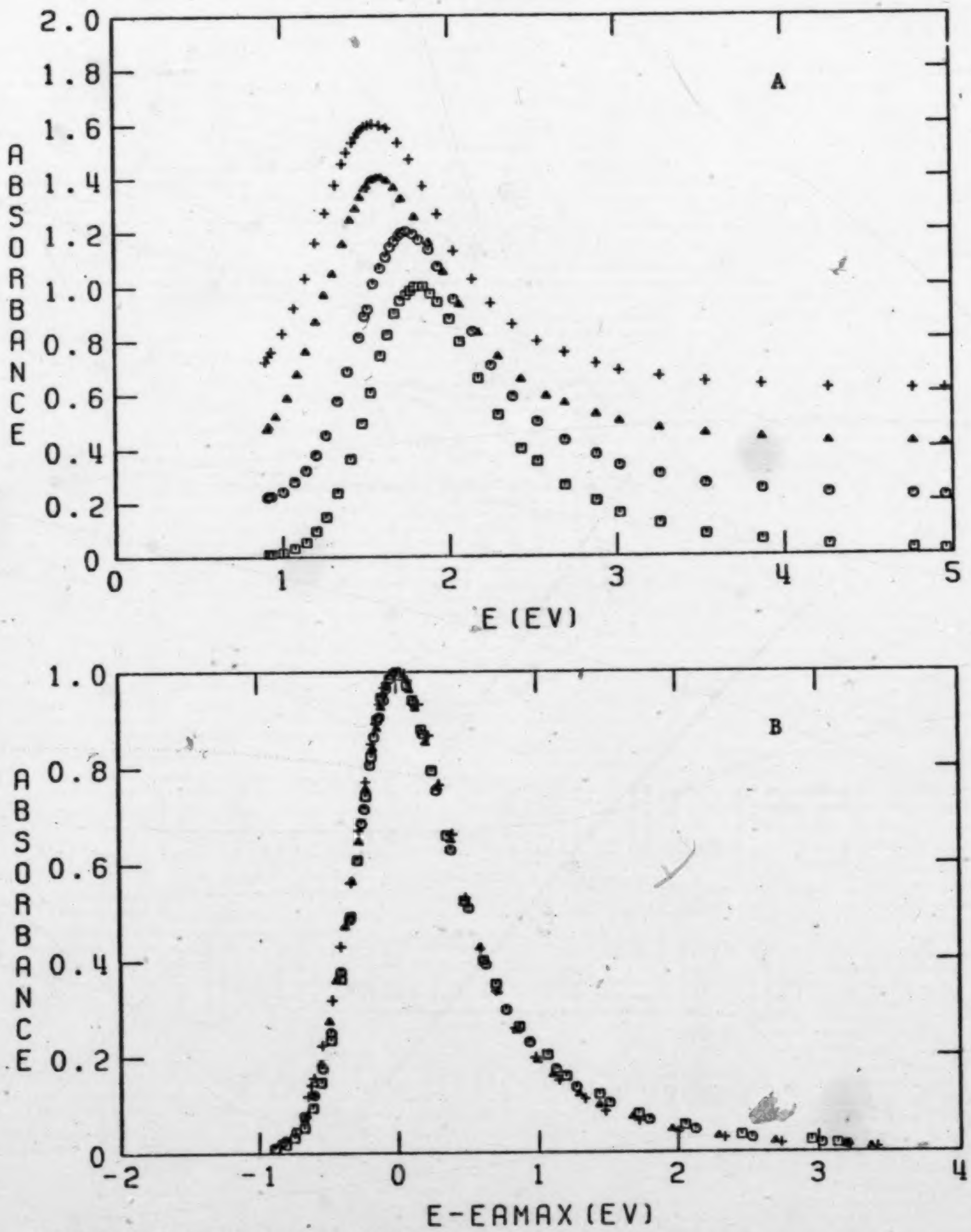

FIGURE III-78. The Optical Absorption Spectrum of Solvated Electrons in a Solution of 98 Mole % Water in 2-Butanol at Different Temperatures.

A: Successive spectra are displaced vertically by 0.2 units.

B: The spectra are normalized at E_{Amax}. □, 273K; O, 298K; △, 350K; +, 370K.

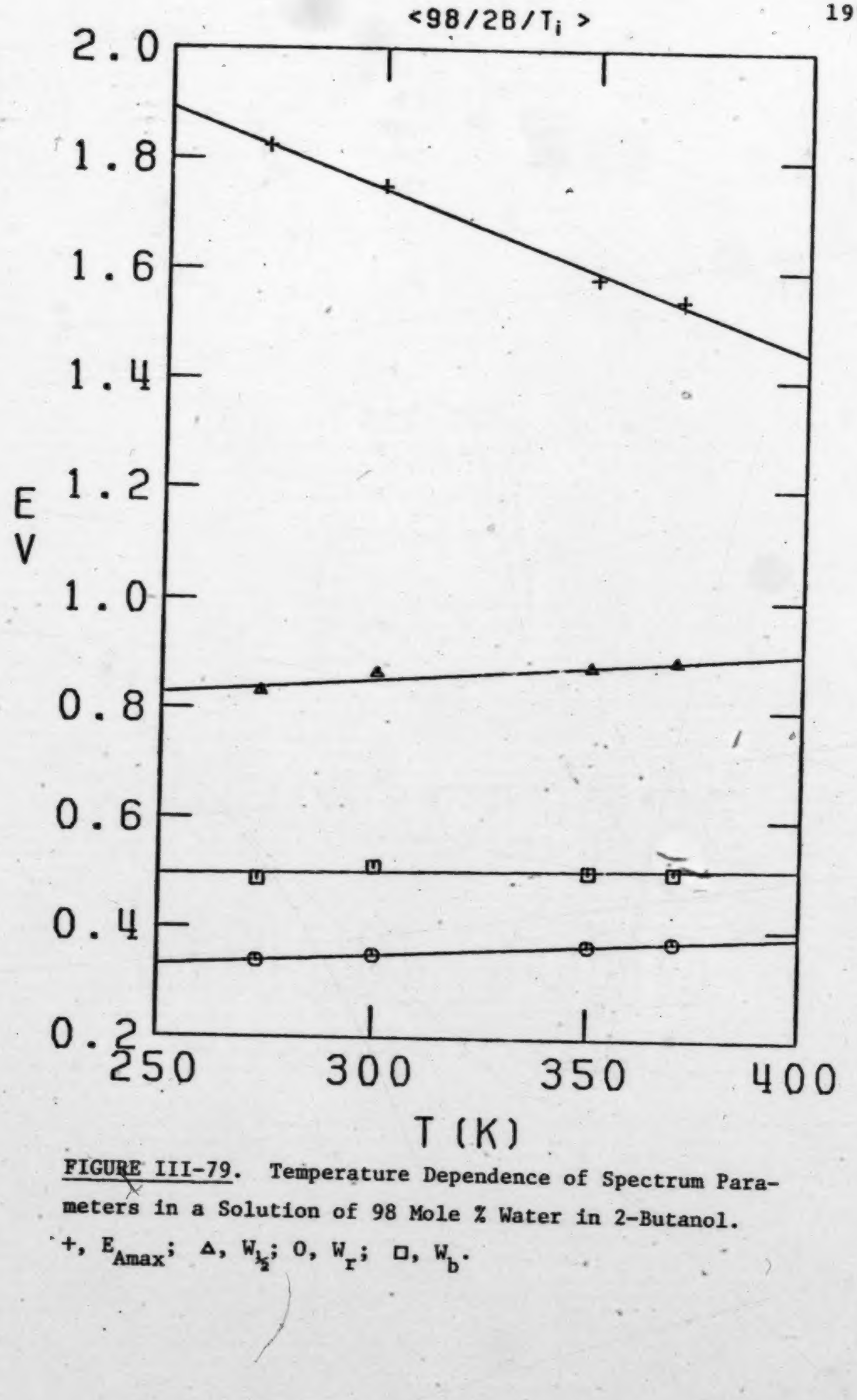

FIGURE III-79. Temperature Dependence of Spectrum Parameters in a Solution of 98 Mole % Water in 2-Butanol. +, E_{Amax}; Δ, $W_{\frac{1}{2}}$; O, W_r; □, W_b.

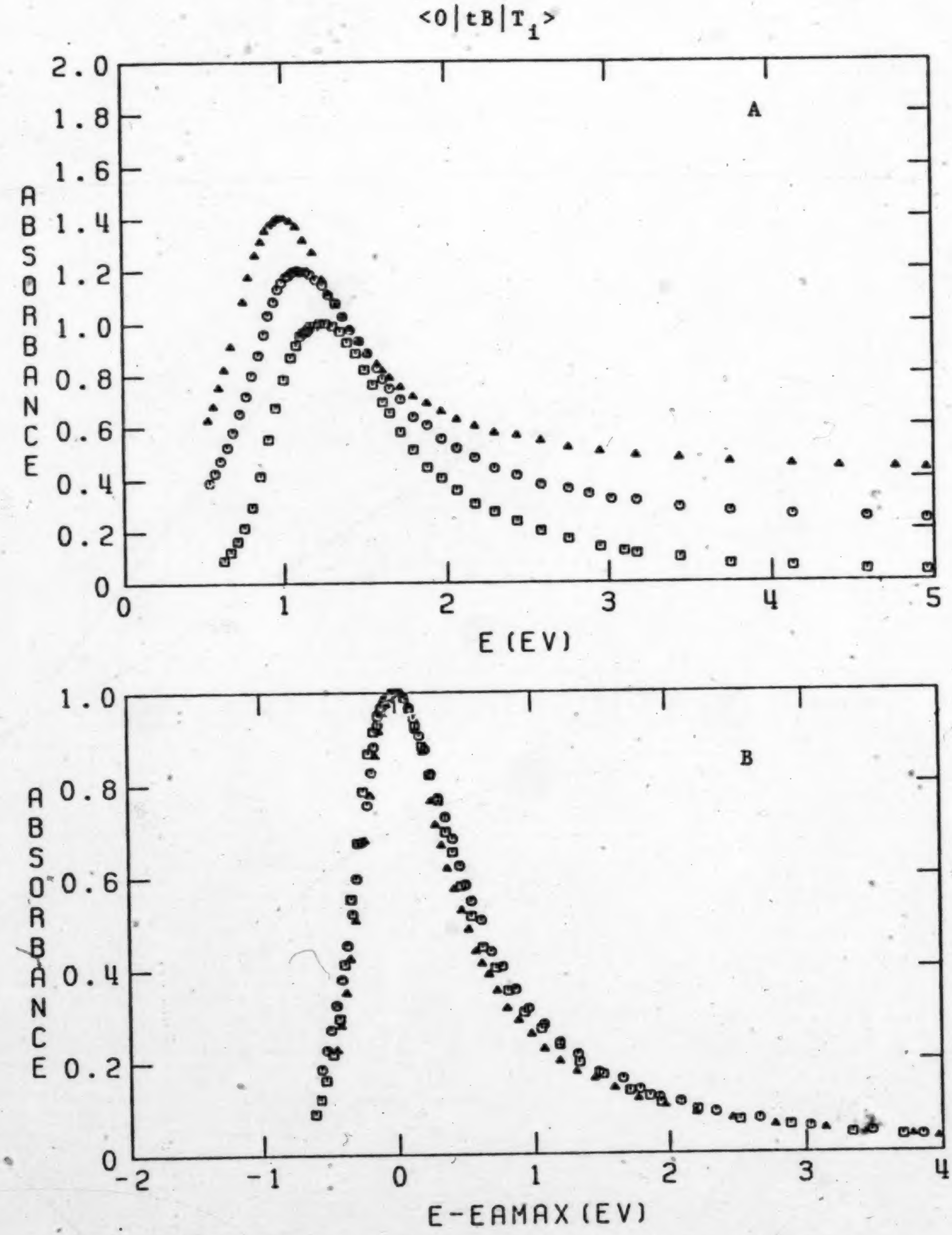

FIGURE III-80. The Optical Absorption Spectrum of Solvated Electrons in t-Butanol at Different Temperatures.

A: Successive spectra are displaced vertically by 0.2 units.

B: The spectra are normalized at E_{Amax}. □, 298K; O, 325K; △, 350K.

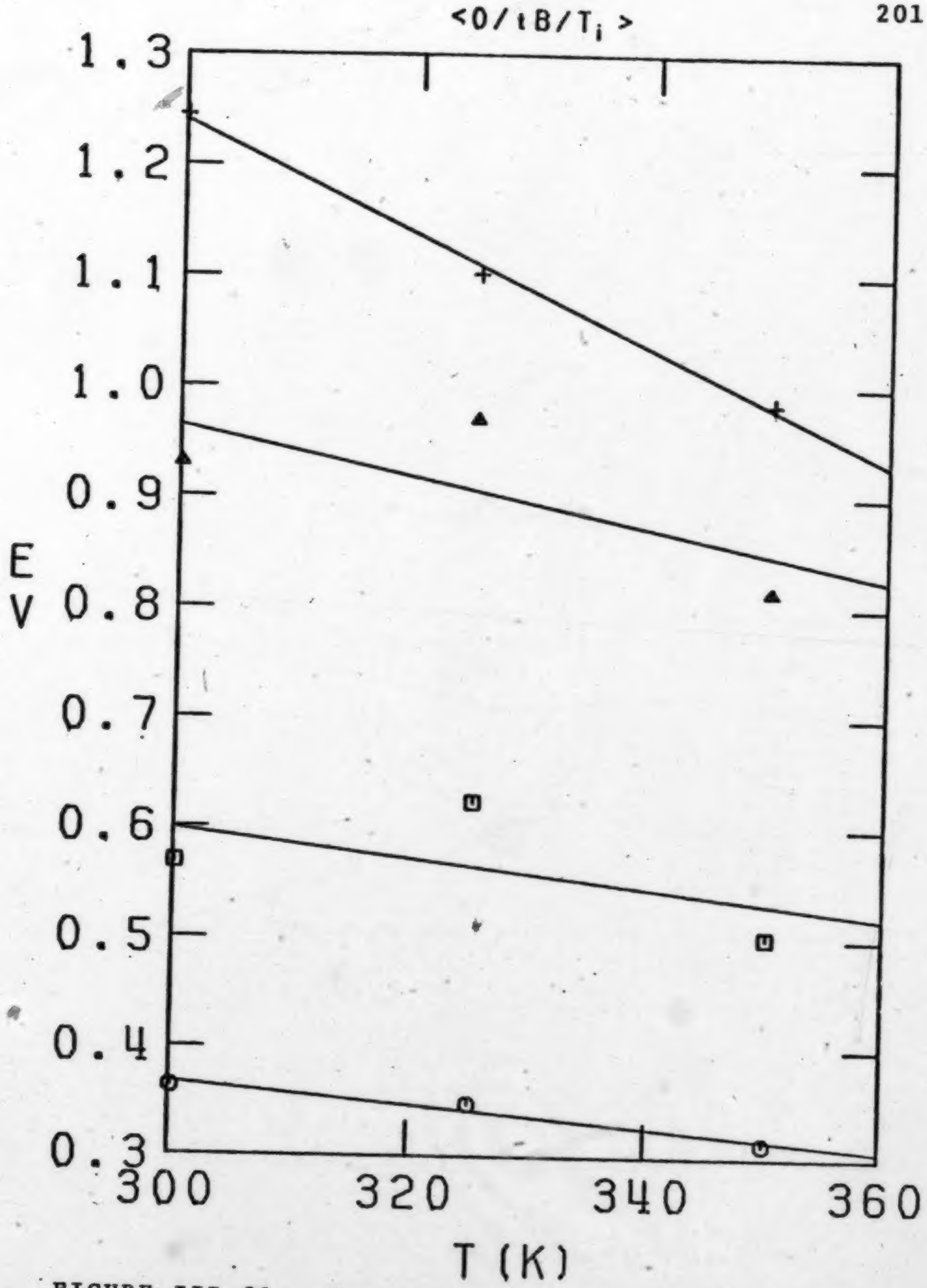

FIGURE III-81. Temperature Dependence of Spectrum Parameters in t-Butanol.

+, E_{Amax}; △, $W_{\frac{1}{2}}$; ○, W_r; □, W_b.

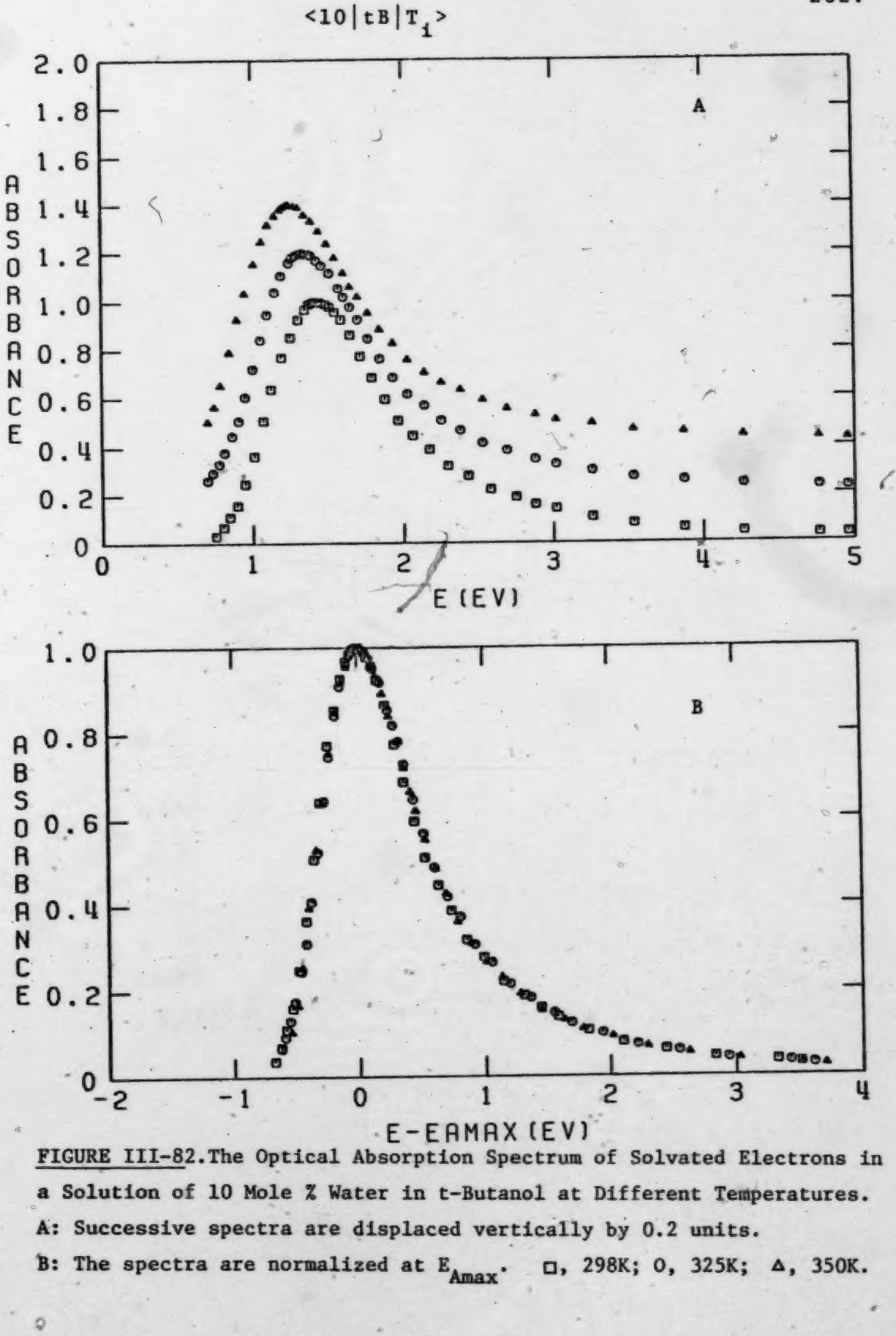

FIGURE III-82. The Optical Absorption Spectrum of Solvated Electrons in a Solution of 10 Mole % Water in t-Butanol at Different Temperatures. A: Successive spectra are displaced vertically by 0.2 units. B: The spectra are normalized at E_{Amax}. □, 298K; O, 325K; △, 350K.

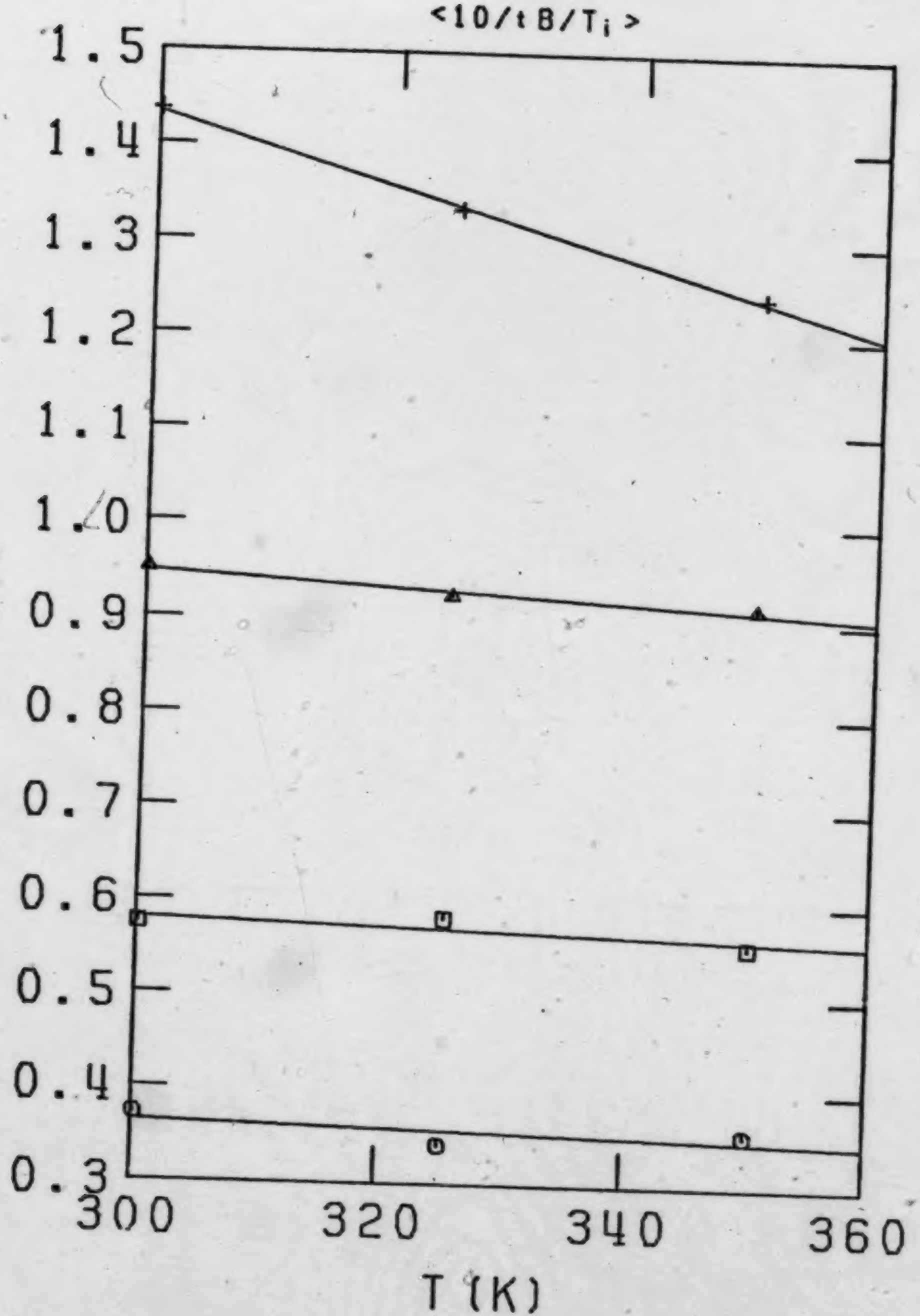

FIGURE III-83. Temperature Dependence of Spectrum Parameters in a Solution of 10 Mole % Water in t-Butanol. +, E_{Amax}; Δ, $W_{½}$; O, W_r; □, W_b.

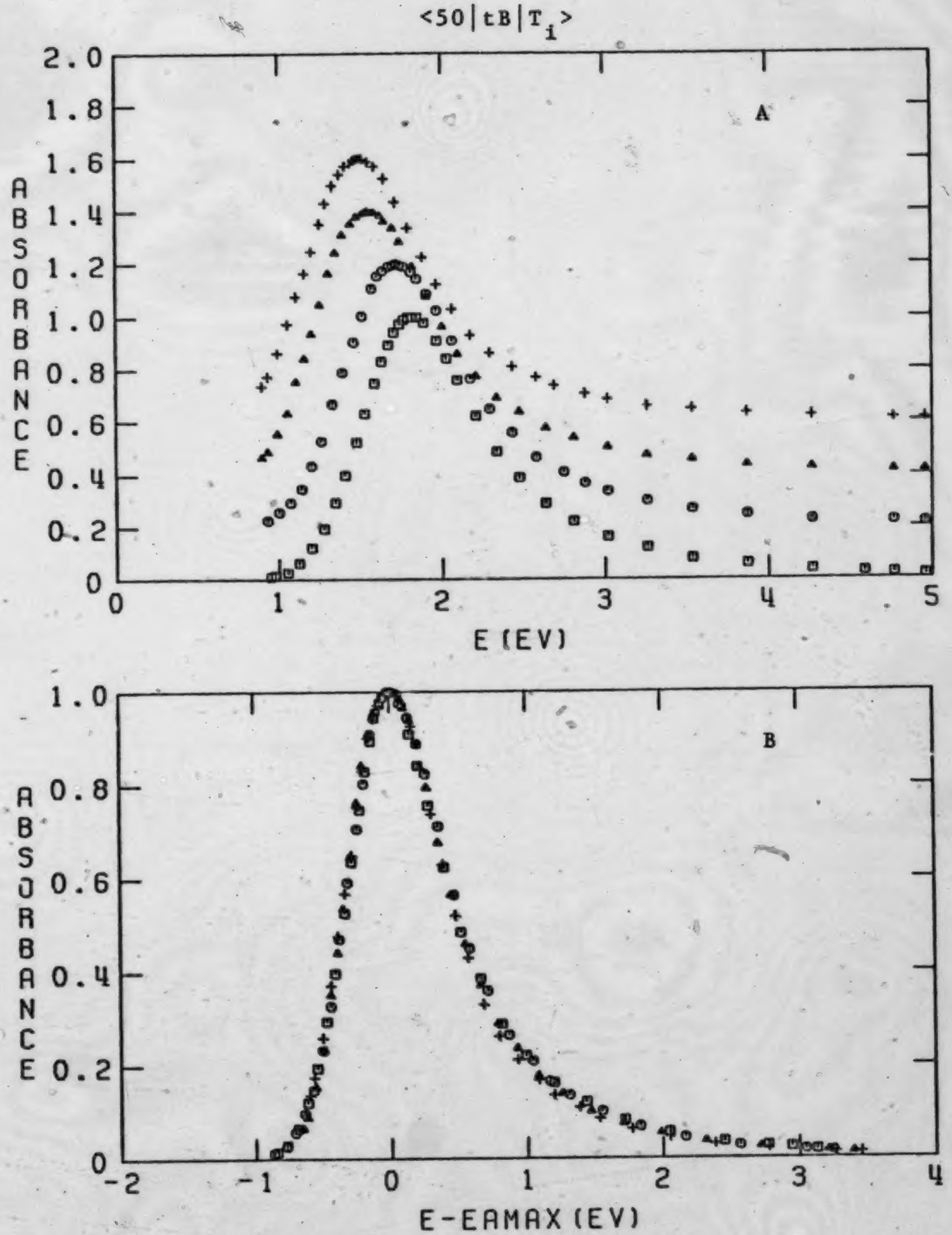

FIGURE III-84. The Optical Absorption Spectrum of Solvated Electrons in a Solution of 50 Mole % Water in t-Butanol at Different Temperatures.

A; Successive spectra are displaced vertically by 0.2 units.

B: The spectra are normalized at E_{Amax}.

□, 273K; O, 298K; Δ, 350K; +, 368K.

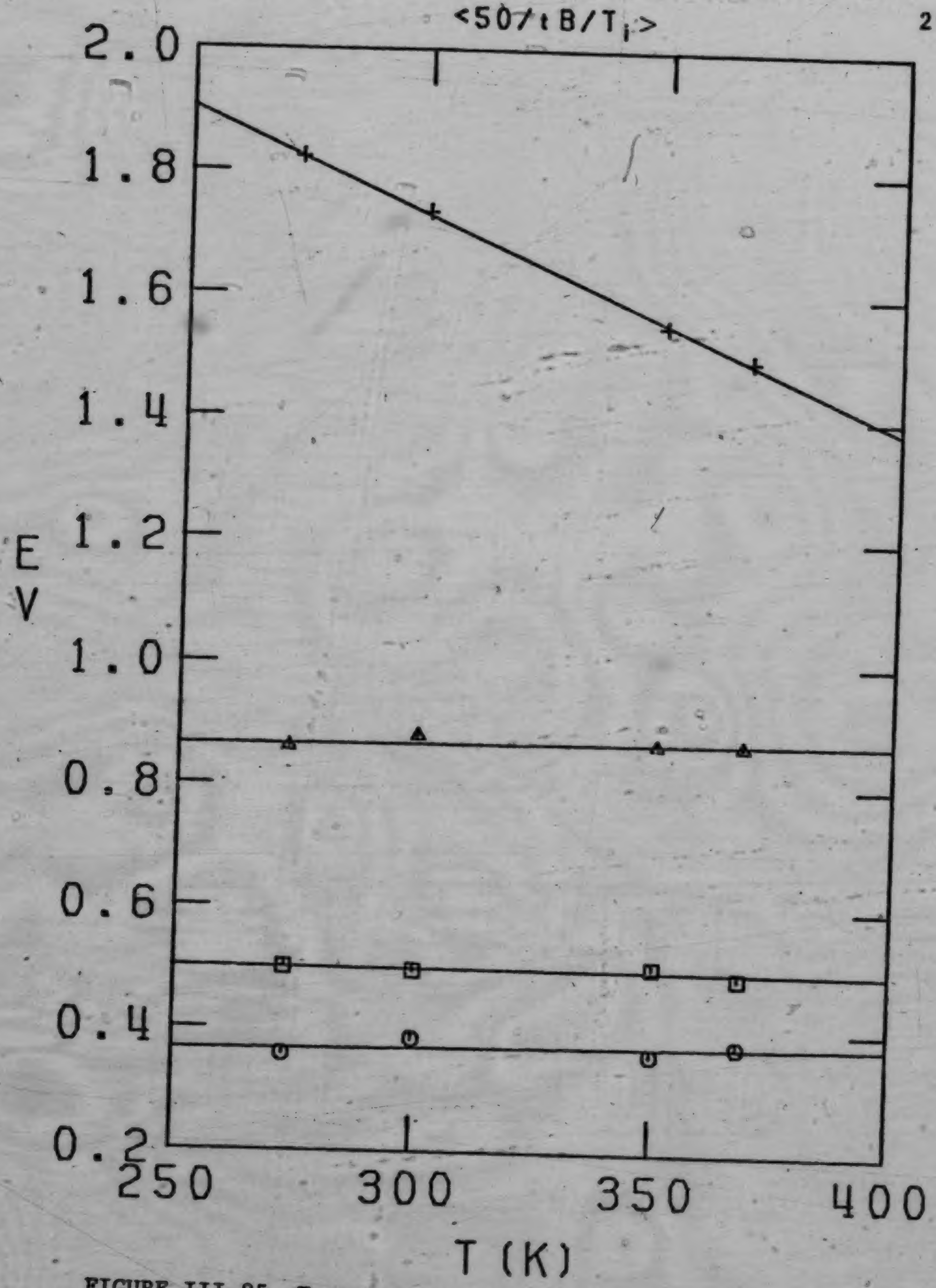

FIGURE III-85. Temperature Dependence of Spectrum Parameters in a Solution of 50 Mole % Water in t-Butanol.
+, E_{Amax}; △, $W_{\frac{1}{2}}$; O, W_r; □, W_b.

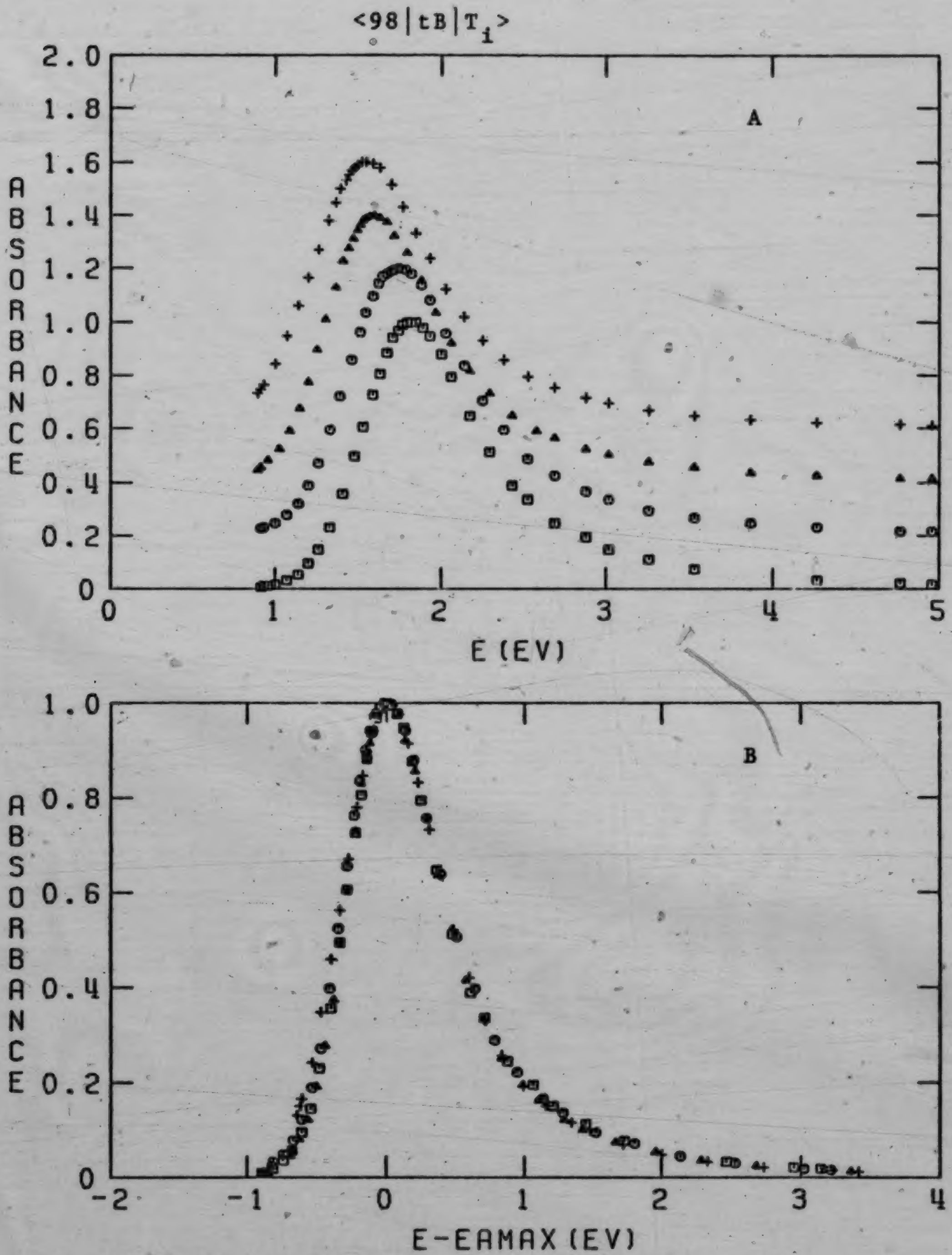

FIGURE III-86. The Optical Absorption Spectrum of Solvated Electrons in a Solution of 98 Mole % Water in t-Butanol at Different Temperatures.

A: Successive spectra are displaced vertically by 0.2 units.

B: The spectra are normalized at E_{Amax}. □, 273K; O, 298K, △, 350K; +, 370K.

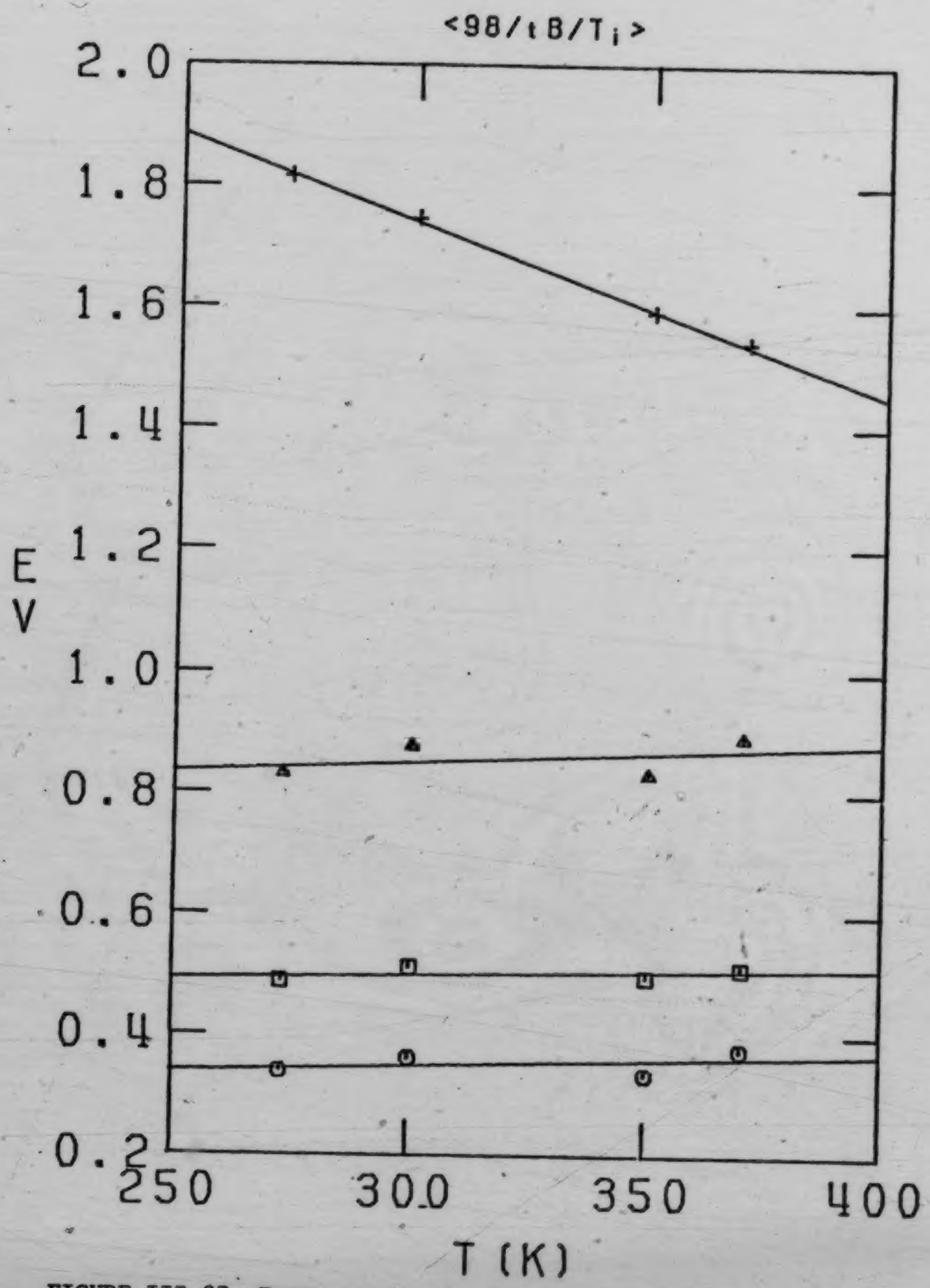

FIGURE III-87. Temperature Dependence of Spectrum Parameters in a Solution of 98 Mole % Water in t-Butanol.
+, E_{Amax}; △, $W_{\frac{1}{2}}$; O, W_r; □, W_b.

From these figures it can be seen that:

(i) The shape of the absorption spectrum changes very little with temperature, in contrast to the changes with composition;

(ii) The E_{Amax} decreases as temperature increases in all the liquids. The rate of decrease is smallest for water and greatest for tertiary butanol;

(iii) The behavior of $W_{\frac{1}{2}}$ with temperature shows much more variability:

(a) It increases with temperature for water, all methanol/water solutions, all primary alcohols, as well as the 98 mole % aqueous solution of all alcohols, which are water-like in all parameters;

(b) It decreases with increasing temperature for secondary and tertiary alcohols, as well as the 10 mole % aqueous solutions of primary, secondary, and tertiary alcohols;

(c) It is independent of temperature for the 50 mole % aqueous solution of primary, secondary, and tertiary alcohols.

(iv) The increase (decrease) in $W_{\frac{1}{2}}$ is due mainly to:

(a) The increase (decrease) of W_b for methanol, all primary alcohols, and 10 mole % water in methanol (for 10 mole % water in primary, secondary except for 2-butanol, and tertiary alcohols);

(b) The increase (decrease) of W_r for water, 50 mole % aqueous solution of methanol, and 98 mole % aqueous solution of all alcohols (for 2-butanol and t-butanol).

C. Effect of Composition upon Temperature Coefficients

Two types of curves were observed for the temperature coefficient of E_{Amax} ($-dE_{Amax}/dT$) as a function of composition (Figure III-88):

(i) For methanol and primary alcohols, $-dE_{Amax}/dT$ increases rapidly to a maximum at around 10 mole % water, then decreases rapidly to around 50 mole % water, followed by a gradual decrease until 98 mole %. After this, it decreases more rapidly again;

(ii) For secondary and tertiary alcohols, it is at its highest for pure alcohol, then decreases sharply as mole % water increases to 10, and gradually until 50 mole % where it again behaves as in (i).

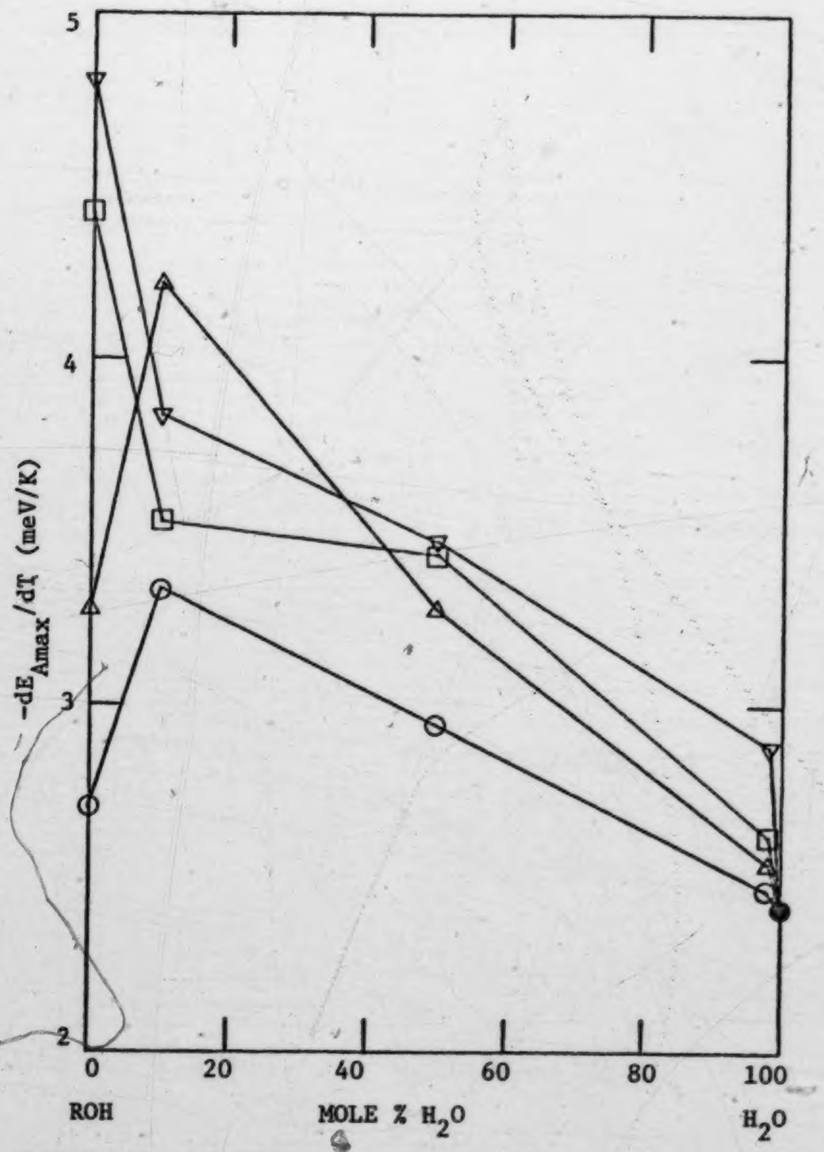

FIGURE III-88. $-dE_{Amax}/dT$ of Alcohol/Water Solutions as a Function of Composition.

○, Methanol; △, 1-propanol; □, 2-propanol; ▽, t-butanol; ●, water.

Shapes for other primary and secondary alcohols are similar to that for △, and for □, respectively.

Three types of curves were observed for the temperature coefficient of $W_{\frac{1}{2}}$ ($dW_{\frac{1}{2}}/dT$) as a function of composition (Figure III-89):

(i) For methanol, it decreases gradually as mole % water increases to 50, and is approximately constant through 50 to 100;

(ii) For primary alcohols, it decreases sharply to a minimum at around 10 mole % water, then increases rapidly to around 50 mole % water, followed by a gradual increase to 100 mole %;

(iii) For secondary and tertiary alcohols, it is at its lowest for pure alcohol, then increases sharply until 98 mole % where it again increases sharply.

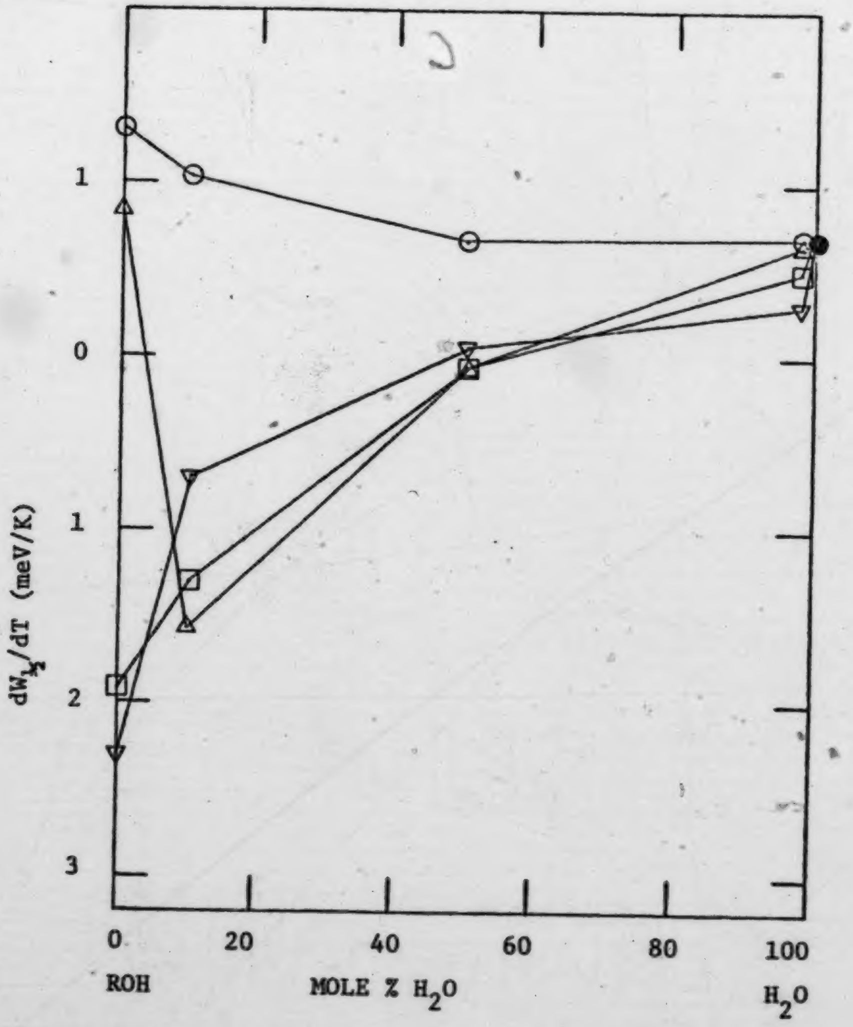

FIGURE III-89 $dW_{1/2}/dT$ of Alcohol/Water Solutions as a Function of Composition.

○, Methanol; △, 1-propanol; □, 2-propanol; ▽, t-butanol; ●, water.

Shapes for other primary and secondary alcohols are similar to that for △, and for □, respectively.

VI. DISCUSSION

A. E_{Amax} of Pure Alcohols from C_1 to C_4 at 298K

From Figures III-4, -6, -8, -12, and -14, it can be seen that for primary alcohols, including methanol, E_{Amax} decreases relatively quickly when a small amount of water is added. By contrast, Figures III-10, -16, and -18 show that for secondary and tertiary alcohols E_{Amax} increases relatively rapidly when a small amount of water is added. From the two sets of figures cited, one can also see that for pure water, E_{Amax} increases when a small amount of any alcohol is added. These observations reflect non-ideal behavior in mixing alcohols with water, as do for instance the viscosities (Figure IV-1) (275,276) and the peculiar behavior of excess enthalpies of mixing (Figure IV-2) (277). These eccentric behaviors will be discussed in the next section.

The E_{Amax} values for pure alcohols and for pure water are listed in Table IV-1, along with values from the literature (14,55,84-87,89,91,95,97,104,106,278). The values differ from one alcohol to another. In order to compare these values, each has been adjusted to 298K by using the temperature coefficients of E_{Amax} from the present study (Tables III-9 to -17). The most reasonably acceptable value of E_{Amax} for each

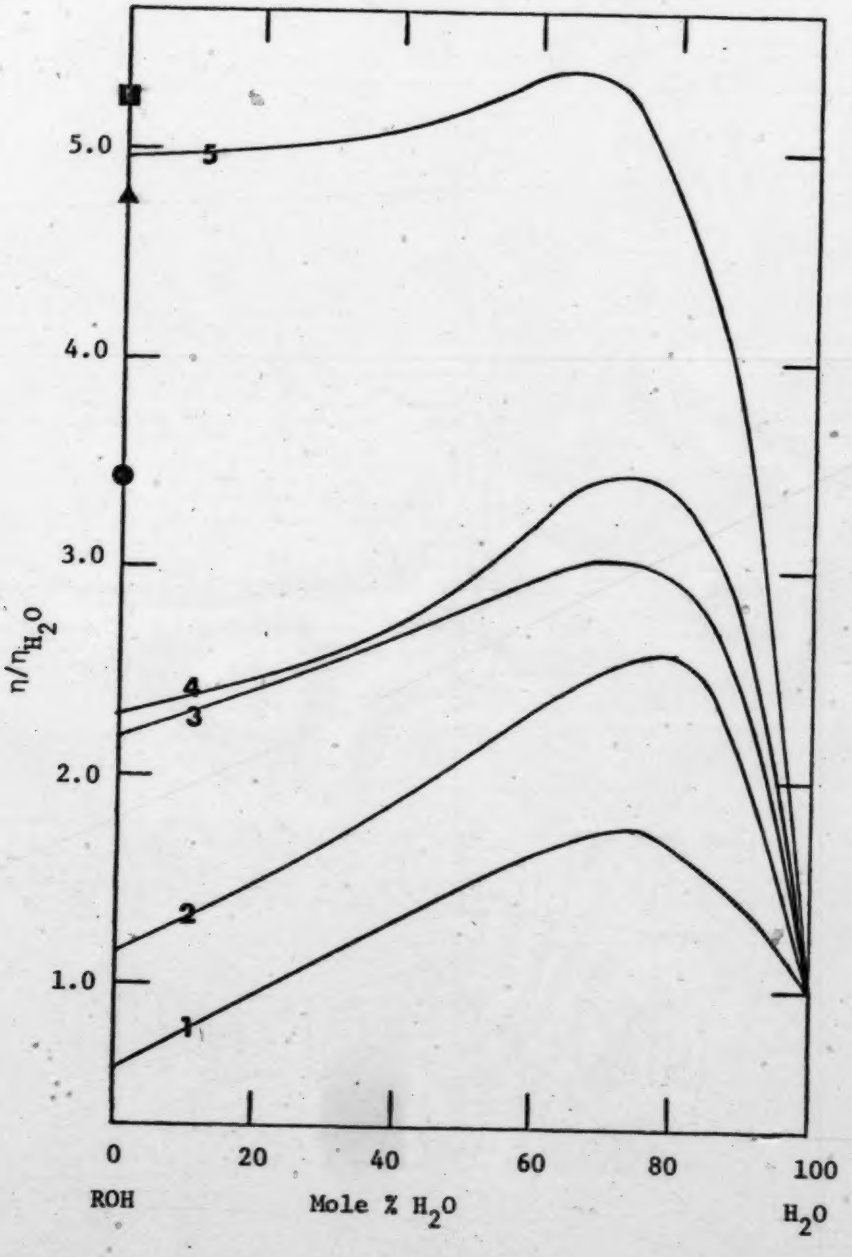

FIGURE IV-1. The Relative Viscosity, η/η_{H_2O} of Pure Alcohols and Alcohol/Water Mixtures at 298K.

1, Methanol; 2, Ethanol; 3, n-Propanol; 4, iso-Propanol; 5, t-Butanol; ●, n-Butanol; ▲, 2-Butanol; ■, iso-Butanol.

1, 2, 3, 4, and 5, Data from ref. 275.

●, ▲, and ■, Data from ref. 276.

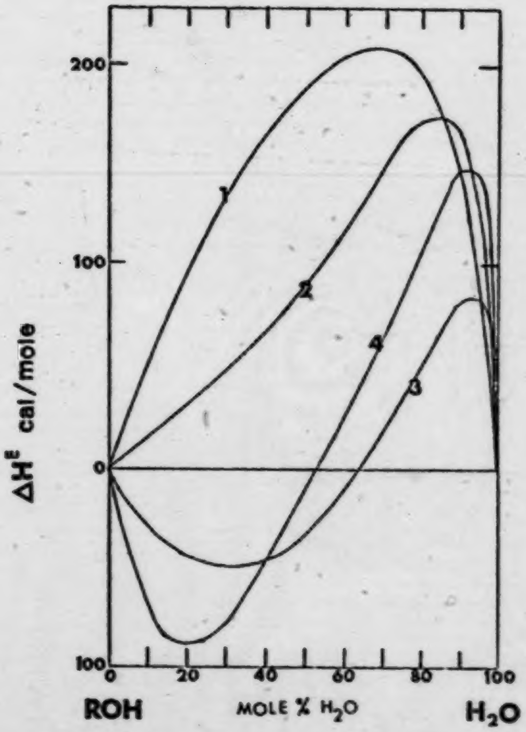

FIGURE IV-2. Excess Enthalpies of Mixing of Alcohol and Water at 298K.

1, Methanol; 2, Ethanol; 3, n-Propanol; 4, t-Butanol.

Data from ref. 277.

TABLE IV-1

Values of E_{Amax} in Pure Alcohols and in Water*

T(K)	M	E	1P	2P	1B	iB	2B	tB	H_2O	Ref.
298	1.98	1.82	1.95	1.52	1.98	1.97	1.59	1.20	1.73	This work
300	1.95	1.79	1.92	1.52				1.14	1.71	84
298	1.96	1.80	1.93	1.53				1.15	1.72	
300			1.93	1.52	1.94			1.14		85
298			1.94	1.53	1.95			1.15		
300	1.95	1.78	1.92		1.93				1.72	86
298	1.96	1.79	1.93		1.94				1.73	
299							1.63			278
298							1.63			
293	1.94									87
298	1.93									
300								1.15		89
298								1.16		
303	1.93	1.70	1.67	1.49	1.82		1.67	0.97	1.72	91
298	1.94	1.72	1.69	1.51	1.84		1.69	0.99	1.73	
298	1.97	1.77	1.67	1.51						14
303	1.93	1.70	1.67	1.49	1.82	1.60		0.99		97
298	1.94	1.72	1.69	1.51	1.84	1.62		1.01		
300	1.97	1.77	1.67	1.51	1.85				1.72	104
298	1.98	1.78	1.68	1.52	1.86				1.73	
298		1.77								106
295	1.95	1.80								95
298	1.94	1.79								
298									1.73	55
298	1.98	1.82	1.92	1.51	1.98	1.97	1.59	1.01	1.73	Most Reasonable value

*FOOTNOTE TO TABLE IV-1

M, Methanol; E, Ethanol; 1P, 1-Propanol; 2P, 2-Propanol; 1B, 1-Butanol; iB, iso-Butanol; 2B, 2-Butanol; tB, t-Butanol; T, Temperature.

$\frac{X}{Y}$, X is the experimental value, Y is the value adjusted to 298K using the temperature coefficients in Tables III-9 to -17.

alcohol and for water has been suggested in the last row of Table IV-1. They are based on the behavior of E_{Amax} in the vicinity of each pure component, either increasing or decreasing sharply when a small amount of solute (water for alcohol; alcohol for water) is added. For the primary alcohols and methanol, the recommended E_{Amax} are the highest reported values. In the case of secondary and tertiary alcohols and water, the recommended E_{Amax} are the lowest reported values. One can see from Table IV-1 that in the case of methanol, ethanol, and 2-propanol, the values of E_{Amax} obtained from the present study are in excellent agreement with the literature values, but there is a big difference in 1-propanol, iso-butanol and t-butanol. A difference also exists in the value of 1-butanol and 2-butanol. The disagreement in 1-propanol and 1-butanol had been first reported from this laboratory by Jou and Freeman in 1977, but they made no comment on this discrepancy (86). Nevertheless, the results obtained from the present study, while obtained earlier than theirs, can also explain why the discrepancy exists.

The literature values of E_{Amax} in 1-propanol and 1-butanol correspond to those obtained in the present study for 10 mole % water in 1-propanol and 3 mole % water in 1-butanol. The discrepancy for iso-butanol is too large to be rationalized from the composition dependence of E_{Amax}. It is due to an unknown error. The literature value, 1.62 eV, is lower than E_{Amax} for pure water (1.73 eV), while the present value, 1.97 eV, is similar to those in other primary alcohols.

The discrepancy for 2-butanol is not as large as those just mentioned. From Figure III-16, one can see that the literature value of 1.69 eV corresponds closely to that obtained in the present study for 17 mole % water in 2-butanol.

The value of E_{Amax} for t-butanol obtained from this work is higher than other values reported. Using Figure III-18, it can be rationalized that the higher value of 1.20 eV is caused by the presence of water. Therefore, the most reasonably acceptable value is 1.0 eV.

The values of E_{Amax} for normal alcohols of C_1 to C_4 (present work) along with C_5 to C_{10} (literature) are shown in Figure IV-3. The purpose of this plot is to see the behavior of E_{Amax} as a function of the number of carbon atoms, and to call attention to the need for justifying it. This is important since the values of E_{Amax} obtained from this laboratory appear to be higher than others, for instance, 1-propanol, 1-butanol and iso-butanol, which have just been mentioned, as well as 1-pentanol (279) and 1-octanol (85), which are shown in Figure IV-3. In this figure, the solid

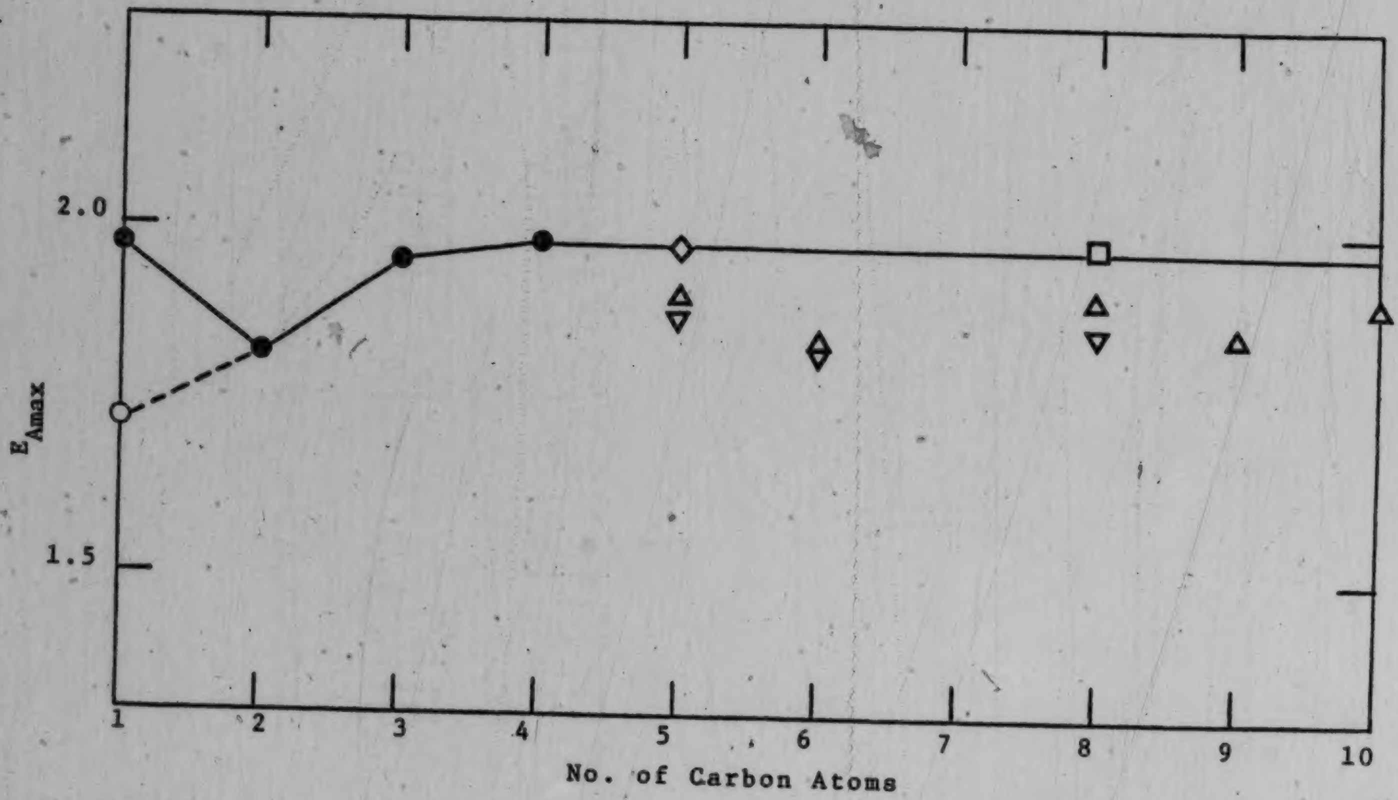

FIGURE IV-3. Plot of E_{Amax} vs the Number of Carbon Atoms in n-Alcohols at 298K. ●, This work; ○, Expected value for methanol; ◇, ref. 279; □, ref. 85; △, ref. 91; ▽, ref. 97.

line drawn from C_5 to C_{10} is the expected value proposed by this study. From this plot, one can argue that the E_{Amax} for ethanol is discrepant from its expected value. However, in the present study the argument leans more heavily toward methanol as the alcohol with eccentric behavior (see Section B-1-iv). The dashed line shows the behavior of methanol that would be expected assuming a trend from ethanol and propanol. Eccentric behavior between methanol and ethanol has been reported by Dolivo and Kevan (280) in their recent work on electrons that have not yet reached the solvated state.

B. Effect of Composition

1. Composition Dependence of E_{Amax} for C_1 to C_4 Alcohol/Water Solutions

The variations of E_{Amax} as a function of composition for methanol, ethanol, 2 isomers of propanol, and 4 isomers of butanol are shown in Figures III-4, -6, -8, -10, -12, -14, -16, and -18. The results are summarized in Figure III-19. From this figure it can be seen that: the overall composition dependence of E_{Amax} can be divided into three categories, one for methanol, another for primary, and a third one for secondary and tertiary alcohols; in the vicinity of pure alcohol the composition dependence can be classified into two categories, one for methanol and primary alcohols, and the other for secondary and tertiary alcohols; in the very high mole % water region, it can be considered to be of only one type, within experimental error.

To facilitate comparison with Figure IV-2 (in Section A), Figure III-19 is transformed into Figure IV-4, by normalizing each E_{Amax} with respect to the E_{Amax} in pure water. The purpose of this comparison is to show the non-ideal behavior of the binary mixture of alcohols with water, with respect to E_{Amax}. The exact reason for this observation is not clear. Since relatively little is known with certainty thus far about the structures of the pure liquids, the structures

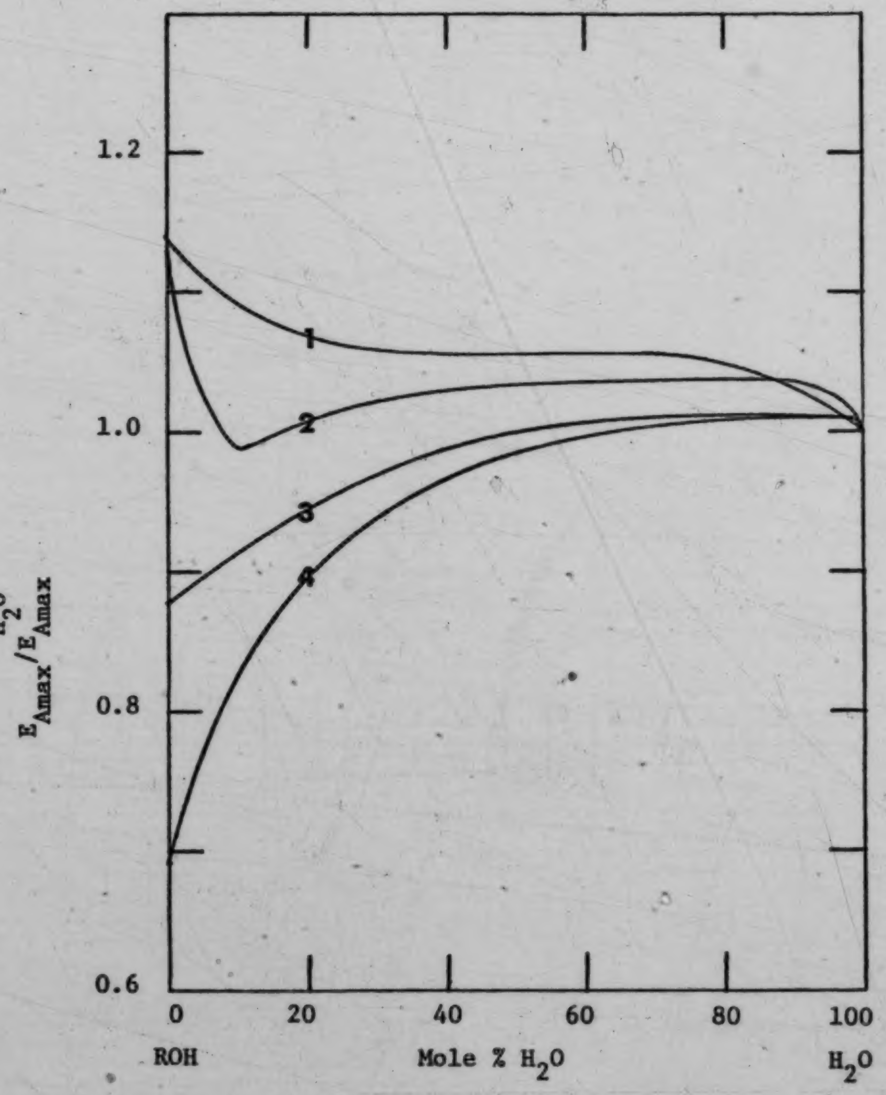

FIGURE IV-4. Composition Dependence of $E_{Amax}/E_{Amax}^{H_2O}$ for Alcohol/Water Mixtures at 298K.

1, Methanol; 2, n-Propanol; 3, iso-Propanol; 4, t-Butanol. Shapes for other primary and secondary alcohols are similar to that for 2 and for 3, respectively.

of the mixtures are even less well defined. Nevertheless, the changes of E_{Amax} indicate that the depth of the trap for the excess electron is changed. Why does this happen? Qualitatively, it is due to mutual interaction of the molecules, and hence, to changes in solution structure. How does this happen? The limited data from the present study do not provide an answer. Therefore, the focus will be on the behavior of E_{Amax} as a function of composition in terms of the changes of trap depth. In addition, solution structure at certain special composition will be proposed to account for the more eccentric of the observed behaviors.

(i) Pure Alcohols

From Figure III-19 or IV-4, one can see that the values of E_{Amax} for alcohols and water are in the following order: methanol > primary alcohol > water > secondary alcohol > tertiary alcohol. This indicates that the depths of the traps are in the same order. The difference in trap depths is probably caused by the difference in solution structure for each category of liquid. For methanol and the primary alcohols, the structure must differ from the secondary and tertiary alcohols, although they have the same functional OH group. From the literature, the following structures have been studied for liquid alcohols: trimer (281), ring polymers (282), and zigzag chain

(283). By comparing the differences in E_{Amax} between methanol and primary alcohols on the one hand and secondary and tertiary alcohols on the other, it is reasonable to assume that in the latter case the function of OH group in trapping the excess electron has been weakened. This could be due to the following factors:

(a) From the inductive effect point of view, the ability of OH group to trap the excess electron has been weakened by the methyl or ethyl group in the α-position to OH, since both methyl and ethyl groups are electron releasing in nature:

(b) The value of E_{Amax} for secondary and tertiary alcohols is lower than for water, methanol and primary alcohols. From the steric effect point of view, branched molecules would form a larger trap than do straight chain molecules, due to steric repulsion of the branched alkyl groups in the α-position with respect to their functional OH group. This can be rationalized from the pressure study of solvated electron spectra in the primary, secondary and tertiary alcohols (84,86), since the ratio of the relative pressure coefficients of E_{Amax}, $\frac{1}{E_{Amax}}\left(\frac{dE_{Amax}}{dP}\right)$, for n-propanol (or n-butanol), iso-propanol, and t-butanol is 1:2:3.

The lower E_{Amax} observed for tertiary than for secondary alcohol is, then, due to the additional methyl group attached to the α-position of the OH group, which enhances both the inductive and the steric effect.

(ii) In the Low Mole % Water Region

From Figure IV-4, it can be seen that in the vicinity of each pure alcohol, when a small amount of water is added E_{Amax} changes relatively rapidly. For methanol and primary alcohols, E_{Amax} decreases with increasing mole % water. By contrast, E_{Amax} for secondary and tertiary alcohols increases as mole % water increases. The exact reasons for the behavior are not clear. The depth of the trap becomes shallower or deeper, causing E_{Amax} to decrease or increase, respectively. The liquid structure of each alcohol is upset by the presence of a small amount of water. This disturbance has two tendencies: one is to decrease the value of E_{Amax} (curves 1 and 2 in Figure IV-5) and the other is to increase it (2, 3 and 4 in Figure IV-5).

The curves 1-4 in Figure IV-5, which represent respectively the behavior in methanol, 1-propanol, 2-propanol, and t-butanol/water mixtures, are nonlinear. The deviation from linearity is due to non-ideal behavior of the alcohol/water mixtures. Non-ideal behavior is also shown in the enthalpies of mixing, Figure IV-2.

FIGURE IV-5. Proposed Two Kinds of Contribution to Account for the Observed E_{Amax} in Alcohol/Water Mixtures at 298K.

O, Ideal mixing of methanol and water;

1, Methanol; 2, n-Propanol; 3, iso-Propanol; 4, t-Butanol. Shapes for other primary and secondary alcohols are similar to that for 2 and for 3, respectively.

A, B, C, or D is the contribution which decreases the value of E_{Amax}, while E is the contribution tending to increase the value of E_{Amax}.

A' and E' are the hypothetical contributions of methanol and water to the ideal behavior of O.

FIGURE IV-5

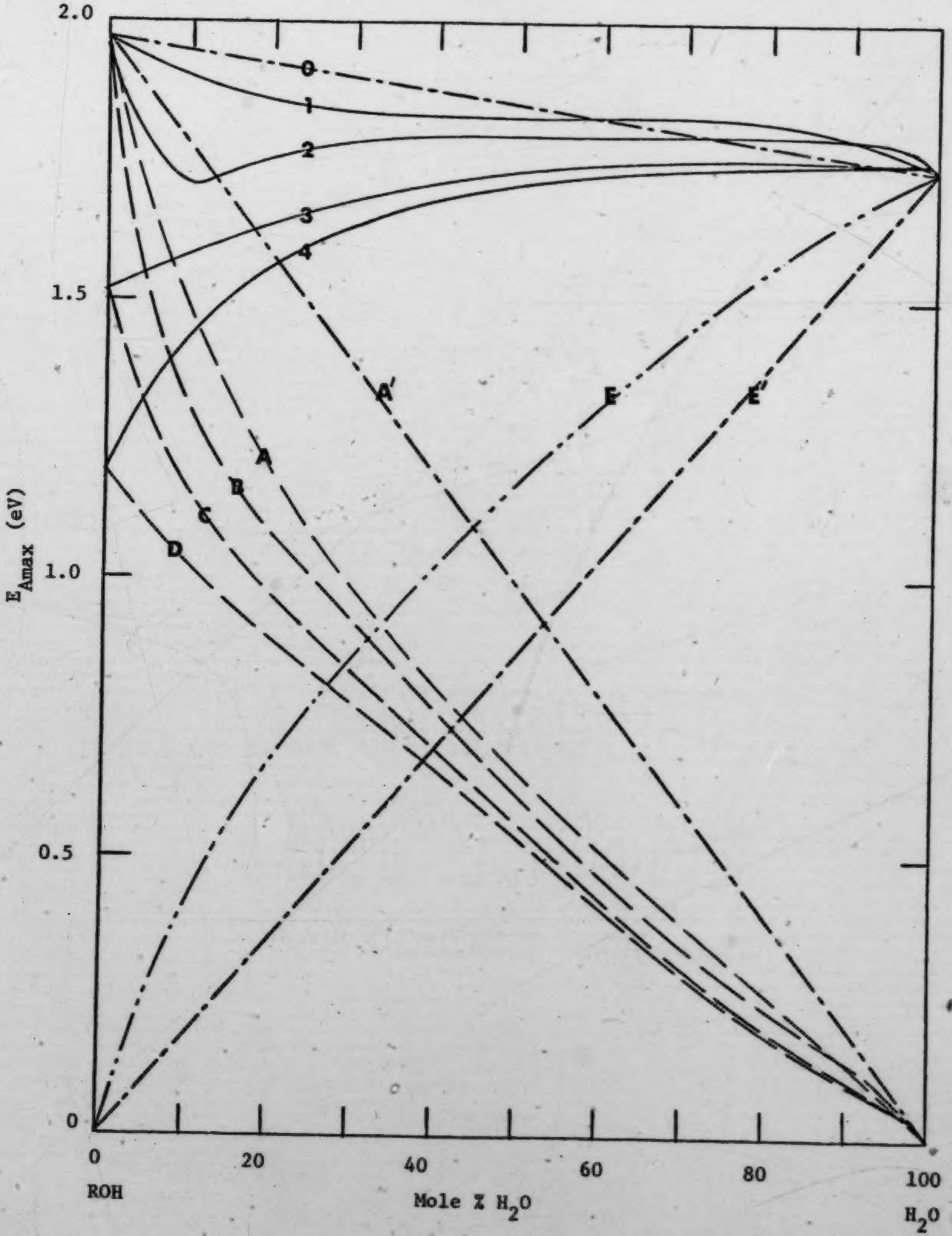
2.0
1.5
1.0
0.5
0
E_{Amax} (eV)
0
1
2
3
4
A'
E
E'
A
B
C
D
0
20
40
60
80
100
ROH
Mole % H_2O
H_2O

The observed curves, 2, 3, and 4 in Figure IV-5 appear to contain a "water component" such as E. The observed curve 2 contains an "alcohol component" such as B, which is obtained by subtracting E from 2. Curve E was drawn arbitrarily to show the general shape of the water component, but the true curve is not known. The true curve is probably different for each alcohol, but for simplicity in the present discussion, E has been taken to represent the contribution of water to the observed E_{Amax} in all alcohol/water mixtures. Curves A, B, C and D are then constructed from the observed curves for E_{Amax} in the methanol, 1-propanol, 2-propanol, and t-butanol/water mixtures, by subtracting curve E.

The line 0 in Figure IV-5 is drawn to indicate the hypothetical ideal mixing of methanol/water. Lines A' and E' are then drawn to represent the ideal contributions of methanol and water respectively to line 0. That is, line 0 is resolved ideally into E' and A'. It can be seen that the observed behavior of methanol/water mixtures (curve 1) deviates little from ideal (line 0). The water contribution to curve 1, in contrast to curves 2, 3, and 4, should not be so heavy weighted as E. A more realistic curve E_1 for the water contribution in methanol/water mixtures would be between curve E and line E', and probably very close to the ideal E'. Hence, curve A for these mixtures is underweighted. A more realistic curve A_1 (Figure IV-6) would be closer to the ideal A', and hence, less sharp than curve A. New curves B_1, C_1 and D_1 are then constructed using the water dominance curve E_1 for methanol and observed curves 2, 3, and 4 for 1-propanol, 2-propanol and t-butanol. Curves B_1 and C_1 are reasonably close to ideal whereas D_1 deviates considerably from ideal.

In comparing Figure IV-5 and -6, the water contribution curve E (in Figure IV-5) seems more appropriate to the case of curve D, whereas E_1 (in Figure IV-6) seems more appropriate to curves A_1, B_1 and C_1. A more realistic representation would probably require a separate water contribution curve for each alcohol.

In the low mole % water region, from Figures IV-5 and IV-6, the slopes of curves A_1, B_1, C_1, and D, indicate the degree of disturbance, and thus the change in trap depth, which causes changes in E_{Amax} when a small amount of water is added to the respective alcohol. The difference in the degree of disturbance between methanol (A_1) and 1-propanol (B_1)/water mixtures shown in Figure IV-6 is parallel to the different rate of change of E_{Amax} with respect to pure methanol and primary alcohols in Figure IV-7, in the vicinity of pure alcohol. The composition de-

FIGURE IV-6. Proposed Two Kinds of Contribution to Account for the Observed E_{Amax} in Alcohol/Water Mixtures at 298K, Based on Water Dominance Curve E_1.

O, Ideal mixing of methanol and water;

1, Methanol; 2, n-Propanol; 3, iso-Propanol; 4, t-Butanol. Shapes for other primary and secondary alcohols are similar to that for 2 and for 3, respectively.

A_1, B_1, C_1, or D_1 is the contribution which decreases the value of E_{Amax}, while E_1 is the contribution tending to increase the value of E_{Amax}.

FIGURE IV-6

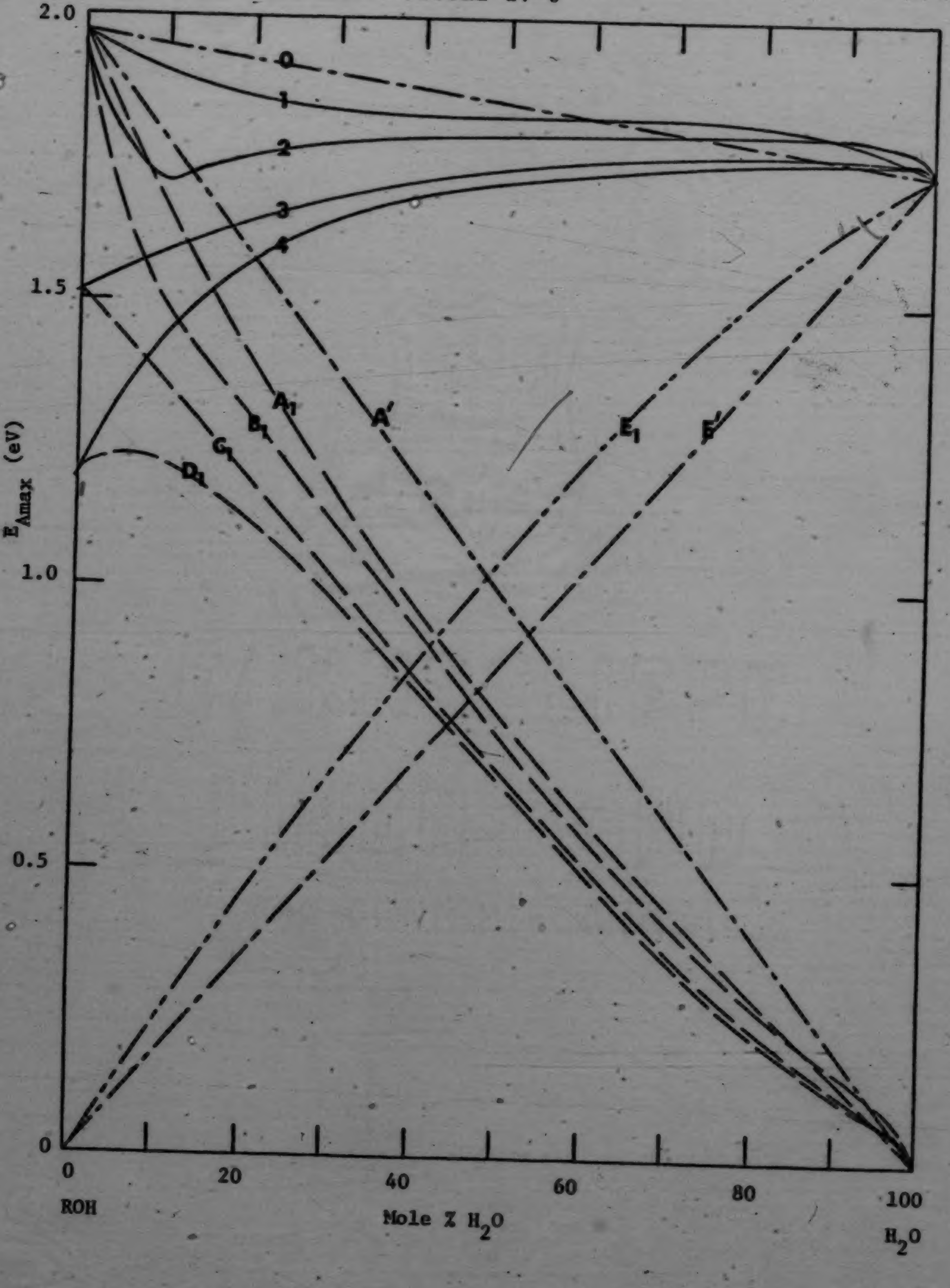
2.0
1.5
1.0
0.5
0
E_{Amax} (eV)
0
1
2
3
4
A_1
A'
B_1
G_1
D_1
E_1
E'
0
20
40
60
80
100
ROH
Mole % H_2O
H_2O

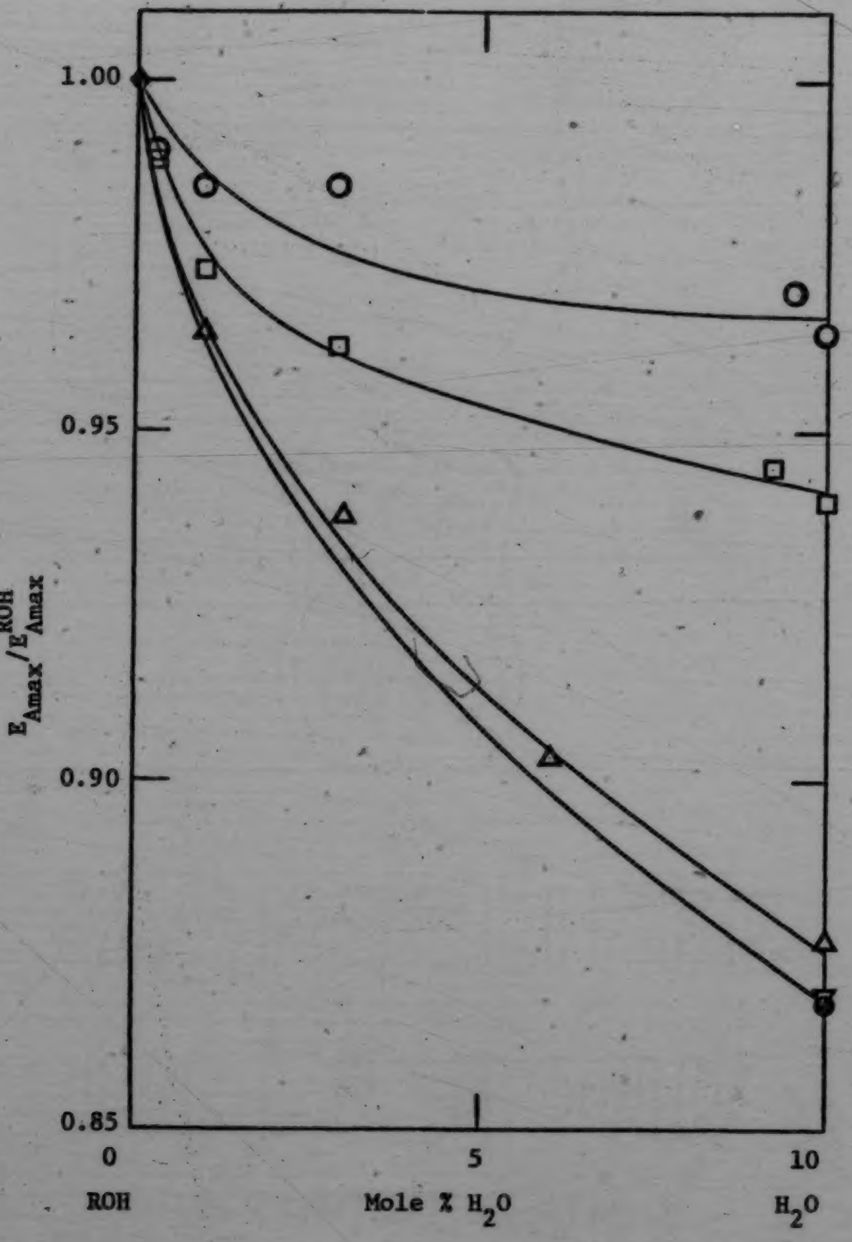

FIGURE IV-7. Composition Dependence of E_{Amax}/E_{Amax}^{ROH} for n-Alcohol/Water Mixtures at 298K.

○, Methanol; □, Ethanol; △, 1-Propanol; ▽, 1-Butanol; ●, iso-Butanol; ◆, Pure ROH.

pendence of E_{Amax} seems to be correlated with the length of carbon chain in methanol and primary alcohols. This suggests that the longer the carbon chain, the greater the disturbance caused by water, for a normal chain containing up to three carbon atoms. The difference in disturbance between C_1 and D seems to be related to the tertiary having greater bulkiness of α-carbon than does the secondary alcohol. That is, when α-carbon is more bulky the relative disturbance by water is greater.

(iii) In the High Mole % Water Region

From Figure IV-4, -5, -6, or -7, one can see that the behavior of E_{Amax} as a function of composition is similar when a small amount of any alcohol is added to water. In all cases, the value of E_{Amax} increases with increasing mole % alcohol. The reasons for this observation are still an open question. However, Franks has cited that when a small amount of a non-electrolyte is added to liquid water, the tetrahedrally coordinated water skeleton, with respect to each oxygen atom, will be changed. This change can be seen from the viscosity-concentration curve in a binary system such as water/ethanol (Figure IV-8). In this figure, $d\eta/dC$ increases with increasing concentration, showing an increased structure effect which reaches a maximum at <10% alcohol (284). By comparing Figure IV-9 and Figure IV-8, it can be

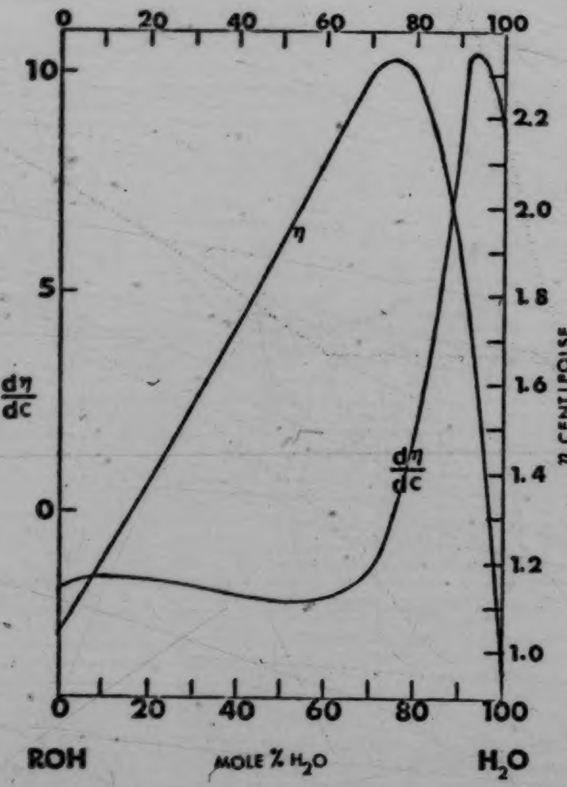

FIGURE IV-8. Viscosity, η, and dη/dC of Ethanol/Water Mixtures at 298K, Data from ref. 284.

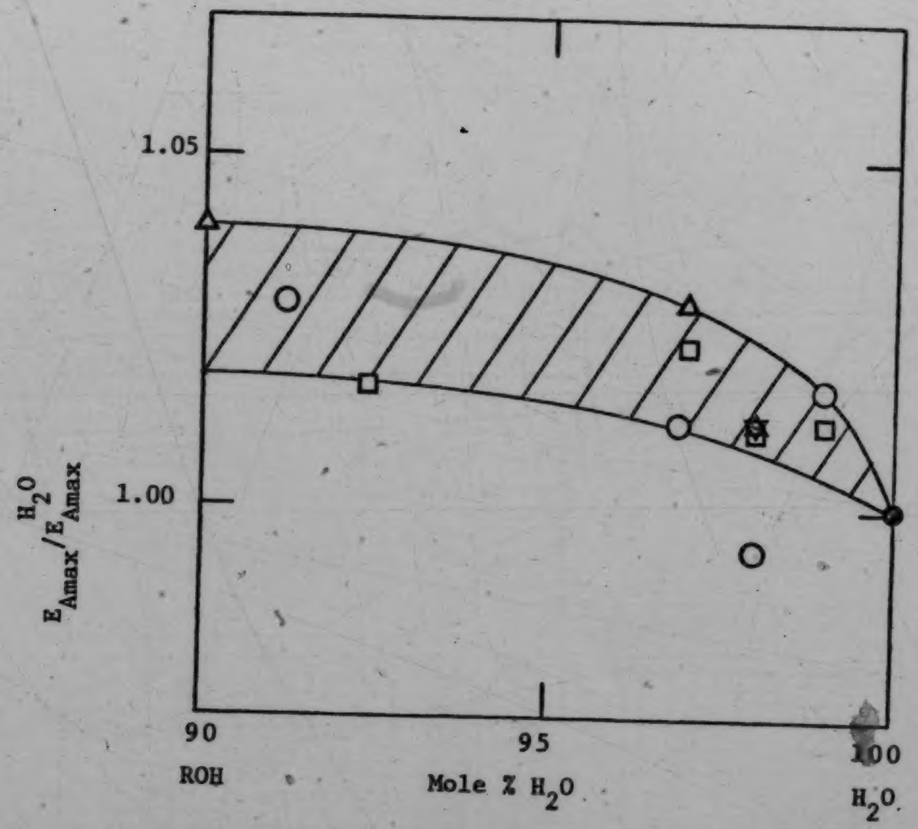

FIGURE IV-9. Composition Dependence of $E_{Amax}/E_{Amax}^{H_2O}$ for Alcohol/Water Mixtures at 298K.

○, Methanol; □, Ethanol; △, 1-Propanol; ▽, 2-Propanol and all 4 isomers of Butanol; ●, Water.

seen that the behavior of E_{Amax} is similar to that of $d\eta/dC$ as a function of composition, especially in the vicinity of pure water. The structure disturbance tends to make the electron trap slightly deeper.

(iv) Around 10 Mole % Water Region

From Figures III-1, -6, -8, -12, -14, -19 and IV-4, it can be seen that near 10 mole % water the value of E_{Amax} in primary alcohol/water solutions passes through a minimum that is equal to or slightly less than the value in pure water. This eccentric behavior is observable in the ethanol/water data of Arai and Sauer (105), but they apparently attributed it to experimental scatter. The minimum indicates that the depth of the trap becomes similar to that in pure water. The reasons for this finding are not yet clear. Two possible reasons are suggested here: (1) the minimum may be an accidental result of the two disturbances mentioned in the above section (ii); (2) an alternate account from the solution structure point of view might be as follows.

The minimum in E_{Amax} indicates that the net strength of interaction between the excess electron and solvent is a minimum when about 10 mole % water is present. The water might enhance formation of alcohol tetramers, which would tend to decrease the availability to the electron solvation site of OH functional groups. Tetramers might result from water-nucleated structures such as that illustrated in Figure IV-10. The structure shown in this figure is based on the ring polymer model for alcohol (282), along with ideas from models such as octahedral (285), tetrahedral (286), and body centered cubic (287-289) that have been proposed for water. Eight alcohol molecules are placed on the corners of a cube 1 to 8, in which 1 to 4 is one tetramer and 5 to 8 is another. A water molecule is placed at the center with H-bonding directions towards sites 1 and 8 by acting as a proton donor, and with other H-bonding directions towards sites 3 and 6 by acting as an electron donor. Thus, two tetramers of alcohol are linked together by one water molecule, and the water molecule is occluded by eight alcohol molecules. The formation of such solution structure around 10 mole % water might account for the observed minimum of E_{Amax}. With this configuration, the net strength of interaction between the excess electron and solvent may then depend upon the size and type of the alkyl group in the α-position to the OH group for each alcohol. Another example of an unusual structural change in the 10 mole % water region of ethanol/water mixtures has been reported by Potts and Davidson (290). They found a eutectic

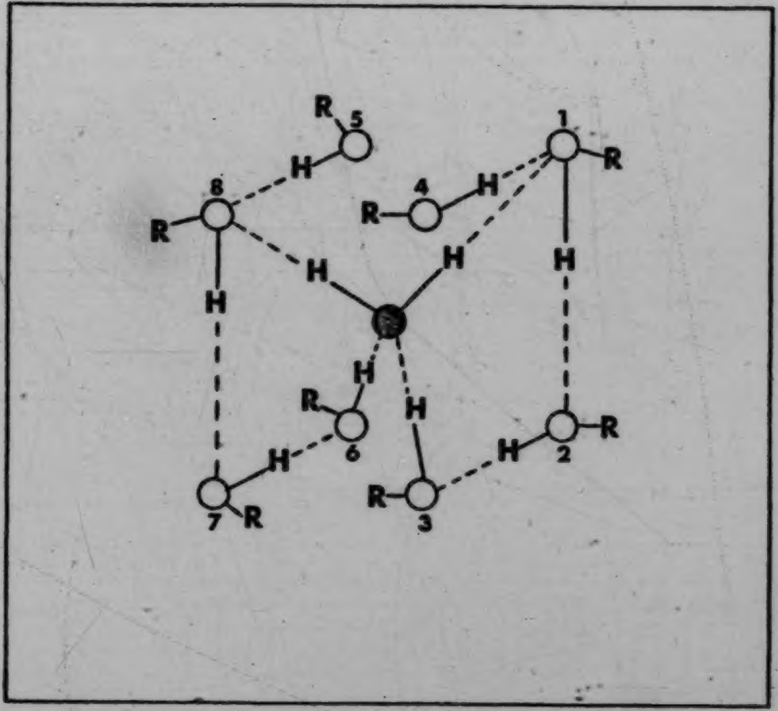

FIGURE IV-10. Proposed Solution Structure for Alcohol/Water Mixtures Around 10 Mole % Water at 298K.

●, Oxygen atom in water molecule;

○, Oxygen atom in alcohol molecule.

point of this ethanol/water system occuring at 15 mole % water.

The different behavior of methanol, compared to that of ethanol and the other primary alcohols, is presumably attributable to the small alkyl group and consequent different liquid structure.

The value of E_{Amax} in methanol is higher than for water. This is another peculiar behavior of methanol that has been observed, in comparison with ethanol. The reason for this could be due to the above configuration and to only one methyl group in the α-position of the OH group. In addition, it might be due to the peculiar character of this alkyl group. The peculiar behavior of this methyl group has been studied by Mulliken as follows (291,292)

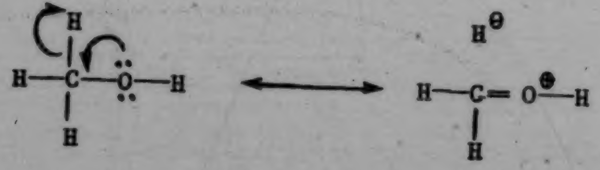

[1]

This eccentric behavior strengthens the power of the solvation site in the OH group, and hence, increases the ability to solvate the excess electron.

In the case of secondary and tertiary alcohol, the corresponding E_{Amax} at 10 mole % water is much lower than for water, although it is higher than for the respective pure alcohol. This could be due to the selective solvation by water.

(v) In the Remaining Composition Range

From Figures IV-4, -5, and -6, it can be seen that, in the 10 to 50 mole % water region, E_{Amax} decreases gradually for methanol, while E_{Amax} increases gradually for primary, secondary and tertiary alcohol/water mixtures. In the 50 to 90 mole % water region, E_{Amax} is nearly composition independent for all alcohols, within experimental error. The former behavior indicates gradual change of the structure of the electron trap, with some preference for water molecules. Above 50 mole % water, the trap appears to be a slightly modified water structure.

2. Composition Dependence of $W_{\frac{1}{2}}$ for Alcohol/Water Mixtures.

The behavior of $W_{\frac{1}{2}}$ as a function of composition is included in the figures mentioned in the previous section for E_{Amax}, and is summarized in Figure III-20. It can be seen from this figure that: $W_{\frac{1}{2}}$ decreases as mole % water increases; most of the decrease occurs up to 50 mole % water; in the low mole % water region, the sharpness of the decrease is in the following order, secondary > primary > methanol >> tertiary alcohol. The $W_{\frac{1}{2}}$ curves reflect non-ideal solution behavior and selective solvation of the electrons by water, as did the E_{Amax} curves.

The non-ideal behavior is accounted for by the mutual disturbance of the liquid structures when water and alcohol molecules are mixed together. Parallel to Section B-1-(ii) above, the observed curves for $W_{\frac{1}{2}}$ are resolved into two components (Figure IV-11). The hypothetical water component curve (E) must be concave towards the composition axis, because the electrons tend to be preferentially solvated by water. The complimentary alcohol curves for methanol (A), 1-propanol (B), 2-propanol (C), and t-butanol (D) were obtained by subtracting E from the observed curves 1, 2, 3, and 4, respectively. From Figure IV-5 and -6 in the previous section, it can be seen that the behavior of E_{Amax} as a function of composition in t-butanol/water is

FIGURE IV-11. Proposed Two Kinds of Contribution to Account for the Observed $W_{\frac{1}{2}}$ in Alcohol/Water Mixtures at 298K.

1, Methanol; 2, n-Propanol; 3, iso-Propanol; 4, t-Butanol. Shapes for other primary and secondary alcohols are similar to that for 2 and for 3, respectively. A, B, C, and D' are the contributions which decrease the value of $W_{\frac{1}{2}}$ in methanol, n-propanol, iso-propanol and t-butanol/water, respectively. E' is the contribution tending to increase the value of $W_{\frac{1}{2}}$ for t-butanol/water mixtures, while E is the corresponding contribution for the rest. E_o is the hypothetical ideal contribution of water.

FIGURE IV-11

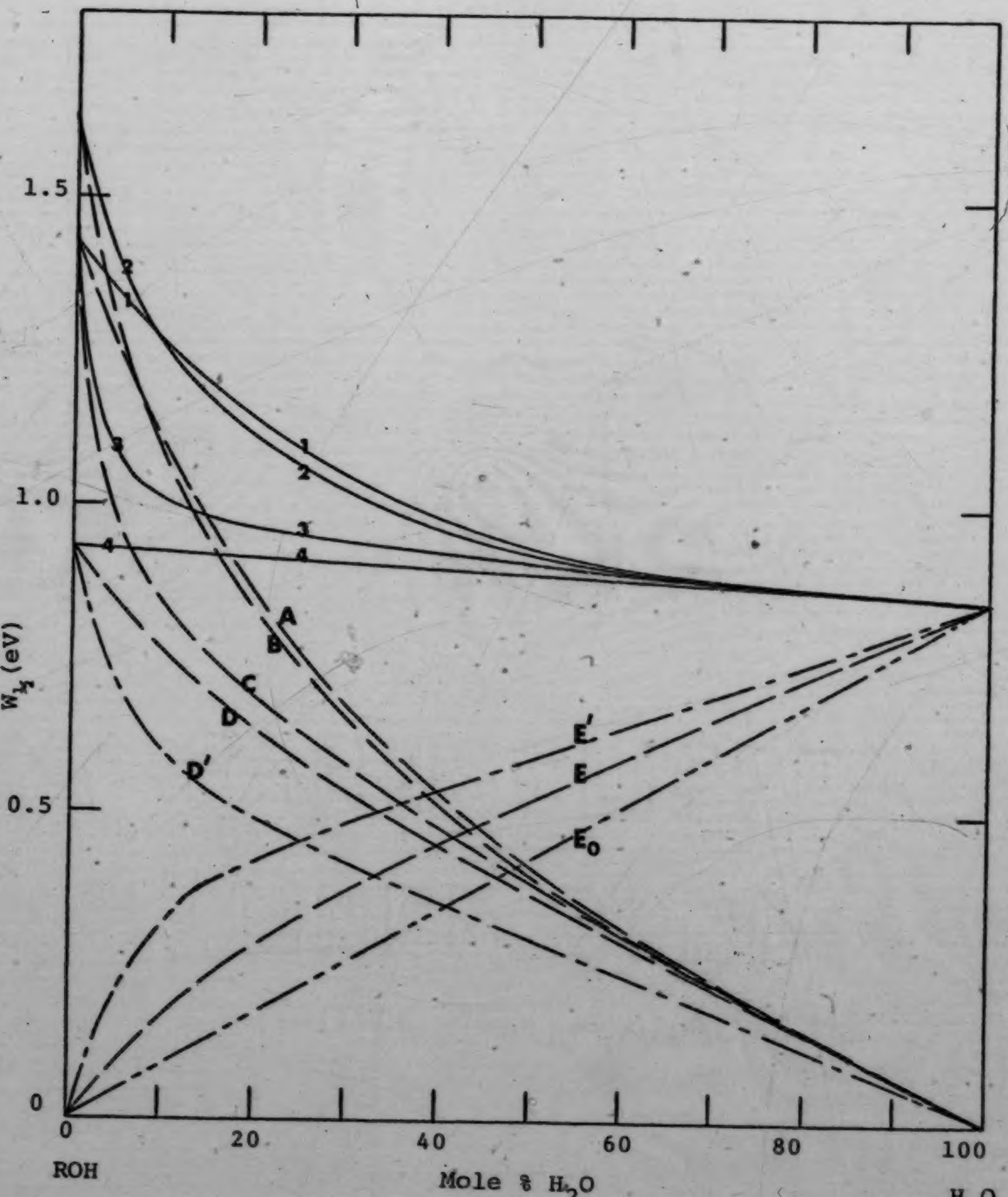
1.5
1.0
0.5
0
$W_{1/2}$ (eV)
0
20
40
60
80
100
ROH
Mole % H_2O
H_2O
1
2
3
4
A
B
C
D
D'
E'
E
E_0

more non-ideal than methanol/water. In Figure IV-11, if the same water component curve E were used for all the alcohol solutions, the behavior of $W_{\frac{1}{2}}$ as a function of composition in t-butanol/water (curve D) would be less non-ideal than in methanol/water (curve A). This is in contrast to the behavior of E_{Amax} mentioned above. Therefore, another hypothetical water component curve (E') is needed in order to obtain a more suitable complimentary curve for t-butanol (D'). With the curve D', the degree of non-ideal behavior of E_{Amax} and of $W_{\frac{1}{2}}$ for t-butanol/water has more or less the same trend compared with methanol/water. Line E_o represents an ideal contribution to $W_{\frac{1}{2}}$ from water, and is used for indicating the deviation from ideal. The slopes of the curves such as A and D' then indicate the relative disturbance of $W_{\frac{1}{2}}$ by water when a small amount is added to the respective alcohol. The apparent composition dependence of $W_{\frac{1}{2}}$ in t-butanol/water shown in Figure IV-11 is nearly linear. This is a coincidence due mainly to the increase of E_{Amax} with increasing mole % water. The ratio $W_{\frac{1}{2}}/E_{Amax}$ does not vary linearly with composition.

Figure IV-12 shows that the apparent $W_{\frac{1}{2}}$ for n-alcohols is nearly independent of carbon chain length, except for methanol. This exception could be expected since the behavior of methanol differs from other primary alcohols as mentioned in the previous two

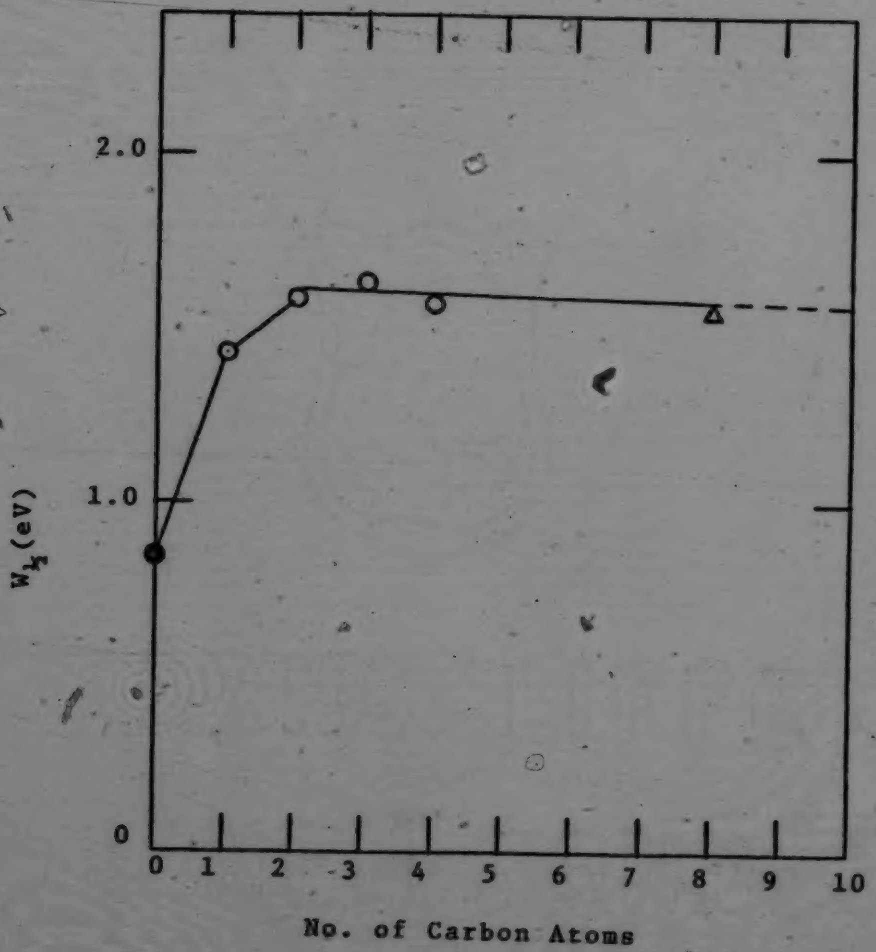

FIGURE IV-12. Plot of $W_{\frac{1}{2}}$ vs the Number of Carbon Atoms in n-Alcohols at 298K.

●, Water; ○, n-Alcohols, this work. Δ, ref. 85.

-----, Expected value.

sections. The value of $W_{\frac{1}{2}}$ in alcohol is much higher than in water. Jou and Freeman have postulated a reason for the observation that the breadth of $W_{\frac{1}{2}}$ in alcohol is wider than in water. This is due to the alkyl group providing a higher excited state in the course of optical transition (86).

From Figure IV-13, it can be seen that the value of $W_{\frac{1}{2}}$ in pure alcohols seems to be correlated to the number and nature of H atoms attached to the carbon atom which is in the α-position of the functional group of alcohols. In other words, the value of $W_{\frac{1}{2}}$ in pure alcohols might depend upon the environment of the carbon atom which is in the α-position to the OH group.

Figure IV-14 shows that in the low mole % water region, the rate of decrease in $W_{\frac{1}{2}}$ with respect to the values in the pure alcohols is as follows, secondary alcohol > primary alcohol > methanol >> tertiary alcohol. This seems to parallel the trend observed in Figure IV-13. Therefore, the non-ideal composition dependence of $W_{\frac{1}{2}}$ might be somehow correlated with the disturbance caused by water upon the environment of the α-carbon to the OH group. The mechanism whereby the environment of the α-carbon affects the $W_{\frac{1}{2}}$ of the absorption spectrum is not known. Nevertheless as shown in the following section, the behavior of $W_{\frac{1}{2}}$

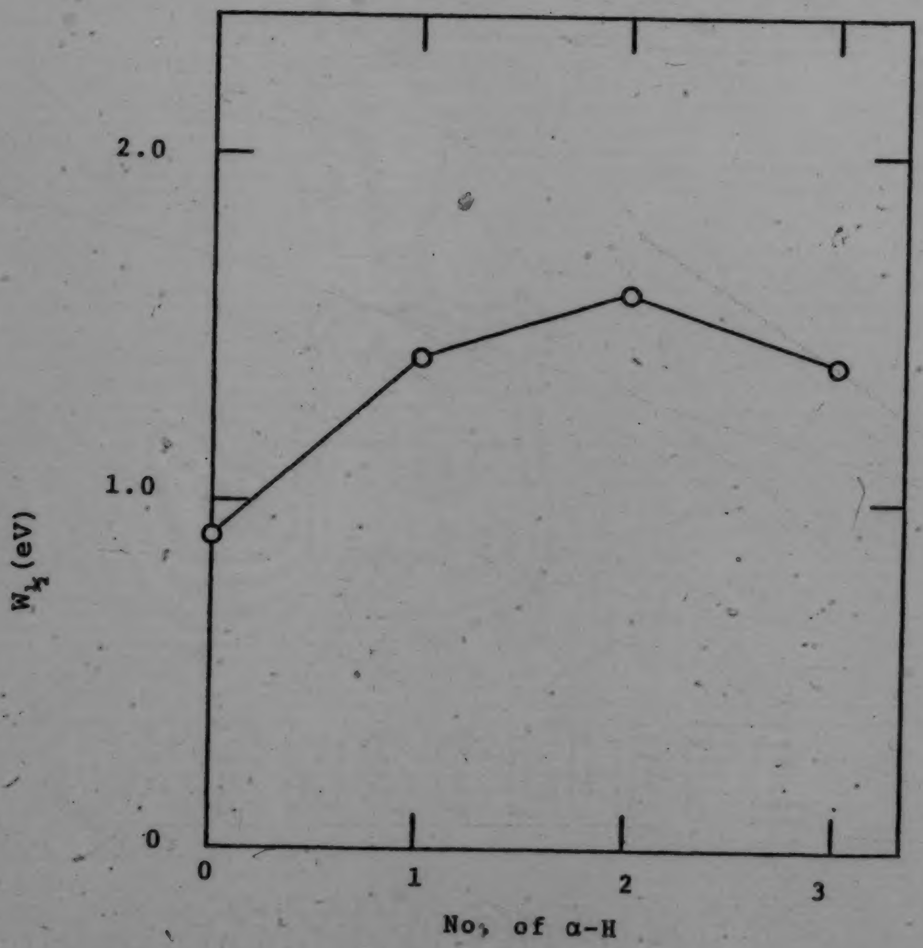

FIGURE IV-13. Plot of $W_{\frac{1}{2}}$ vs the Number of α-H in Alcohols at 298K.

0, t-Butanol; 1, iso-Propanol; 2, n-Propanol; 3, Methanol.

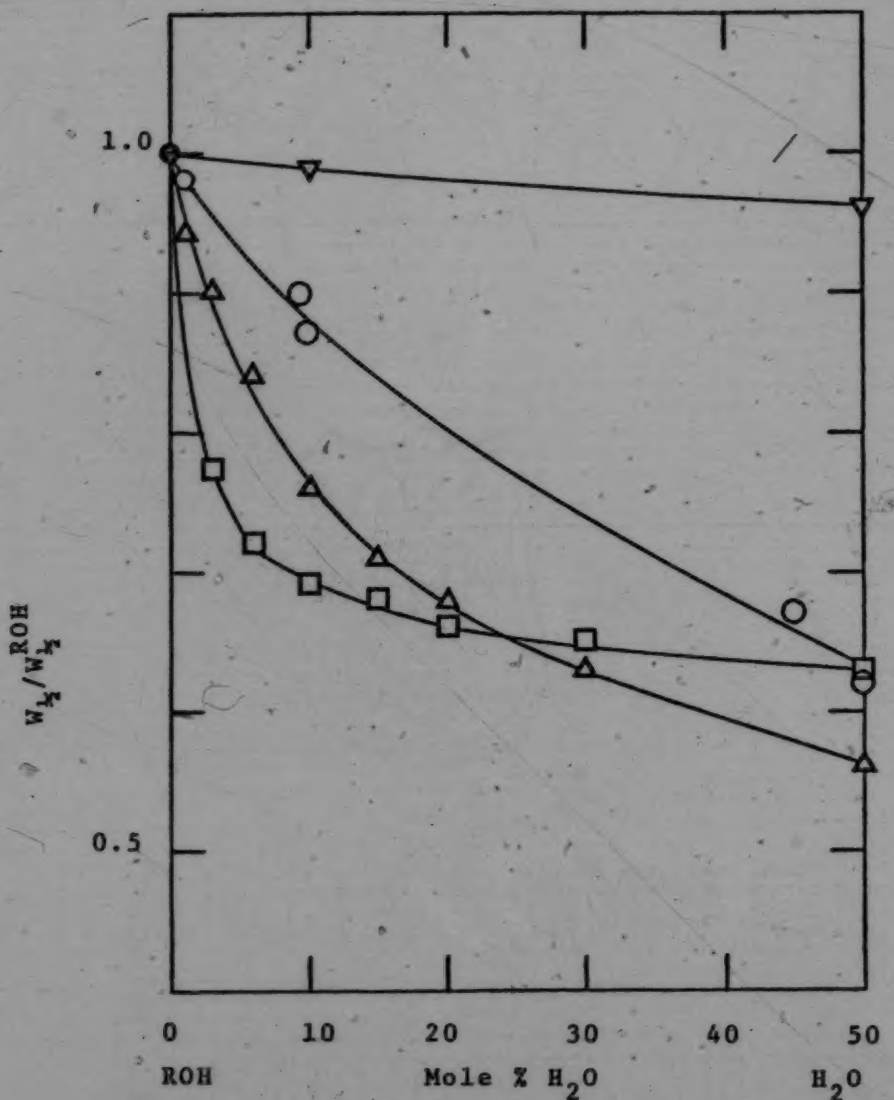

FIGURE IV-14. Composition Dependence of $W_{\frac{1}{2}}/W_{\frac{1}{2}}^{ROH}$ for Alcohol/Water Mixtures at 298K.

●, ROH; ○, Methanol; △, 1-Propanol; □, 2-Propanol; ▽, t-Butanol.

Trends for other primary and secondary alcohols are similar to that for △ and for □, respectively.

is determined largely by changes in W_b. Thus, further research should be aimed at changes in the high energy side of the spectrum with changes in solution structure.

From Figure IV-11, one can see that above 50 mole % water, $W_{\frac{1}{2}}$ is nearly composition independent for all alcohols. This is similar to the behavior of E_{Amax} as a function of composition in the same concentration region (see Figure IV-5 or -6). This consistency supports the suggestion that above 50 mole % water the electron rests preferentially in a trap that is a slightly modified water structure.

3. Composition Dependence of W_b and W_r

The values of W_b and W_r are given by (Figure II-15):

$$W_{\frac{1}{2}} = W_b + W_r \qquad [2]$$

$$W_b = E_b - E_{Amax} \qquad [3]$$

and

$$W_r = E_{Amax} - E_r \qquad [4]$$

where E_b is the energy at half-height of absorption maximum on the blue side of the spectrum and E_r is the corresponding energy on the red side of the spectrum. The reported values of W_b and W_r depend upon the value chosen for E_{Amax}, for a fixed value of $W_{\frac{1}{2}}$. The value of E_{Amax} is obtained visually from the plot, and could differ from one person to another by ±0.02 eV. The values of W_b and W_r are therefore subject to this amount of error.

The behaviors of W_b and W_r as functions of composition are shown in the figures mentioned above for E_{Amax} and $W_{\frac{1}{2}}$, and are summarized in Figure III-21. One can see from this figure that: W_b is more sensitive to changing composition than is W_r, especially in the low mole % water region; from 0 to 50 mole % water, both W_b and W_r decrease with increasing mole % water; above 50 mole % water, both of them are almost composition independent, and the value is nearly the same for pure water. The W_b curves reflect non-ideal solution behavior and selective solvation of the electrons by water more than the W_r curves do.

By comparing Figure III-20 and -21, one can see that composition dependence of $W_{\frac{1}{2}}$ is generated mainly through W_b. This supports the interpretation that the shapes of the low and high energy sides of the bands are determined by different processes (86). The absorption band may therefore be deconvoluted into overlapping component bands (85). The lower energy side of the band represents the bound-bound (b-b) transition between the ground state and a first excited state, both of which are determined mainly by the potential well created by the OH groups. The higher energy side of the band in water represents bound-continuum (b-c) transitions. The greater width of the band in alcohol solvents, compared with that in water, is attributed to the alkyl group which may provide an extra, higher excited bound state. That is, in alcohols there may exist an additional b-b transition in between the b-b and b-c transitions just mentioned.

From Figure IV-15, one can see that, within the inherent error (see next paragraph), composition dependence of W_b/W_r is similar to the behavior of $W_{\frac{1}{2}}$ as a function of composition (Figure IV-11). Above 50 mole % water, W_b/W_r is nearly independent of composition for all alcohols. This is similar

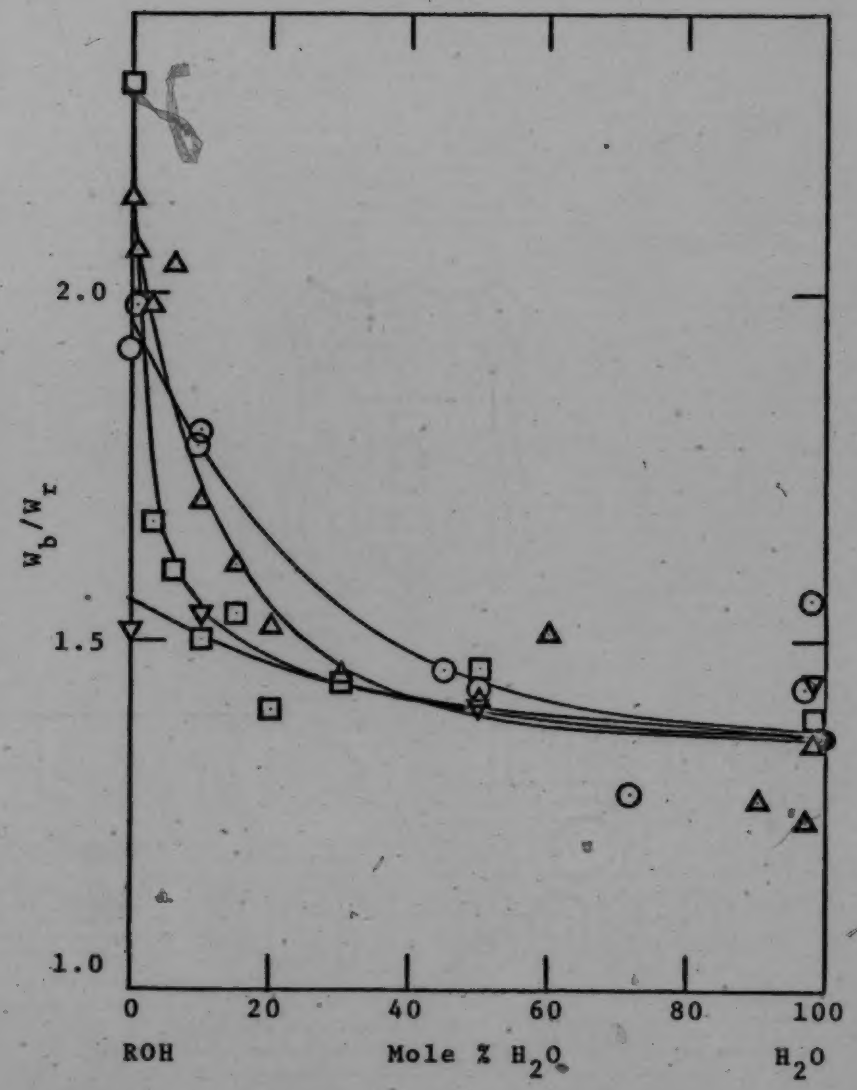

FIGURE IV-15. Composition Dependence of W_b/W_r for Alcohol/Water Mixtures at 298K.

●, Water; ○, Methanol; △, 1-Propanol; □, 2-Propanol; ▽, t-Butanol. Shapes for other primary and secondary alcohols are similar to that for △ and for □, respectively.

to the behavior of E_{Amax} (Figure IV-5 or -6) and of $W_{\frac{1}{2}}$ (Figure IV-11) as a function of composition in the same concentration region. This consistency again supports the suggestion that above 50 mole % water the electron rests preferentially in a trap that is a slightly modified water structure.

The ratio of W_b to W_r has been used to indicate the asymmetry factor of the absorption spectra for the solvated electron (52,85). The values of W_b/W_r obtained from the present study are listed in Tables III-1 to -8. As mentioned above, W_b and W_r are dependent on the value of E_{Amax} chosen for a fixed value of $W_{\frac{1}{2}}$. Given that the error in determining the value of E_{Amax} is ±1%, the error inherited in calculating the ratio of W_b to W_r will be ±10%. Therefore, this ratio is good for qualitatively indicating the asymmetry of a given absorption spectrum; however, it is useful for quantitative comparison of the asymmetry of absorption spectra only when the inherited error can be ignored (Figures IV-15 and -16).

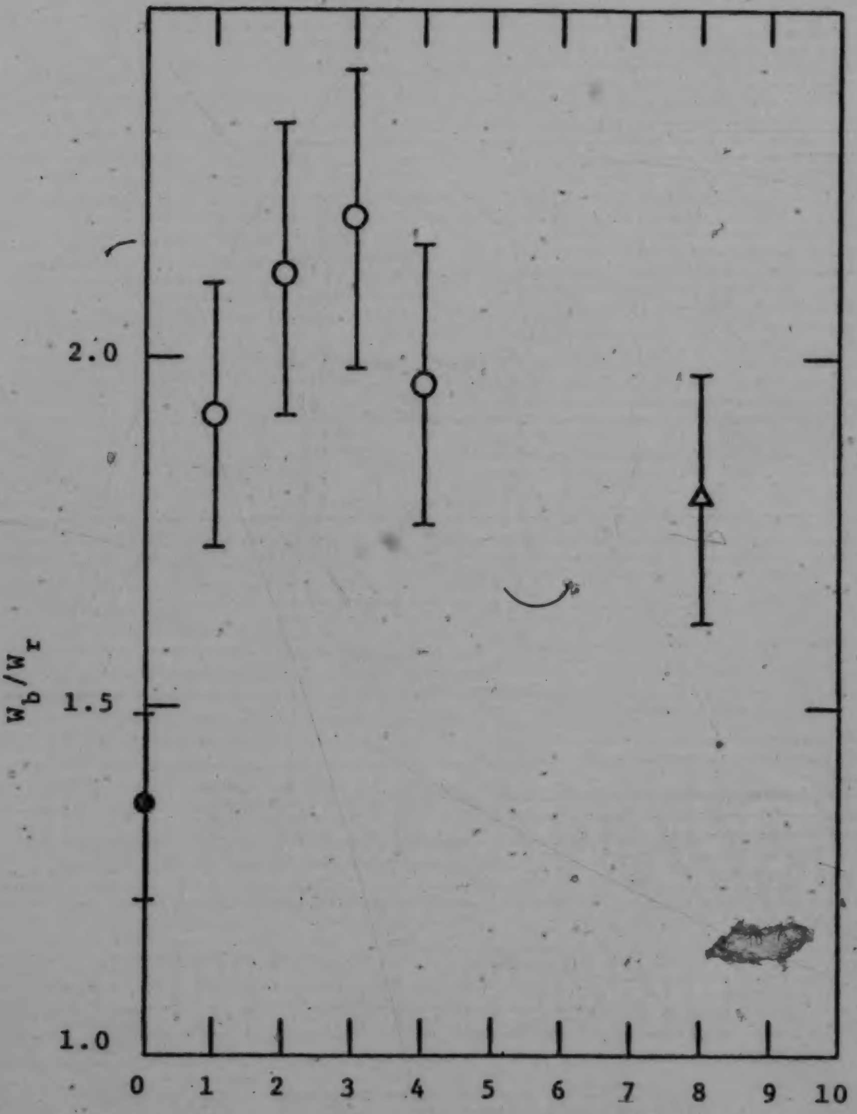

FIGURE IV-16. Plot of W_b/W_r vs the Number of Carbon Atoms in n-Alcohols at 298K.

●, Water; ○, n-Alcohols, this work.

△, ref. 85.

4. Composition Dependence of $G\varepsilon_{max}$

As shown in Figure III-2, $G\varepsilon_{max}$ changes relatively rapidly with composition in the vicinity of pure water and pure alcohol. The most attractive and challenging phenomenon is that of the $G\varepsilon_{max}$ having a maximum in the very high mole % water region. The increase of $G\varepsilon_{max}$ upon the addition of ~2 mole % of an alcohol to water coincides with the small increase of E_{Amax} (Figure III-1 or -19). This behavior suggests that the addition of a few mole % of alcohol to water enhances the orderliness of the water structure, which might increase the thermalization range of the excess electrons and thereby the free ion yield G (yield per 100 eV). There is physical evidence that the presence of a small amount of monohydric alcohol affects the structure of liquid water: ethanol can form a clathrate hydrate of $C_2H_5OH.17H_2O$ at 94 mole % water (290); there is a maximum for the velocity of sound and for the sound absorption coefficient around 96 to 90 mole % water in t-butanol/water (293); there is a minimum of solute partial molar volume in ethanol (Figure IV-17) and in t-butanol/water mixtures around 93 and 97 mole % water, respectively (294); the critical micelle concentration curve of sodium dodecyl sulfate at 25°C in t-butanol/water

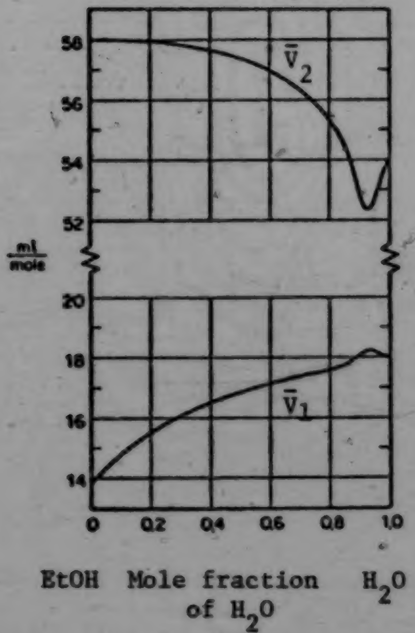

FIGURE IV-17. Partial Molar Volumes in Ethanol/Water Mixtures at 293K.

Data from ref. 294(b).

$\bar{V}_1$, Water; $\bar{V}_2$, Ethanol; EtOH represents Ethanol.

$\bar{V}$, indicates partial molar volume.

mixtures has a minimum at 96 mole % water (295); the composition dependence curve of sodium chloride concentration required for the flocculation of polystyrene emulsions in ethanol/water mixtures has a maximum at 95 mole % water (296); in the hydrolysis of t-butyl chloride in ethanol/water mixtures, it has been found that there exist maxima at 97 mole % water in the composition dependence curves for the enthalpy and entropy of activation (297); and there is a maximum for the structural contribution to the temperature of maximum density in aqueous solutions of ethanol and t-butanol around 98 to 96 mole % water (298).

Finally, by comparing Figure III-2 and Figure IV-8, it can be seen that the behavior of $G\varepsilon_{max}$ is similar to that of $d\eta/dC$ as a function of composition (284), especially in the vicinity of pure water, where both reach a very pronounced maximum, then decline sharply.

Thus, the peculiar behavior of $G\varepsilon_{max}$ could be due to changes in the solution structure. The importance of changes in solution structure indicates the need for a structural configuration similar to the one above for the 10 mole % water region, but with an alcohol molecule contained by a number of water molecules. How such configuration might affect G and ε_{max} are openings for future study.

C. Effect of Temperature

1. Temperature Dependence of Spectra Shape of Alcohol/Water Mixtures

From the A sections of the even numbered Figures III-22 to -86, one can see that the E_{Amax} for each spectrum decreases as temperature increases. But from the B sections in these figures, it appears that the shape of the solvated electron absorption spectrum changes very little with temperature, for a given composition. This is in contrast to the behavior of spectrum shape as a function of composition (Figures III-3, -5, -7, -9, -11, -13, -15, and -17). This contrast indicates that over the temperature range examined (up to the boiling point for each solution) the nature of the solvation site is sensitive to composition but insensitive to temperature changes for a given composition. Thus, the extent of selective solvation of the electrons in a solvent of particular composition is approximately invariant with temperature.

2. Temperature Dependence of E_{Amax}

The decrease of E_{Amax} with increasing temperature is consistent with models mentioned in Chapter 1, Section C. According to these models, the behavior of E_{Amax} as a function of temperature can be considered to be mainly due to the expansion of the solvation trap as the temperature increases. In other words, the depth of the trap becomes shallower with increasing temperature. Hence, the value of E_{Amax} decreases as the temperature increases.

Tables III-9 to -17 show that the temperature coefficient of E_{Amax} is smallest for pure water and greatest for pure t-butanol. This indicates that the trap solvating the excess electron is relatively less sensitive to temperature in water than in the pure alcohols. In the alcohols the sensitivity varies with structure in the order methanol < primary alcohols < secondary alcohols < t-butanol (Figure IV-18). This is related to differences in the thermal stability of the electron solvation structure in each solvent.

The composition dependence of the temperature coefficient for each category alcohol/water solutions is shown in Figure III-88. From this figure, one can see that: (a) from 0 to 10 mole % water region, the temperature coefficient increases drastically in methanol and primary alcohols, but decreases sharply in secondary alcohols and t-butanol. This indicates that the thermal stability of the solvation site in the solution is less for the former and more for the latter, compared with pure alcohols; (b) in 10 to 98 mole % water region, the corresponding thermal stability increases (temperature coefficient decreases) gradually with increasing

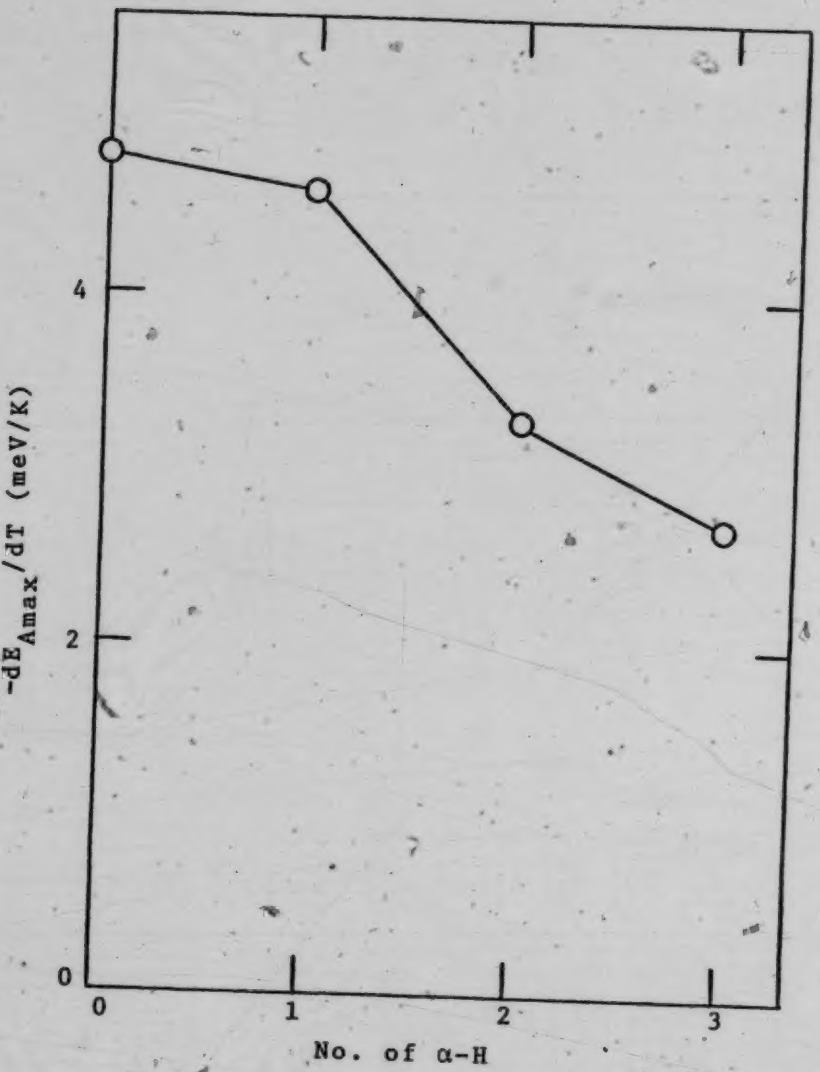

FIGURE IV-18. Plot of $-dE_{Amax}/dT$ vs the number of α-H in alcohols.

0, t-Butanol; 1, iso-Propanol; 2, n-Propanol; 3, Methanol.

water concentration; (c) between 98 and 100 mole % water, the stability again increases significantly. This last change is consistent with the phenomena mentioned in Section B-4, and supports the suggestion that the addition of a few mole % of alcohol to water affects the water structure.

3. Temperature Dependence of $W_{\frac{1}{2}}$

From the odd numbered Figures III-23 to -87 or Tables III-9 to -17, one can see that the value of $W_{\frac{1}{2}}$ changes only slightly with increasing temperature and that it can increase or decrease or remain nearly constant. This is in contrast to the much larger change of $W_{\frac{1}{2}}$ as a function of composition (Figures III-4, -6, -8, -10, -12, -18, and III-20, -21).

The behavior of $W_{\frac{1}{2}}$ as a function of temperature can be considered to be due to the overall results of (a) electron-phonon interaction (EPI) (2) and (b) electron-dipole interaction (EDI) (188). The former tends to increase $W_{\frac{1}{2}}$ as temperature increases, while the latter tends to decrease $W_{\frac{1}{2}}$. Limiting considerations to these two interactions, if the effect of (a) dominates (b) then the observed temperature coefficient of $W_{\frac{1}{2}}$, $dW_{\frac{1}{2}}/dT$, is positive. It is negative if the effect of (a) is dominated by (b). It can be nearly zero, if the effect of (a) is more or less the same as that of (b).

From Tables III-9 to -17, one can see that the $dW_{\frac{1}{2}}/dT$ is positive for methanol, primary alcohols and water, and is negative for secondary alcohols and t-butanol. This indicates that the $dW_{\frac{1}{2}}/dT$ is dominated by EDI in the latter and is dominated by EPI in the former.

The composition dependence of the $dW_{\frac{1}{2}}/dT$ for each category of alcohol/water mixture is shown in Figure III-89. From this figure, the following four phenomena can be observed.

(i) The values of $dW_{\frac{1}{2}}/dT$ in the pure alcohols are widely scattered, but with the exception of methanol, addition of 10 mole % water brings them close together. From 0 to 10 mole % water, the $dW_{\frac{1}{2}}/dT$ decreases drastically in primary alcohol, but increases sharply in t-butanol. In addition, it decreases slightly in methanol, but increases gradually in secondary alcohols. This indicates that in primary alcohol/water solutions, the dominant contribution to the $dW_{\frac{1}{2}}/dT$ has shifted from EPI to EDI. In secondary alcohols and t-butanol/water mixtures, the relative strength of contribution has shifted from EDI toward EPI, compared with pure alcohols, although the value of $dW_{\frac{1}{2}}/dT$ is still negative. The behavior of $dW_{\frac{1}{2}}/dT$ in methanol/water differs from primary alcohol/water solutions. All these observed trends for the $dW_{\frac{1}{2}}/dT$ are similar to that for

E_{Amax} (Figure III-19), and supports the suggestion that when a small amount of water is added to alcohols, there are at least two different interferences affecting the solution structure. Just as E_{Amax} reaches a minimum (Figure III-19) around 10 mole % water, so does $dW_{\frac{1}{2}}/dT$ reach a minimum (Figure III-89) in this region. This observation also suggests the occurrence of a solution structure such as that proposed earlier to account for the peculiar behavior of E_{Amax} for primary alcohol.

(ii) In the 10 to 50 mole % water region, for all the alcohols except methanol, $dW_{\frac{1}{2}}/dT$ becomes progressively less negative. This indicates an increasing contribution from EPI. In methanol/water mixtures, it seems nearly independent of composition. This behavior of $dW_{\frac{1}{2}}/dT$ is again similar to the behavior of E_{Amax} in the same region.

(iii) From 50 to 98 mole % water, within the precision of measurement, the behavior of $dW_{\frac{1}{2}}/dT$ can be considered as composition independent. This trend is similar to that mentioned above for both E_{Amax} (Figure III-19) and $W_{\frac{1}{2}}$ (Figure III-20). This observation supports the suggestion that in this region, the excess electron rests preferentially in a trap that is a slightly modified water structure.

(iv) Between 98 and 100 mole % water, the $dW_{\frac{1}{2}}/dT$ again increases significantly, except for methanol. This change is consistent with the behavior discussed in previous sections for dE_{Amax}/dT, $G\varepsilon_{max}$ and E_{Amax}, and again supports the suggestion that adding a small amount of alcohol to water affects the water structure.

In order to check the correlations of $dW_{\frac{1}{2}}/dT$ with dE_{Amax}/dT and E_{Amax}, the ratios $(dW_{\frac{1}{2}}/dT)/(dE_{Amax}/dT)$ and $(dW_{\frac{1}{2}}/dT)/E_{Amax}$ have been plotted against mole % water for methanol, 1-propanol, 2-propanol and t-butanol/water mixtures (Figures IV-19, -20). The trends obtained from these two plots are similar to Figure III-89.

By comparing Figure III-88 and -89, except for methanol/water mixtures, the following correlation can be obtained: with increasing mole % water, the behavior of the temperature coefficient of E_{Amax} is opposite to that of the temperature coefficient of $W_{\frac{1}{2}}$. This indicates that when the solvation trap is thermally more stable in a given alcohol/water mixture than in the pure alcohol solvent, then $dW_{\frac{1}{2}}/dT$ is mainly governed by EPI. On the other hand, if the trap is thermally less stable in the solution than in the pure solvent, then $dW_{\frac{1}{2}}/dT$ is mainly determined by EDI. The latter case is observed only for primary alcohol in the 0 to 10 mole % water region. The former case is observed for primary alcohols in the remaining mole % water regions and for secondary alcohols and t-butanol in all regions.

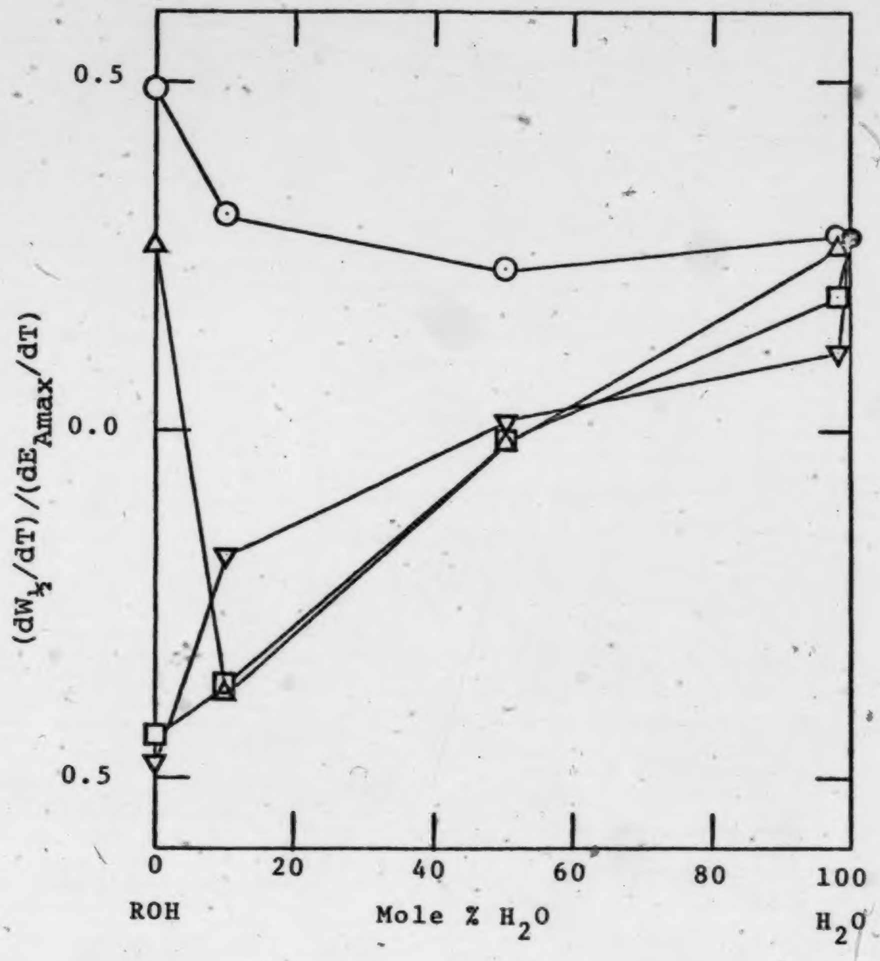

FIGURE IV-19. Composition Dependence of $(dW_{1/2}/dT)/(dE_{Amax}/dT)$ for Alcohol/Water Mixtures.

●, Water; ○, Methanol; △, 1-Propanol; □, 2-Propanol; ▽, t-Butanol. Trends for other primary and secondary alcohols are similar to that for △ and for □, respectively.

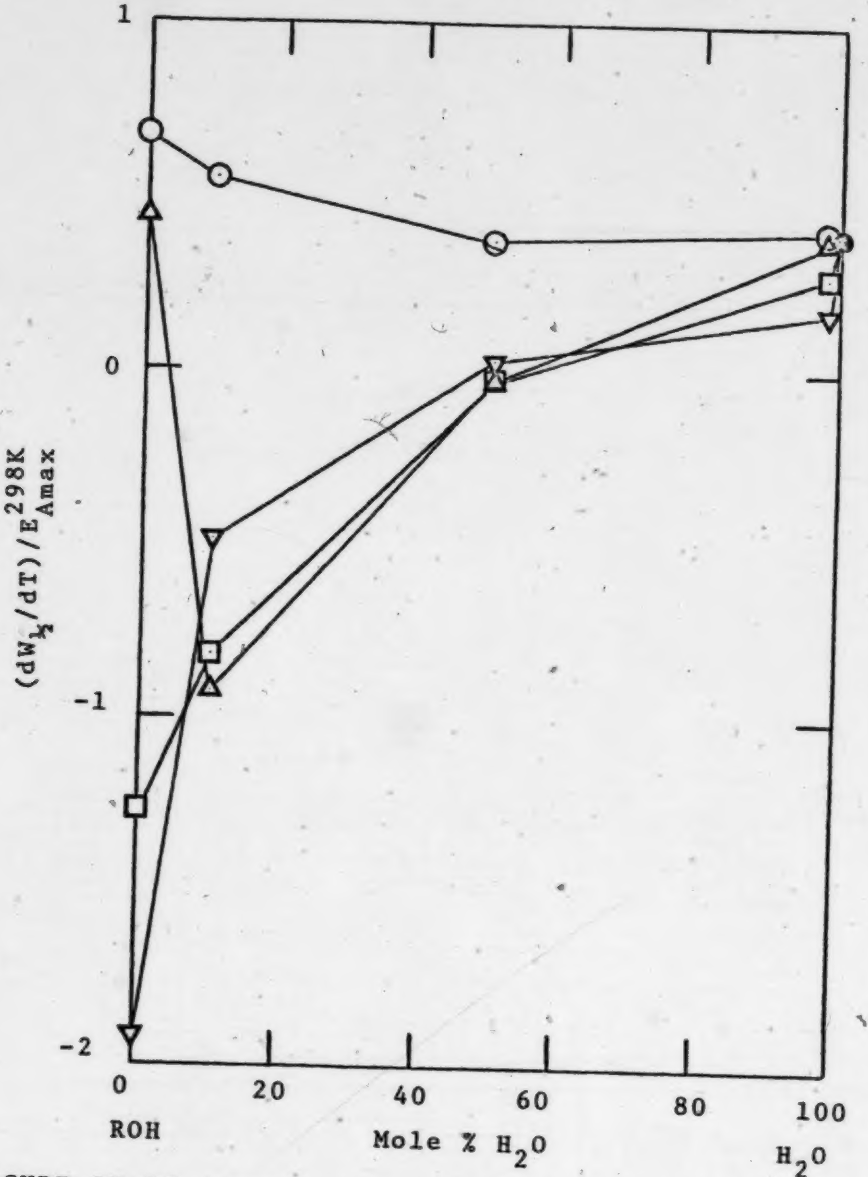

FIGURE IV-20. Composition Dependence of $(dW_{1/2}/dT)/E^{298}_{Amax}$ for Alcohol/Water Mixtures.

●, Water; ○, Methanol; △, 1-Propanol; □, 2-Propanol; ▽, t-Butanol. Trends for other primary and secondary alcohols are similar to that for △ and for □, respectively.

The values of the ratio $W_{\frac{1}{2}}/E_{Amax}$ for water, methanol, 1-propanol, 2-propanol, and t-butanol, and also for 10 and 50 mole % water in these alcohols, are listed in Table IV-2, and plotted against temperature in Figures IV-21 to -24. The relationship between $W_{\frac{1}{2}}/E_{Amax}$ and temperature is approximately linear. All these plots have a positive slope, indicating that $W_{\frac{1}{2}}$ decreases less rapidly with increasing temperature than does E_{Amax}.

The value of $W_{\frac{1}{2}}/E_{Amax}$ is higher for pure alcohols than for pure water (Table IV-2 or Figures IV-21 to -24). Upon adding 10 mole % water into alcohols, the value of $W_{\frac{1}{2}}/E_{Amax}$ decreases towards the value of pure water by more than the 10 % change expected for ideal mixing. At 298K, the % decreases are respectively 26, 38, 65, and 43 for 10 mole % water in methanol, 1-propanol, 2-propanol, and t-butanol. All these decreases indicate selective solvation by water. When 50 mole % water is added, the value of $W_{\frac{1}{2}}/E_{Amax}$ decreases by much more than the 50%. At 298K, the % decreases are respectively 99, 91, 96 and 90 in methanol, 1-propanol, 2-propanol, and t-butanol. These decreases again indicate selective solvation by water and also show that, above 50 mole % water, the excess electron rests preferentially in a trap that is a slightly modified water structure. Figures IV-21 to -24 show that at temperatures higher than 298K, the corresponding % decrease in $W_{\frac{1}{2}}/E_{Amax}$

TABLE IV-2

The Temperature Coefficient of $W_{\frac{1}{2}}/E_{Amax}$ in Alcohol/Water Mixtures.

							10^3(dR/dT)
$\langle 0 \mid M \mid T_i \rangle$	180	200	250	298	350		
R	0.55	0.56	0.63	0.72	0.81		1.8
$\langle 10 \mid M \mid T_i \rangle$	180	200	250	298	350		
R	0.49	0.50	0.59	0.66	0.74		1.5
$\langle 50 \mid M \mid T_i \rangle$		200	250	298	350		
R		0.40	0.43	0.49	0.56		1.2
$\langle 0 \mid 1P \mid T_i \rangle$	150	200	250	298	350	369	
R	0.63	0.68	0.75	0.83	0.95	0.99	2.5
$\langle 10 \mid 1P \mid T_i \rangle$		200	250	298	350		
R		0.62	0.67	0.70	0.76		0.9
$\langle 50 \mid 1P \mid T_i \rangle$			260	298	350	360	
R			0.48	0.52	0.56	0.57	0.8
$\langle 0 \mid 2P \mid T_i \rangle$		200	250	298	350		
R		0.75	0.81	0.95	1.09		2.7
$\langle 10 \mid 2P \mid T_i \rangle$		200	250	298	350		
R		0.61	0.63	0.65	0.68		0.5
$\langle 50 \mid 2P \mid T_i \rangle$			250	298	339	352	
R			0.46	0.52	0.54	0.57	1.1
$\langle 0 \mid tB \mid T_i \rangle$				298	325	350	
R				0.78	0.88	0.83	2.5
$\langle 10 \mid tB \mid T_i \rangle$				298	325	350	
R				0.65	0.70	0.73	1.5

(continued)

Table IV-2 (continued)

$\langle 50\|tB\|T_i\rangle$	273	298	350	368	
R	0.47	0.52	0.56	0.69	1.3
$\langle 100\|W\|T_i\rangle$	273	298	350	373	
R	0.47	0.49	0.55	0.57	1.0

$R \equiv W_{\frac{1}{2}}/E_{Amax}$

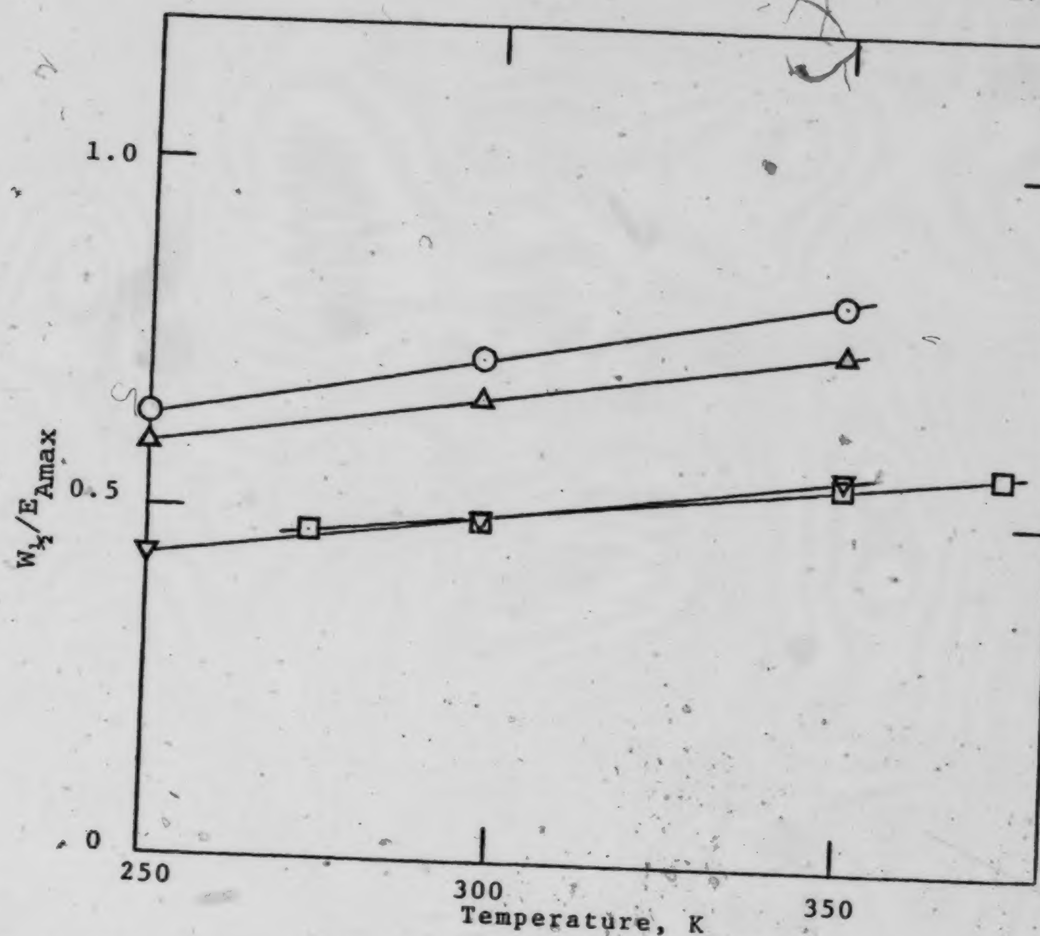

FIGURE IV-21. Temperature Dependence of $W_{\frac{1}{2}}/E_{Amax}$ for Methanol/Water Mixtures.

○, Pure methanol; △, 10 mole % water; ▽, 50 mole % water; □, Pure water.

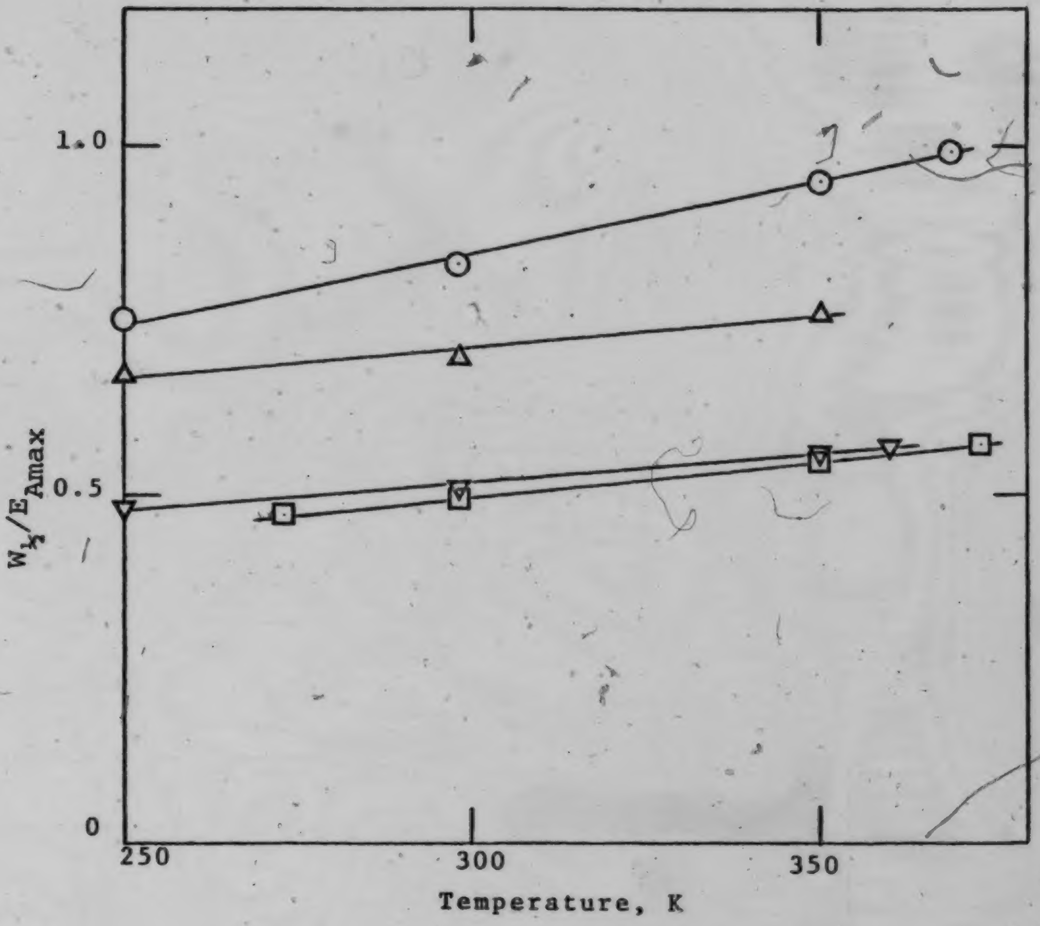

FIGURE IV-22. Temperature Dependence of $W_{\frac{1}{2}}/E_{Amax}$ for 1-Propanol/Water Mixtures.

○, Pure 1-propanol; △,10 mole % water; ▽, 50 mole % water; □, Pure water.

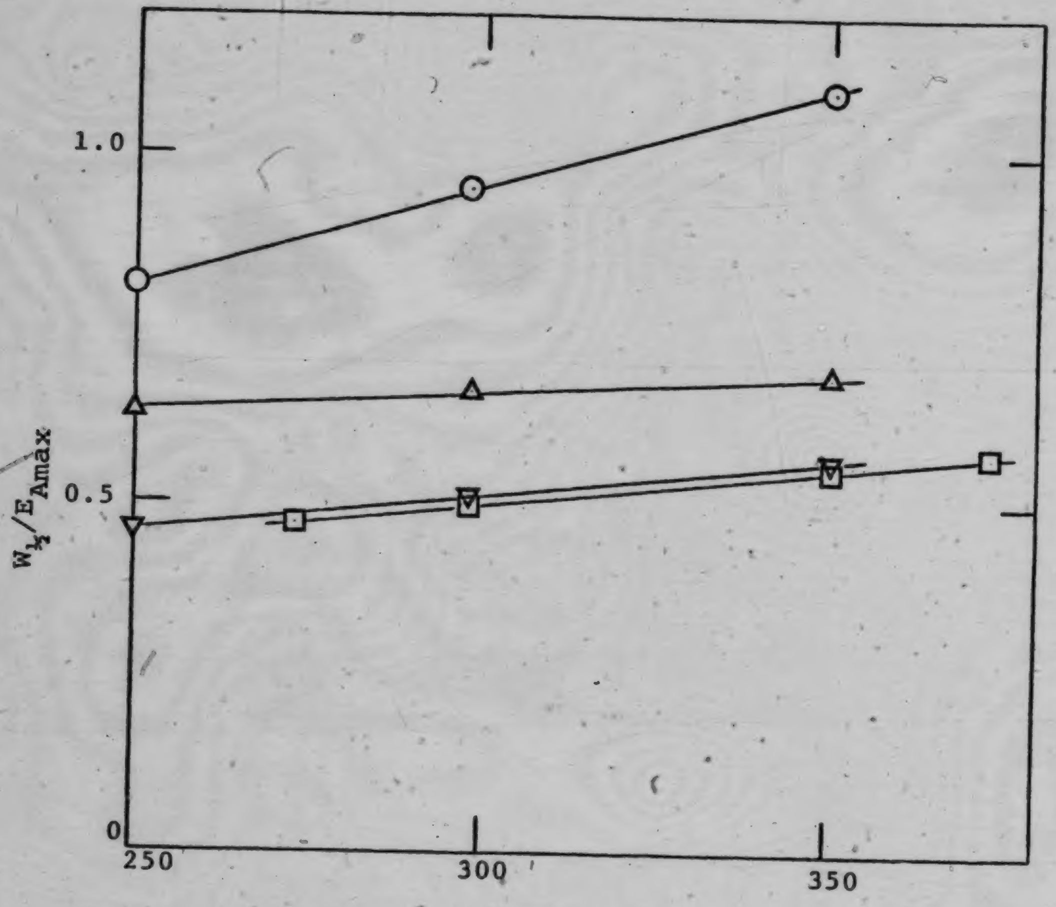

FIGURE IV-23. Temperature Dependence of $W_{½}/E_{Amax}$ for 2-Propanol/Water Mixtures.

○, Pure 2-propanol; △, 10 mole % water; ▽, 50 mole % water; □, Pure water.

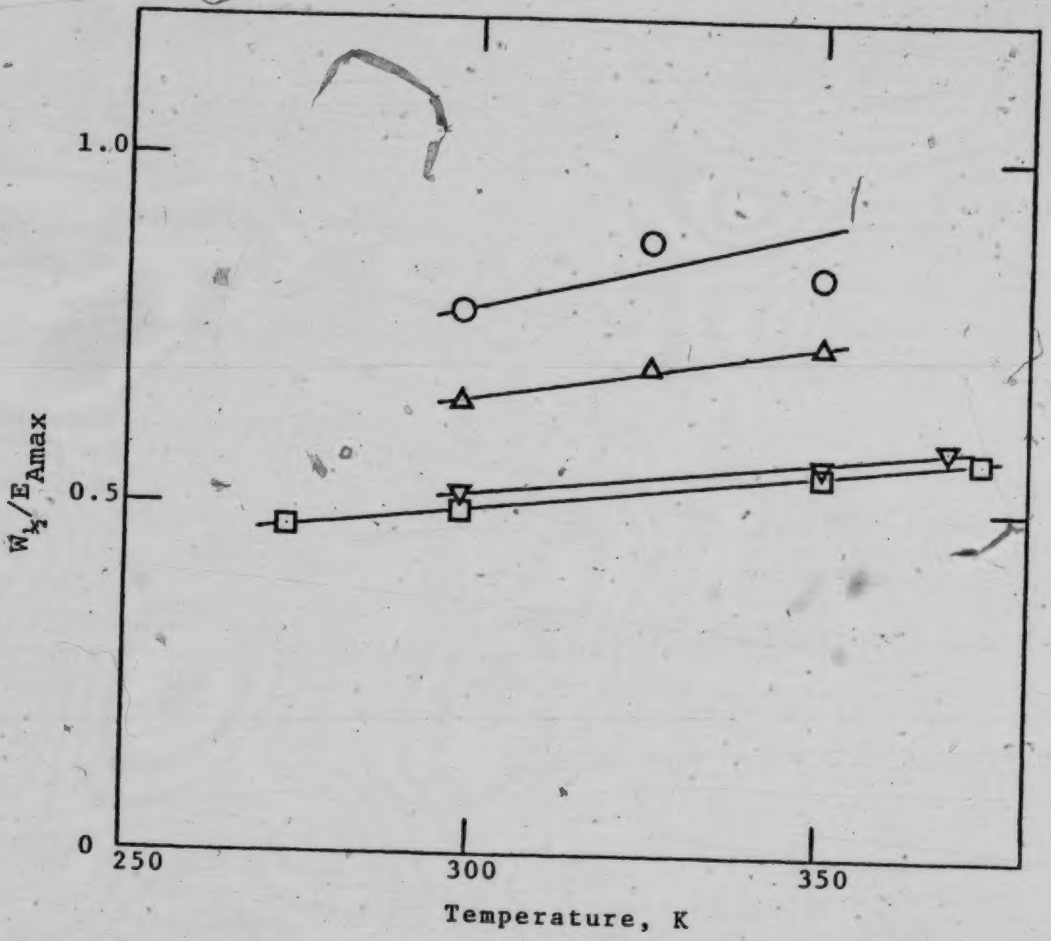

FIGURE IV-24. Temperature Dependence of $W_{\frac{1}{2}}/E_{Amax}$ for t-Butanol/Water Mixtures.

○, Pure t-butanol; △, 10 mole % water; ▽, 50 mole % water; □, Pure water.

is larger than those just mentioned for 10 mole % water mixtures. It appears that increasing the temperature favors selective solvation by water.

D. Summary

A number of observations can be made about the optical absorption spectra for solvated electrons in alcohol/water mixtures.

1. Pure Solvents

The values of E_{Amax} for alcohols and water are found as follows: methanol ≈ primary alcohols (except ethanol) > water > secondary alcohols > t-butanol. This is due to the difference in each liquid's structure. The values of $W_{\frac{1}{2}}$ are as follows: primary alcohols > methanol > secondary alcohols > t-butanol ≃ water. This is accounted for by the environment of the α-carbon in the alkyl group which provides an extra, higher excited state.

2. Alcohol/Water Mixtures

(a) Effect of Composition

In the vicinity of pure alcohols, when a small amount of water is added the E_{Amax} for the solution has two trends, depending upon the nature of the alcohol. The value of E_{Amax} decreases as mole % water increases in methanol and primary alcohols, and it increases for secondary alcohols and t-butanol. The plots are concave upward for the former and concave downward for the latter. In contrast, the values of $W_{\frac{1}{2}}$ decrease with increasing mole % water, all curves being concave upward. All these indicate the selective solvation of the excess electrons by water.

In the very high mole % water region, the values of E_{Amax} increase significantly for all alcohol/water mixtures, but the values of $W_{\frac{1}{2}}$ are independent of composition. This indicates that when a small amount of alcohol is added, the liquid structure of water is altered to make the depth of solvation trap slightly deeper. The observed eccentric behavior of $G\varepsilon_{max}$ in this region, that is, $G\varepsilon_{max}$ increases sharply as mole % alcohol increases and then decreases, also indicates that the liquid structure of water is changed.

Around 10 mole % water in primary alcohols, E_{Amax} has been found to reach a minimum that is close to or slightly less than the value for pure water. This premature minimum shows the existence of a solution structure that is peculiar to this mole % region. Between 10 and 50 mole % water, E_{Amax} gradually increases to a plateau value which is slightly higher than that for pure water.

From 50 to about 97 mole % water, both E_{Amax} and $W_{\frac{1}{2}}$ are nearly composition independent. This indicates that the excess electron rests preferentially in a trap composed of a slightly modified water structure.

(b) Effect of Temperature

In contrast to the spectrum behavior as a function of composition, the shape of the solvated electron absorption spectrum changes little with temperature. The value of E_{Amax} decreases as temperature increases for electrons in all the solutions and pure compounds. This is mainly due to the trap becoming more shallow with increasing temperature. The temperature coefficient, $-dE_{Amax}/dT$, of water is less than for pure alcohols, indicating the trap to solvate the excess electron is relatively less sensitive to temperature in water than in the pure alcohols.

The value of $W_{\frac{1}{2}}$ changes only slightly with increasing temperature. In some solutions it increases, in others it decreases or remains nearly constant. This may be accounted for by the competition between the effects of the electron-phonon interaction and the electron-dipole interaction.

Temperature dependence of $W_{\frac{1}{2}}/E_{Amax}$ is approximately linear with positive slope for all solutions, including pure compounds. The value of $W_{\frac{1}{2}}/E_{Amax}$ is higher for alcohols than for water. In 10 mole % water solutions, it decreases towards the value of water by more than the 10% change expected for ideal mixing.

This indicates the selective solvation by water. In 50 mole % water solution, the % decrease towards the pure water value is more than 90%, indicating that the excess electron rests preferentially in a trap that is a slightly modified water structure. The % decrease in $W_{1/2}/E_{Amax}$ is larger with increasing temperature, for a given solution. This shows that increasing the temperature favors selective solvation by water.

(c) Composition Dependence of Temperature Coefficient.

In the 0 to 10 mole % water region, $-dE_{Amax}/dT$ increases drastically in methanol and primary alcohols, but decreases sharply in secondary alcohols and t-butanol. An increasing temperature coefficient indicates a decreasing thermal stability of the solvation structure, and vice versa. In the 10 to 98 mole % water region, $-dE_{Amax}/dT$ decreases gradually with increasing water concentration. Between 98 and 100 mole % water, $-dE_{Amax}/dT$ again decreases significantly. The last change indicates that the addition of a small amount of alcohol to water affects the water structure.

The behaviors of $-dE_{Amax}/dT$ and $dW_{1/2}/dT$ as a function of composition are similar to that of E_{Amax} itself. The behavior of $W_{1/2}$ itself with composition is quite different from these.

REFERENCES

1. J. Jortner, S. A. Rice and E. G. Wilson, in "Metal-Ammonia Solutions", G. Lepoutre and M. J. Sienko (Eds.), W. A. Benjamin, Inc., New York, 1964, p.222.
2. D. A. Copeland, N. R. Kestner and J. Jortner, J. Chem. Phys., 53, 1189 (1970).
3. G. R. Freeman, J. Chem. Phys., 46, 2822 (1967).
4. W. Kauzmann, "Quantum Chemistry", Academic Press Inc., New York, 1957, p.188.
5. W. Weyl, Ann. Phys., 121, 601 (1864).
6. C. A. Kraus, "The Properties of Electrically Conducting Systems", Chemical Catalogue Co., New York, 1922, p.375.
7. R. A. Ogg, Phys. Rev., 69, 668 (1946).
8. G. W. A. Fowles, W. R. McGregor and M. C. R. Symons, J. Chem. Soc., 3329 (1957).
9. J. L. Down, J. Lewis, B. Moore and G. Wilkinson, J. Chem. Soc., 3767 (1959).
10. J. E. Bennett, B. Mile and A. Thomas, J. Chem. Soc., (A), 1393 (1967).
11. W. L. Jolly, C. J. Hallada and M. Gold, in "Metal Ammonia Solutions", W. A. Benjamin, Inc., New York, 1964 p.174.
12. L. M. Dorfman, F. Y. Jou and R. Wagerman, Ber. Bunsenges. Phys. Chem., 75, 681 (1971).

13. E. J. Hart and J. W. Boag, J. Am. Chem. Soc., 84, 4090 (1962).

14. M. C. Sauer, Jr., S. Arai and L. M. Dorfman, J. Chem. Phys., 42, 708 (1965).

15. J. H. Baxendale, E. M. Fielden and J. P. Keene, Science, 148, 637 (1965).

16. G. R. Freeman, Actions Chimiques et Biologiques des Radiations, 14, 73 (1970).

17. F. Y. Jou and L. M. Dorfman, J. Chem. Phys., 58, 4715 (1973).

18. J. Jortner and R. M. Noyes, J. Phys. Chem., 70, 770 (1966).

19. U. Schindewolf, Angew. Chem. Int. Ed., 7, 190 (1968).

20. J. H. Baxendale, Rad. Res. Suppl., 4, 139 (1964).

21. C. A. Kraus, J. Chem. Edcn., 30, 83 (1953).

22. C. A. Kraus and W. W. Lucasse, J. Am. Chem. Soc., 45, 2551 (1923).

23. K. Schmidt and M. Anbar, J. Phys. Chem., 73, 2846 (1969).

24. D. S. Berns, Adv. Chem. Ser., 50, 82 (1965).

25. W. J. Moore, "Physical Chemistry", 3rd Edn., Prentice Hall, Englewood Cliffs, N.J. 1962, p.337.

26. C. A. Kraus and W. C. Bray, J. Am. Chem. Soc., 35, 1315 (1913).

27. P. H. Tewari and G. R. Freeman, J. Chem. Phys, 51, 1276 (1969).

28. W. F. Schmidt and A. O. Allen, J. Chem. Phys., 52, 4788 (1970).

29. R. M. Minday, D. L. Schmidt and H. T. Davis, J. Phys. Chem., 76, 442 (1972).

30. J.-P. Dodelet and G. R. Freeman, Can. J. Chem., 50, 2267 (1972).

31. J.-P. Dodelet, K. Shinsaka and G. R. Freeman, J. Chem. Phys., 59, 1293 (1973).

32. C. A. Hutchinson and R. C. Pastor, J. Chem. Phys., 21, 1959 (1953).

33. Y. Claeys, C. F. Baes and W. K. Wilmarth, J. Chem. Phys., 16, 425 (1948).

34. E. J. Hart, S. Gordon and E. M. Fielden, J. Phys. Chem., 70, 150 (1966).

35. J. E. Bennett, B. Mile and A. Thomas, J. Chem. Soc., A, 1399 (1967).

36. J. H. Baxendale, Nature, 201, 468 (1964).

37. J. K. Thomas, S. Gordon and E. J. Hart, J. Phys. Chem., 68, 1524 (1964).

38. E. J. Hart, J. K. Thomas and S. Gordon, Rad. Res. Suppl., 4, 74 (1964).

39. S. Gordon, E. J. Hart, M. S. Matheson, J. Rabani and J. K. Thomas, Faraday Soc., Disc., 36, 193 (1963).

40. S. Gordon, E. J. Hart, M. S. Matheson, J. Rabani and J. K. Thomas, J. Am. Chem. Soc., 85, 1375 (1963).

41. K. D. Asmus and A. Henglein, Ber. Bunsenges. Phys. Chem., 68, 348 (1964).

42. M. Anbar and E. J. Hart, J. Phys. Chem., 69, 973 (1965).

43. E. J. Hart, S. Gordon and J. K. Thomas, J. Phys. Chem., 68, 1271 (1964).

44. M. Anbar and E. J. Hart, J. Phys. Chem., 69, 271 (1965).

45. I. A. Taub, M. C. Sauer, Jr., and L. M. Dorfman, Faraday Soc. Disc., 36, 206 (1963).

46. S. Arai and L. M. Dorfman, J. Chem. Phys., 41, 2190 (1964).

47. G. R. Freeman, J. Phys. Chem., 77, 7 (1973).

48. C. A. Kraus, (a) J. Am. Chem. Soc., 30, 1323 (1908); (b) J. Am. Chem. Soc., 43, 749 (1921).

49. G. Stein, Disc. Faraday Soc., 12, 227 (1952).

50. R. L. Platzman, in "Physical and Chemical Aspects of Basic Mechanisms in Radiobiology", U. S. Natl. Res. Council Publ., 305, 34 (1953).

51. J. W. Boag and E. J. Hart, Nature, 197, 45 (1963).

52. F. Y. Jou and G. R. Freeman, J. Phys. Chem., 83, 2382, (1979).

53. B. D. Michael, E. J. Hart and K. H. Schmidt, J. Phys. Chem., 75, 2798 (1971).

54. E. J. Hart and M. Anbar, in "The Hydrated Electron", Wiley Interscience, John Wiley & Sons, New York, 1970, p.44.

55. E. J. Hart and M. Anbar, in "The Hydrated Electron", Wiley Interscience, John Wiley & Sons, New York, 1970, p.40.

56. W. C. Gottschall and E. J. Hart, J. Phys. Chem., 71, 2102 (1967).

57. U. Schindewolf and R. Olinger, Ber. Bunsenges. Phys. Chem., 72, 1066 (1968).

58. D. M. Brown, F. S. Dainton, J. P. Keene and D. C. Walker, Proc. Chem. Soc., 266 (1964).

59. J. Belloni, F. Billiau and E. Saito, Nouveau J. de Chimie, 3, 157 (1979).

60. Farhataziz, J. Phys. Chem., 81, 827 (1977).

61. R. Covetto, S. Hahne and U. Schindewolf, Z. Phys. Chem. (N.F.), 102, 283 (1976).

62. Farhataziz and L. M. Perkey, J. Phys. Chem., 79, 1651 (1975).

63. G. I. Khaikin and V. A. Zhigunov, High Engy. Chem., 9, 183 (1975).

64. W. A. Seddon, J. W. Fletcher, F. C. Sopchyshyn and J. J. Jevcak, Can. J. Chem., 52, 3269 (1974).

65. J. Belloni, P. Cordier and J. Delaire, Chem. Phys. Lett., 27, 241 (1974).

66. Farhataziz, L. M. Perkey and R. R. Hentz, J. Chem. Phys., 60, 4383 (1974).

67. G. Rubinstein, T. R. Tuttle, Jr. and S. Golden, J. Phys. Chem., 77, 2872 (1973).

68. W. A. Seddon, J. W. Fletcher, J. Jevcak and F. C. Sopchyshyn, Can. J. Chem., 51, 3653 (1973).

69. M. T. Lok, F. J. Tehan and J. L. Dye, J. Phys. Chem., 76, 2975 (1972).

70. G. I. Khaikin, V. A. Zhigunov and P. I. Dolin, High Engy. Chem., 5, 44 (1971).

71. R. Catterall, Nature, Phys. Science, 229, 10 (1971).

72. J. L. Dye, M. G. DeBacker and L. M. Dorfman, J. Chem. Phys., 52, 6251 (1970).

73. W. H. Koehler and J. J. Lagowski, J. Phys. Chem., 73, 2329 (1969).

74. R. K. Quinn and J. J. Lagowski, J. Phys. Chem., 73, 2326 (1969).

75. R. K. Quinn and J. J. Lagowski, J. Phys. Chem., 72, 1374 (1968).

76. C. Hallada and W. L. Jolly, Inorg. Chem., 2, 1076 (1963).

77. M. Gold and W. L. Jolly, Inorg. Chem., 1, 818 (1962).

78. R. C. Douthit and J. L. Dyen, J. Am. Chem. Soc., 82, 4472 (1960).

79. F.Y. Jou and G. R. Freeman, J. Phys. Chem., in press, (1979).

80. J. Corset and G. Lepoutre, in Proc. Colloque Weyl I: Metal Ammonia Solution, G. Lepoutre and M. J. Sienko (Eds.), W. A. Benjamin, Inc., New York, 1964, p.187.

81. I. Hurley, T. R. Tuttle, Jr. and S. Golden, in Proc. Colloque Weyl II: Metal Ammonia Solutions, J. J. Lagowski and M. J. Sienko (Eds.), Butterworths, London, 1970, p.508.

82. V. N. Shubin, V. A. Zhigunov, G. I. Khaihin, L. P. Beruchashvili and P. I. Dolin, Adv. Chem. Ser., 81, 95 (1968).

83. D. F. Burow and J. J. Lagowski, Adv. Chem. Ser., 50, 125 (1965).

84. F. Y. Jou and G. R. Freeman, J. Phys. Chem., 83, 261 (1979).

85. F. Y. Jou and G. R. Freeman, Can. J. Chem., 57, 591 (1979).

86. F. Y. Jou and G. R. Freeman, J. Phys. Chem. 81, 909 (1977).

87. T. A. Chubakova and N.A. Bakh, High Engy. Chem., 12, 315 (1977).

88. A. K. Kostin, V. V. Golovanov, V. I. Zolotarevskii,

and A. V. Vannikov, High Engy. Chem., 11, 209 (1977).

89. G. G. Teather and N. V. Klassen, Int. J. Rad. Phys. Chem., 7, 475 (1975).

90. R. S. Dixon, V. J. Lopata and C. R. Roy, Int. J. Rad. Phys. Chem., 8, 707 (1976).

91. R. R. Hentz and G. A. Kenney-Wallace, J. Phys. Chem., 78, 514 (1974).

92. L. M. Perkey, Farhataziz and R. R. Hentz, Chem. Phys. Lett., 27, 531 (1974).

93. L. I. Grossweiner, E. F. Zwicker and G. W. Swenson, Science, 141, 1180 (1963).

94. A. Namiki, M. Noda and T. Higashimura, Chem. Phys. Lett., 23, 402 (1973).

95. K. N. Jha, G. L. Bolton and G. R. Freeman, J. Phys. Chem., 76, 3876 (1972).

96. H. Hase, T. Warashina, M. Noda, A. Namiski and T. Higashimura, J. Chem. Phys., 57, 1039 (1972).

97. R. R. Hentz and G. Kenney-Wallace, J. Phys. Chem., 76, 2931 (1972).

98. T. Shida, S. Iwata and T. Watanabe, J. Phys. Chem., 76, 3683 (1972).

99. T. Shida, S. Iwata and T. Watanabe, J. Phys. Chem., 76, 3691 (1972).

100. J. H. Baxendale and P. Wardman, Nature, 230, 449 (1971).

101. A. Bernas and D. Grand, Chem. Comm., 1667 (1970).

102. H. Habersbergerová, Lj. Josimović and J. Teplý Trans. Faraday Soc., 66, 669 (1970).

103. H. Habersbergerová, Lj. Josimović and J. Teplý, Trans. Faraday Soc., 66, 656 (1970).

104. A. Ekstrom, Rad. Res. Rev., 2, 381 (1970).

105. S. Arai and M. C. Sauer, Jr., J. Chem. Phys., 44, 2297 (1966).

106. I. A. Taub, D. A. Harter, M. C. Sauer, Jr. and L. M. Dorfman, J. Chem. Phys., 41, 979 (1964).

107. L. Kevan, Adv. Rad. Chem., 4, 181 (1974).

108. L. M. Dorfman, Adv. Chem. Ser., 50, 36 (1965).

109. G. M. Zimia and N. A. Bakh, High Engy. Chem., 12, 25 (1977).

110. M. Ogasawara, K. Shimizu, K. Yoshida, J. Kroh and H. Yoshida, Chem. Phys. Lett., 64, 43 (1979).

111. J. F. Gavlas, F. Y. Fou and L. M. Dorfman, J. Phys. Chem., 78, 2631 (1974).

112. L. M. Dorfman and F. Y. Jou, in "Electrons in Fluids", J. Jornter and N. R. Kestner (Eds.), Springer-Verlag, Berlin, 1973, p.447.

113. D. Huppert, Ph. Avourls and P. M. Rentzepis, J. Phys. Chem., 82, 2282 (1978).

114. T. Ito, K. Fueki, A. Namiki and H. Hase, J. Phys. Chem., 77, 1803 (1973).

115. M. Anbar and E. J. Hart, J. Phys. Chem., 69, 1244 (1965).

116. J. Delaire, P. Cordier, J. Belloni, F. Billiau and M. O. Delcourt, J. Phys. Chem., 80, 1687 (1976).

117. J. W. Fletcher, W. A. Seddon and F. C. Sopchyshyn, Can. J. Chem., 51, 2975 (1973).

118. W. A. Seddon, J. W. Fletcher and F. C. Sopchyshyn, Can. J. Chem., 54, 2807 (1976).

119. R. Cooper and J. K. Thomas, J. Chem. Phys., 48, 5103 (1968).

120. J. H. Baxendale and M. A. J. Rodgers, J. Phys. Chem., 72, 3849 (1968).

121. F. S. Dainton, J. P. Keene, T. J. Kemp, G. A. Salmon and J. Teplý, Proc. Chem. Soc., 265 (1964).

122. A. Ekstrom and J. E. Willard, J. Phys. Chem., 72, 4599 (1968).

123. G. A. Salmon and W. A. Seddon, Chem. Phys. Lett., 24, 366 (1974).

124. T. Huang, I. Eisele, D. P. Lin and L. Kevan, J. Chem. Phys., 56, 4702 (1972).

125. F. Y. Jou and G. R. Freeman, Can. J. Chem., 54, 3696 (1976).

126. W. A. Seddon, J. W. Fletcher, F. C. Sopchyshyn and R. Catterall, Can. J. Chem., 55, 3356 (1977).

127. J.-P. Dodelet, F. Y. Jou and G. R. Freeman, J. Phys. Chem., 79, 2876 (1975).

128. H. Y. Wang and J. E. Willard, J. Chem. Phys., 69, 2964 (1978).

129. M. Nishida, J. Chem. Phys., 66, 2760 (1977).

130. N. Kato, T. Kimura and K. Fueki, J. Chem. Phys., 65, 5020 (1976).

131. S. L. Hager and J. E. Willard, J. Chem. Phys., 61, 3244 (1974).

132. J. H. Baxendale, C. Bell and P. Wardman, J.C.S., Faraday Trans. I, 69, 776 (1973).

133. T. Huang and L. Kevan, J. Am. Chem. Soc., 95, 3122 (1973).

134. H. Hase, T. Higashimura and M. Ogasawara, Chem. Phys. Lett., 16, 214 (1972).

135. J. H. Baxendale, C. Bell and P. Wardman, Chem. Phys. Lett., 12, 347 (1972).

136. J. T. Richards and J. K. Thomas, Chem. Phys. Lett., 10, 317 (1971).

137. K. Funabashi and Y. Maruyama, J. Chem. Phys., 55, 4494 (1971).

138. S. L. Hager and J. E. Willard, Chem. Phys. Lett., 24, 102 (1974).

139. N. V. Klassen, H. A. Gillis and G. G. Teather, J. Phys. Chem., 76, 3847 (1972).

140. J. T. Richards and J. K. Thomas, J. Chem. Phys., 53, 218 (1970).

141. J. P. Guarino and W. H. Hamill, J. Am. Chem. Soc., 86, 777 (1964).

142. J. Lin, K. Tsuji and F. Williams, J. Am. Chem. Soc., 90, 2766 (1968).

143. W. H. Hamill, J. P. Guarino, M. R. Ronayne and J. A. Ward, Disc. Faraday Soc., 36, 169 (1963).

144. L. Kevan, H. A. Gillis, K. Fueki and T. Kimura, J. Chem. Phys., 68, 5203 (1978).

145. H. A. Gillis, N. V. Klassen, G. G. Teather and H. K. Lokan, Chem. Phys. Lett., 10, 481 (1971).

146. I. A. Taub and H. A. Gillis, J. Am. Chem. Soc., 91, 6507 (1969).

147. A. Banerjee and J. Simons, J. Chem. Phys., 68, 415 (1978).

148. T. Shida and S. Iwata, J. Am. Chem. Soc., 95, 3473 (1973).

149. R. Bensasson and E. J. Land, Chem. Phys. Lett., 15, 195 (1972).

150. D. C. Walker, N. V. Klassen and H. A. Gillis, Chem. Phys. Lett., 10, 636 (1971).

151. A. M. Koulkes-Pujo, L. Gilles, B. Lesigne and J. Sutton, Chem. Comm., 749 (1971).

152. E. A. Shaede, L. M. Dorfman, G. J. Flynn and D. C. Walker, Can. J. Chem., 51, 3905 (1973).

153. H. Nauta and C. Van Huis, J.C.S., Faraday Trans., I, 68, 647 (1972).

154. N. Hayashi, E. Hayon, T. Ibata, N. N. Lichtin and A. Matsumoto, J. Phys. Chem., 75, 2267 (1971).

155. N. S. Fel', P. I. Dolin and V. I. Zolotarevskii, High Engy. Chem., 1, 132 (1967).

156. R. Olinger and U. Schindewolf, Ber. Bunsenges. Phys. Chem., 75, 639 (1971).

157. J. W. Fletcher and W. A. Seddon, J.C.S., Faraday Disc., 63, 18 (1977).

158. B. G. Ershov and A. K. Pikaev, Rad. Res. Rev., 2, 1 (1969).

159. E. I. Mal'tsev, A. M. Koulkes-Pujo, A. V. Vannivov and N.A. Bakh, High Engy. Chem., 9, 168 (1975).

160. T. K. Cooper, D. C. Walker, H. A. Gillis and N. V. Klassen, Can. J. Chem., 51, 2195 (1973).

161. J. H. Baxendale and E. J. Rasburn, J.C.S., Faraday Trans., I, 70, 705 (1974).

162. T. J. Kepm, G. A. Salmon and P. Wardman, in "Pulse Radiolysis", M. Ebert, J. P. Keene, A. J. Swallow, and J. H. Baxendale, (Eds.), Academic Press, London & New York, 1965, p.247.

163. L. Shields, J. Phys. Chem., 69, 3186 (1965).

164. F. S. Dainton and R. J. Whewell, J.C.S. Chem. Comm., 493 (1974).

165. T. Sawai and W. H. Hamill, J. Phys. Chem., 73, 3452 (1969).

166. J. R. Brandon and R. F. Firestone, J. Phys. Chem., 78, 792 (1974).

167. V. S. Marevtsev and A. V. Vannikov, High Engy. Chem., 7, 104 (1973).

168. T. Ito, N. Ujikawa and K. Fueki, J. Phys. Chem., 79, 2479 (1975).

169. J. Mayer, J. L. Gebicki, and J. Kroh, Rad. Phys. Chem., 11, 101 (1978).

170. J. H. Baxendale, J. P. Keene and E. J. Rasburn, J.C.S., Faraday Trans., I, 70, 718 (1974).

171. J. H. Baxendale and P. H. G. Sharpe, Chem. Phys. Lett., 41, 440 (1976).

172. L. B. Magnusson, J. T. Richards and J. K. Thomas, Int. J. Rad. Phys. Chem., 3, 295 (1971).

173. B. J. Brown, N. T. Barker and D. F. Sangster, Aust. J. Chem., 26, 2089 (1973).

174. G. A. Kenney-Wallace and C. D. Jonah, Chem. Phys. Lett., 39, 596 (1976).

175. P. S. Childs and R. R. Dewald, J. Phys. Chem., 79, 58 (1975).

176. J. Jortner, Molec. Phys., 5, 257 (1962).

177. M. Born and J. R. Oppenheimer, Ann. Phys. Lpz., 84, 457 (1927).

178. L. D. Landau, Physik Z. Sowiet Union, 3, 664 (1933).

179. S. I. Pekar, J. Phys. USSR., 10, 341, 347 (1946).

180. A. S. Davydov, J. Exp. Theor. Phys., USSR., 18, 913 (1948).

181. M. F. Deigen, J. Exp. Theor. Phys., USSR., 26, 300 (1954).

182. Yu. T. Mazurenko and V. K. Mukhomorov, Opt. Spectros., USSR, 41, 28 (1976).

183. V. K. Mukhomorov and Yu. T. Mazurenko, Opt. Spectros., USSR., 41, 550 (1976).

184. V. K. Mukhomorov and Yu. T. Mazurenko, Opt. Spectros., USSR., 43, 494 (1977), and references contained therein.

185. M. G. Robinson, K. N. Jha and G. R. Freeman, J. Chem. Phys., 55, 4933 (1971).

186. A. K. Pikaev, "The Solvated Electron in Radiation Chemistry", Nauka, Moscow, 1969, quoted by ref. 184.

187. U. Schindewolf, in "Metal Ammonia Solutions", J. J. Lagowski and M. J. Sienko, Eds., Butterworths, London, 1970, p.199.

188. R. L. Bush and K. Funabashi, J.C.S., Faraday Trans., II, 73, 274 (1977).

189. T. Holstein, Ann. Phys., 8, 325, 343 (1959).

190. G. L. Borisenko and A. V. Vannikov, High Engy. Chem., 12, 413 (1978).

191. W. N. Lipscomb, J. Chem. Phys., 21, 52 (1953).

192. R. A. Stairs, J. Chem. Phys., 27, 1431 (1957).

193. M. Smith and M. C. R. Symons, Faraday Soc. Trans., 24, 206 (1957).

194. M. Smith and M. C. R. Symons, Faraday Soc. Trans., 54, 346 (1958).

195. M. J. Blandamer, R. Catterall, L. Shields and M. C. R. Symons, J. Chem. Soc., 4357 (1964).

196. M. J. Blandamer, L. Shields and M. C. R. Symons, J. Chem. Soc., 3759 (1965).

197. S. Ishimaru, T. Yamabe, K. Fukui and H. Kato, Chem. Phys. Lett., 17, 264 (1972).

198. J. A. Pople and R. K. Nesbet, J. Chem. Phys., 22, 571 (1954).

199. J. A. Pople, D. L. Beveridge and P. A. Dobosh, J. Chem. Phys., 47, 2026 (1967).

200. E. J. Hart and W. C. Dottschall, J. Am. Chem. Soc., 71, 2102 (1967).

201. R. G. Gordon, Adv. Magn. Reson. 3, 1 (1968).

202. J. Jortner, J. Chem. Phys., 30, 839 (1959).

203. J. Jortner, Rad. Res. Suppl., 4, 24 (1964).

204. U. Schindewolf, H. Kohrmann and G. Lang, Angew. Chem. Int. Edn. Engl., 7, 512 (1969).

205. R. R. Hentz, Farhataziz and E. M. Hansen, J. Chem. Phys. 56, 4485 (1972).

206. R. R. Hentz, Farhataziz and E. M. Hansen, 57, 2959 (1972).

207. K. Iguchi, J. Chem. Phys., 48, 1735 (1968).

208. K. Iguchi, J. Chem. Phys., 51, 3137 (1967).

209. K. Fueki, J. Chem. Phys., 49, 765 (1968).

210. M. Tachiya, Y. Tabata and K. Ohima, J. Phys. Chem., 77, 263 (1973).

211. I. Carmichael and B. Webster, J.C.S., Faraday Trans., II, 70, 1570 (1974).

212. K. Funabashi, I. Carmichael and W. H. Hamill, J. Chem. Phys., 69, 2652 (1978).

213. N. R. Kestner, J. Logan and J. Jortner, J. Phys. Chem., 78, 2148 (1974).

214. J. McHale and J. Simons, J. Chem. Phys., 67, 389 (1977).

215. D. E. O'Reilly, J. Chem. Phys., 41, 3736 (1964).

216. R. H. Land and D. E. O'Reilly, J. Chem. Phys., 46, 4496 (1967).

217. K. Fueki, D. F. Feng and L. Kevan, J. Phys. Chem., 74, 1976 (1970).

218. K. Fueki, D. F. Feng, L. Kevan and R. E. Christoffersen, J. Phys. Chem., 75, 2297 (1971).

219. K. Fueki, D. F. Feng and L. Kevan, J. Chem. Phys., 56, 5351 (1972).

220. D. F. Feng, K. Fueki and L. Kevan, J. Chem. Phys., 57, 1253 (1972).

221. K. Fueki, D. F. Feng and L. Kevan, J. Am. Chem. Soc., 95, 1398 (1973).

222. D. F. Feng, K. Fueki and L. Kevan, J. Chem. Phys., 58, 3281 (1973).

223. D. F. Feng, D. Ebbing and L. Kevan, J. Chem. Phys., 61, 249 (1974).

224. K. Fueki, D. F. Feng and L. Kevan, J. Phys. Chem., 78, 393 (1974).

225. D. F. Feng, H. Yoshida and L. Kevan, J. Chem. Phys., 61, 4440 (1974).

226. T. Kimura, K. Fueki, P. A. Narayama and L. Kevan, Can. J. Chem., 55, 1940 (1977).

227. J. H. Baxendale and P. Wardman, J.C.S., Faraday Trans., I, 69, 584 (1973).

228. J. Jortner, Ber. Bunsenges. Phys. Chem., 75, 696 (1971).

229. J. Logan and N. R. Kestner, J. Phys. Chem., 76, 2738 (1972).

230. N. Kestner and J. Jortner, J. Phys. Chem., 77, 1040 (1973).

231. N. Kestner in "Electrons in Fluids", J. Jortner and N. R. Kestner, Eds., Springer-Verlag, New York - Berlin, 1973, p.1.

232. A. Gaathon and J. Jortner, in "Electrons in Fluids", J. Jortner and N. R. Kestner, Eds., Springer-Verlag, New York - Berlin, 1973, p. 429.

233. N. R. Kestner, J. Jortner and A. Gaathon, Chem. Phys. Lett., 19, 328 (1973).

234. N. R. Kestner and J. Logan, J. Phys. Chem., 79, 2815 (1975).

235. N. R. Kestner, in "Electron-Solvent and Anion-Solvent Interactions,", L. Kevan and B. C. Webster, Eds., Elsevier Scientific Publ. Co., Amsterdam, 1976, p.1.

236. N. R. Kestner, Can. J. Chem., 55, 1937 (1977).

237. R. R. Hentz, Farhataziz and E. M. Hansen, J. Chem. Phys., 55, 4974 (1971).

238. B. C. Webster and I. C.Carmichael, J. Chem. Phys., 68, 4086 (1978).

239. I. Carmichael, Chem. Phys. Lett., 56, 339 (1978).

240. H. Aulich, L. Nemec and P. Delahay, J. Chem. Phys., 61, 4235 (1974).

241. L. Nemec, L. Chia and P. Delahay, J. Phys. Chem., 79, 2935 (1975).

242. A. M. Brodsky and A. V. Tsarevsky, Int. J. Rad. Phys. Chem., 8, 455 (1976).

243. M. G. DeBacker, J. N. Decarpigny and M. Lannoo, J. Phys. Chem., 81, 159 (1977).

244. L. Raff and H. Pohl, Adv. Chem. Ser., 50, 173 (1965).

245. M. Natori and T. Watanabe, J. Phys. Soc. Jap., 21, 1573 (1966).

246. M. Natori, J. Phys. Soc. Jap., 24, 918 (1968).

247. M. Natori, J. Phys. Soc. Jap., 27, 1309 (1969).

248. B. J. McAloon and B. C. Webster, Theor. Chim. Acta (Berl.), 15, 385 (1969).

249. S. Ray, Chem. Phys. Lett., 11, 573 (1971).

250. S. Ishimaru, H. Tomita, T. Yamabe, K. Fueki and H. Kato, Chem. Phys. Lett., 23, 106 (1973).

251. S. Ishimaru, H. Kato, T. Yamabe and K. Fueki, J. Phys. Chem., 77, 1450 (1973).

252. M. Weissman and N. V. Cohan, Chem. Phys. Lett., 7, 445 (1970).

253. M. Weissman and N. V. Cohan, J. Chem. Phys., 59, 1385 (1973).

254. C. A. Naleway and M. E. Schwartz, J. Phys. Chem., 76, 3905 (1972).

255. T. Kajiwara, K. Funabashi and C. A. Naleway, Phys. Rev., A, 6, 808 (1972).

256. G. Howat and B. C. Webster, J. Phys. Chem., 76, 3714 (1972).

257. M. D. Newton, J. Chem. Phys., 58, 5833 (1973).

258. M. D. Newton, J. Phys. Chem., 79, 2795 (1975).

259. M. Tachiya and A. Mozumder, J. Chem. Phys., 60, 3037 (1974).

260. M. Tachiya and A. Mozumder, J. Chem. Phys., 61, 3890 (1974).

261. J. M. Moskowitz, M. Boring and J. H. Wood, J. Chem. Phys., 62, 2254 (1975).

262. B. Webster, J. Phys. Chem., 79, 2809 (1975).

263. S. Golden, C. Guttman and T. R. Tuttle, Jr., J. Chem. Phys., 44, 3791 (1966).

264. T. R. Tuttle, Jr., G. Rubinstein and S. Golden, J. Phys. Chem., 75, 3635 (1971).

265. S. Golden and T. R. Tuttle, Jr., J. Phys. Chem., 82, 944 (1978).

266. S. M. S. Akhtar and G. R. Freeman, J. Phys. Chem., 75, 2756 (1971).

267. ICRU Report 21, Radiation Dosimetry: Electrons with Initial Energies Between 1 and 50 MeV, International Commission on Radiation Units and Measurements, Washington, D.C., May 15, 1972, pp. 33-37.

268. National Research Council, "International Critical Tables", McGraw-Hill, New York, 1926, Vol. 1, p.58.

269. R. E. Rondeau, J. Chem. & Eng. Data, 11, 124 (1966).

270. R. Lugo and P. Delahay, J. Chem. Phys., 57, 2122 (1972).

271. J. P. Chenier, in "APL Functions for Random Number and Probability", Computing Service Reference Manual #49, The University of Alberta, Edmonton, Canada, November, 1978.

272. C. Leibovitz, in "APL Functions for Numerical Analysis", Computing Service Reference Manual #46, The University of Alberta, Edmonton, Canada, April, 1975.

273. G. L. Bolton, K. N. Jha, and G. R. Freeman, Can. J. Chem., 54, 1497 (1976), and references contained therein.

274. A. J. Swallow, "Radiation Chemistry", Longman, London, 1973, Chap. 7, pp. 136-166.

275. J. Timmermans, "Physico-Chemical Constants of Binary Systems", Vol. 4, Interscience, New York, N.Y., 1960, pp. 163-236.

276. J. A. Riddick and W. B. Bunger, Techniques of Chemistry, Vol. II, "Organic Solvents", Physical Properties and Methods of Purification, 3rd Edn., Wiley-Interscience, John and Sons, Inc., New York, 1970, pp.145-155.

277. F. Franks, "Physico-Chemical Processes in Mixed Aqueous Solvents", American Elsevier Publ. Co., Inc., New York, 1967, p.54.

278. K. Okazaki and G. R. Freeman, Can. J. Chem., 56, 2313 (1978).

279. K. Okazaki, A. D. Leu and G. R. Freeman, to be published.

280. G. Dolivo and L. Kevan, J. Chem. Phys., 70, 2599 (1979).

281. W. C. Coburn, Jr., and E. Grunwald, J. Am. Chem. Soc., 80, 1318 (1958).

282. L. Pauling, "The Nature of the Chemical Bond", 3rd Edn., Cornell Univ. Press, New York, 1960, p.473.

283. K. J. Tauer and W. N. Liscomb, Acta Cryst., 5, 606 (1952).

284. R. L. Kay, private communication quoted by F. Franks, in "Physico-Chemical Processes in Mixed Aqueous Solvents", American Elsevier Publ. Co., Inc., New York, 1967, p.67.

285. C. L. V. P. Van Eck, H. Mendel and W. Boag, Faraday Soc. Disc., 24, 200 (1957).

286. L. Pauling, in "Hydrogen Bonding", D. Hadzi, Ed., Pergamon Press, London, 1959, p.1.

287. G. M. Bell, J. Phys., C, Solid State Phys., 5, 889 (1972).

288. O. Weres and S. A. Rice, J. Am. Chem. Soc., 94, 8983 (1972).

289. J. W. Perram, in "The Hydrogen Bond", P. Schuster, G. Zundel and C. Sandorfy, Eds., North-Holland Publ. Co., Amsterdam - Oxford, 1976, Vol. 1, Chap. 7, pp. 358-389.

290. A. D. Potts and D. W. Davidson, J. Phys. Chem., 69, 996 (1965).

291. R. S. Mulliken, C. A. Rieke and W. G. Brown, J. Am. Chem. Soc., 63, 41 (1941).

292. R. S. Mulliken, Tetrahedron, 5, 259 (1959).

293. F. Franks, in "Physico-Chemical Processes in Mixed Aqueous Solvents", F. Franks, Ed., American Elsevier Publ. Co., Inc., New York, 1967, p.55.

294. (a) P.61 of ref. 293. (b) P.122 of ref. 25.

295. D. Eagland and G. Armitage, private communication, quoted by ref. 293, p.62.

296. R. H. Ottewill, private communication; B. Vincent, M.Sc. Thesis, University of Bristol, 1965, quoted by ref. 293, p.63.

297. A. Winstein and A. H. Fainberg, J. Am. Chem. Soc., 79, 5937 (1957).

298. F. Franks and B. Watson, Trans. Faraday Soc., 63, 329 (1967).

299. C. Capellos and B. H. J. Bielski, in "Kinetic Systems" Mathematical Description of Chemical Kinetic in Solution, Wiley-Interscience, New York, 1972, p.112.

V. APPENDIX

Spectra Analysis

A. Deconvolution of Absorption Spectra

In obtaining secondary parameters of an absorption spectrum, the choice of constraints in the method of deconvolution mentioned on pages 75 and 76 is arbitrary. Examples of attempts to deconvolute the optical absorption spectrum of solvated electrons in pure methanol at 298K are shown in Figures V-1 to -3. In Figures V-1 and -2, for the first Gaussian band the relative absorbance A_{1max}/A_{max} for the band maximum is required to be greater than 80% of the observed band maximum, and the maximum error for fit between generated and observed bands is required to be less than ±2%. For the second Gaussian band, in Figure V-1 the maximum error has been kept the same as for the first Gaussian, ±2%, whereas in Figure V-2 a maximum error of ±3% has been allowed for the second Gaussian band. The restrictions are less stringent in Figure V-3. The value of A_{1max}/A_{max} for the maximum of the first Gaussian band is only required to be greater than 60% of the observed band maximum, and the maximum error between generated and observed bands is only required to be less than ±3% for each of the three Gaussians that were extracted.

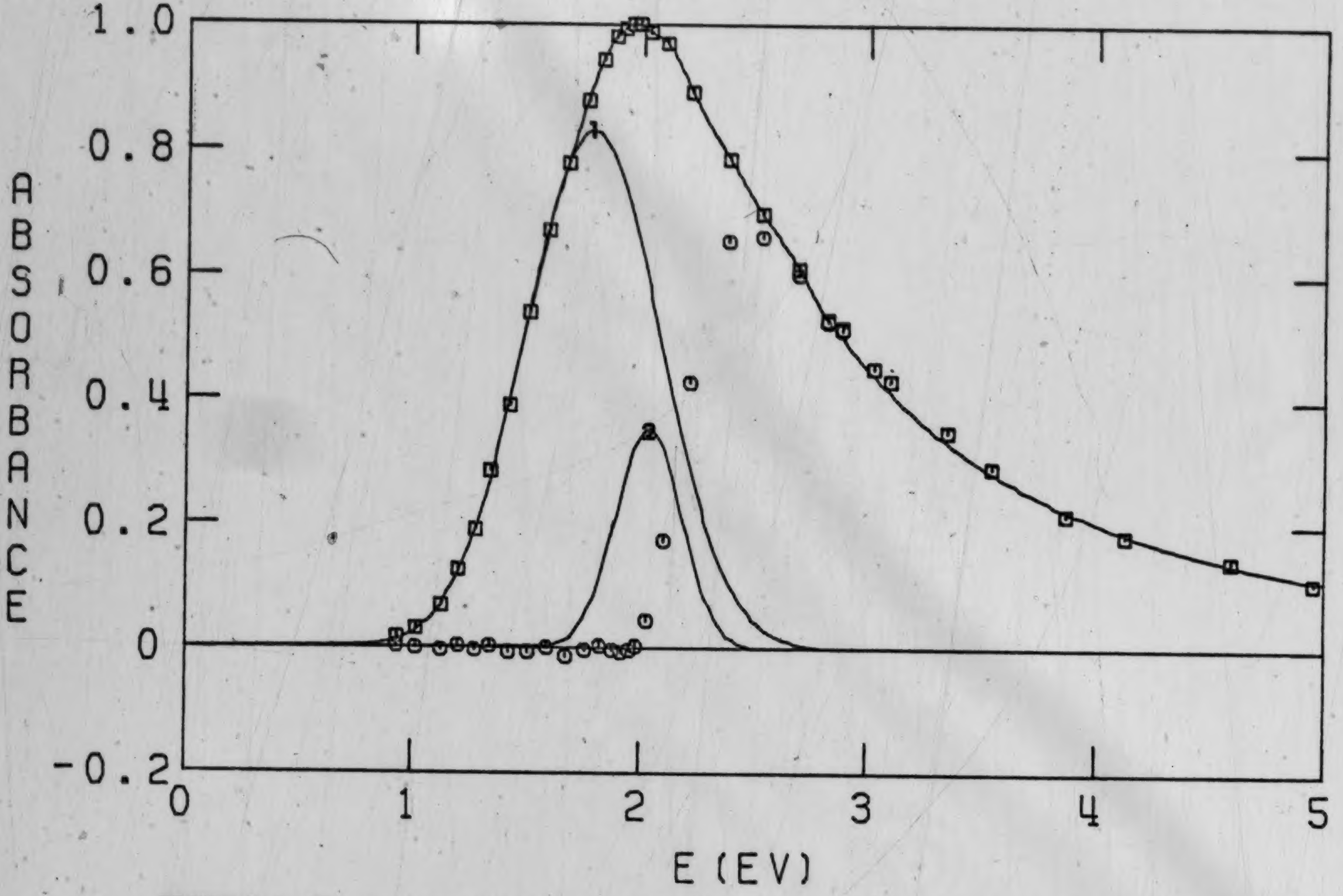

FIGURE V-1. The Band Deconvolution of the Optical Absorption Spectrum of Solvated Electrons in Methanol at 298K. □, Experimental; 1, First Gaussian; 2, Second Gaussian; 0, Residual High Energy Tail.

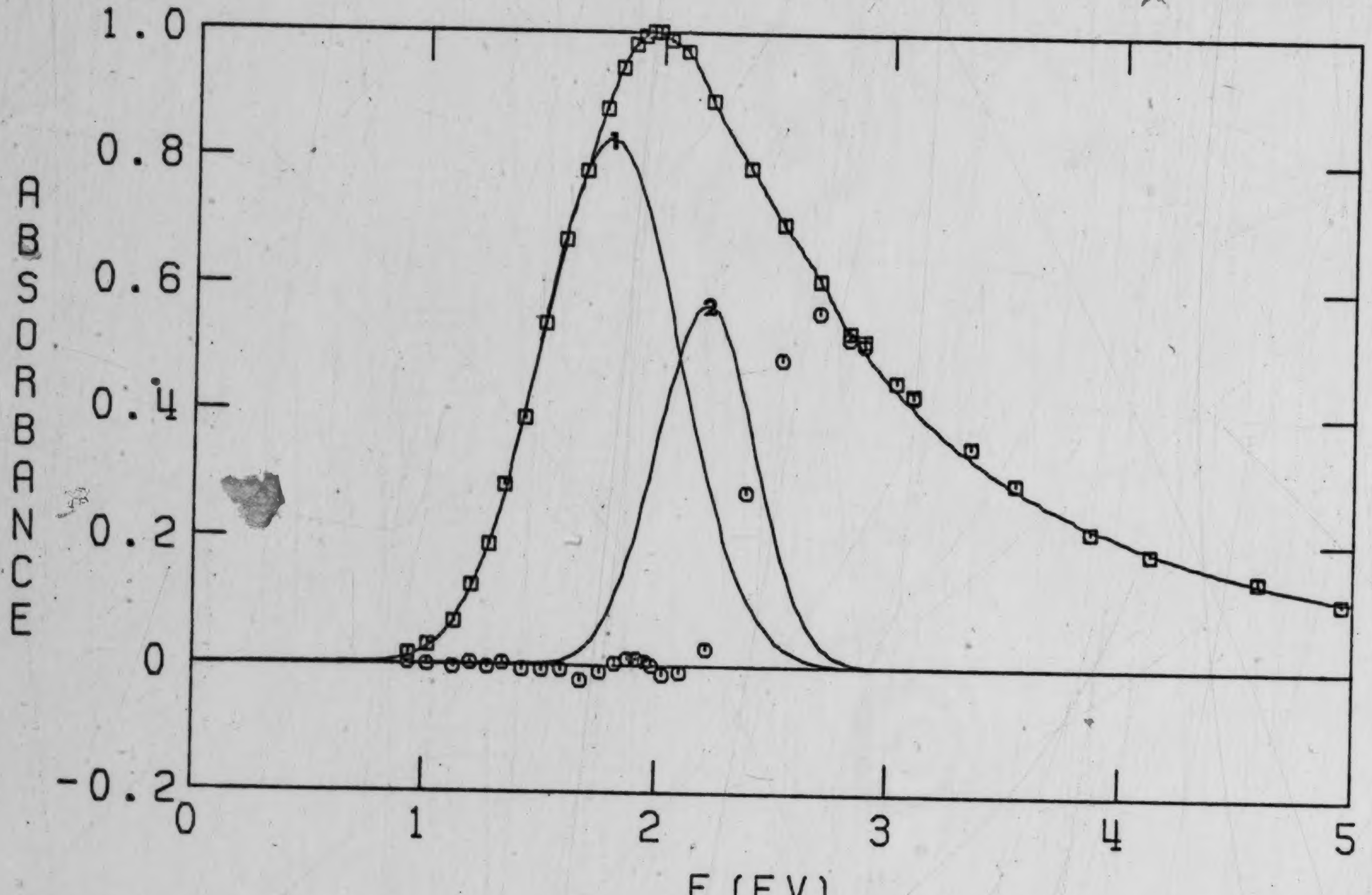

FIGURE V-2. Band Deconvolution in Methanol at 298K. Symbols as in Figure V-1.

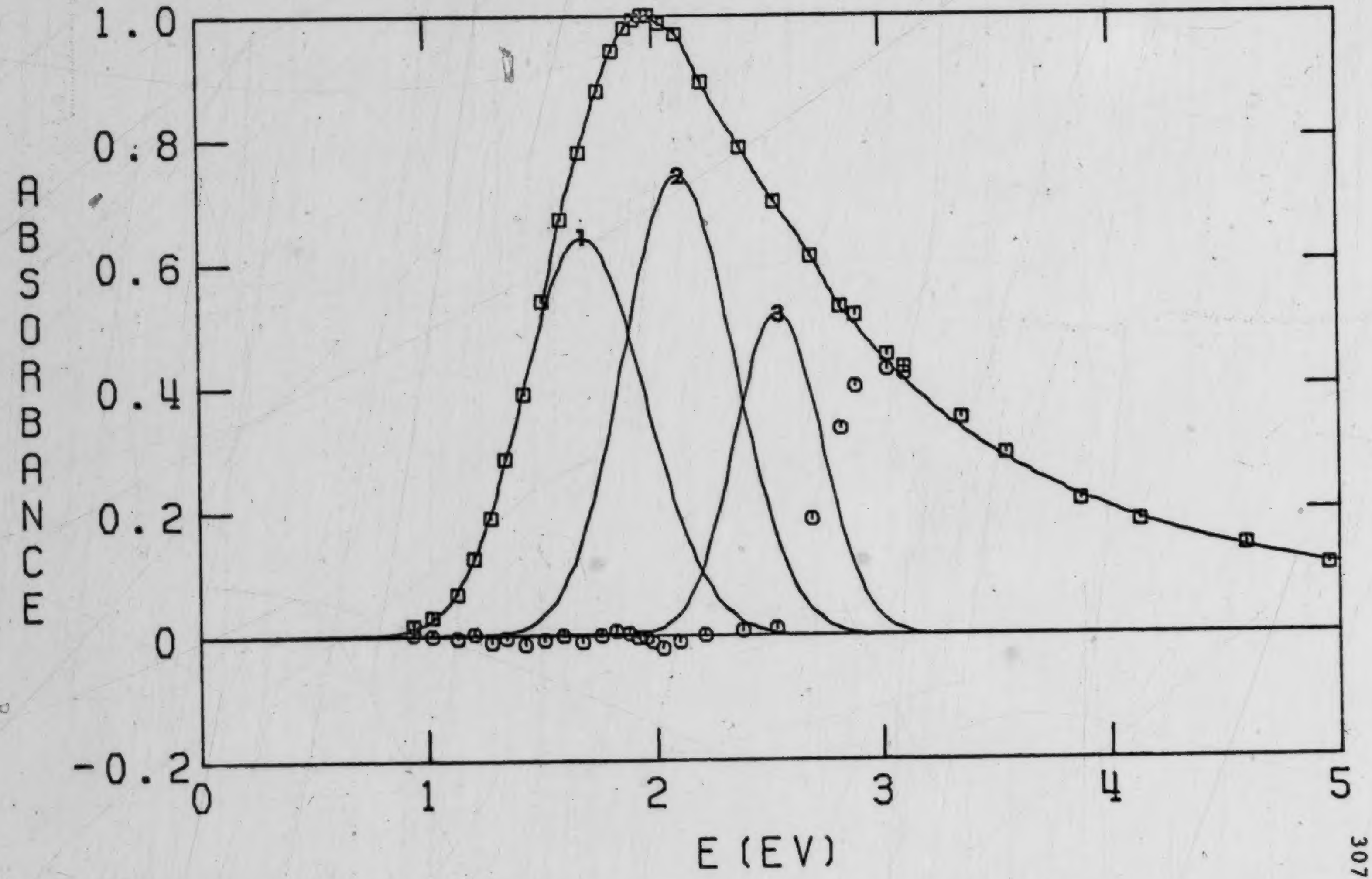

FIGURE V-3. Band Deconvolution in Methanol at 298K. Symbols as in Figure V-1, and 3, Third Gaussian.

The results obtained from these figures are summarized in Table V-1. From this table, it can be seen that:

(1) Allowing the maximum % error to be changed from 1.7 to 2.5 for deconvoluting the second Gaussian band allows about 60, 8, and 47% increases in A_{2max}/A_{max}, E_{A2max}, and g_2, respectively.

(2) Allowing the relative absorbance A_{1max}/A_{max} of the first Gaussian to be changed from 0.83 to 0.64 causes 5 and 10% decreases in E_{A1max} and g_1, respectively. The resulting changes allowed in the second Gaussian band are: A_{2max}/A_{max} and g_2 increase respectively 30 and 14%, and E_{A2max} decreases 4%. If the values of A_{1max}/A_{max} and g_1 are lower, then the corresponding values for the second Gaussian can be higher.

(3) The magnitudes of the g values for the three Gaussians in case III, decrease in the order of $g_1 > g_2 > g_3$.

Although the arbitrariness in the choice of constraints to deconvolute the absorption spectrum has been illustrated in Figures V-1 to -3, the deconvolution of the spectra in mixed solvents has been done under the following constraints:

TABLE V-1

Parameters for Deconvoluting the Absorption Spectra of Methanol into Gaussian Bands at 298K

		The First Band			The Second Band			The Third Band
		I[§]	II[§]	III[§]	I[§]	II[§]	III[§]	III[§]
A_{imax}/A_{max}		0.83	0.83	0.64	0.35	0.57	0.74	0.52
E_{Aimax}	eV	1.79	1.79	1.69	2.04	2.21	2.11	2.55
g_i[*]	eV	0.35	0.35	0.32	0.17	0.25	0.29	0.22
Δ_{max}[†]	%	1.7	1.7	1.7	1.7	2,5	2.5	2.5

[§] I, II and III indicate Figures V-1, -2 and -3, respectively.

[*] g represents half of the width at half-height in generated Gaussian band.

[†] Δ_{max} = The maximum % error between the generated and the observed bands in terms of the relative absorbance.

(a) Tentatively, only two Gaussian bands are extracted from each absorption spectrum.

(b) For the first Gaussian band, the constraints are the same as required for the band deconvolution in Figure V-2.

(c) For the second Gaussian band, the value of A/A_{max} for the band maximum is required to be greater than 80% of the band maximum for the residual band obtained from (b).

(d) The maximum difference between the sum of the two generated bands and the observed band will be ±3%.

The results obtained from this type of deconvolution for each alcohol/water mixture are summarized in Tables V-3 to -10. The results for water are listed in Table V-2. Representative spectra obtained from this deconvolution are shown in Figures V-4 to -20 for water, methanol, 1-propanol, 2-propanol, and t-butanol. These alcohols were selected to represent the four categories used in this study, i.e., methanol, primary, secondary and tertiary alcohols. The temperature in all cases is 298K. The validity of these parameters will be discussed in the last section of this chapter.

TABLE V-2

Secondary Parameters of Solvated Electrons in Water at Different Temperatures*

$<100\|W\|T_i>$	Code No.	155	152	153	154
T	K	273	298	350	373
A_1		0.98	0.99	0.99	0.99
A_2		0.33	0.27	0.21	0.21
E_1	eV	1.79	1.74	1.62	1.57
E_2	eV	2.36	2.29	2.34	2.26
g_1	eV	0.34	0.35	0.40	0.41
g_2	eV	0.27	0.23	0.29	0.29
f_1		0.60	0.64	0.73	0.74
f_2		0.16	0.12	0.11	0.11
f_3		0.24	0.24	0.16	0.15
E_b^c	eV	2.38	2.27	2.35	2.27
α		3.9	4.0	4.1	4.3

* where A is the relative absorbance of band maximum with respect to (w.r.t.) the observed A/A_{max}; E is the energy of band maximum; g is the half of the width at half-height of Gaussian band; and f is the area ratio of Gaussian band w.r.t. the observed band. Subscript 1 indicates first Gaussian band, 2 indicates second Gaussian band, 3 indicates residual high energy tail. E_b^c represents the threshold energy of bound-continuum transition, while α indicates the descending power of A/A_{max} vs E curve, in which E is greater than E_{Amax}.

TABLE V-3

Secondary Parameters of Solvated Electrons in Methanol/Water at Different Temperatures

$\langle 0\|M\|T_1\rangle$	Code No.	5	4	3	1	2
T	K	180	200	250	298	350
A_1		0.89	0.90	0.90	0.82	0.90
A_2		0.63	0.54	0.57	0.59	0.63
E_1	eV	2.12	2.10	1.95	1.79	1.66
E_2	eV	2.49	2.56	2.41	2.22	2.19
g_1	eV	0.28	0.33	0.34	0.35	0.35
g_2	eV	0.19	0.26	0.25	0.26	0.30
f_1		0.28	0.32	0.33	0.30	0.33
f_2		0.13	0.15	0.15	0.16	0.19
f_3		0.59	0.53	0.52	0.54	0.48
E_b^c	eV	2.48	2.49	2.35	2.20	2.09
α		2.8	2.7	2.8	2.7	2.7

$\langle 10\|M\|T_1\rangle$	Code No.	16	15	14	13	17
T	K	180	200	250	298	350
A_1		0.90	0.92	0.93	0.90	0.91
A_2		0.51	0.47	0.50	0.47	0.52
E_1	eV	2.19	2.14	1.98	1.80	1.59
E_2	eV	2.61	2.51	2.44	2.30	2.05
g_1	eV	0.31	0.31	0.36	0.38	0.35
g_2	eV	0.25	0.20	0.24	0.29	0.26

(continued)

TABLE V-3 (continued)

f_1		0.36	0.38	0.41	0.42	0.39
f_2		0.16	0.12	0.15	0.17	0.16
f_3		0.48	0.50	0.44	0.41	0.45
E_b^c	eV	2.54	2.44	2.41	2.24	1.99
α		3.3	3.3	3.3	3.1	3.0
$<50\|M\|T_i>$	Code No.	20	19	18	21	
T	K	200	250	298	350	
A_1		0.92	0.91	0.92	0.91	
A_2		0.48	0.42	0.44	0.51	
E_1	eV	2.07	1.94	1.75	1.56	
E_2	eV	2.52	2.45	2.16	1.93	
g_1	eV	0.26	0.31	0.31	0.30	
g_2	eV	0.28	0.33	0.24	0.20	
f_1		0.41	0.47	0.47	0.44	
f_2		0.23	0.23	0.17	0.17	
f_3		0.36	0.30	0.36	0.39	
E_b^c	eV	2.48	2.25	2.10	1.89	
α		3.7	3.7	3.6	3.6	
$<98\|M\|T_i>$	Code No.	23	22	24	25	
T	K	273	298	350	370	
A_1		0.98	0.96	0.99	0.99	
A_2		0.33	0.39	0.33	0.26	
E_1	eV	1.79	1.68	1.58	1.55	

(continued)

TABLE V-3 (continued)

E_2	eV	2.27	2.09	2.13	2.15
g_1	eV	0.32	0.31	0.34	0.37
g_2	eV	0.26	0.21	0.27	0.30
f_1		0.59	0.55	0.63	0.68
f_2		0.16	0.16	0.16	0.15
f_3		0.25	0.29	0.21	0.17
E_b^c	eV	2.28	2.08	2.08	2.16
α		4.3	4.3	4.2	4.2

TABLE V-4

Secondary Parameters of Solvated Electrons in Ethanol/Water at Different Temperatures

$\langle 0\vert E\vert T_i\rangle$	Code No.	28	27	26	6	29
T	K	160	200	250	298	350
A_1		0.86	0.89	0.90	0.89	0.88
A_2		0.63	0.66	0.61	0.63	0.59
E_1	eV	2.08	1.97	1.84	1.67	1.48
E_2	eV	2.51	2.43	2.32	2.20	1.94
g_1	eV	0.32	0.32	0.34	0.37	0.35
g_2	eV	0.25	0.24	0.26	0.29	0.26
f_1		0.22	0.24	0.26	0.27	0.26
f_2		0.13	0.13	0.13	0.15	0.13
f_3		0.65	0.63	0.61	0.58	0.61
E_b^c	eV	2.46	2.39	2.26	2.12	1.87
α		2.2	2.2	2.3	2.3	2.1

$\langle 10\vert E\vert T_i\rangle$	Code No.	34	33	32	31	30
T	K	160	200	250	298	350
A_1		0.93	0.94	0.88	0.88	0.91
A_2		0.60	0.55	0.56	0.53	0.53
E_1	eV	2.12	2.04	1.77	1.56	1.41
E_2	eV	2.56	2.57	2.19	1.93	1.78
g_1	eV	0.31	0.36	0.34	0.32	0.31
g_2	eV	0.23	0.28	0.24	0.20	0.20

(continued)

TABLE V-4 (continued)

f_1		0.27	0.35	0.32	0.33	0.35
f_2		0.13	0.16	0.14	0.12	0.13
f_3		0.60	0.49	0.54	0.55	0.52
E_b^c	eV	2.52	2.49	2.15	1.90	1.73
α		2.5	2.7	2.7	2.6	2.6

$<50\|E\|T_1>$	Code No.	38	37	36	35
T	K	222	250	298	350
A_1		0.98	0.94	0.94	0.93
A_2		0.41	0.35	0.41	0.42
E_1	eV	1.99	1.90	1.70	1.54
E_2	eV	2.44	2.35	2.10	1.93
g_1	eV	0.31	0.33	0.32	0.31
g_2	eV	0.22	0.27	0.21	0.22
f_1		0.51	0.53	0.51	0.52
f_2		0.15	0.16	0.15	0.16
f_3		0.34	0.31	0.34	0.32
E_b^c	eV	2.47	2.34	2.08	1.94
α		3.9	3.9	3.9	3.8

$<98\|E\|T_1>$	Code No.	40	39	41	42
T	K	273	298	350	366
A_1		0.98	0.98	0.97	0.98
A_2		0.32	0.31	0.29	0.29
E_1	eV	1.80	1.72	1.58	1.53

(continued)

TABLE V-4 (continued)

E_2	eV	2.28	2.16	2.13	2.02
g_1	eV	0.32	0.33	0.36	0.36
g_2	eV	0.25	0.23	0.29	0.24
f_1		0.61	0.62	0.66	0.66
f_2		0.15	0.13	0.15	0.13
f_3		0.24	0.25	0.19	0.21
E_b^c	eV	2.21	2.17	2.14	2.01
α		4.5	4.4	4.4	4.4

TABLE V-5

Secondary Parameters of Solvated Electrons in 1-Propanol/Water at Different Temperatures

$\langle 0\|1p\|T_i\rangle$	Code No.	47	46	45	7	43	44
T	K	150	200	250	298	350	369
A_1		0.86	0.91	0.89	0.93	0.89	0.89
A_2		0.66	0.59	0.66	0.52	0.71	0.66
E_1	eV	2.19	2.09	1.92	1.78	1.53	1.47
E_2	eV	2.65	2.54	2.43	2.25	2.05	2.08
g_1	eV	0.35	0.37	0.37	0.40	0.36	0.41
g_2	eV	0.25	0.22	0.27	0.24	0.28	0.34
f_1		0.28	0.31	0.30	0.33	0.29	0.32
f_2		0.15	0.12	0.16	0.11	0.17	0.20
f_3		0.57	0.57	0.54	0.56	0.54	0.48
E_b^c	eV	2.61	2.50	2.39	2.16	2.01	2.07
α		2.7	2.7	2.7	2.6	2.5	2.5

$\langle 10\|1P\|T_i\rangle$	Code No.	61	60	59	62
T	K	200	250	298	350
A_1		0.94	0.90	0.87	0.90
A_2		0.55	0.56	0.66	0.53
E_1	eV	2.09	1.83	1.55	1.42
E_2	eV	2.63	2.39	1.98	1.75
g_1	eV	0.38	0.39	0.32	0.30
g_2	eV	0.28	0.32	0.24	0.18

(continued)

TABLE V-5 (continued)

f_1		0.40	0.40	0.35	0.37
f_2		0.17	0.21	0.20	0.13
f_3		0.43	0.39	0.45	0.50
E_b^c	eV	2.60	2.35	1.97	1.71
α		3.1	3.1	3.2	3.2
$<50\|1P\|T_i>$	Code No.	52	51	53	54
T	K	260	298	350	360
A_1		0.97	0.97	0.97	0.96
A_2		0.37	0.35	0.38	0.38
E_1	eV	1.86	1.73	1.55	1.53
E_2	eV	2.29	2.16	1.96	1.97
g_1	eV	0.33	0.34	0.32	0.33
g_2	eV	0.23	0.22	0.21	0.22
f_1		0.55	0.56	0.55	0.56
f_2		0.14	0.13	0.14	0.15
f_3		0.31	0.31	0.31	0.29
E_b^c	eV	2.26	2.14	1.95	1.92
α		4.1	3.9	4.0	4.0
$<98\|1P\|T_i>$	Code No.	58	57	55	56
T	K	273	298	350	363
A_1		0.99	0.99	0.99	1.00
A_2		0.31	0.33	0.28	0.21
E_1	eV	1.80	1.72	1.59	1.59

(continued)

TABLE V-5 (continued)

E_2	eV	2.24	2.25	2.13	2.22
g_1	eV	0.33	0.34	0.35	0.39
g_2	eV	0.22	0.26	0.25	0.25
f_1		0.60	0.60	0.66	0.73
f_2		0.13	0.18	0.13	0.10
f_3		0.27	0.22	0.21	0.17
E_b^c	eV	2.23	2.18	2.10	2.23
α		4.3	4.3	4.3	4.6

TABLE V-6

Secondary Parameters of Solvated Electrons in 2-Propanol/Water at Different Temperatures

$\langle 0\|2P\|T_i\rangle$	Code No.	49	48	8	50
T	K	200	250	298	350
A_1		0.92	0.91	0.85	0.87
A_2		0.69	0.66	0.52	0.72
E_1	eV	1.80	1.63	1.40	1.11
E_2	eV	2.27	2.10	1.88	1.56
g_1	eV	0.30	0.31	0.36	0.29
g_2	eV	0.25	0.25	0.31	0.25
f_1		0.25	0.25	0.27	0.23
f_2		0.16	0.15	0.14	0.16
f_3		0.59	0.60	0.59	0.61
E_b^c	eV	2.27	2.08	1.80	1.53
α		2.3	2.2	2.1	2.0

$\langle 10\|2P\|T_i\rangle$	Code No.	64	63	83	66
T	K	200	250	298	350
A_1		0.87	0.84	0.90	0.97
A_2		0.47	0.54	0.59	0.38
E_1	eV	1.79	1.56	1.50	1.37
E_2	eV	2.24	1.92	1.98	1.80
g_1	eV	0.35	0.31	0.35	0.33
g_2	eV	0.28	0.21	0.29	0.21

(continued)

TABLE V-6 (continued)

f_1		0.37	0.35	0.36	0.49
f_2		0.16	0.15	0.16	0.13
f_3		0.47	0.50	0.48	0.38
E_b^c	eV	2.17	1.88	1.77	1.78
α		2.8	2.9	3.0	3.0

$<50\|2P\|T_i>$	Code No.	70	67	68	69
T	K	250	298	339	352
A_1		0.96	0.97	0.91	0.93
A_2		0.30	0.35	0.42	0.41
E_1	eV	1.88	1.69	1.56	1.49
E_2	eV	2.35	2.13	1.92	1.86
g_1	eV	0.35	0.33	0.31	0.31
g_2	eV	0.26	0.23	0.21	0.21
f_1		0.59	0.58	0.52	0.54
f_2		0.14	0.14	0.16	0.16
f_3		0.27	0.27	0.32	0.30
E_b^c	eV	2.31	2.13	1.87	1.85
α		4.2	4.2	4.2	4.2

$<98\|2P\|T_i>$	Code No.	71	72	73	74
T	K	273	298	339	360
A_1		0.98	0.99	0.99	0.98
A_2		0.31	0.29	0.40	0.28
E_1	eV	1.80	1.74	1.61	1.56

(continued)

TABLE V-6 (continued)

E_2	eV	2.32	2.27	2.01	2.11
g_1	eV	0.33	0.35	0.30	0.36
g_2	eV	0.25	0.25	0.19	0.28
f_1		0.60	0.62	0.56	0.67
f_2		0.15	0.16	0.14	0.15
f_3		0.25	0.24	0.30	0.18
E_b^c	eV	2.31	2.25	1.96	2.10
α		4.1	4.2	4.3	4.3

TABLE V-7

Secondary Parameters of Solvated Electrons in 1-Butanol/Water at Different Temperatures

$\langle 0\|1B\|T_i\rangle$	Code No.	87	88	9	89	90
T	K	200	250	298	350	388
A_1		0.85	0.80	0.89	0.85	0.81
A_2		0.64	0.66	0.53	0.54	0.63
E_1	eV	2.08	1.87	1.84	1.62	1.33
E_2	eV	2.56	2.33	2.35	2.21	1.84
g_1	eV	0.36	0.35	0.43	0.46	0.41
g_2	eV	0.28	0.27	0.30	0.37	0.29
f_1		0.29	0.26	0.35	0.35	0.29
f_2		0.17	0.17	0.14	0.18	0.16
f_3		0.54	0.57	0.51	0.47	0.55
E_b^c	eV	2.52	2.24	2.30	2.08	1.75
α		2.7	2.8	2.6	2.6	2.4

$\langle 10\|1B\|T_i\rangle$	Code No.	130	129	126	127	128
T	K	200	250	298	350	373
A_1		0.95	0.93	0.92	0.92	0.91
A_2		0.53	0.51	0.51	0.52	0.48
E_1	eV	2.12	1.87	1.66	1.45	1.40
E_2	eV	2.70	2.44	2.27	1.91	1.95
g_1	eV	0.39	0.42	0.39	0.34	0.36
g_2	eV	0.31	0.31	0.35	0.25	0.32

(continued)

TABLE V-7 (continued)

f_1		0.36	0.41	0.42	0.41	0.45
f_2		0.16	0.17	0.21	0.17	0.21
f_3		0.48	0.42	0.37	0.42	0.34
E_b^c	eV	2.68	2.44	2.30	1.88	1.92
α		2.6	2.8	2.8	2.9	2.9

$<50\|1B\|T_i>$	Code No.	148	149	150	151
T	K	298	325	350	364
A_1		0.98	0.98	0.98	0.98
A_2		0.29	0.32	0.36	0.33
E_1	eV	1.77	1.67	1.57	1.54
E_2	eV	2.40	2.18	2.09	2.12
g_1	eV	0.36	0.35	0.34	0.35
g_2	eV	0.32	0.26	0.25	0.25
f_1		0.60	0.59	0.58	0.59
f_2		0.16	0.14	0.15	0.14
f_3		0.24	0.27	0.27	0.27
E_b^c	eV	2.39	2.16	2.08	2.04
α		3.7	3.8	3.8	3.8

$<98\|1B\|T_i>$	Code No.	123	122	124	125
T	K	273	298	350	363
A_1		0.99	0.98	0.99	1.00
A_2		0.35	0.35	0.26	0.31
E_1	eV	1.79	1.72	1.61	1.55

(continued)

TABLE V-7 (continued)

E_2	eV	2.26	2.21	2.25	2.01
g_1	eV	0.32	0.33	0.38	0.35
g_2	eV	0.22	0.24	0.31	0.19
f_1		0.59	0.60	0.68	0.64
f_2		0.15	0.16	0.14	0.11
f_3		0.26	0.24	0.18	0.25
E_b^c	eV	2.27	2.18	2.25	2.04
α		4.2	4.2	4.1	4.0

TABLE V-8

Secondary Parameters of Solvated Electrons in iso-Butanol/Water at Different Temperatures

$\langle 0\|iB\|T_i\rangle$	Code No.	95	95	93	10	91	92
T	K	170	200	250	298	350	378
A_1		0.83	0.86	0.84	0.90	0.84	0.92
A_2		0.61	0.58	0.64	0.59	0.56	0.48
E_1	eV	2.15	2.17	1.94	1.76	1.60	1.45
E_2	eV	2.64	2.68	2.44	2.25	2.20	2.13
g_1	eV	0.40	0.40	0.37	0.38	0.48	0.53
g_2	eV	0.28	0.31	0.28	0.25	0.37	0.39
f_1		0.31	0.32	0.29	0.31	0.36	0.41
f_2		0.16	0.17	0.17	0.14	0.18	0.16
f_3		0.53	0.51	0.54	0.55	0.46	0.43
E_b^c	eV	2.58	2.55	2.36	2.18	2.14	2.08
α		2.8	2.8	2.8	2.6	2.6	2.4

$\langle 10\|iB\|T_i\rangle$	Code No.	135	134	131	132	133
T	K	200	250	298	350	365
A_1		0.97	0.95	0.93	0.95	0.94
A_2		0.51	0.46	0.50	0.45	0.48
E_1	eV	2.14	1.89	1.66	1.50	1.41
E_2	eV	2.71	2.58	2.26	2.14	1.95
g_1	eV	0.41	0.42	0.38	0.38	0.36
g_2	eV	0.28	0.38	0.34	0.35	0.29

(continued)

TABLE V-8 (continued)

f_1		0.39	0.43	0.43	0.48	0.46
f_2		0.14	0.19	0.21	0.21	0.19
f_3		0.47	0.38	0.36	0.31	0.35
E_b^c	eV	2.68	2.55	2.27	2.16	1.95
α		2.8	2.8	2.8	2.9	2.9

$\langle 50 \vert iB \vert T_i \rangle$	Code No.	144	145	146	147
T	K	286	298	325	350
A_1		0.98	0.99	0.99	0.98
A_2		0.34	0.34	0.34	0.32
E_1	eV	1.78	1.75	1.66	1.58
E_2	eV	2.26	2.27	2.16	2.11
g_1	eV	0.34	0.34	0.34	0.35
g_2	eV	0.25	0.27	0.24	0.26
f_1		0.57	0.58	0.59	0.61
f_2		0.15	0.16	0.14	0.15
f_3		0.28	0.26	0.27	0.24
E_b^c	eV	2.22	2.26	2.19	2.09
α		4.0	3.9	3.9	3.8

$\langle 98 \vert iB \vert T_i \rangle$	Code No.	119	118	120	121
T	K	273	298	350	363
A_1		0.99	0.99	1.00	0.99
A_2		0.31	0.32	0.23	0.23
E_1	eV	1.81	1.73	1.61	1.58

(continued)

TABLE V-8 (continued)

E_2	eV	2.37	2.25	2.17	2.20
g_1	eV	0.34	0.34	0.38	0.38
g_2	eV	0.25	0.26	0.22	0.29
f_1		0.62	0.62	0.70	0.70
f_2		0.14	0.15	0.10	0.12
f_3		0.24	0.23	0.20	0.18
E_b^c	eV	2.36	2.26	2.18	2.18
α		4.1	4.2	4.3	4.1

TABLE V-9

Secondary Parameters of Solvated Electrons in 2-Butanol/Water at Different Temperatures

$\langle 0\|2B\|T_i\rangle$	Code No.	100	99	98	156	96	97
T	K	163	200	250	298	350	370
A_1		0.89	0.84	0.86	0.88	0.88	0.87
A_2		0.66	0.69	0.71	0.57	0.53	0.49
E_1	eV	1.88	1.81	1.65	1.51	1.25	1.14
E_2	eV	2.40	2.25	2.13	1.99	1.79	1.65
g_1	eV	0.36	0.33	0.32	0.39	0.40	0.39
g_2	eV	0.29	0.24	0.27	0.26	0.32	0.31
f_1		0.15	0.15	0.18	0.25	0.25	0.25
f_2		0.09	0.10	0.12	0.11	0.12	0.11
f_3		0.76	0.75	0.70	0.64	0.63	0.64
E_b^c	eV	2.37	2.20	2.05	1.93	1.75	1.62
α		1.6	1.7	1.9	1.9	1.7	1.6

$\langle 10\|2B\|T_i\rangle$	Code No.	139	138	136	137
T	K	200	250	298	350
A_1		0.97	0.95	0.93	0.96
A_2		0.33	0.36	0.37	0.43
E_1	eV	1.96	1.75	1.58	1.41
E_2	eV	2.70	2.44	2.23	1.96
g_1	eV	0.45	0.40	0.39	0.32
g_2	eV	0.39	0.40	0.39	0.26

(continued)

TABLE V-9 (continued)

f_1		0.57	0.53	0.53	0.50
f_2		0.17	0.20	0.22	0.18
f_3		0.26	0.27	0.25	0.32
E_b^c	eV	2.73	2.43	2.30	1.96
α		3.4	3.2	3.1	3.0

$\langle 50\|2B\|T_1\rangle$	Code No.	143	140	141	142
T	K	273	298	325	350
A_1		0.97	0.98	0.99	0.97
A_2		0.33	0.32	0.35	0.35
E_1	eV	1.82	1.74	1.61	1.54
E_2	eV	2.31	2.22	2.10	1.96
g_1	eV	0.34	0.35	0.33	0.32
g_2	eV	0.25	0.24	0.22	0.21
f_1		0.60	0.62	0.60	0.58
f_2		0.15	0.14	0.15	0.14
f_3		0.25	0.24	0.25	0.28
E_b^c	eV	2.30	2.26	2.12	1.97
α		4.4	4.3	4.1	4.1

$\langle 98\|2B\|T_1\rangle$	Code No.	115	114	116	117
T	K	273	298	350	370
A_1		0.99	0.99	0.99	1.00
A_2		0.33	0.31	0.27	0.24
E_1	eV	1.80	1.74	1.58	1.54

(continued)

TABLE V-9 (continued)

E_2	eV	2.31	2.28	2.14	2.00
g_1	eV	0.32	0.34	0.36	0.37
g_2	eV	0.25	0.25	0.26	0.21
f_1		0.60	0.64	0.68	0.69
f_2		0.15	0.14	0.14	0.10
f_3		0.25	0.22	0.18	0.21
E_b^c	eV	2.31	2.27	2.16	2.01
α		4.2	4.3	4.3	4.4

TABLE V-10

Secondary Parameters of Solvated Electrons in t-Butanol/Water at Different Temperatures

$\langle 0\|tB\|T_1\rangle$	Code No.	157	101	102
T	K	298	325	350
A_1		0.98	1.00	0.99
A_2		0.53	0.43	0.38
E_1	eV	1.14	1.08	0.97
E_2	eV	1.49	1.59	1.50
g_1	eV	0.26	0.32	0.30
g_2	eV	0.16	0.23	0.27
f_1		0.39	0.47	0.48
f_2		0.13	0.15	0.16
f_3		0.48	0.38	0.36
E_b^c	eV	1.46	1.62	1.52
α		2.6	2.4	2.3

$\langle 10\|tB\|T_1\rangle$	Code No.	103	104	105
T	K	298	325	350
A_1		0.86	0.98	0.96
A_2		0.50	0.47	0.44
E_1	eV	1.31	1.29	1.20
E_2	eV	1.65	1.73	1.70
g_1	eV	0.27	0.30	0.32
g_2	eV	0.17	0.21	0.27

(continued)

TABLE V-10 (continued)

f_1		0.37	0.48	0.49
f_2		0.14	0.16	0.19
f_3		0.49	0.36	0.32
E_b^c	eV	1.56	1.74	1.69
α		3.1	3.0	3.0

$\langle 50\|tB\|T_1\rangle$	Code No.	109	158	107	108
T	K	273	298	350	368
A_1		0.98	0.97	0.97	0.98
A_2		0.32	0.34	0.41	0.31
E_1	eV	1.80	1.68	1.49	1.46
E_2	eV	2.34	2.12	1.87	1.92
g_1	eV	0.34	0.34	0.31	0.34
g_2	eV	0.28	0.23	0.19	0.23
f_1		0.61	0.60	0.55	0.63
f_2		0.16	0.15	0.15	0.13
f_3		0.23	0.25	0.30	0.24
E_b^c	eV	2.35	2.14	1.87	1.92
α		4.2	4.3	4.1	4.1

$\langle 98\|tB\|T_1\rangle$	Code No.	113	110	111	112
T	K	273	298	350	370
A_1		0.99	0.99	0.99	0.99
A_2		0.30	0.33	0.35	0.24
E_1	eV	1.81	1.71	1.57	1.54

(continued)

TABLE V-10 (continued)

E_2	eV	2.30	2.17	2.03	2.14
g_1	eV	0.33	0.33	0.31	0.38
g_2	eV	0.23	0.23	0.22	0.26
f_1		0.62	0.61	0.61	0.70
f_2		0.13	0.14	0.15	0.12
f_3		0.25	0.25	0.25	0.18
E_b^c	eV	2.29	2.12	2.04	2.14
α		4.3	4.3	4.2	4.2

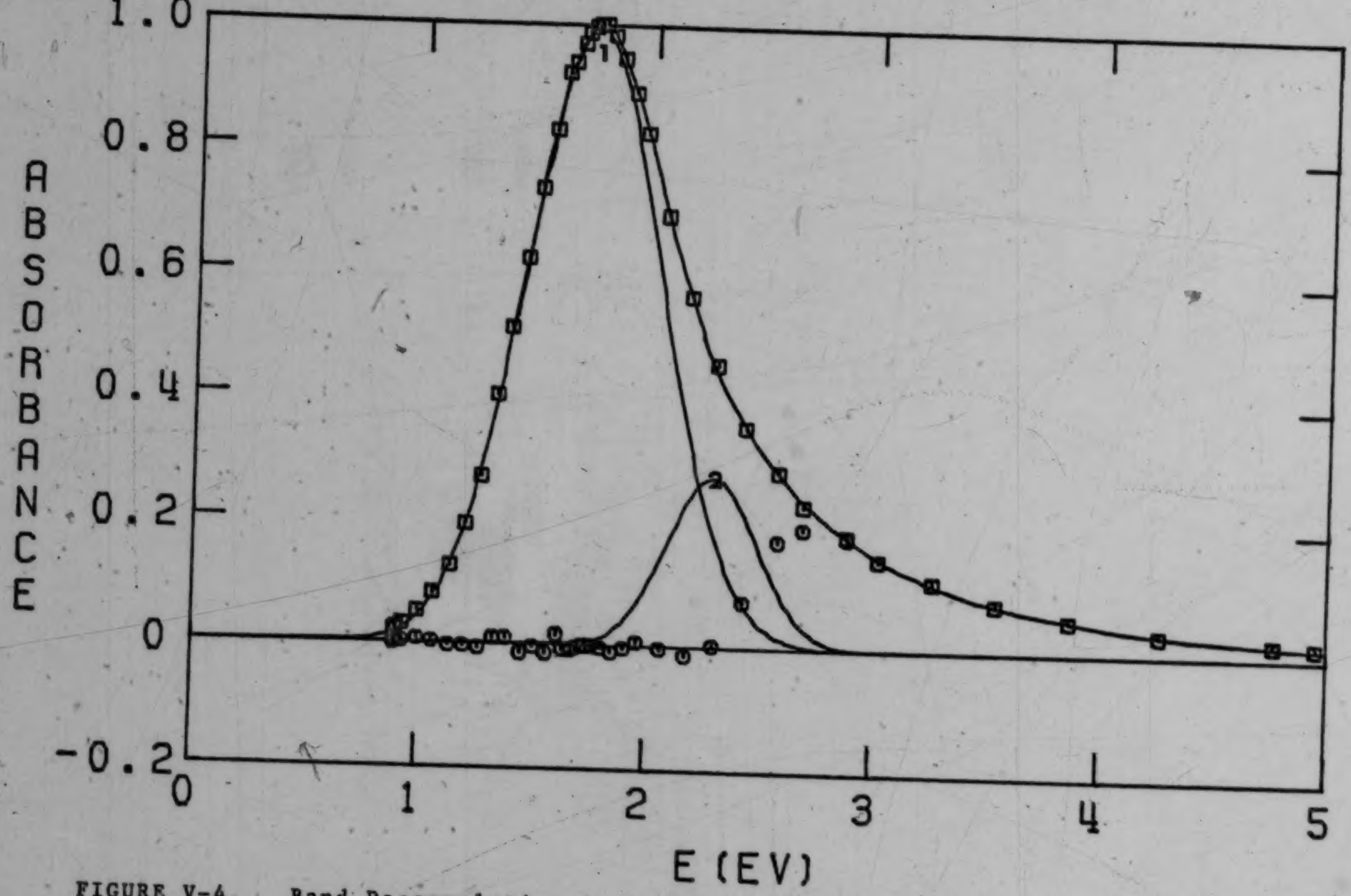

FIGURE V-4. Band Deconvolution in Water at 298K. Symbols as in Figure V-1.

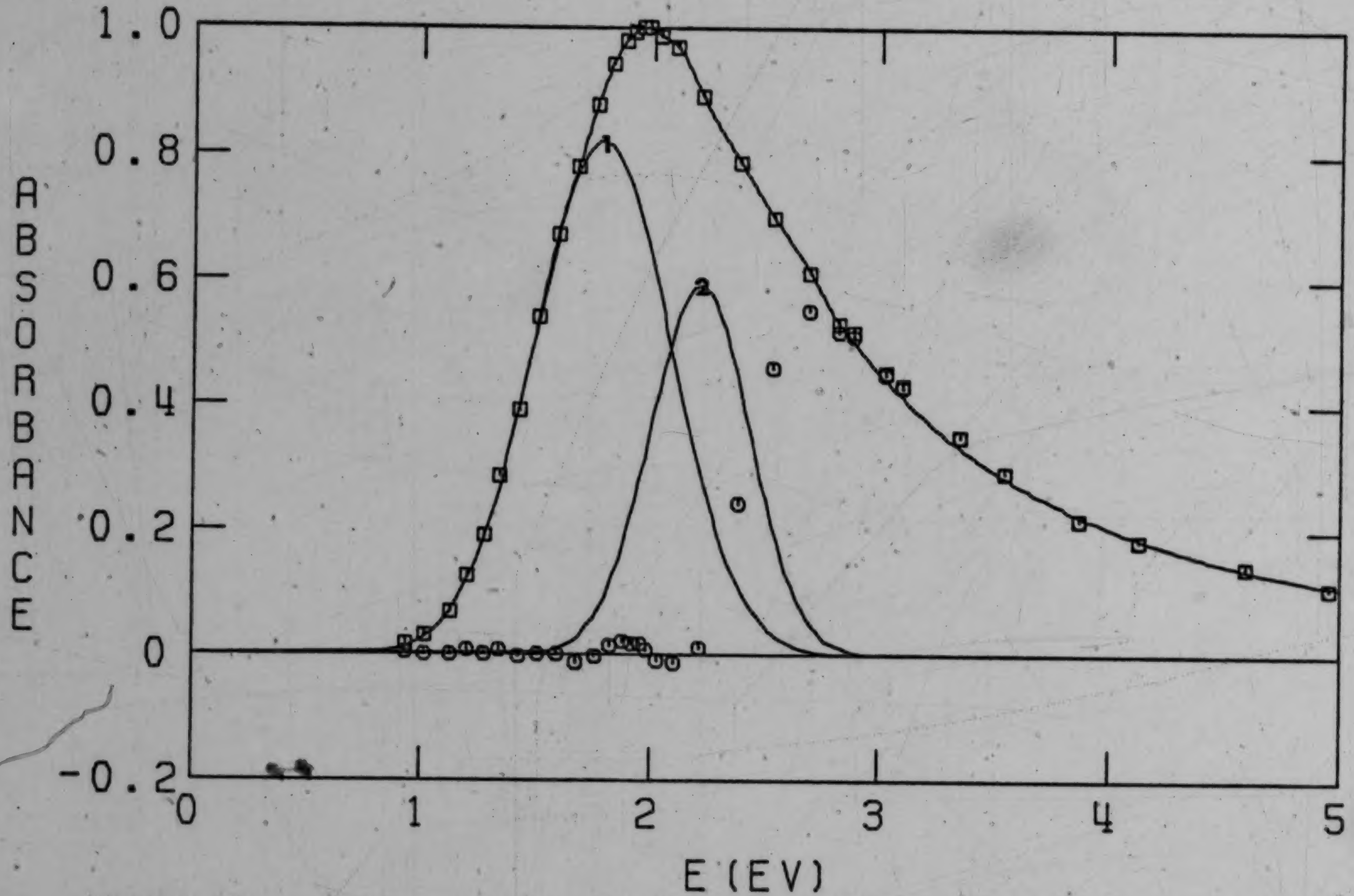

FIGURE V-5. Band Deconvolution in Methanol at 298K. Symbols as in Figure V-1.

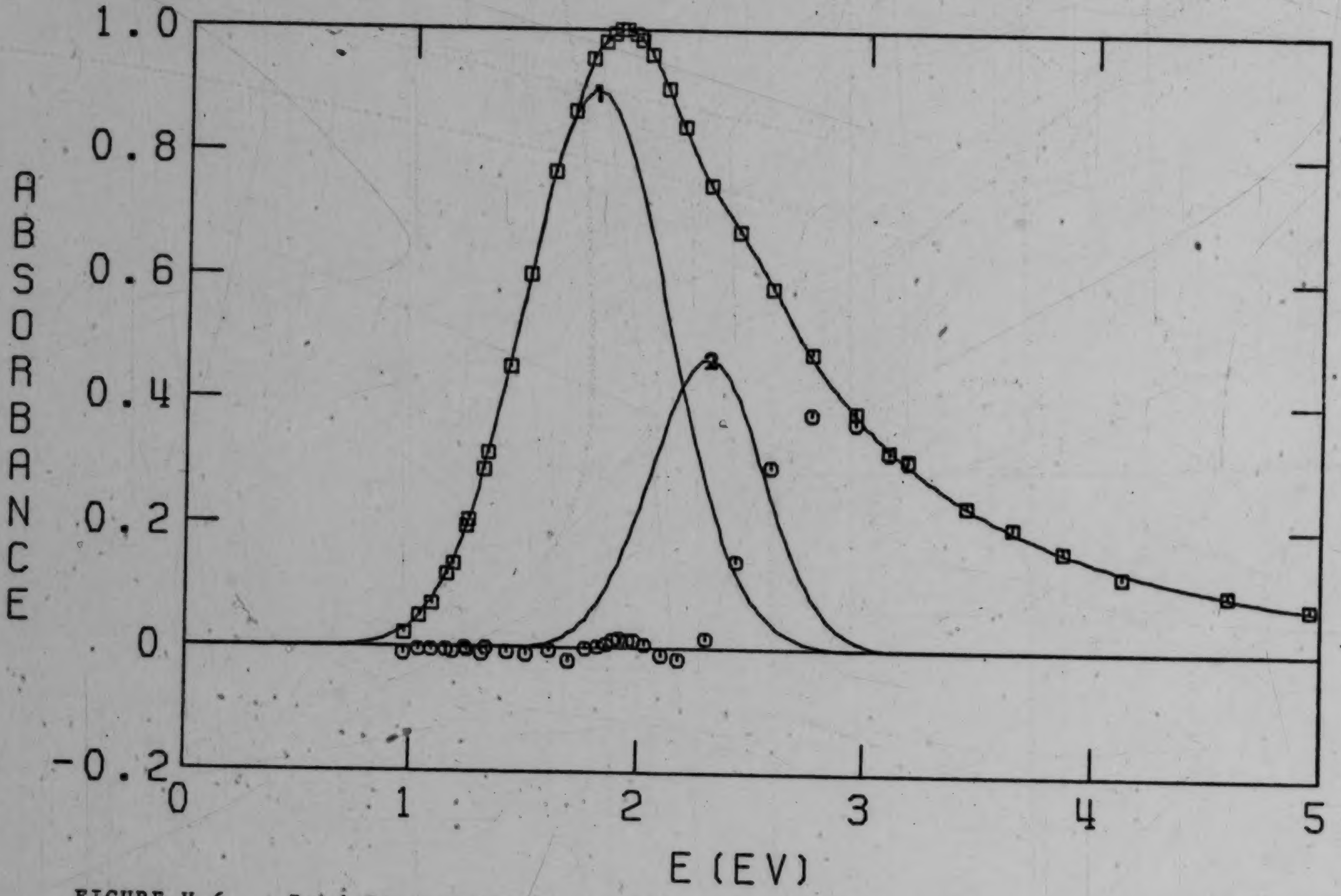

FIGURE V-6. Band Deconvolution in Methanol Containing 10 Mole % Water at 298K. Symbols as in Figure V-1.

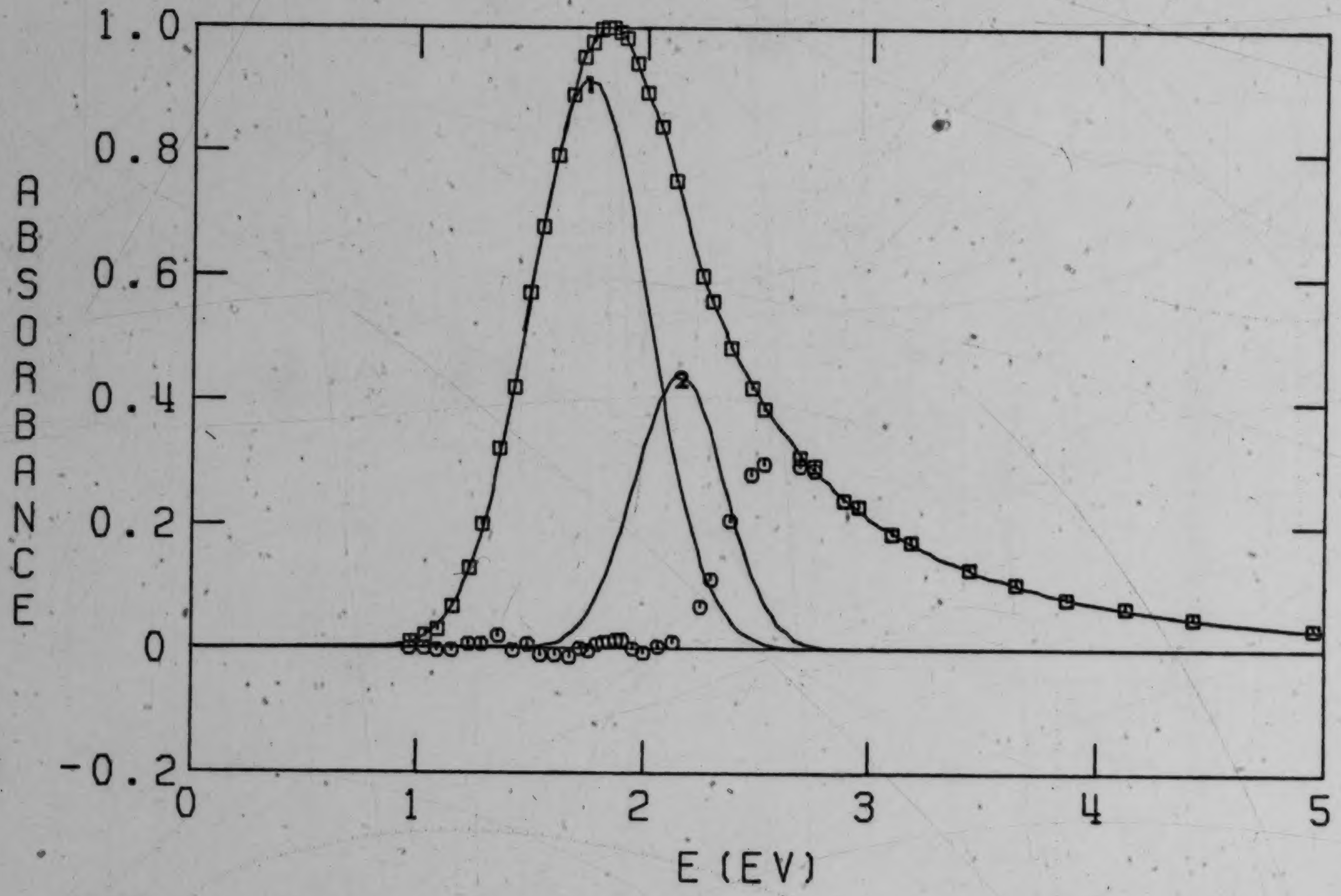

FIGURE V-7. Band Deconvolution in Methanol Containing 50 Mole % Water at 298K. Symbols as in Figure V-1.

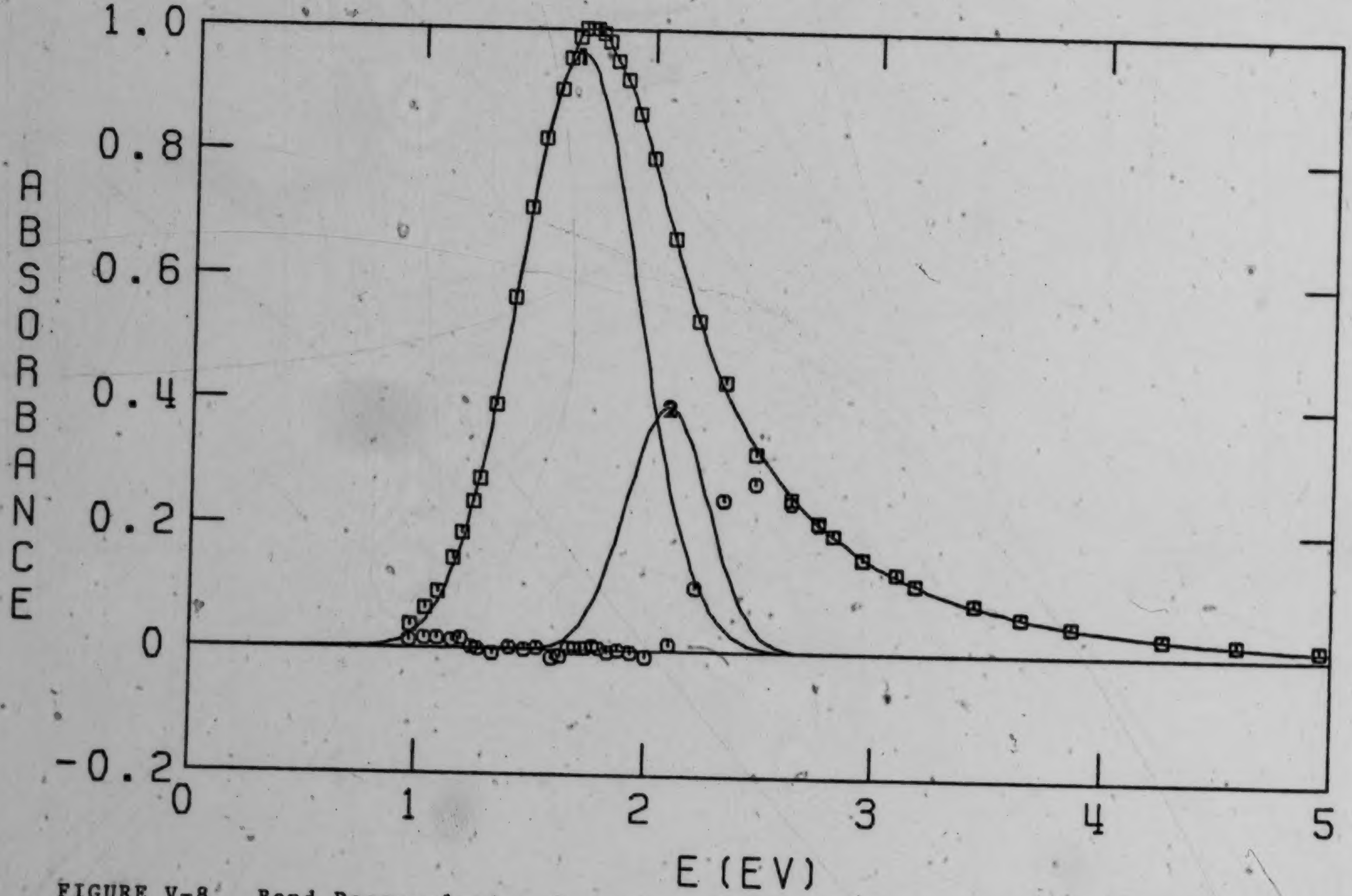

FIGURE V-8. Band Deconvolution in Methanol Containing 98 Mole % Water at 298K Symbols as in Figure V-1.

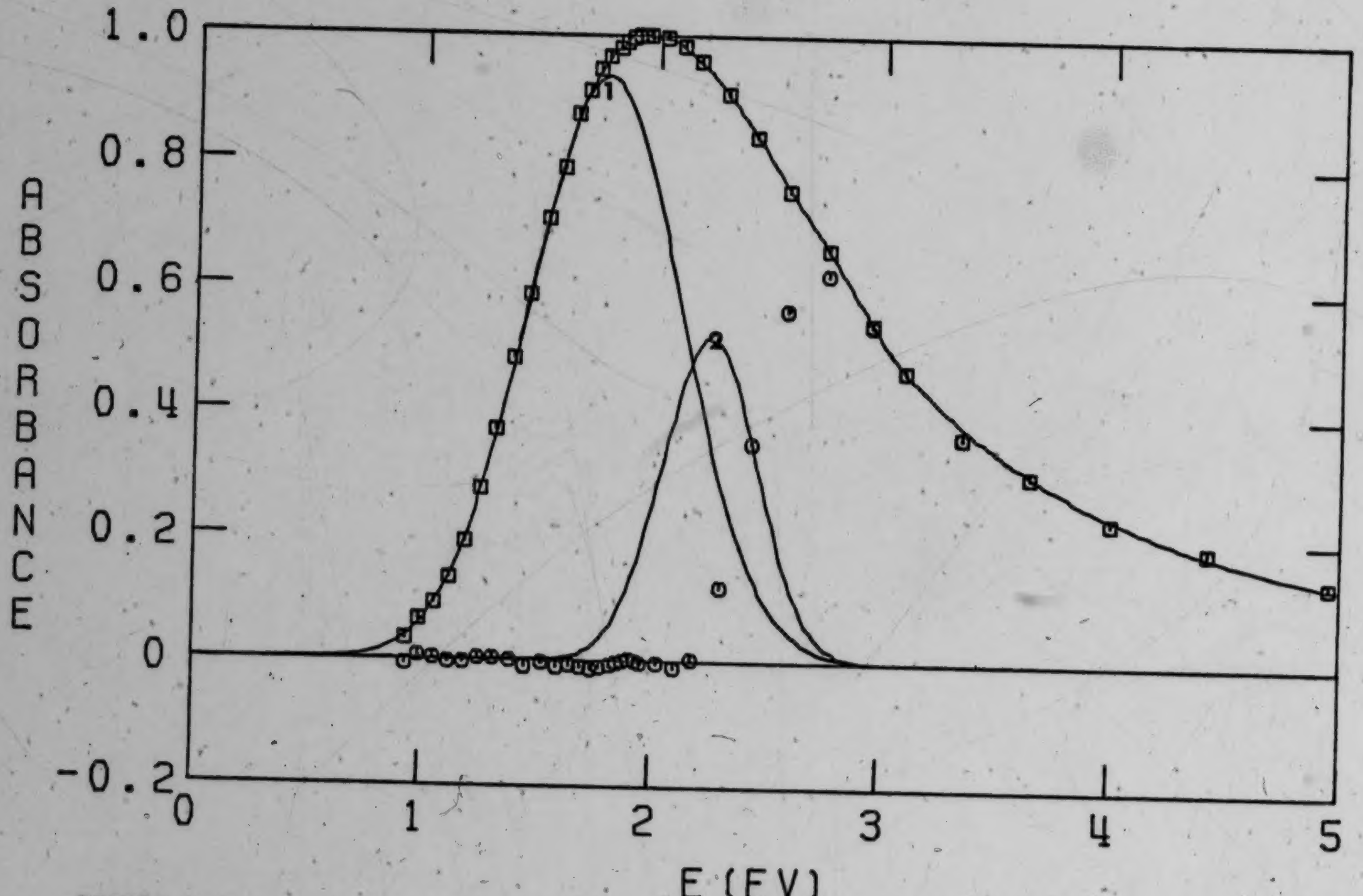

FIGURE V-9. Band Deconvolution in 1-Propanol at 298K. Symbols as in Figure V-1.

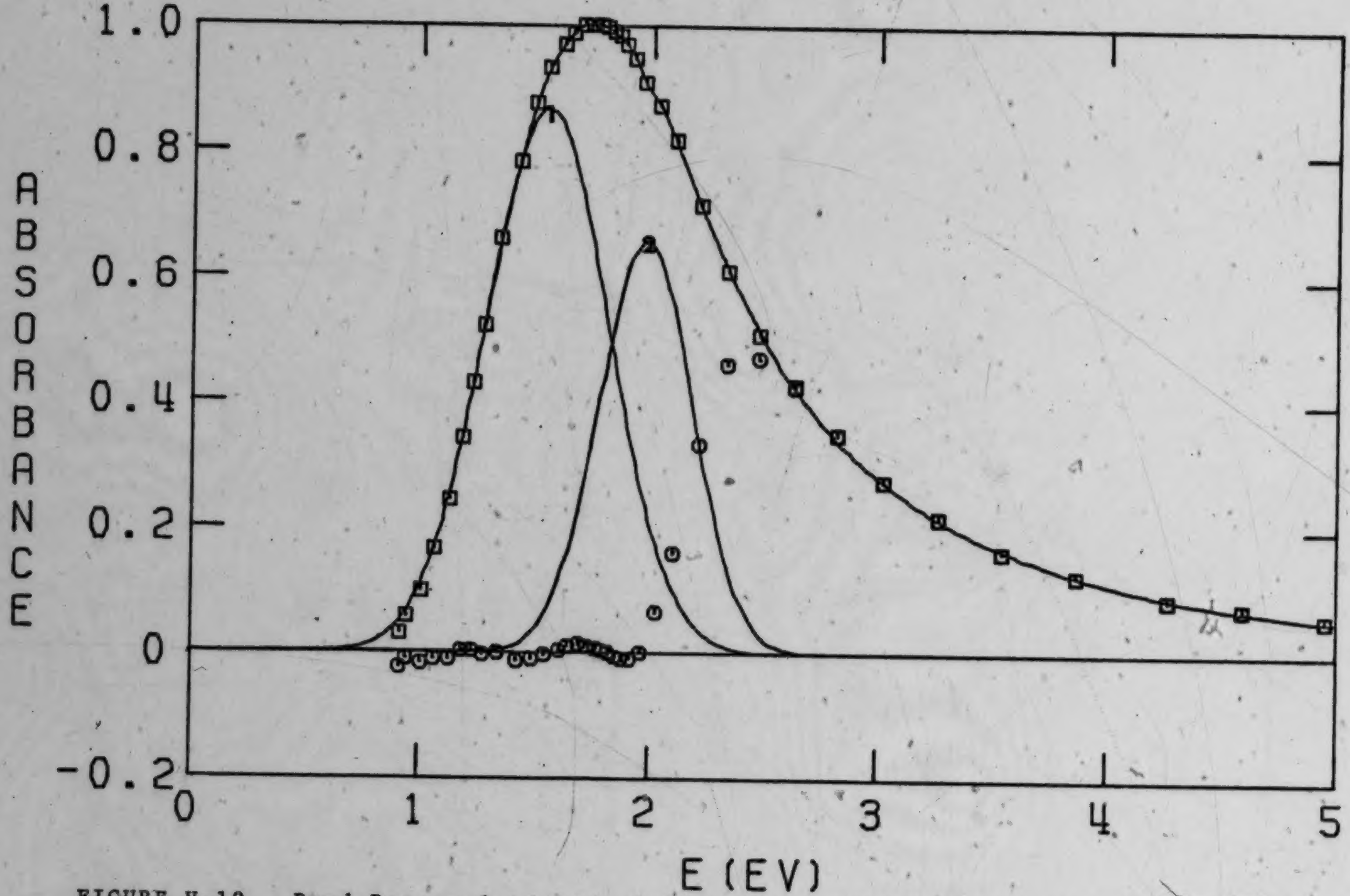

FIGURE V-10. Band Deconvolution in 1-Propanol Containing 10 Mole % Water at 298K. Symbols as in Figure V-1.

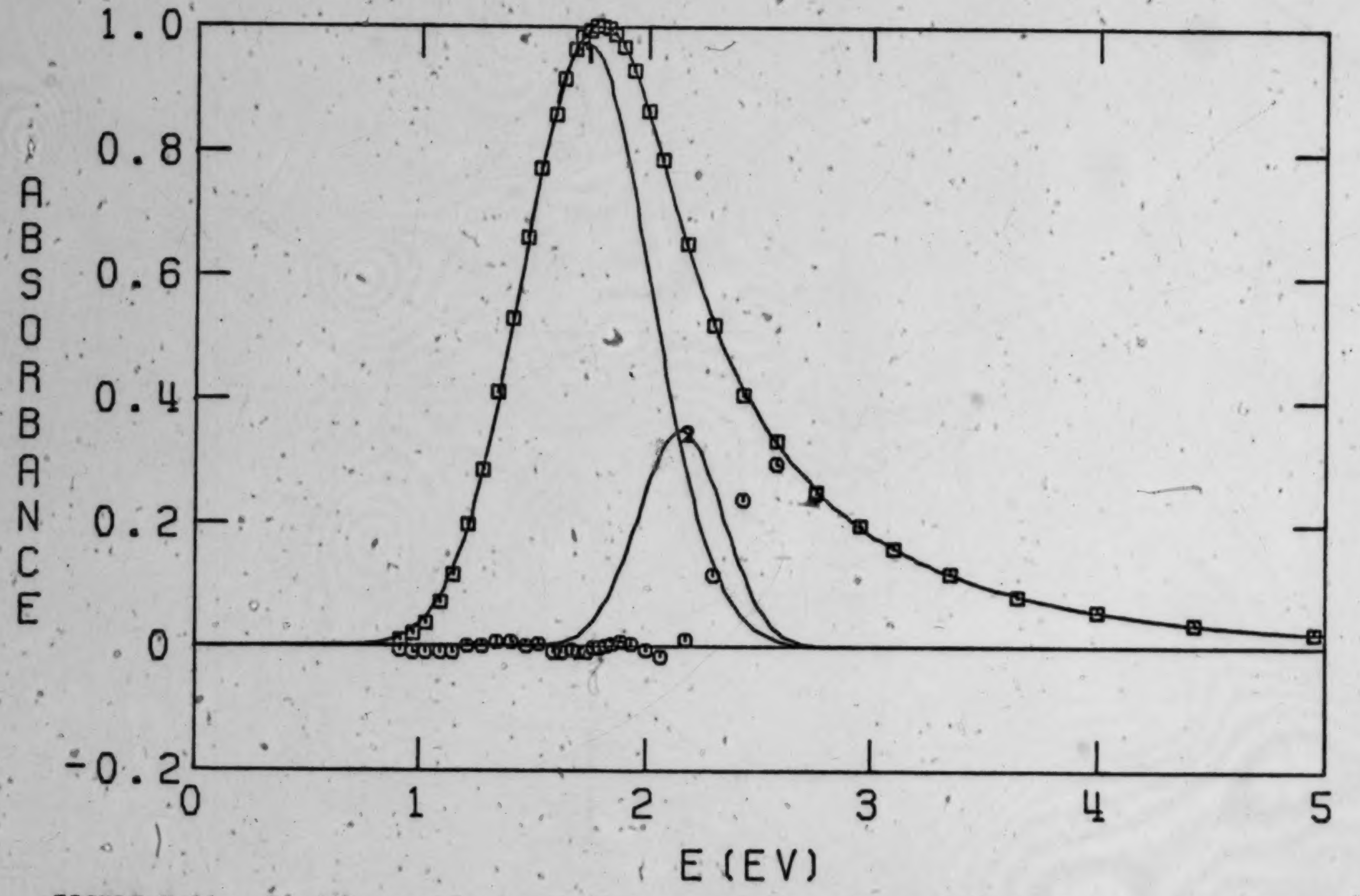

FIGURE V-11. Band Deconvolution in 1-Propanol Containing 50 Mole % Water at 298K.

Symbols as in Figure V-1.

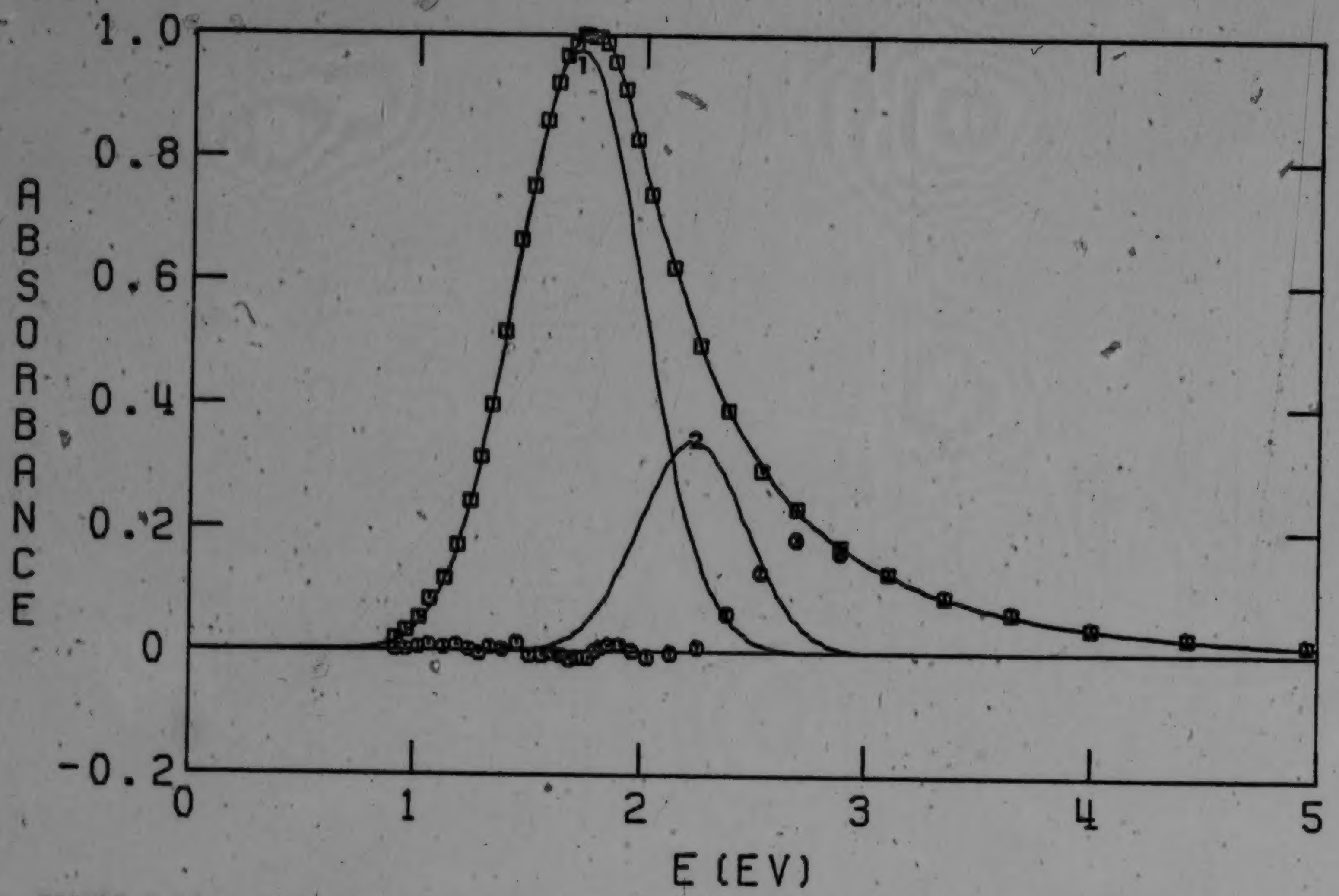

FIGURE V-12. Band Deconvolution in 1-Propanol Containing 98 Mole % Water at 298K. Symbols as in Figure V-1.

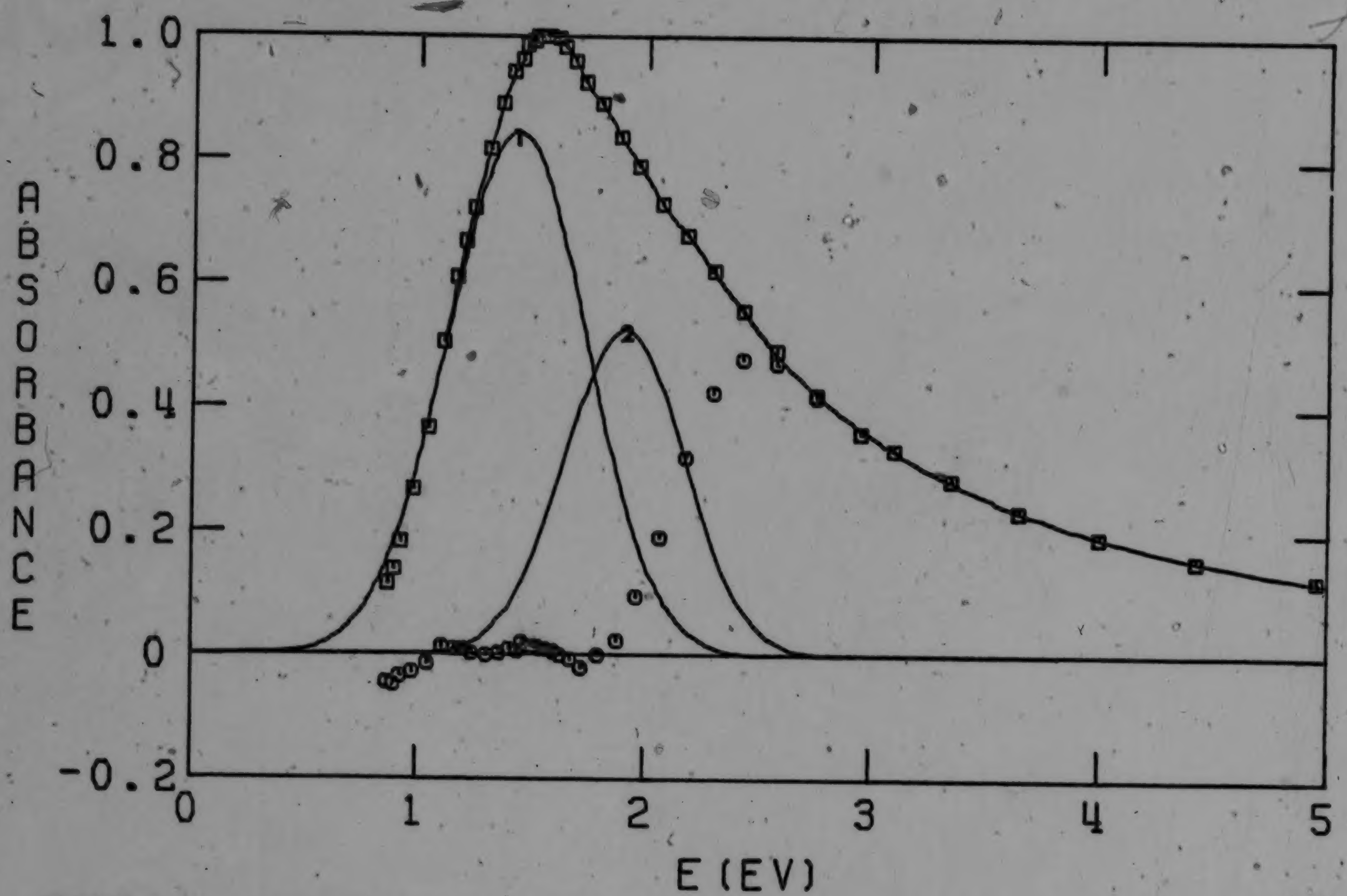

FIGURE V-13. Band Deconvolution in 2-Propanol at 298K. Symbols as in Figure V-1.

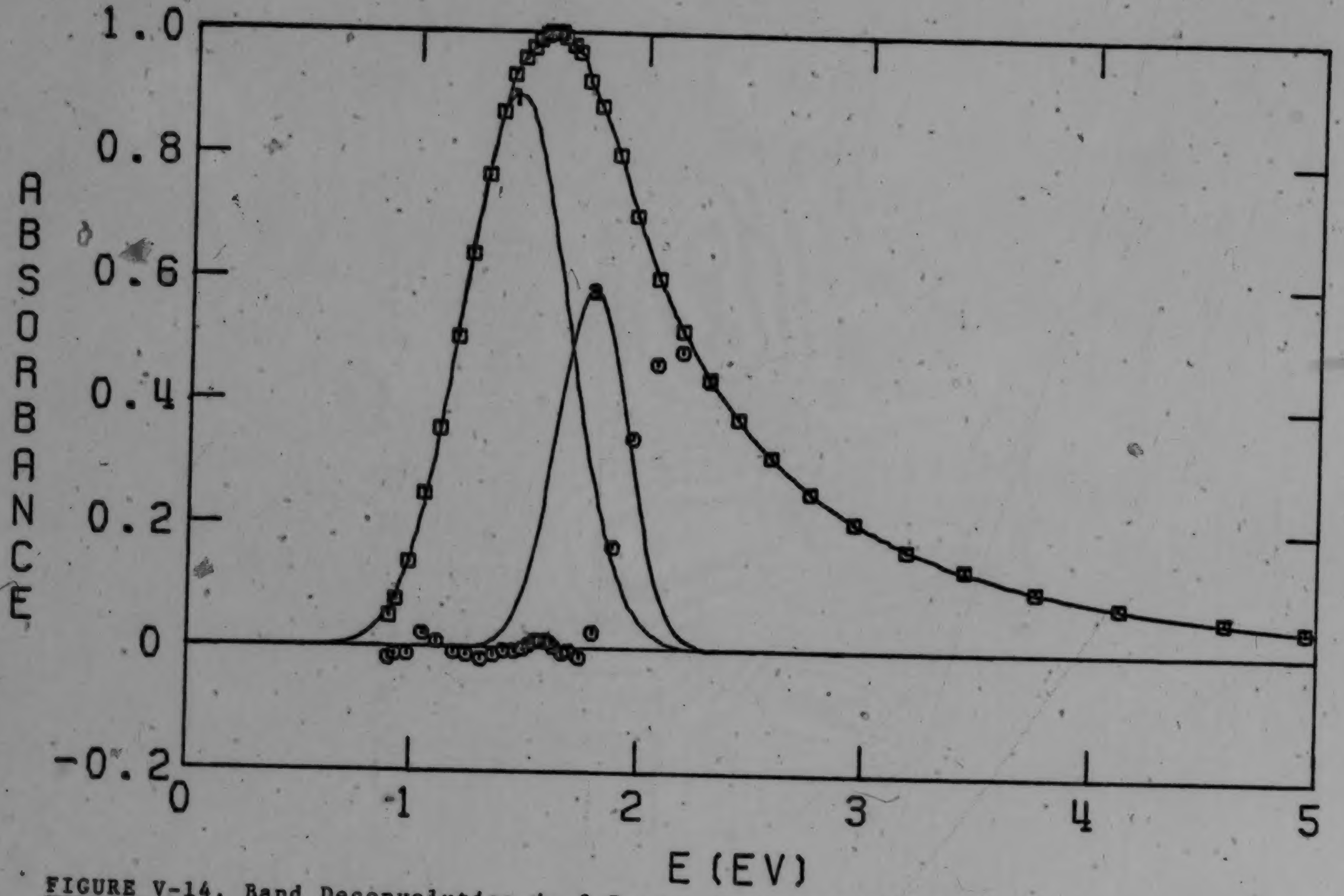

FIGURE V-14. Band Deconvolution in 2-Propanol Containing 10 Mole % Water at 298K. Symbols as in Figure V-1.

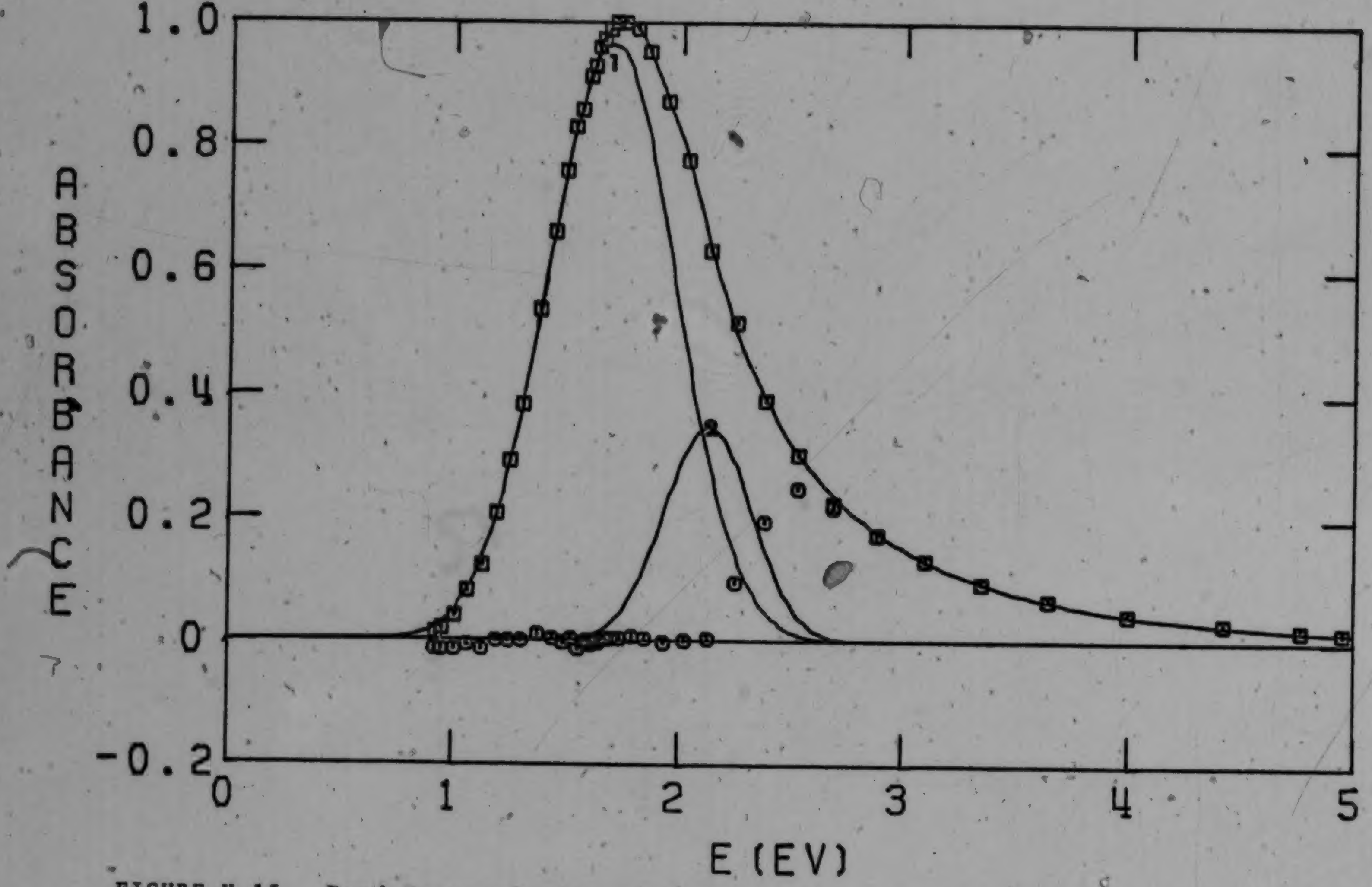

FIGURE V-15. Band Deconvolution in 2-Propanol Containing 50 Mole % Water at 298K. Symbols as in Figure V-1.

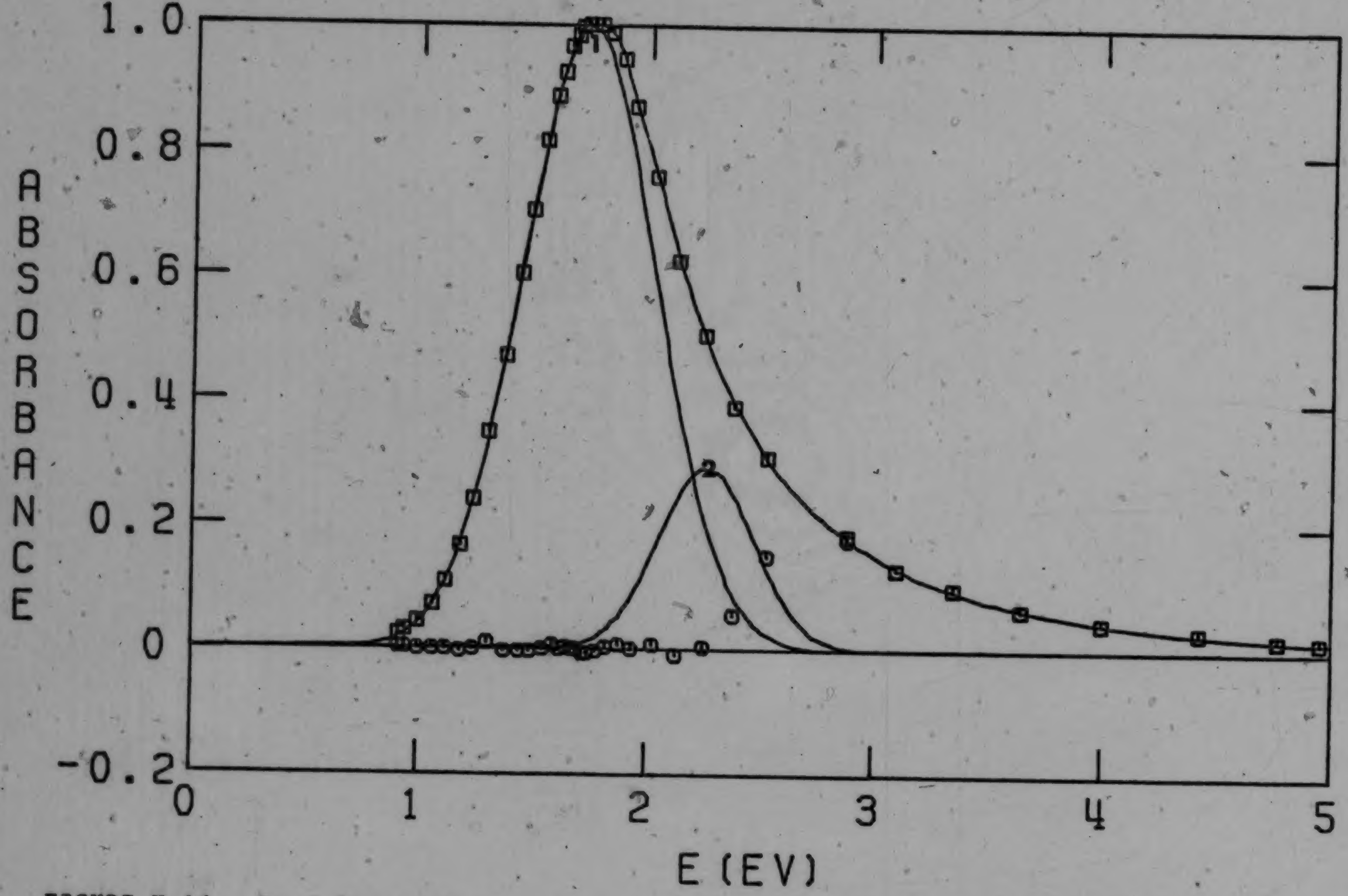

FIGURE V-16. Band Deconvolution in 2-Propanol Containing 98 Mole % Water at 298K.

Symbols as in Figure V-1.

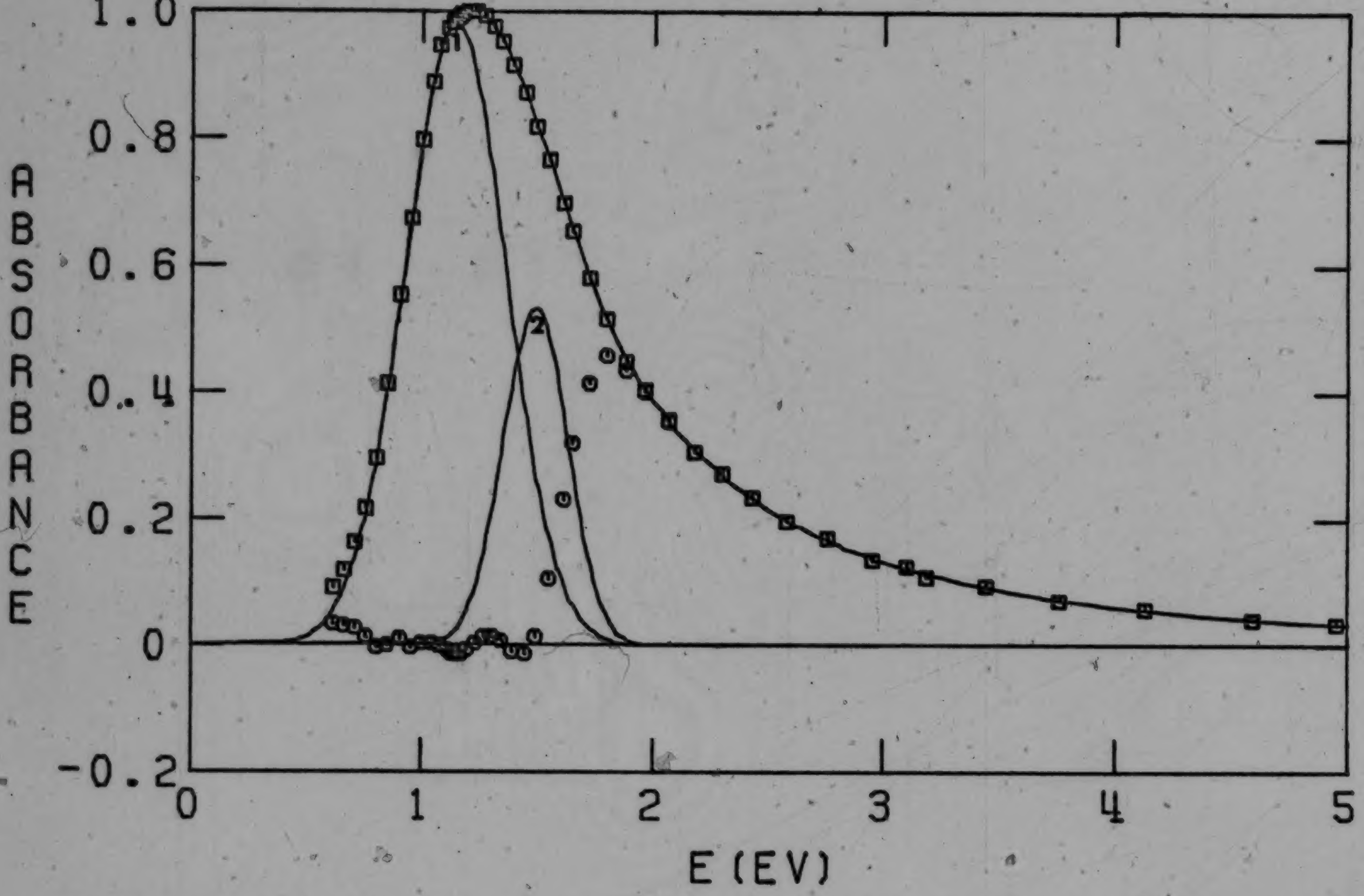

FIGURE V-17. Band Deconvolution in t-Butanol at 298K. Symbols as in Figure V-1.

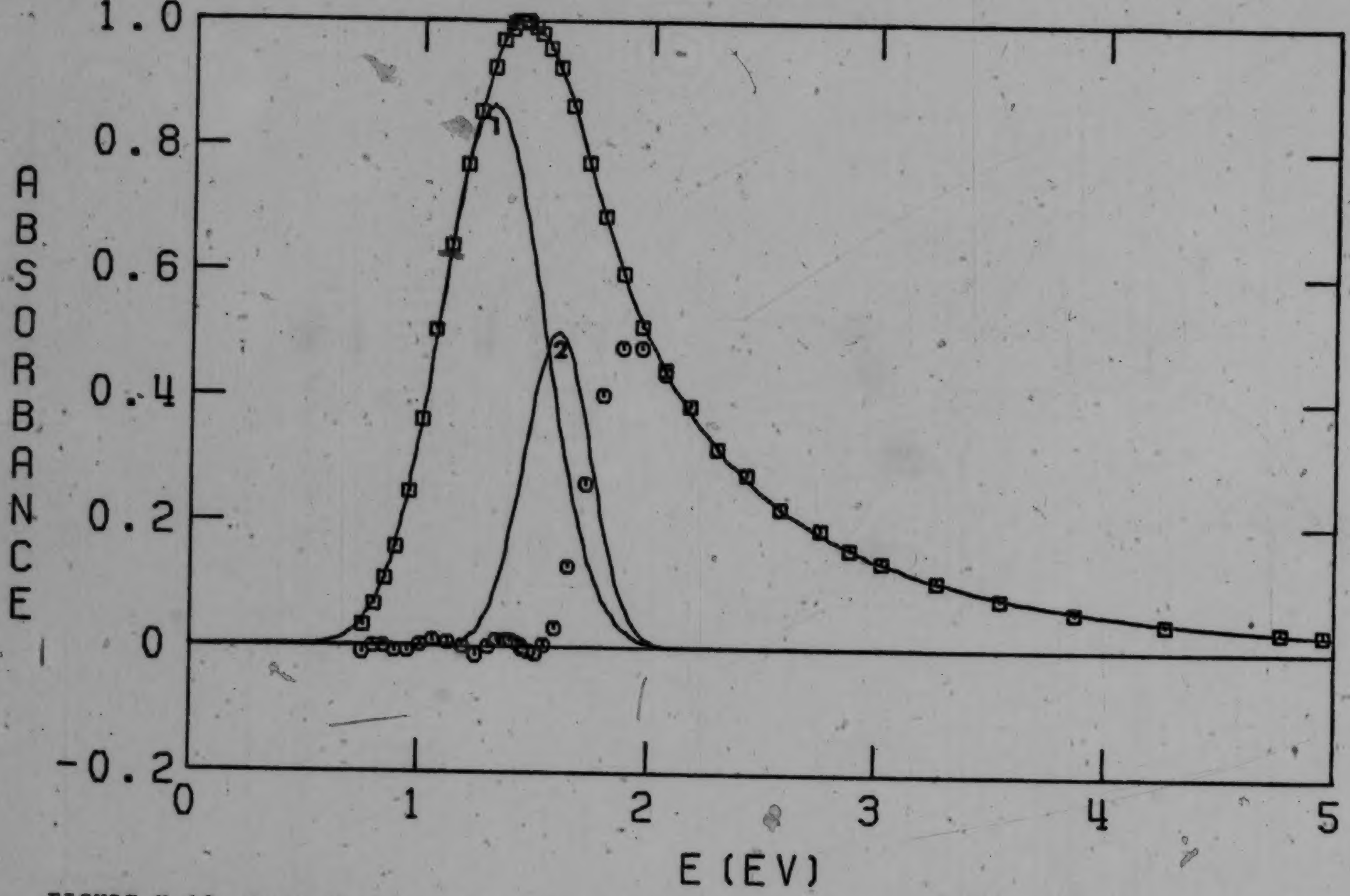

FIGURE V-18. Band Deconvolution in t-Butanol Containing 10 Mole % Water at 298K. Symbols as in Figure V-1.

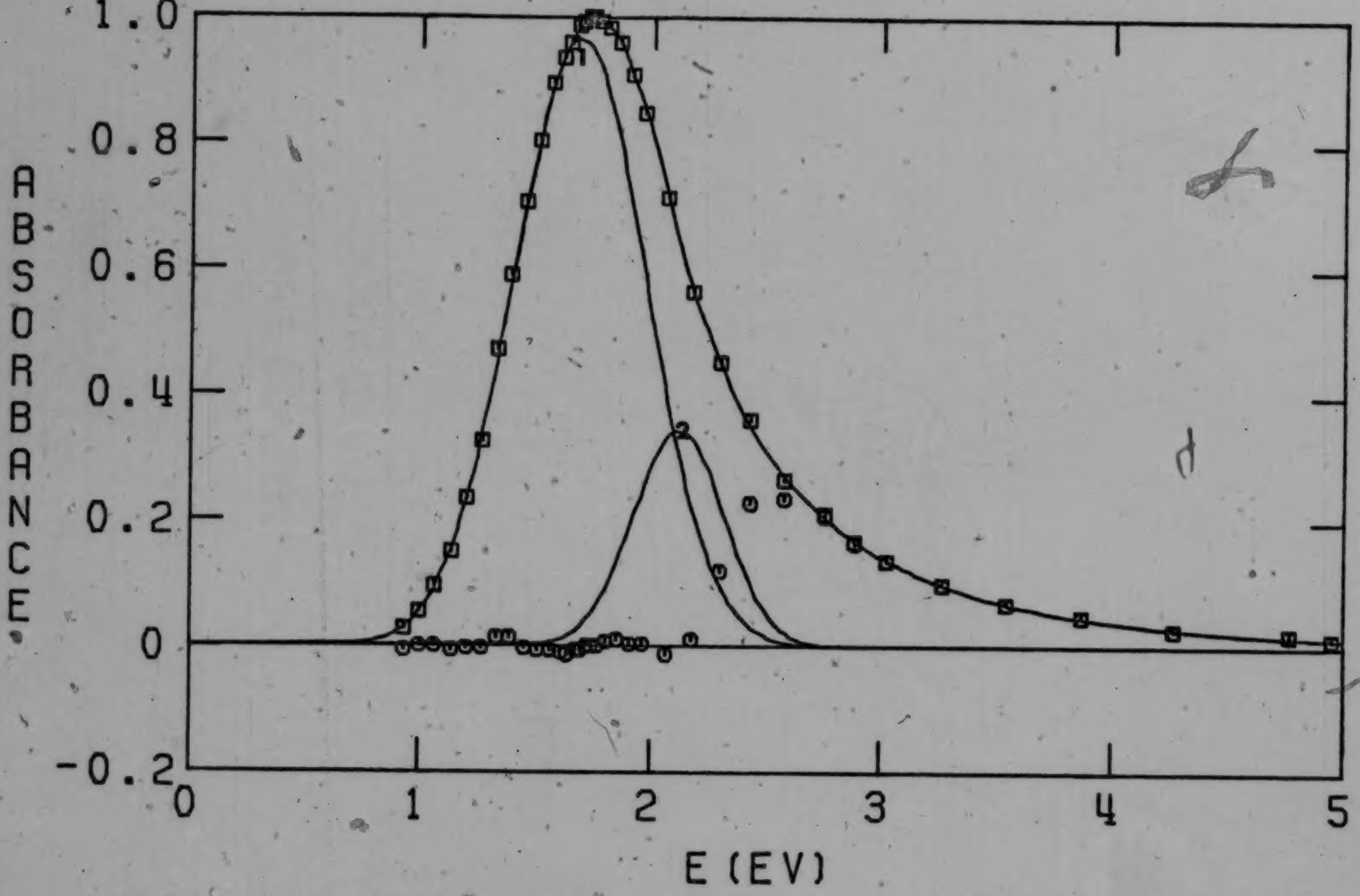

FIGURE V-19. Band Deconvolution in t-Butanol Containing 50 Mole % Water at 298K.

Symbols as in Figure V-1.

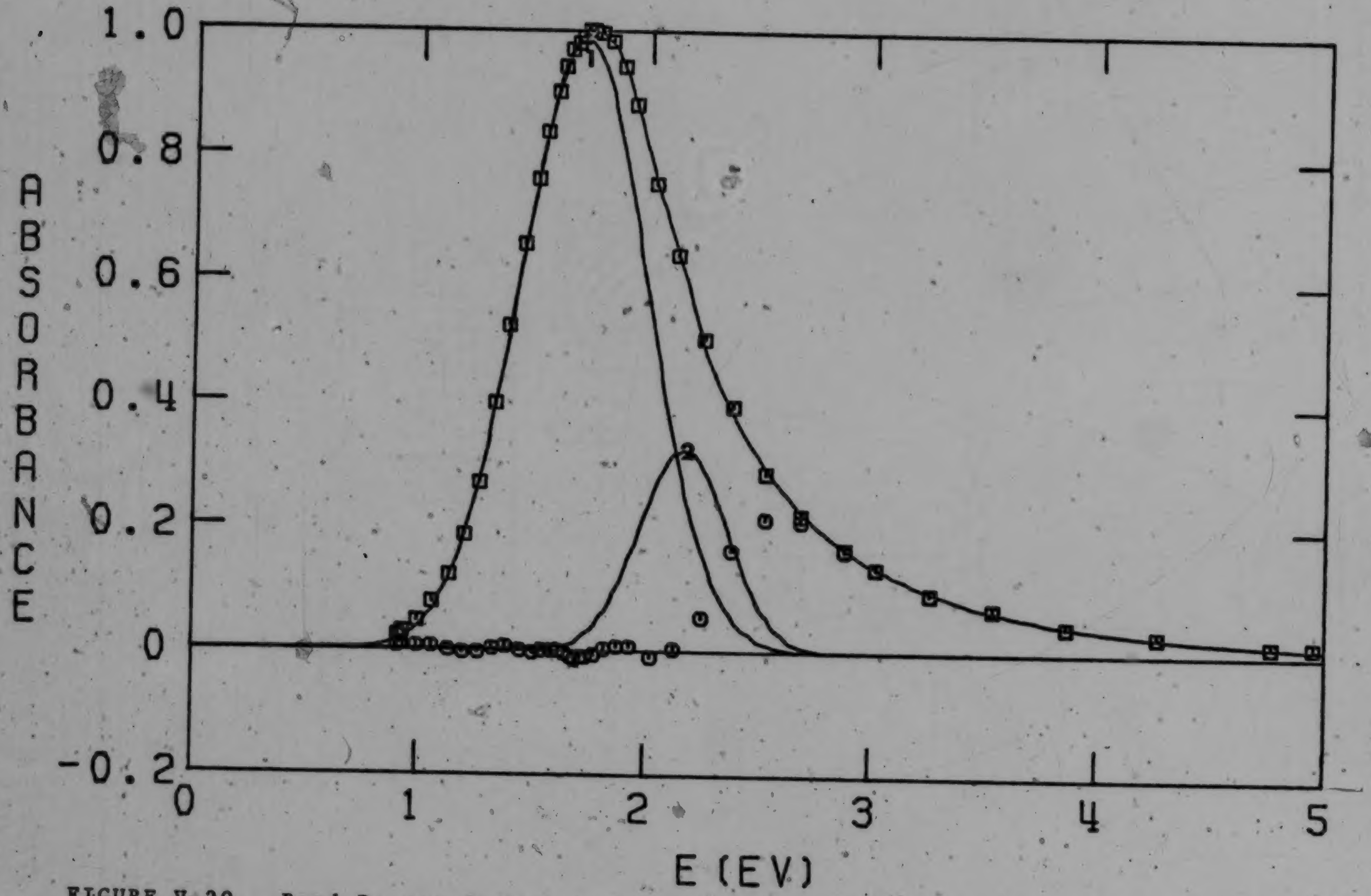

FIGURE V-20. Band Deconvolution in t-Butanol Containing 98 Mole % Water at 298K. Symbols as in Figure V-1.

B. High Energy Side of the Absorption Spectra

For the high energy side of the spectra, the values of α in $A/A_{max} = \text{constant}\cdot E^{-\alpha}$, obtained by the method described on page 76, are listed in Tables V-2 to -10. Lugo and Delahay (270) found that α, for 3-methylpentane glass and for liquids tetrahydrofuran and hexamethylphosphoric triamide, is 8/3. Jou and Freeman (85, 86) found that α is around 3 and 4 for alcohols and water, respectively. The values obtained in this study at 298K for the alcohol/water mixtures are shown in Table V-11. The values for the alcohols are between 2 and 3, the value for water is 4, and those for the solutions are intermediate.

C. Area Measurements

In order to compare for relative contribution of each deconvoluted band to the observed absorption band, the area under each band has been calculated (see pages 76 and 81). The area ratio, f, of each resolved band to the total observed spectrum is listed in Tables V-2 to -10.

D. The Secondary Parameters

The representative plots of the secondary parameters (listed in Section A), such as E_1, E_2, g_1, g_2, and $f_i/f_i^{H_2O}$ (i = 1, 2, 3) against composition are

TABLE V-11

The Values of α for Alcohol/Water Mixtures at 298K*

Mole % H_2O Alcohols	0	10	50	98	100
M	2.7	3.1	3.6	4.3	4.0
E	2.3	2.6	3.9	4.4	4.0
1P	2.6	3.2	3.9	4.3	4.0
2P	2.1	3.0	4.2	4.2	4.0
1B	2.6	2.8	3.7	4.2	4.0
iB	2.6	2.9	3.9	4.2	4.0
2B	1.9	3.1	4.3	4.3	4.0
tB	2.6	3.1	4.3	4.3	4.0

---

* The symbols used in this table are:

M for methanol; E for ethanol; 1P for 1-propanol; 2P for 2-propanol; 1B for 1-butanol; iB for iso-butanol; 2B for 2-butanol, and tB for t-butanol.

shown in Figures V-21 to -27. The trends in E_1 and E_2 (Figures V-21 and -22) are similar to those in E_{Amax} (Figure IV-4). With the exception of the 2-propanol solutions, the trends in g_1 (Figure V-23) are also somewhat similar to those in E_{Amax}. However, the uncertainties in the g_2 values render possible correlations obscure (Figure V-24). Figure V-25 shows that the behavior of $f_1/f_1^{H_2O}$ as a function of composition, seems to be slightly concave downward as mole % water increases. From Figure V-26, one can see that except for 1-propanol/water mixtures, composition dependence of $f_2/f_2^{H_2O}$ has an inverted U shape. Figure V-27 shows that the trend for the behavior of $f_3/f_3^{H_2O}$ as a function of composition is concave upward with increasing mole % water.

Since it is in the developing stage to choose appropriate constraints, the parameters obtained from this type of deconvolution will not be discussed further. How to eliminate the "subjective" factor in deconvolution and obtain parameters more useful for insight into electron solvation is a problem for future study.

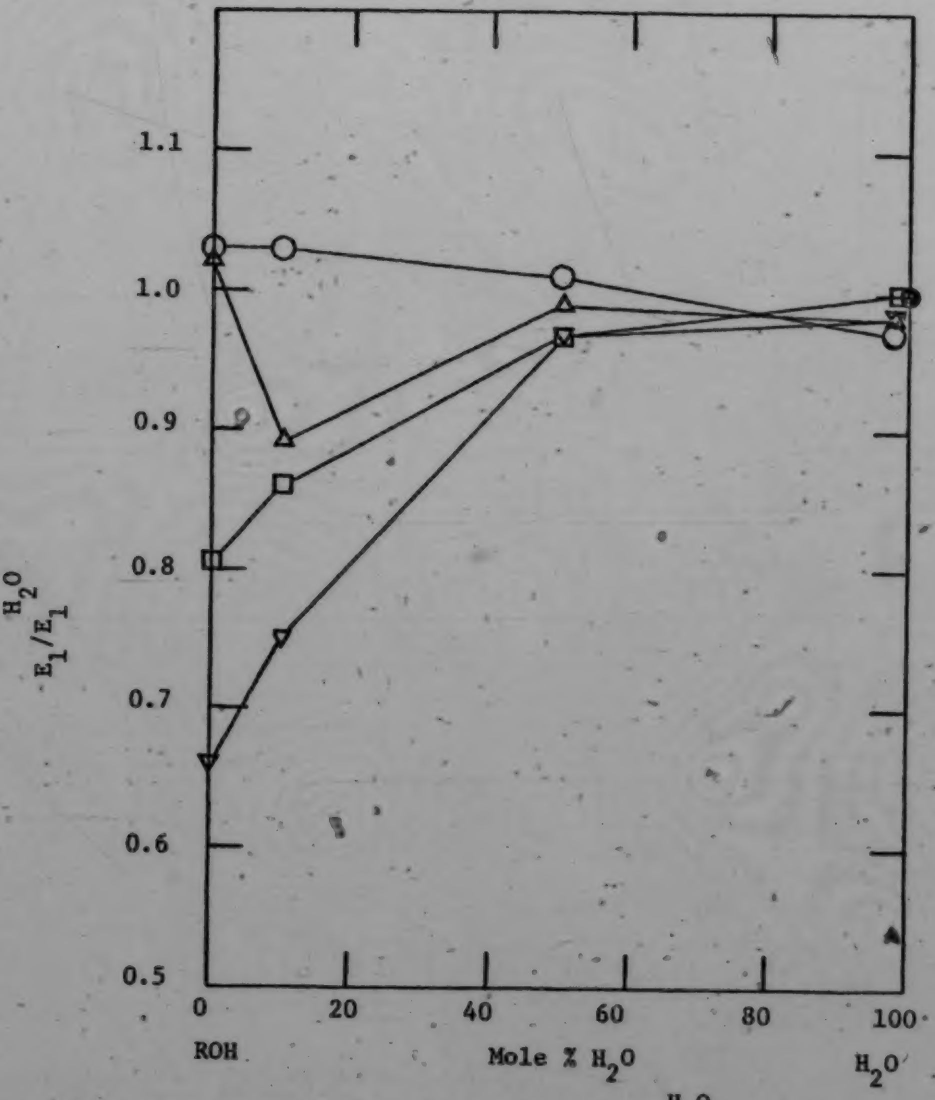

FIGURE V-21. Composition Dependence of $E_1/E_1^{H_2O}$ for Alcohol/Water Mixtures at 298K.

●, Water; ○, Methanol; △, 1-Propanol; □, 2-Propanol; ▽, t-Butanol.

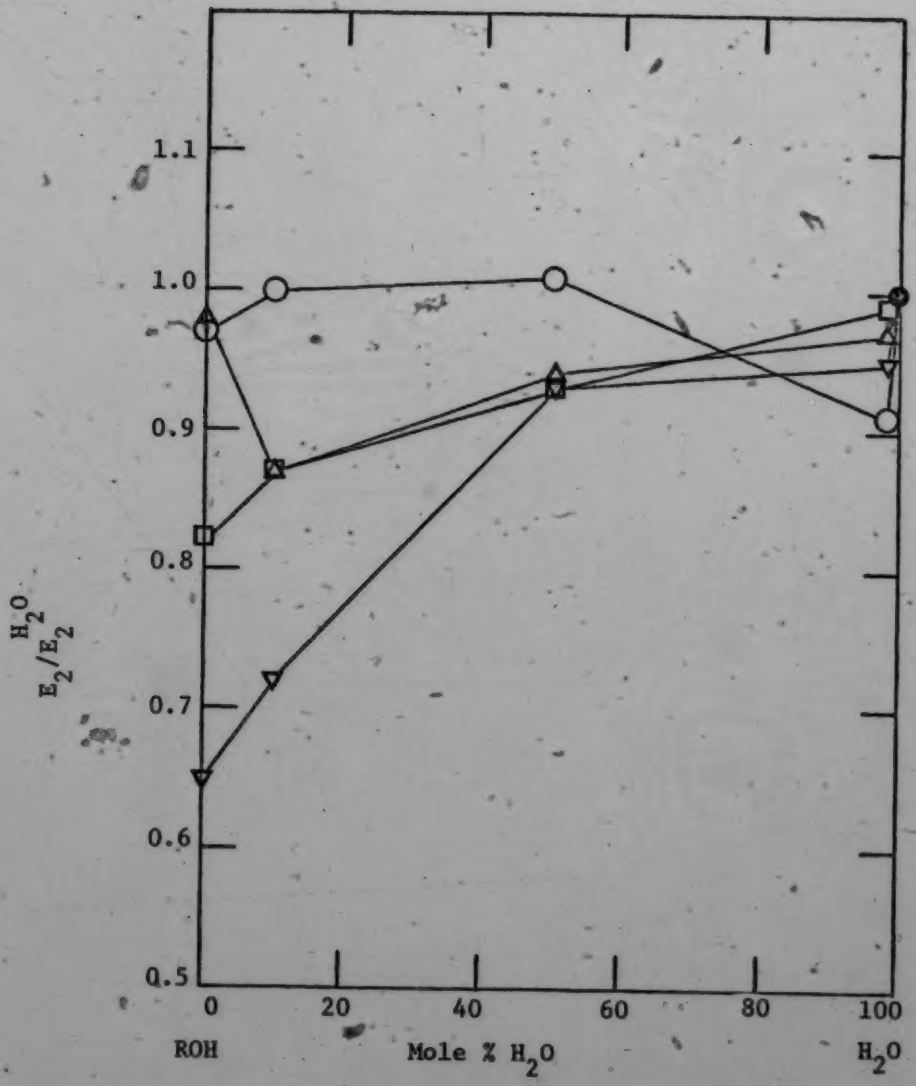

FIGURE V-22. Composition Dependence of $E_2/E_2^{H_2O}$ for Alcohol/ Water Mixtures at 298K.

●, Water; ○, Methanol; △, 1-Propanol; □, 2-Propanol; ▽, t-Butanol.

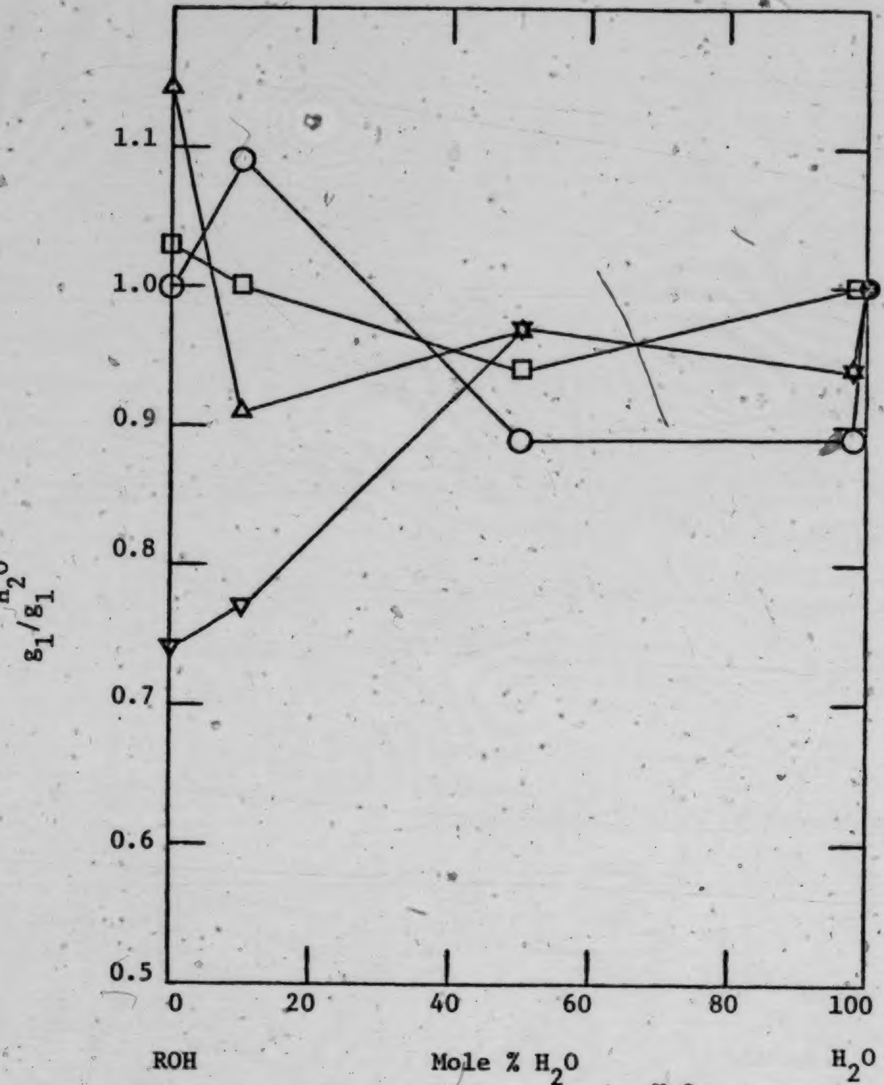

FIGURE V-23. Composition Dependence of $g_1/g_1^{H_2O}$ for Alcohol/ Water Mixtures at 298K.

●, Water; ○, Methanol; △, 1-Propanol; □, 2-Propanol; ▽, t-Butanol.

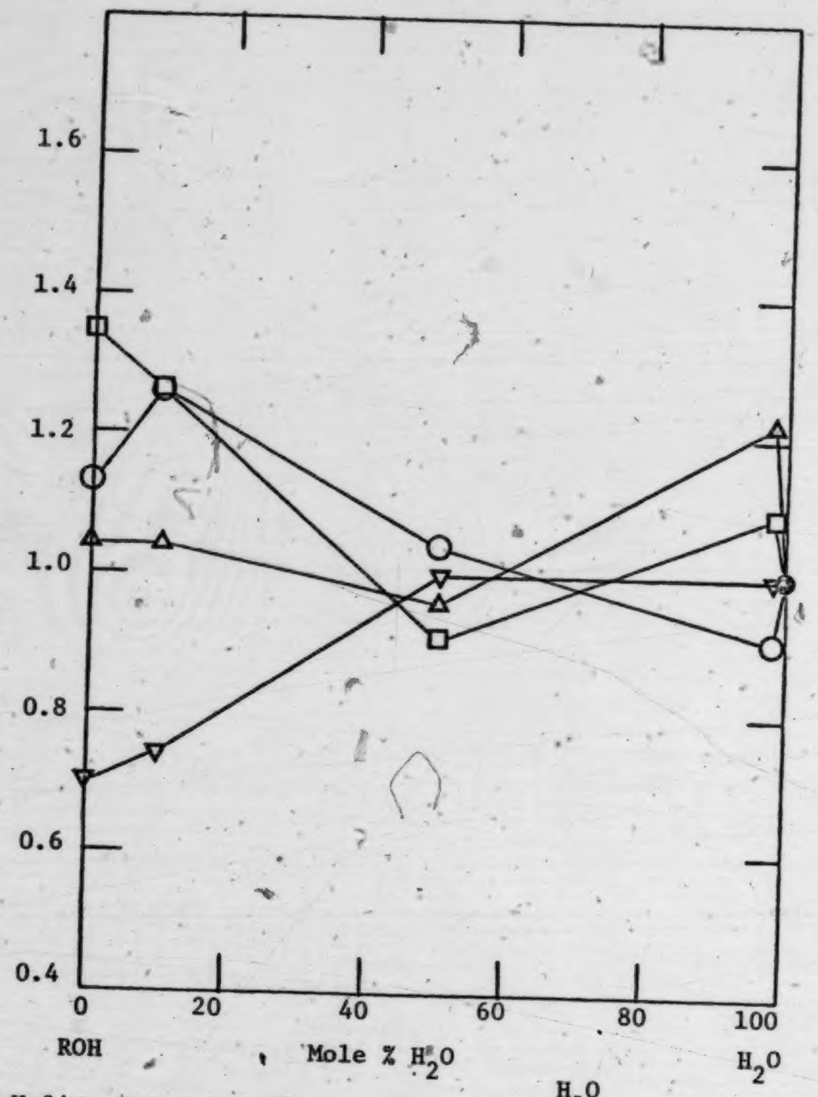

FIGURE V-24. Composition Dependence of $g_2/g_2^{H_2O}$ for Alcohol/ Water Mixtures at 298K.

●, Water; ○, Methanol; △, 1-Propanol; □, 2-Propanol; ▽, t-Butanol.

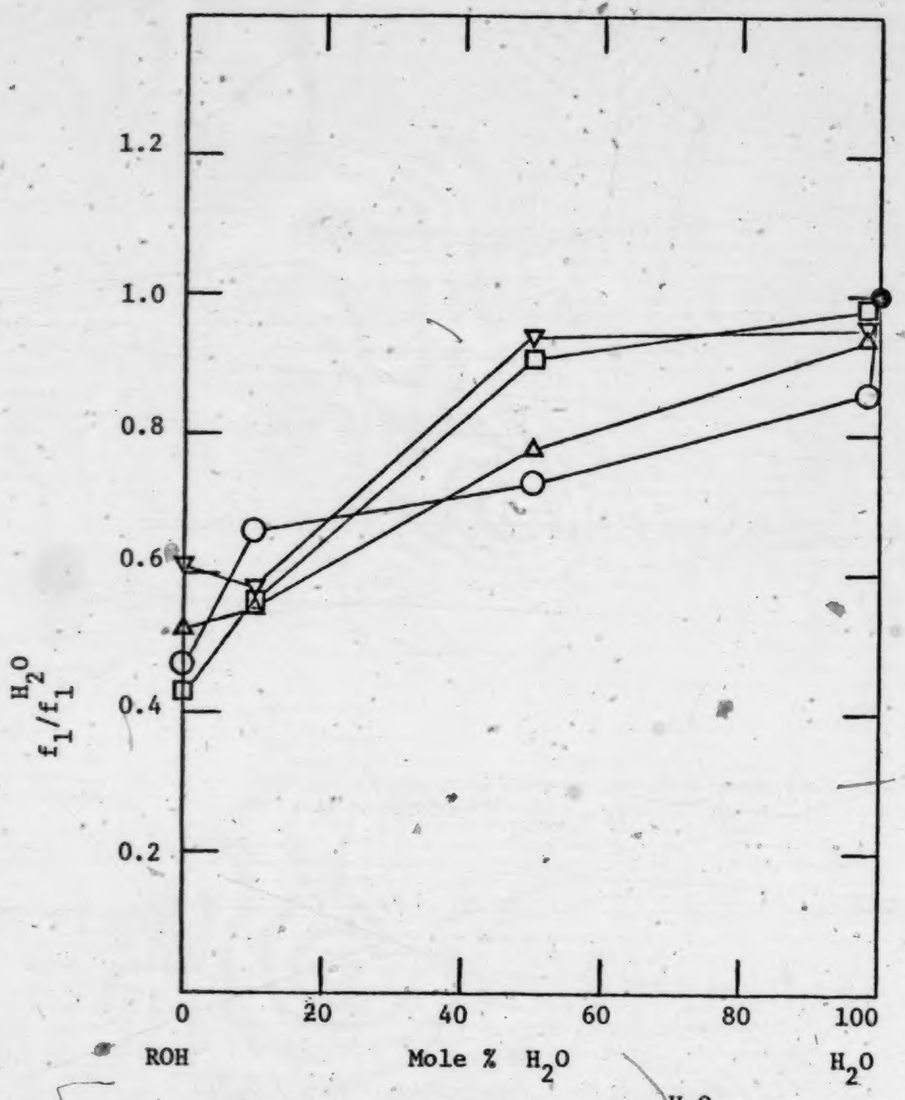

FIGURE V-25. Composition Dependence of $f_1/f_1^{H_2O}$ for Alcohol/ Water Mixtures at 298K.

●, Water; ○, Methanol; △, 1-Propanol; □, 2-Propanol; ▽, t-Butanol.

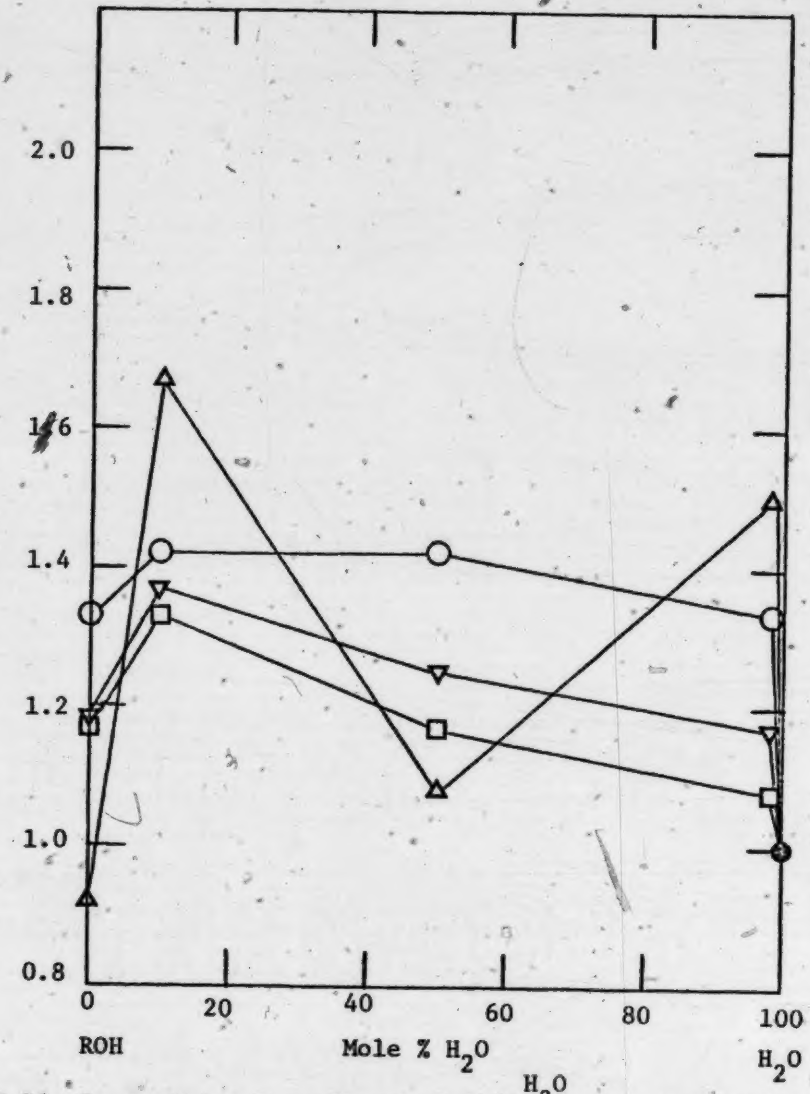

FIGURE V-26. Composition Dependence of $f_2/f_2^{H_2O}$ for Alcohol/ Water Mixtures at 298K.

●, Water; ○ , Methanol; △, 1-Propanol; □, 2-Propanol; ▽, t-Butanol.

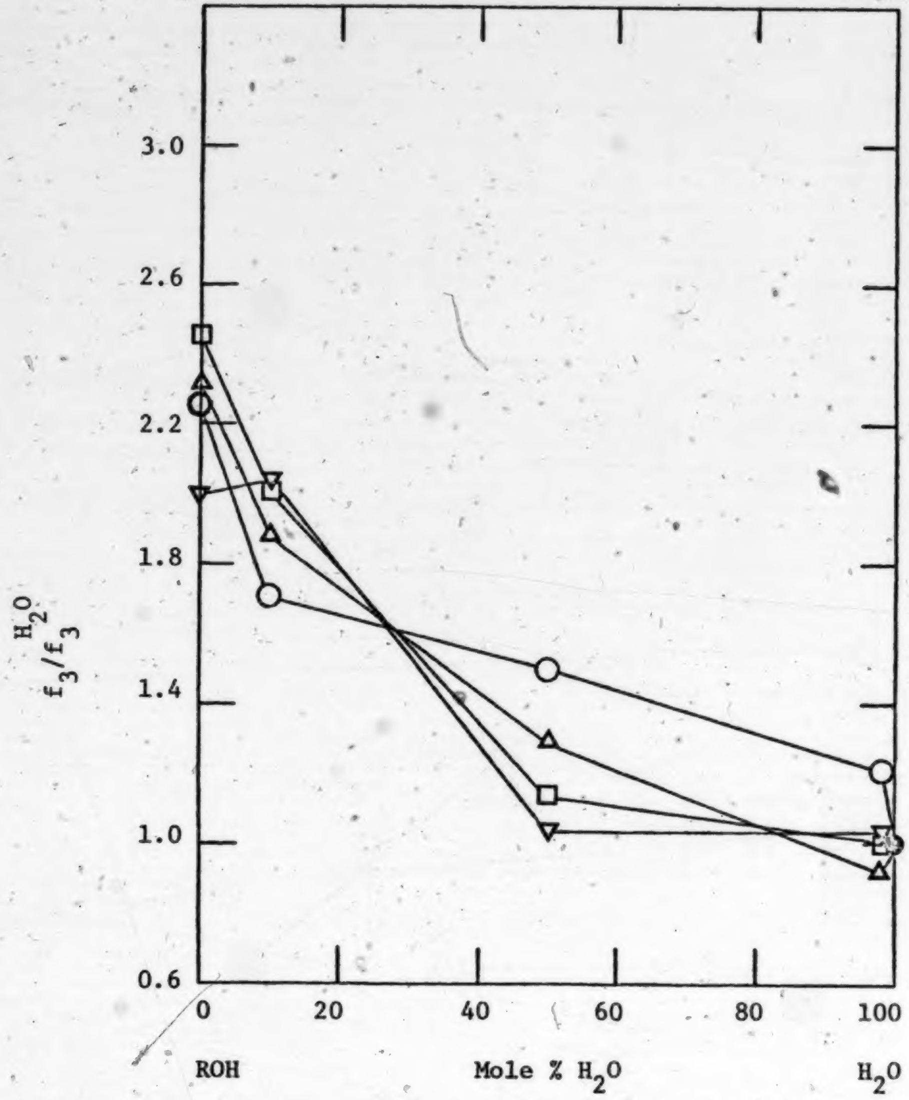

FIGURE V-27. Composition Dependence of $f_3/f_3^{H_2O}$ for Alcohol/ Water Mixtures at 298K.

●, Water; ○, Methanol; △, 1-Propanol; □, 2-Propanol; ▽, t-Butanol.